THE DISK POPULATION OF THE TAURUS STAR-FORMING REGION[1]

K. L. Luhman[2,3], P. R. Allen[2], C. Espaillat[4,5], L. Hartmann[4], and N. Calvet[4]

Draft version November 6, 2018

ABSTRACT

We have analyzed nearly all images of the Taurus star-forming region at 3.6, 4.5, 5.8, 8.0, and 24 μm that were obtained during the cryogenic mission of the *Spitzer Space Telescope* (46 deg^2) and have measured photometry for all known members of the region that are within these data, corresponding to 348 sources, or 99% of the known stellar population. By combining these measurements with previous observations with the *Spitzer* Infrared Spectrograph and other facilities, we have classified the members of Taurus according to whether they show evidence of circumstellar disks and envelopes (classes I, II, and III). Through these classifications, we find that the disk fraction in Taurus, N(II)/N(II+III), is $\sim$ 75% for solar-mass stars and declines to $\sim$ 45% for low-mass stars and brown dwarfs (0.01–0.3 $M_\odot$). This dependence on stellar mass is similar to that measured for Chamaeleon I, although the disk fraction in Taurus is slightly higher overall, probably because of its younger age (1 Myr vs. 2–3 Myr). In comparison, the disk fraction for solar-mass stars is much lower ($\sim$ 20%) in IC 348 and σ Ori, which are denser than Taurus and Chamaeleon I and are roughly coeval with the latter. These data indicate that disk lifetimes for solar-mass stars are longer in star-forming regions that have lower stellar densities. Through an analysis of multiple epochs of *Spitzer* photometry that are available for $\sim$ 200 Taurus members, we find that stars with disks exhibit significantly greater mid-infrared variability than diskless stars, which agrees with the results of similar variability measurements for a smaller sample of stars in Chamaeleon I. The variability fraction for stars with disks is higher in Taurus than in Chamaeleon I, indicating that the IR variability of disks decreases with age. Finally, we have used our data in Taurus to refine the observational criteria for primordial, evolved, and transitional disks. The ratio of the number of evolved and transitional disks to the number of primordial disks in Taurus is 15/98 for spectral types of K5–M5, indicating a timescale of $0.15 \times \tau_{\rm primordial} \sim 0.45$ Myr for the clearing of the inner regions of optically thick disks. After applying the same criteria to older clusters and associations (2–10 Myr) that have been observed with *Spitzer*, we find that the proportions of evolved and transitional disks in those populations are consistent with the measurements in Taurus when their star formation histories are properly taken into account.

ERRATUM: In Table 7, we inadvertently omitted the spectral type bins in which class II sources were placed in Table 8 based on their bolometric luminosities (applies only to stars that lack spectroscopic classifications). The bins were K6–M3.5 for FT Tau, DK Tau B, and IRAS 04370+2559, M3.5–M6 for IRAS 04200+2759, IT Tau B, and ITG 1, and M6–M8 for IRAS 04325+2402 C. In addition, the values of $K_s - [3.6]$ in Table 13 and Figure 26 for spectral types of M4–M9 are incorrect. We present corrected versions of Table 13 and Figure 26.

Subject headings: accretion disks — planetary systems: protoplanetary disks — stars: formation — stars: low-mass, brown dwarfs — stars: pre-main sequence

1. INTRODUCTION

Much of our knowledge of the processes of star and planet formation has been derived from observations of circumstellar disks around newborn stars. The Taurus complex of dark clouds is one of the principle sites for studies of disks. Taurus is among the nearest star-forming regions to the Sun (d = 140 pc) and contains more than 300 young stars and brown dwarfs (Kenyon et al. 2008). Because of the low stellar den-

sity and the absence of photoionizing stars, most members of Taurus are not embedded within bright nebulae, and thus are not subject to high levels of background emission that would hinder infrared (IR) observations of disks. The low density of Taurus also permitted resolved photometry of individual stars with the low-resolution imaging that was offered by the first major far-IR telescope, the *Infrared Astronomical Satellite* (IRAS, Beichman et al. 1986; Kenyon et al. 1990, 1994). By combining 12–100 μm photometry from IRAS with 1–10 μm data from ground-based telescopes, Kenyon & Hartmann (1995) performed the most comprehensive census of disks in a star-forming region at that time. The disk-bearing stars identified in Taurus have served as targets for a multitude of detailed observations of circumstellar disks (Kenyon et al. 2008, references therein).

The census of the stellar population of Taurus has expanded significantly since the disk study of

[1] Based on observations performed with the *Spitzer Space Telescope*.
[2] Department of Astronomy and Astrophysics, The Pennsylvania State University, University Park, PA 16802; kluhman@astro.psu.edu.
[3] Center for Exoplanets and Habitable Worlds, The Pennsylvania State University, University Park, PA 16802.
[4] Department of Astronomy, The University of Michigan, Ann Arbor, MI 48109.
[5] Current address: Harvard-Smithsonian Center for Astrophysics, Cambridge, MA 02138.

Kenyon & Hartmann (1995), particularly at masses below 0.5 $M_\odot$. The sensitivities of IR telescopes also have improved dramatically, most notably with the deployment of the *Spitzer Space Telescope* (Werner et al. 2004), which is capable of detecting members of Taurus with masses below 0.01 $M_\odot$. The Taurus stellar population has been imaged extensively by *Spitzer* through pointed observations of individual stars as well as wide-field maps. These images have been used to measure photometry for known members of Taurus (Hartmann et al. 2005; Luhman et al. 2006; Guieu et al. 2007) and search for new disk-bearing members (Luhman et al. 2006, 2009a,b; Rebull et al. 2010).

With the recent completion of the cryogenic mission of *Spitzer*, we wish to present a study of disks in Taurus that makes use of all *Spitzer* images of the region, which cover a total area of 46 deg^2 and encompass 99% of the known stellar population. We begin by analyzing all *Spitzer* images of Taurus at 3.6–24 μm that are publicly available and measuring photometry for all known members that are detected in these data (§ 2). We use these measurements in conjunction with previous observations by the *Spitzer* Infrared Spectrograph and other telescopes to classify the spectral energy distributions of all members of Taurus (§ 3). Through these classifications, we investigate how the prevalence of disks depends on stellar mass (§ 4) and location (§ 5). We then characterize the mid-IR variability of disks in Taurus with the multi-epoch photometry from *Spitzer* (§ 6). Finally, we use our mid-IR data in Taurus to refine the observational criteria for the advanced stages of disk evolution and we apply these criteria to *Spitzer* measurements in nearby clusters and associations with ages of 2–10 Myr (§ 7).

2. INFRARED IMAGES

2.1. *Observations*

For our census of the disk population in Taurus, we use images at 3.6, 4.5, 5.8, and 8.0 μm obtained with *Spitzer*'s Infrared Array Camera (IRAC; Fazio et al. 2004) and images at 24 μm obtained with the Multiband Imaging Photometer for *Spitzer* (MIPS; Rieke et al. 2004). The fields of view are $5'.2 \times 5'.2$ and $5'.4 \times 5'.4$ for IRAC and the 24 μm channel of MIPS, respectively. The cameras produced images with FWHM= $1''.6$–$1''.9$ from 3.6 to 8.0 μm and FWHM=$5''.9$ at 24 μm.

We consider all IRAC and MIPS 24 μm observations that have been performed in the vicinity of the Taurus clouds with the exception of some of the data with program identifications (PIDs) of 50477 and 50584, which are not yet available to the public. The images from the latter programs encompass only a small number of known members of Taurus, as discussed later in this section. The available data were obtained through Guaranteed Time Observations for PID=6, 36, 37 (G. Fazio), 53 (G. Rieke), 94 (C. Lawrence), 30540 (G. Fazio, J. Houck), and 40302 (J. Houck), Director's Discretionary Time for PID=462 (L. Rebull), Legacy programs for PID=139, 173 (N. Evans), and 30816 (D. Padgett), and General Observer programs for PID=3584 (D. Padgett), 20302 (P. André), 20386 (P. Myers), 20762 (J. Swift), 30384 (T. Bourke), 40844 (C. McCabe), and 50584 (D. Padgett). The IRAC and MIPS observations were performed through 180 and 137 Astronomical Observation Requests

(AORs), respectively. The characteristics of the resulting images are summarized in Tables 1 and 2. All AORs in Taurus with publicly available data are included in these observing logs, even those that do not contain known members and thus do not contribute photometry to our disk census. The boundaries of the IRAC and MIPS images are indicated in maps of the Taurus dark clouds in Figures 1 and 2, respectively. Each camera observed a total area of 46 deg^2. The fields covered by the two cameras closely overlap, as demonstrated in Figures 1 and 2.

We adopt the census of the stellar population in Taurus that was described by Luhman et al. (2009b), which is an updated version of the one presented by Kenyon et al. (2008). This census consists of 352 and 341 sources that are resolvable by IRAC and MIPS 24 μm images, respectively, 346 and 299 of which are within the available IRAC and MIPS images. Two of the members in the MIPS images were not observed by IRAC. Thus, a total of 348 resolved members appear within images from either IRAC or MIPS, corresponding to 99% of the known stellar population. All known members of Taurus are included in the tabulations of photometry in the next section. The stars that are outside of all available images for a given camera are indicated in those tables. The IRAC and MIPS images that are not yet available to the public encompass three and four known members, respectively. One and three of these stars are outside of the currently available IRAC and MIPS images, which consist of XEST 06-006 for IRAC and XEST 06-006, 2MASS J04163048+3037053, and 2MASS J04162725+2053091 for MIPS.

2.2. *Data Reduction*

Initial processing of the IRAC and MIPS images was performed by the Spitzer Science Center (SSC) pipeline. The pipeline versions were S14.0.0, S14.4.0, S15.3.0, S16.1.0, and S18.7.0 for IRAC and S16.0.1, S16.1.0, S16.1.1, and S17.2.0 for MIPS. The IRAC images produced by the SSC pipeline were combined into mosaics using R. Gutermuth's WCSmosaic IDL package (Gutermuth et al. 2008). We selected a plate scale of $0''.86$ pixel^{-1} for these final images. For MIPS, we used the mosaics produced by the SSC pipeline, which had a plate scale of $2''.45$ pixel^{-1}.

We measured photometry for the known members of Taurus with methods similar to those employed in our previous *Spitzer* studies of star-forming regions (Luhman et al. 2008a,b). We used the IRAF task STARFIND to measure the positions of the Taurus members in the IRAC and MIPS images and we performed aperture photometry at those locations using the IRAF task PHOT. For MIPS sources, the radii of the apertures and inner and outer boundaries of the sky annuli were 3, 3, and 4 pixels, respectively. For a given IRAC source, we selected one of the apertures listed in Table 3. The 4 pixel apertures were the default choices. We visually inspected the IRAC images of all stars to determine if smaller apertures were needed because of close proximity to other sources. Based on this inspection, we adopted aperture radii of 3 pixels and sky annuli extending from 3 to 4 pixels for the IRAC measurements of JH 112 and 2MASS J04324938+2253082. For sources that were very close to other stars, we attempted to remove the

light from the latter by subtracting a scaled IRAC point spread function (PSF, Marengo et al. 2006). We performed this step prior to the measurement of photometry for UZ Tau Ba+Bb, DK Tau B, IT Tau B, HV Tau C, MHO 1, MHO 2, Haro 6-37 A and B, V710 Tau A and B, J1-4872 A and B, IRAS 04191+1523 B, HD 28867 A and B, and FU Tau B (Luhman et al. 2009a). We measured photometry from each PSF-subtracted image with aperture radii and inner and outer sky annuli of either 2, 14, and 15 pixels or 3, 3, and 4 pixels, respectively. We selected the aperture from these two options that minimized contamination by the residuals of the neighboring PSF-subtracted star.

Many of the protostars in Taurus are surrounded by extended emission in the IRAC images. We measured photometry for these sources using both the default 4-pixel apertures as well as larger apertures that encompass most of the scattered light. L1521F-IRS and IRAS 04166+2706 exhibit only extended emission and no point sources at 3.6–5.8 and 3.6 μm, respectively. Therefore, we did not apply the 4-pixel apertures to these images and measured photometry from only the large apertures. Because IRAS 04325+2402 C is faint compared to its surrounding emission, we estimated its IRAC photometry through PSF fitting.

To calibrate the photometry, we adopted zero point magnitudes (ZP) of 19.670, 18.921, 16.855, 17.394, and 15.119 in the 3.6, 4.5, 5.8, 8.0, and 24 μm bands, where $M = -2.5 \log(DN/sec) + ZP$ (Reach et al. 2005; Engelbracht et al. 2007). For each AOR that contained stars that were isolated, bright, and unsaturated, we used these stars to measure aperture corrections between our adopted apertures and the larger ones employed by Reach et al. (2005) and Engelbracht et al. (2007). For the MIPS data, we combined our aperture corrections with the one estimated by Engelbracht et al. (2007) between their aperture and an infinite one. These aperture corrections were then applied to our photometry for all other sources in that AOR. If an AOR did not contain stars that were suitable for estimating aperture corrections, we adopted the averages of the corrections measured among all of the AORs. The average aperture corrections for IRAC are given in Table 3. The spread in these measurements was less than ±0.01 mag for a given band and aperture. The corrections to an infinite aperture for MIPS ranged between 0.78–0.84 mag with an average value of 0.80 mag.

We present the IRAC and MIPS photometry for the known members of Taurus in Tables 4, 5, and 6. If an object is saturated or is not detected in all MIPS images of that position, it appears only once in Table 6 and the observing dates are omitted. Our quoted photometric errors include the Poisson errors in the source and background emission and the 2% and 4% uncertainties in the calibrations of IRAC and MIPS, respectively (Reach et al. 2005; Engelbracht et al. 2007). The errors do not include an additional error of ±0.05 mag due to location-dependent variations in the IRAC calibration.

3. CLASSIFICATIONS OF SPECTRAL ENERGY DISTRIBUTIONS

3.1. *Known Class 0 and Class I Sources*

Spectral energy distributions (SEDs) of young stars are sensitive to the presence of circumstellar dust, and thus can be used to constrain the evolutionary stages of the members of a young stellar population. These stages consist of a protostar surrounded by an accretion disk and an infalling envelope (classes 0 and I), a star with a disk but no envelope (class II), and a star that is no longer surrounded by primordial dust (class III, Lada & Wilking 1984; Lada 1987; André et al. 1993; Greene et al. 1994). We wish to classify the members of Taurus with SEDs constructed from our *Spitzer* photometry. However, while class III stars are easily distinguished from less evolved systems, some class I and class II sources can exhibit similar SEDs in the *Spitzer* bands (Hartmann et al. 2005). The definitive identification of class I sources requires other observations that better constrain the presence of an envelope, such as mid-IR spectroscopy, far-IR and millimeter photometry, and high-resolution images. Therefore, before classifying the *Spitzer* SEDs in Taurus, we assign classes 0 and I to all members of Taurus that exhibit evidence of envelopes in previous data. These stars consist of all targets from Watson et al. (2004) and Furlan et al. (2008)[6], IRAS 04108+2803 A (Zasowski et al. 2009), L1551NE (Moriarty-Schieven et al. 1995), IRAS 04191+1523 A (Tamura et al. 1991; Moriarty-Schieven et al. 1992), IRAS 04191+1523 B (Motte 1998; Duchêne et al. 2004; Dunham et al. 2006), IRAM 04191+1522 (André et al. 1999; Dunham et al. 2006), L1521F-IRS (Bourke et al. 2006), IRAS 04111+2800G (Prusti et al. 1992), and IRAS 04166+2706 (Kenyon et al. 1990; Bontemps et al. 1996; Motte & André 2001). Haro 6-5B also is a class I source according to unpublished data from the *Spitzer* Infrared Spectrograph (IRS, D. Watson, private communication). Among these protostars, IRAS 04368+2557 and IRAM 04191+1522 are the clearest examples of class 0 sources based on their low bolometric temperatures ($T_{\rm bol} < 70$ K, Chen et al. 1995; André et al. 1999; Motte & André 2001). We adopt class I designations for the remaining stars. A few of these sources appear to be in transition between classes 0 and I (L1551NE, Chen et al. 1995) or between classes I and II (IRAS 04154+2823, Furlan et al. 2008). The latter stage has been referred to as flat-spectrum or class I-II in some studies, but we denote them as class I for the purposes of this work since they show evidence of envelopes (albeit tenuous ones).

The stars described in this section that exhibit evidence of envelopes in previous observations comprise all class 0 and I sources in Table 7. Sources that have class I SEDs but lack supporting observations that are sensitive to the presence of envelopes are listed as "class I?" (§ 3.3).

3.2. *Infrared Color-Color & Color-Magnitude Diagrams*

To provide an initial demonstration of how stars with disks are identified with *Spitzer* photometry, we can construct color-color and color-magnitude diagrams from our *Spitzer* data for Taurus. These diagrams are frequently applied to young stellar populations because they effectively discriminate between stars with and without

---

[6] The IRS data from Furlan et al. (2008) that were attributed to IRAS 04166+2706 actually apply to IRAS 04166+2708. This misidentification of IRAS 04166+2706 with the counterpart of IRAS 04166+2708 also appears in Luhman (2006), Luhman et al. (2006), and Kenyon et al. (2008), and probably originated in the former two papers.

disks and yet they do not require knowledge of the individual stellar properties, such as spectral types and extinctions (Allen et al. 2004; Megeath et al. 2004).

If multiple measurements are available in a given band for a star, we adopt the mean of those measurements weighted by the inverse square of their flux errors in the color-color and color-magnitude diagrams. Some Taurus members lack photometry in one or more bands and thus are absent from a given diagram because they are unresolved from brighter sources, outside the field of view of the *Spitzer* images, saturated, detected only as extended emission, or below the detection limit (only applies to the 24 μm data). If a binary is resolved by IRAC but not by MIPS, we plot the total system magnitudes when data from both cameras are used in a diagram.

In Figure 3, we present two IRAC color-color diagrams for the members of Taurus that have been measured in all of the IRAC bands. Some of the stars reside in a tight group near the origin while others form a broad distribution of redder sources, which correspond to stellar photospheres and stars with disks, respectively. As expected, the known class 0/I sources exhibit the reddest colors since they are surrounded by the both circumstellar disks and envelope, although a few protostars have relatively blue colors because they appear nearly edge-on from our point of view (e.g., IRAS 04302+2247).

In Figure 4, we plot the members of Taurus in a color-color diagram that combines IRAC and MIPS data and an IRAC color-magnitude diagram. As in the IRAC color-color diagrams, two distinct populations of diskless and disk-bearing stars are apparent in both diagrams. The IRAC/MIPS color-color diagram is useful for identifying stars that exhibit excess emission at 24 μm but not in the IRAC bands, which is a signature of a disk with an inner hole. Disks of this kind are discussed in more detail in § 7. Meanwhile, the color-magnitude diagram in Figure 4 illustrates the dependence of mid-IR colors on magnitude, which acts as a proxy for luminosity, spectral type, and stellar mass. At fainter magnitudes, the sequence of diskless stars becomes slightly redder, reflecting a variation of the photospheric colors with spectral type, while the average excess at 8 μm of the sources with disks becomes smaller. The same trends have been found in previous IRAC measurements for Taurus (Luhman et al. 2006).

3.3. *Classification with Spectral Slopes*

Most members of Taurus are easily classified as either class III or class 0/I/II with *Spitzer* color-color diagrams. However, the color-color diagrams do not offer a straightforward means of dividing disk-bearing stars among classes 0, I, and II. In addition, some stars have ambiguous colors that are neither neutral nor very red, which can arise from diskless stars that are highly reddened or very cool, or stars that harbor disks in advanced stages of evolution. We can perform more refined and quantitative classifications by characterizing the SED of each star in terms of spectral slopes that are defined as $\alpha = d \log(\lambda F_\lambda)/d \log(\lambda)$ (Adams et al. 1987; Lada 1987; Greene et al. 1994), correcting the slopes for reddening, and comparing the resulting values to the typical slopes of stellar photospheres near the spectral type in question.

As done in Chamaeleon I (Luhman et al. 2008a), we have computed slopes in Taurus between four pairs of

bands, $K_s/[8.0]$, $K_s/[24]$, $[3.6]/[8.0]$, and $[3.6]/[24]$. For most stars, we use measurements of K_s (2.2 μm) from the Point Source Catalog of the Two-Micron All-Sky Survey (2MASS, Skrutskie et al. 2006). We adopt photometry from multiplicity surveys for a few systems that are marginally resolved by 2MASS. As in the color-color diagrams, we have used the weighted average in a given band if an object has been observed at multiple epochs. For binaries that are resolved in K_s and the IRAC bands but not at 24 μm, we computed the 24 μm slopes with the total system fluxes at shorter wavelengths. These systems are noted in Table 7. We have dereddened the observed slopes using the extinctions described by Luhman et al. (2009b) and the reddening law from Flaherty et al. (2007), except for members that lack reliable estimates of extinctions. The observed and dereddened values of α_{2-8}, α_{2-24}, $\alpha_{3.6-8}$, and $\alpha_{3.6-24}$ are presented in Table 7. All known members of Taurus are included in Table 7, even those for which none of these slopes could be computed. The classifications for the latter sources are determined from other data, as discussed at the end of this section.

Histograms of the dereddened spectral slopes from Table 7 are shown in Figure 5. The observed slopes are used for stars that lack extinction estimates. Like the data in the color-color diagrams, the slopes form a narrow group of blue sources and a broader distribution of redder objects, corresponding to stellar photospheres and stars with disks, respectively. To better distinguish between these two populations, we plot the slopes as a function of spectral type in Figure 6. Our adopted spectral types are listed with the spectral slopes in Table 7 (Cowley 1972; Hartigan et al. 1994; Strom & Strom 1994; Kenyon & Hartmann 1995; Torres et al. 1995; Wichmann et al. 1996; Briceño et al. 1998, 2002; Kenyon et al. 1998; Luhman & Rieke 1998; Malfait et al. 1998; Duchêne et al. 1999; White et al. 1999; Martín 2000; Martín et al. 2001; Steffen et al. 2001; White & Ghez 2001; Hartigan & Kenyon 2003; Muzerolle et al. 2003; Walter et al. 2003; White & Basri 2003; Luhman 2004b, 2006; Luhman et al. 2003a, 2006, 2009a,b; Guieu et al. 2006; Slesnick et al. 2006; Beck 2007; Prato et al. 2009). The sequences of class III stars are narrow and well-separated from the redder population of class 0/I/II sources. The class III sequence is tighter at 8 μm while the separations from the disk-bearing stars are larger at 24 μm. The photospheric slopes also vary with spectral type, particularly for α_{2-8}. All of these characteristics apply to the data for Chamaeleon I from Luhman et al. (2008a). Indeed, we find that the photospheric sequences for Taurus and Chamaeleon I are very similar. As a result, we adopt the same thresholds for distinguishing between classes II and III that were defined by Luhman et al. (2008a), except that we have used the colors of young field L dwarfs from Luhman et al. (2009b) to revise the boundaries at L0.

We have used the spectral slopes in Figure 6 to classify the Taurus members that were not already assigned to classes 0 and I in § 3.1 based on previous detections of envelopes. Stars below the thresholds in Figure 6 are classified as class III while redder stars with $\alpha \leq 0$ are designated as class II (Lada 1987). Sources with $\alpha > 0$ are labeled as "class I?" if no other data are available to verify the presence of an envelope. Unlike in our study

of Chamaeleon I, we do not employ the "flat-spectrum" class ($-0.3 \leq \alpha \leq 0.3$, Greene et al. 1994) because most Taurus members within this range of slopes have been observed with mid-IR spectroscopy, which is sensitive to the presence of envelopes and thus discriminates fairly reliably between classes I and II (Furlan et al. 2006, 2008). If a star exhibits excess emission at 24 μm but not at 8 μm, we classify it as class II. A few objects that are slightly bluer than the II/III thresholds at 24 μm and are labeled as class III may have small amounts of excess emission. The SEDs of these stars are discussed in § 7.

We discuss in more detail the classifications of several sources, particularly ones for which the four spectral slopes disagree with each other or with classifications derived from previous mid-IR spectroscopy. Although IRAS 04385+2550, IRAS 04301+2608, IRAS 04260+2642, CZ Tau, CoKu Tau/4, and 2MASS J04210795+2702204 have $\alpha_{3.6-24} > 0$, we classify them as class II rather than class I based on the absence of signatures of envelopes (e.g., strong silicate and ice absorption features) in IRS spectra from D'Alessio et al. (2005), Furlan et al. (2006), and unpublished observations in *Spitzer* programs PID=2, 3303, and 30765 (D. Watson, private communication). The 8 and 24 μm slopes for 2MASS J04381486+2611399 imply class I and class II, respectively. It is probably a class II object since high-resolution images and mid-IR spectroscopy do not show any evidence of an envelope, indicating that it is not a class I source (Luhman et al. 2007a). Those data do reveal an edge-on disk, which is the cause of its red SED. Although the dereddened 24 μm slopes of 2MASS J04194657+2712552 are slightly below the I/II threshold of $\alpha = 0$, we list it as "class I?" since it has the reddest SED of any known member of Taurus with a measured spectral type later than M6 (excluding the edge-on system 2MASS J04381486+2611399). For IRAS 04187+1927, α_{2-8} and $\alpha_{3.6-8}$ produce different classifications (II vs. I). Slopes extended to 24 μm are unavailable since this star was not observed by MIPS. We have assigned it to class II based on IRS data (Furlan et al. 2006). J1-4872 A and B are class II based on α_{2-8} but are class III according to the other slopes. We adopt the latter classification for these stars because of the possibility of variability between the dates of the K_s and *Spitzer* observations. For the same reason, we classify CIDA-9 using $\alpha_{3.6-8}$ (class II) rather than with α_{2-8} (class I). Although 2MASS J04373705+2331080 is slightly redder in α_{2-8} than the II/III threshold, this color excess is not reliable given the large uncertainty in the measurement of K_s. When compared to 3.6 μm, the 5.8 and 8.0 μm measurements for this object do not exhibit significant excess emission relative to stellar photospheres (Luhman et al. 2009b), indicating that it is a class III source. Similarly, V710 Tau B has a small excess at 8 μm, but the significance of this excess is marginal since the uncertainty in the 8 μm measurement is large. We classify this star as "class II?". IRAS 04173+2812 is class I and class II according to the 8 and 24 μm slopes, respectively. We adopt the 24 μm classification since the presence of an envelope is more easily detected at longer wavelengths.

Finally, we discuss the classifications of the Taurus members for which none of the four spectral slopes in Table 7 could be computed because the necessary *Spitzer*

photometry is not available. We could not measure photometry at 8 and 24 μm for V892 Tau, RY Tau, T Tau N, and AB Aur because they are either saturated or outside of the images. We assign these stars to class II based on the mid-IR spectroscopy from Furlan et al. (2006). 2MASS J04390637+2334179 was observed at 3.6 and 5.8 μm but not at 4.5 and 8.0 μm. The photometry in the former two bands and a non-detection at 24 μm indicate that this star is class III. Six known members of Taurus were not observed by IRAC in any of its bands. Two of these stars, 2MASS J04381630+2326402 and 2MASS J04385871+2323595, were within the field of view of MIPS images, but were not detected. The detection limits at 24 μm are sufficiently faint to demonstrate that these stars are class III. One star, MWC 480, is known to be a class II source from previous observations (Mannings et al. 1997). The remaining three sources have weak Hα emission (Luhman 2004b, 2006; Luhman et al. 2009b; Slesnick et al. 2006), suggesting that they are not undergoing significant accretion. We classify these stars as "class III?".

The SED classifications for all known members of Taurus are presented in Table 7. For multiple systems that are unresolved by IRAC, these classifications apply to the component that dominates at mid-IR wavelengths. However, it is possible for different components to dominate at different IR wavelength ranges, as in the case of T Tau N and S (Furlan et al. 2006). For that system, the designation of class II in Table 7 refers to T Tau N, whereas the southern component may be a class I source (Furlan et al. 2006).

4. DISK FRACTION

We would like to use our tabulation of SED classifications in Taurus to measure the fraction of members that have disks as a function of stellar mass. However, some of the known members of Taurus were originally discovered because they exhibited evidence of disks. As a result, the census of Taurus could be biased in favor of stars with disks, in which case the disk fraction computed from all known members would not be representative of the stellar population. To address this possibility, we have measured a disk fraction from a sample of members that is likely to be unbiased in terms of disks. For this sample, we have selected all known members within the fields observed during the *XMM-Newton* Extended Survey of the Taurus Molecular Cloud (XEST, Güdel et al. 2007). These fields have been searched extensively for new members with a variety of methods and offer relatively well-defined completeness limits (Luhman et al. 2009b). As done in Chamaeleon I (Luhman et al. 2008a), we compute the disk fraction as a function of spectral type, which acts as a proxy for stellar mass. For both the XEST fields and all of Taurus, we list in Table 8 the number of members as a function of SED class and spectral type. For members that lack measured spectral types, most of which are class I sources, we estimated the spectral type bins in which they belong by combining their luminosities (e.g., Furlan et al. 2008) with the values predicted by the evolutionary models for an age of 1 Myr. The two class 0 sources are excluded from Table 8.

We now consider the question of how to define the disk fraction in a young population. The ultimate objective

of studies of disk fractions is the measurement of the average lifetime of disks by comparing disk fractions among clusters with different ages (Haisch, Lada, & Lada 2001). In these comparisons, the ages that are typically adopted for clusters apply only to the class II and III members since the class I sources usually lack the temperature and luminosity measurements that are needed for isochronal ages. If class I sources are younger than stars in classes II and III (e.g., § 5), then it would be inappropriate to include them in disk fractions when estimating disk lifetimes. Therefore, we define the disk fraction as N(II)/N(II+III) in our analysis of Taurus. In comparison, many previous studies have included both classes I and II in their disk fractions. Because the frequency of class I sources decreases rapidly with cluster age, disk fractions for clusters older than Taurus ($\tau > 1$ Myr) do not depend significantly on the treatment of these objects. However, the adopted definition does have a noticeable effect on the disk fractions in the youngest regions.

The values of N(II)/N(II+III) for Taurus from Table 8 are plotted versus spectral type in Figure 7. The boundaries of the spectral type bins in Figure 7 have been converted to stellar masses by combining the temperature scale of Luhman et al. (2003b) and the evolutionary models of Baraffe et al. (1998) and Chabrier et al. (2000). As shown in Figure 7, the disk fractions for the known members in the XEST fields and across all of Taurus are similar. If the true disk fraction is the same within and outside of the XEST fields, then the agreement in these disk fractions suggests that the total census of Taurus is not strongly biased for or against stars with disks. These disk fractions in Taurus exhibit a dependence on spectral type and stellar mass, declining steadily from $\sim$ 75% for solar-mass stars to $\sim$ 45% for low-mass stars and brown brown dwarfs. For comparison, we have included in Figure 7 the disk fractions measured from *Spitzer* observations of Chamaeleon I and IC 348 (Lada et al. 2006; Muench et al. 2007; Luhman et al. 2005, 2008a). The fractions for Taurus and Chamaeleon I vary with spectral type in a similar manner while an opposite dependence on spectral type is present in the data for IC 348. Like Taurus and Chamaeleon I, roughly half of its low-mass members have disks, but the disk fraction is much lower among its solar-mass stars. The σ Ori cluster closely resembles IC 348 in this respect (Hernández et al. 2007a; Luhman et al. 2008b). Given that Chamaeleon I, IC 348, and σ Ori have similar ages (2–3 Myr, Luhman 2007; Luhman et al. 2008b), these differences in disk fractions are presumably tied to the star-forming conditions of these regions. For instance, Luhman et al. (2008a) suggested that the low disk fraction at higher masses in IC 348 relative to Chamaeleon I might be related to the higher stellar density of IC 348 combined with the segregation of the more massive stars toward the center of the cluster. The high and low disk fractions for solar-mass stars in Taurus and σ Ori, respectively, provide further support for this hypothesis since the former is even more sparse than Chamaeleon I while the latter is comparable in density to IC 348. Thus, it appears that the disk lifetimes for stars more massive than 0.5 $M_\odot$ may be shorter in denser clusters.

Finally, we note that the ratio of the number of class II sources to the number of class I sources in Taurus (~ 4.4)

is similar to the values measured in previous studies of Taurus (Kenyon & Hartmann 1995) and in *Spitzer* surveys of other nearby regions of ongoing star formation ($\tau < 5$ Myr, Evans et al. 2009; Gutermuth et al. 2009). This ratio is typically interpreted as the ratio of the lifetimes of these stages. For instance, if an average lifetime of 3 Myr is adopted for class II sources, then the measurement of N(I)/N(II) in Taurus implies a lifetime of 0.7 Myr for class I objects.

5. SPATIAL DISTRIBUTIONS OF SED CLASSES

In addition to measuring the disk fraction as a function of stellar mass in Taurus, we can also use our SED classifications to compare the spatial distributions of the SED classes. To arrive at meaningful results in this comparison, the completeness of the stellar census should not vary significantly with SED class. The images of Taurus from *Spitzer* have demonstrated that the current census has a high level of completeness for classes I and II across most of the cloud complex (Luhman et al. 2006, 2009b). The completeness for class III stars is not well-defined outside of the denser stellar aggregates and may be lower than that of the class I/II sources in those outer areas, but correcting for such incompleteness would reinforce the primary result regarding the class III sources that we are about to describe, which is that they are more widely distributed than the less evolved stars.

The locations of Taurus members in classes I, II, and III are shown on maps of the cloud complex in Figures 8 and 9. The class I/II sources tend to appear near the dense gas, as found previously in Taurus and other star-forming regions (Hartmann 2002; Gutermuth et al. 2009, references therein), while the class III stars are more frequently scattered far from the dark clouds. To perform a quantitative comparison of these spatial distributions, we have computed for each star the distance to the nearest known member from any SED class. The median of these distances is 2.2, 3.3, and 5.′5 for classes I, II, and III, respectively, which corresponds to 0.09, 0.13, and 0.22 pc at the distance of Taurus. Histograms of the nearest neighbor distances for classes I+II and III are presented in Figure 10. According to a two-sided Kolmogorov-Smirnov test, the probability that those two samples are drawn from the same parent distribution is 0.3%. The probability that classes I and II are drawn from the same distribution is 10%, which does not represent a significant difference.

Spitzer has been used to measure the spatial distributions of young stars in dozens of other star-forming regions (Gutermuth et al. 2009). Because most of those clusters have not been searched extensively for members prior to the *Spitzer* imaging, and only the disk-bearing members can be identified with mid-IR photometry, the *Spitzer* surveys have primarily measured the spatial distributions of classes I and II. For instance, the nearest neighbor distances from Gutermuth et al. (2009) were computed among class I/II sources without the inclusion of class III stars. To enable a comparison of our results to those of Gutermuth et al. (2009), we have computed nearest neighbor distances in Taurus in the same manner. We find that the median of the distance to the nearest member in classes I or II is 2.2, 4.1, and 3.′6 for classes I, II, and I+II, respectively, or 0.09, 0.17, and 0.15 pc at the distance of Taurus. The class II sources again ap-

pear to be more widely distributed than the protostars. The probability that the nearest neighbor distances for classes I and II are drawn from the same distribution is 2%. Thus, the exclusion of the class III stars has enhanced the difference between the class I and II distributions. A marginally significant difference of this kind also was found by Gutermuth et al. (2009) in their analysis of 36 young clusters.

The median of the nearest neighbor distances for the class I+II sample in Taurus, 0.15 pc, is twice as large as the average median for the clusters from Gutermuth et al. (2009), which is consistent with the measurement of larger protostellar envelopes in Taurus than in denser clusters like Ophiuchus (Motte et al. 1998). For several clusters, Gutermuth et al. (2009) found that the distributions of nearest neighbor distances among classes I and II peaked near 0.02–0.05 pc, while the distribution in Taurus reaches a sharp maximum in the lowest bin below $15''$, or 0.01 pc, as shown in the top panel of Figure 10. This difference is likely a reflection of the close proximity of Taurus relative to the clusters from Gutermuth et al. (2009, $d = 140$–1700 pc), which allows higher spatial resolution. To give the Taurus sample a resolution that is comparable to that from Gutermuth et al. (2009), we can count neighboring members in Taurus that are within $10''$ of each other as single sources. By doing so, the maximum in the Taurus distribution moves out to 0.02–0.03 pc and the median increases by $\sim 20\%$.

Guieu et al. (2007) measured *Spitzer* photometry for 23 late-type (M5.5–M9.5) members of Taurus and used these data to check for spatial variations in the disk fraction of brown dwarfs. They found that the disk fraction for low-mass objects in their sample was lower in the southern filaments than in northern ones. In comparison, the more massive members did not appear to exhibit the same trend. Guieu et al. (2007) suggested that the spatial dependence of the disk fraction for low-mass sources could result from an older age for southern filaments combined with shorter disk lifetimes for brown dwarfs. We have investigated this issue with our SED classifications. The northern and southern filaments compared by Guieu et al. (2007) can be separated by a declination of $\delta = 25°10'$ (J2000). We have computed disk fractions on each side of this boundary for low- and high-mass members, arriving at $128/175 = 0.73 \pm 0.03$ for $\leq$M6 and $15/30 = 0.50 \pm 0.09$ for >M6 in the north and $75/121 = 0.62 \pm 0.04$ for $\leq$M6 and $5/22 = 0.23^{+0.11}_{-0.06}$ for >M6 in the south[7]. The ratio of southern to northern disk fractions is 0.85 ± 0.07 and $0.46^{+0.23}_{-0.14}$ for $\leq$M6 and >M6, respectively. Since these ratios differ by only slightly more than 1 σ, we find that there is no significant evidence to indicate that the disk fraction of brown dwarfs varies with position in a different manner than the disk fraction of stars. The suggestion by Guieu et al. (2007) that disk lifetimes are shorter for brown dwarfs also is not supported by the disk fractions measured in older clusters like Chamaeleon I, IC 348, and σ Ori that were described in the previous section.

6. DISK VARIABILITY

[7] The statistical errors in the disk fractions are computed in the manner described by Burgasser et al. (2003).

A majority of the members of Taurus have been observed more than once with the cameras on board *Spitzer*. We can use these multi-epoch measurements to measure the mid-IR variability of disks in Taurus.

We have measured photometry at multiple epochs for 201, 206, 214, and 207 members of Taurus at 3.6, 4.5, 5.8, and 8.0 μm, respectively. As done in Chamaeleon I by Luhman et al. (2008a), we have quantified the variability of the data in Taurus by computing the difference between each magnitude and the average magnitude for a given object and wavelength (Δm). In Figure 11, we present histograms of Δm for class III stars and for sources that are class 0, I, or II. Each measurement of Δm is weighted by the inverse of the number of measurements so that all members contribute equally to the distributions. The data in Figure 11 demonstrate that stars with disks exhibit significantly greater levels of mid-IR variability than diskless stars, which agrees with variability measurements in Chamaeleon I (Luhman et al. 2008a). Among stars that have been observed at multiple epochs in at least two bands, 92 of 144 class 0/I/II sources and 16 of 75 class III stars have $\Delta m > 0.05$ in one or more bands. If we require $\Delta m > 0.05$ in at least two bands, then these fractions become 64/144 and 2/75 respectively. Thus, the difference in the variability fractions is more pronounced when variability in two bands is required, which is a reflection of the fact that the different IRAC bands usually vary simultaneously for stars with disks but not for class III stars.

It is useful to compare our variability statistics for Taurus to those in Chamaeleon I. We have updated the variability measurements from Luhman et al. (2008a) by combining the IRAC photometry from that study with additional data from Luhman & Muench (2008). Multiple epochs of photometry are available for 49, 52, 88, and 76 members of Chamaeleon I at 3.6, 4.5, 5.8, and 8.0 μm, respectively. For sources that have been observed more than once in at least two bands, 15 of 57 class 0/I/II sources and 2 of 48 class III stars exhibit $\Delta m > 0.05$ in two or more bands. Thus, the variability fraction for stars with disks is higher in Taurus than in Chamaeleon I ($64/144 = 0.44 \pm 0.04$ vs. $15/57 = 0.26^{+0.07}_{-0.05}$). Since Chamaeleon I is older than Taurus, this comparison indicates that the variability of disks decreases with age.

7. ADVANCED STAGES OF DISK EVOLUTION

Taurus offers a unique opportunity for studying the advanced stages of disk evolution. Because Taurus is nearby and does not suffer from crowding or bright nebular emission, mid-IR photometry can be measured more accurately for its stellar population than for most other star-forming regions. Furthermore, since most members of Taurus have been classified spectroscopically, we can reliably estimate the SEDs of their underlying stellar photospheres. The high quality of both the observed and photospheric SEDs makes it possible to detect the small levels of IR excess emission that arise from the most evolved disks, even those surrounding low-mass stars and brown dwarfs. Because the stellar population in Taurus is large and contains significant numbers of both protostars and diskless stars, the intervening stages of disk evolution should be sampled with the best available uniformity and number statistics. For these reasons, Taurus was the site of much of the earliest work on

the advanced stages of disk evolution (Strom et al. 1989; Skrutskie et al. 1990) and is the one region to which most other young clusters are compared.

In this section, we use our *Spitzer* data in Taurus to refine the classification of the evolutionary phases of disks and to identify the Taurus members that harbor the most evolved disks. We then apply our classification criteria to other young populations that have been observed with *Spitzer* so that we can constrain the timescale of disk clearing.

7.1. *Terminology*

A variety of names, definitions, and observational criteria for the stages of disk evolution have been employed in previous studies. We describe our adopted terms in this section and develop observational criteria for them in § 7.2.

We define *primordial disks* as disks that are optically thick at IR wavelengths and have not experienced inner clearing[8]. Observationally, primordial disks in Taurus form a large, continuous population in terms of mid-IR color excesses, as demonstrated in § 7.2. There are several possible mechanisms that may drive the evolution of primordial disks, including giant planet formation and the growth and settling of dust grains (Najita et al. 2007, references therein).

Pre-transitional disks are primordial disks that have formed gaps in which dust is optically thin or absent. These disks exhibit less excess emission at $\lambda \lesssim 10~\mu$m than the average primordial disk but still retain strong disk emission at longer wavelengths. Because they are not distinct from the main population of disks in terms of their mid-IR excess emission (§ 7.2), we treat pre-transitional disks as a subset of primordial disks. Examples of pre-transitional disks in Taurus include UX Tau A and LkCa 15 (Furlan et al. 2006; Espaillat et al. 2007b, 2008a).

The IR excesses from members of Taurus do not decrease monotonically from primordial disks to stellar photospheres. Instead, stars in Taurus are found predominantly in two groups that are well-separated from each other in terms of their IR colors (Skrutskie et al. 1990). The gap between these populations does contain a few stars, including those with *transitional disks* and *evolved disks* (Skrutskie et al. 1990; Hernández et al. 2007a). Transitional disks have large inner holes, and thus produce little or no emission at shorter IR wavelengths followed by a sudden onset of strong emission at longer wavelengths. Taurus members that are known to harbor transitional disks include CoKu Tau/4, GM Aur, and DM Tau (Rice et al. 2003; Forrest et al. 2004; Quillen et al. 2004; Calvet et al. 2005; D'Alessio et al. 2005), although the inner hole in the disk of CoKu Tau/4 was probably produced by a stellar companion rather than processes associated with disk evolution and planet formation (Ireland & Kraus 2008). Meanwhile, evolved disks are full disks without inner holes that are in the process of becoming optically thin. As a result, they exhibit weak emission at all mid-IR wavelengths and their spectral slopes do not show the abrupt increase that

is observed in transitional disks. Other terms used for these disks include anemic, thin, weak, and homologously depleted (Lada et al. 2006; Barrado y Navascués et al. 2007; Dahm & Hillenbrand 2007; Currie et al. 2009a).

An optically thin disk that contains an inner hole could arise when an evolved disk is inwardly truncated or a transitional disk becomes optically thin. We refer to these disks as *evolved transitional disks*. They produce little or no excess emission at $\lambda < 10~\mu$m and weak emission at longer wavelengths. The SEDs of evolved transitional disks closely resemble those of *debris disks*, which are disks of second-generation dust that is generated by collisions among planetesimals (Kenyon & Bromley 2005; Rieke et al. 2005; Hernández et al. 2006; Currie et al. 2008; Carpenter et al. 2009).

7.2. *Classification of Evolutionary Stages*

The stages of disk evolution described in the previous section differ from each other in terms of the strength of mid-IR excess emission as a function of wavelength. We can characterize these differences by examining excesses at multiple wavelengths for all members of Taurus that have been observed by *Spitzer*. In a transitional disk, the wavelength beyond which excess emission appears depends on the size of the inner hole. Therefore, we consider a range of wavelengths covered by *Spitzer*, namely 4.5, 5.8, 8.0, and 24 μm. To measure the excess emission in each band, we subtract the *Spitzer* data from photometry at K_s (2.2 μm), which is short enough in wavelength that the stellar photosphere usually dominates the total flux while red enough that extinction is low. These colors were corrected for extinction in the manner described for the spectral slopes in § 3.3. We plot $K_s-[8.0]$, $K_s-[5.8]$, and $K_s-[4.5]$ versus $K_s-[24]$ for class II and III members of Taurus in Figures 12, 13, and 14, respectively. Since both the average excess emission and the photospheric colors vary with spectral type (Figure 6, Luhman et al. 2008a), we divide the data into four ranges of spectral types (sp), consisting of $sp \leq$K4.5, K4.5$< sp \leq$M2.5, M2.5$< sp \leq$M5.75, and $sp \geq$M6. We exclude members that lack measured spectral types and that have photometric uncertainties greater than 0.1 mag. The positions of the known pre-transitional and transitional systems UX Tau A, LkCa 15, GM Aur, DM Tau, and CoKu Tau/4 are indicated in the color-color diagrams. Since DM Tau was not observed by MIPS, we have substituted the 25 μm measurement from IRAS.

As found in previous studies of Taurus (Skrutskie et al. 1990), the IR colors in Figures 12, 13, and 14 exhibit two distinct populations. The gap between them is larger for bands at longer wavelengths and for earlier spectral types, and is nearly absent in $K_s - [4.5]$ for late-type stars. We define the large, continuous population of red sources as primordial disks and objects within the gaps as evolved disks, transitional disks, and evolved transitional or debris disks. The approximate locations of these disks within a gap are indicated in Figure 12. The colors in which a transitional disk can be distinguished from the primordial population depends on the size of its inner hole. For instance, a disk that is primordial according to its 4.5–24 μm excesses could have a small hole that produces a deficit of excess emission only at shorter wavelengths.

---

[8] Alternatively, primordial disks can be defined to include the transitional and evolved stages, i.e., any disks that are less evolved than debris disks.

7.3. Models of Settled Disks

We have performed modeling of accretion disks with large degrees of dust settling to assess whether the sources near the bottom of the primordial populations in Figures 12–14 can be explained in terms of optically thick disks. For these calculations, we have employed models of irradiated accretion disks from D'Alessio et al. (2005, 2006). For comparison to the K5–M2 and M3–M5 populations in Taurus, we consider models for two stars that have spectral types of M0 and M4. We adopt stellar masses of 0.7 and 0.2 $M_\odot$, effective temperatures of 3850 and 3240 K, and stellar radii of 2.3 and 1.4 $R_\odot$, respectively. The model disks are composed of amorphous silicates and graphite grains with opacities and dust-to-gas mass ratios from Draine & Lee (1984). The grain size distribution follows the form $a^{-3.5}$ where a varies between a_{min} and a_{max}. The upper disk layers contain grains that are similar in size to those in the interstellar medium (i.e., a_{min}=0.005 μm and a_{max}=0.25μm). In the midplane, the maximum grain size is 1 mm. We adopt an outer disk radius of 300 AU and the inner disk edge or "wall" is located at the radius where the dust sublimation temperature (1400 K) is reached. The disks are given accretion rates of 10^{-10} $M_\odot$ yr^{-1}, a viscosity parameter (α) of 0.01, and a settling parameter (ϵ) of 0.001, where ϵ is the dust-to-gas mass ratio in the upper disk layers relative to the standard dust-to-gas mass ratio. We selected values for these parameters, particularly ϵ, that are likely to minimize the IR excess emission for comparison to the bluest primordial disks in Taurus.

The IR colors produced by our two models are shown with the data for K5–M2 and M3–M5 members of Taurus in Figures 12–14. For both ranges of spectral types, the model colors appear near the upper boundary of the gaps, indicating that the objects in the main population of disks above the gap can be interpreted as optically thick disks. Thus, the observational criteria defined in the previous section (i.e., gap boundaries) appear to be physically meaningful and consistent with the theoretical distinction between primordial disks and the later stages of disk evolution (§ 7.1). In addition, our comparison of the observed and model colors demonstrates that Taurus contains a substantial number of optically thick disks that are highly settled, which is not surprising given that $\sim 1/3$ of the members of Taurus have fully cleared their inner disks (Table 8).

7.4. New Transitional and Evolved Disks in Taurus

The SEDs of Taurus members that have transitional, evolved, and evolved transitional/debris disks according to their 4.5–24 μm colors are presented in Figures 15, 16, and 17. For reference, we include the pre-transitional systems UX Tau A and LkCa 15 in Figure 15. These SEDs consist of our 3.6–24 μm photometry from *Spitzer* and JHK_s data (1.2–2.2 μm) from the 2MASS Point Source Catalog. Since DM Tau was not observed at 24 μm by MIPS, we have used the 25 μm measurement from IRAS in its SED. The sizes of the solid points that comprise the SEDs are equivalent to ±0.12 mag. All of the measurements in these SEDs have uncertainties less than this value. To characterize the excess emission in each SED, we compare it to an estimate of the SED of the stellar photosphere, which is based on the average colors of

class III stars near the spectral type in question (§ A). We have reddened the photospheric SEDs by combining the extinction estimates described by Luhman et al. (2009b) with the reddening laws from Rieke & Lebofsky (1985) and Flaherty et al. (2007).

Evidence of evolved and transitional disks has been previously presented for several of the stars in Figures 15–17. CoKu Tau/4, GM Aur, and DM Tau were observed with IRS spectroscopy and the resulting data were successfully modeled in terms of disks with inner holes (D'Alessio et al. 2005; Calvet et al. 2005; Furlan et al. 2006). Similar analysis was applied to UX Tau A and LkCa 15, which show evidence of disk gaps (Furlan et al. 2006; Espaillat et al. 2007b). Furlan et al. (2006, 2009) detected excess emission longward of 12 μm in an IRS spectrum of V819 Tau. Furlan et al. (2006) also reported a tentative detection of excess emission beyond 20 μm in an IRS spectrum of V410 X-ray 3, but that excess is no longer present in a new reduction of those observations (Furlan et al. 2009). Nevertheless, we do find that V410 X-ray 3 exhibits a small excess of $\sim$ 0.4 mag at 24 μm, which is below the detection limit of the IRS data (Furlan et al. 2009). Andrews & Williams (2005) suggested that FW Tau could be a transitional disk based on a detection at submillimeter wavelengths. The spatial resolution of those observations is insufficient to determine whether the source of the submillimeter emission is the 0''08 binary FW Tau A+B or their 2''3 companion FW Tau C, which is known to have a disk (White & Ghez 2001). Although MIPS cannot fully resolve a pair with this separation, the 24 μm emission does appear to be centered on the former rather than the latter, indicating that FW Tau A+B indeed may be responsible for the submillimeter emission. If so, the disk around FW Tau A+B is an evolved transitional disk or debris disk rather than a transitional disk based on the small size of the 24 μm excess. The SED of IRAS 04125+2902 in Figure 15 was also shown in the study that confirmed its membership in Taurus (Luhman et al. 2009b). The remaining stars in Figures 15–17 have not been previously identified as having disks in advanced stages of evolution. We note that one star in Figure 17 (XEST 17-036) and the stars in Figure 17 have 24 μm excesses that are too small to be classified as class II with the II/III thresholds that were adopted in Figure 6.

Additional data are needed to definitively assess the nature of our new candidates for transitional and evolved disks. For instance, the SEDs in Figure 17 could arise from both evolved transitional disks and debris disks. When SEDs of this kind are observed for early-type stars, they are cited as convincing evidence of debris disks since the dust in an (optically thin) evolved transitional disk would be removed very quickly. However, a source of dust replenishment may not be necessary to explain the SEDs in Figure 17 since the dust removal timescale is roughly comparable to the age of Taurus for low-mass stars (Backman & Paresce 1993; Currie et al. 2009b). Because debris disks are depleted of gas, measurements that trace gas can help distinguish between debris disks and evolved transitional disks. The strengths of the Hα emission lines from the candidate evolved transitional/debris systems do not indicate the presence of active accretion, and thus allow

for the possibility of gas depletion (Strom et al. 1989; Kenyon et al. 1998; White & Ghez 2001; Muzerolle et al. 2003; Luhman 2004b; Luhman et al. 2009b).

Binarity also is relevant to the interpretation of our candidates. Excess emission that appears only at longer wavelengths can arise from the disk of an unresolved low-mass companion rather than from a disk with an inner hole. Even if the latter is present, the inner truncation of the disk may be caused by interactions with a stellar companion rather than processes associated with disk evolution (Guenther et al. 2007; Ireland & Kraus 2008). Multiplicity measurements are required to address these possibilities. Finally, millimeter and submillimeter observations would be valuable for verifying the presence of disks for the stars with the smallest 24 μm excesses (Andrews & Williams 2005) and for resolving inner holes (Brown et al. 2008; Dutrey et al. 2008; Hughes et al. 2007, 2009) while mid-IR spectroscopy would provide the high-resolution SEDs that are necessary for detailed modeling of the disks (Calvet et al. 2005; D'Alessio et al. 2005; Espaillat et al. 2007b).

As with V819 Tau and V410 X-ray 3, Furlan et al. (2006) found excess emission at long wavelengths in their IRS spectrum of HBC 427. However, they suggested that a star at a distance of 15″ from HBC 427 may have contributed light into the IRS slit during the observations of HBC 427, resulting in a spurious excess. To assess this possibility, we have inspected the MIPS 24 μm images of HBC 427. We find that the nearby star cited by Furlan et al. (2006) is sufficiently faint and well-resolved that it probably did not contaminate the IRS spectrum of HBC 427. However, another object that is 9″ from HBC 427, corresponding to HBC 427/1 from Massarotti et al. (2005), is ∼ 1.3 mag brighter than HBC 427 at 24 μm and very likely is the source of the apparent excess emission in the IRS data. This conclusion is supported by the fact that our 24 μm photometry of HBC 427 does not exhibit excess emission. The contaminating source is probably a galaxy based on its near- and mid-IR colors. Furlan et al. (2009) arrived at the same conclusion through analysis of the MIPS data as well as peak-up images from IRS.

7.5. *Comparison to Clusters at 2–10 Myr*

Imaging with the *Spitzer Space Telescope* has been widely used to classify the evolutionary stages of disks in nearby clusters and associations. We can apply the observational criteria developed for Taurus to these populations to provide the uniformly-derived classifications that are necessary for meaningful comparisons among them. We have selected clusters and associations that were observed with both IRAC and MIPS down to spectral types of ∼M2 ($M \sim 0.5\ M_\odot$) and that are older than Taurus but within the era of primordial disks ($\tau \sim$ 2–10 Myr). For each region, we will plot $K_s - [5.8]$ and $K_s - [8.0]$ versus $K_s - [24]$ for spectral types of K5–M2 and M3–M5. The *Spitzer* data for a few clusters do not reach the latter range of types. We begin by showing the colors for the class II and class III sources in Taurus in the same format in Figure 18. We have defined boundaries in Figure 18 that follow the upper edges of the color gaps in Taurus, which will be used for identifying transitional and evolved disks in the other clusters. We find that the same boundaries are adequate

for the two ranges of spectral types. These boundaries are defined as lines connecting $(K_s - [5.8], K_s - [8.0], K_s - [24]) = (1, 1.55, 3.4), (0.7, 1.15, 4.1)$, and $(0.7, 1.15, 6)$.

7.5.1. *Chamaeleon I*

The dereddened values of $K_s - [5.8]$, $K_s - [8.0]$, and $K_s - [24]$ for K5–M2 and M3–M5 members of Chamaeleon I ($\tau \sim$ 2–3 Myr, Luhman 2007) are plotted in Figure 19. The *Spitzer* data are from Luhman et al. (2008a) and Luhman & Muench (2008) and the extinction estimates that were used for dereddening the colors are from Luhman (2007) and Luhman & Muench (2008). We adopt the K_s data from 2MASS and Luhman (2007). As shown in Figure 19, the distribution of colors in Chamaeleon I closely resembles that in Taurus. The same gap in colors is present in both regions. Several stars below the boundaries in Figure 19 have been previously recognized as possible transitional systems, consisting of CS Cha, T35, C7-1, CHXR 22E, CHXR 71, and CHXR 76 (Takami et al. 2003; Damjanov et al. 2007; Espaillat et al. 2007a; Luhman et al. 2008a; Kim et al. 2009). Using our terminology (§ 7.1, Figure 12) and the colors in Figure 19, we classify CS Cha, T35, and CHXR 22E as transitional disks, C7-1 and CHXR 71 as evolved disks, and CHXR 76 as an evolved transitional disk or a debris disk. In addition, we identify CHSM 9484 as a new candidate for an evolved disk. The ratio of the number of transitional and evolved disks to the number of primordial disks in Figure 19 is 7/56, which is similar to the value of 15/98 in Taurus for K5–M5. SZ Cha, T21, T25, T54, and T56 also exhibit evidence of transitional disks (Kim et al. 2009), but are absent from Figure 19 because measurements with IRAC or MIPS are unavailable, or they have spectral types earlier than K5.

7.5.2. *IC 348*

The dereddened colors for K5–M2 and M3–M5 members of IC 348 ($\tau \sim$ 2–3 Myr, Luhman et al. 2003b) are shown in Figure 20. The *Spitzer* measurements and extinction estimates are from Lada et al. (2006), Muench et al. (2007), and Currie et al. (2009b) and the K_s data are from 2MASS. The sensitivity of the 24 μm images of IC 348 is lower than that in Taurus and Chamaeleon I because of brighter background emission. As a result, those images do not detect most of the stellar photospheres for spectral types later than K5, making it more difficult to characterize the distribution of colors. However, the available data that are shown in Figure 20 are consistent with the presence of a gap in colors that is similar to the ones observed in Taurus and Chamaeleon I. According to Figure 20, sources 67, 72, 133, and 190 from Luhman et al. (2003b) have transitional disks and source 176 from that study has an evolved disk. Source 72 was previously noted as a possible transitional disk by Lada et al. (2006). Several additional stars appear below the boundaries in Figure 20, but their candidacy as evolved disks or transitional disks is questionable since the uncertainties in their 24 μm data are large (0.1–0.5 mag, Currie et al. 2009b). Currie et al. (2009b) suggested that the frequency of transitional and evolved disks is higher in IC 348 than in Taurus. However, we find that the frequencies are consistent with each other when we apply the same observational criteria to both regions. For instance, even if the IC 348 members

with uncertain 24 μm photometry are included, the ratio of the number of transitional and evolved disks to the number of primordial disks is 15/98 in Taurus and 20/83 in IC 348 for spectral types of K5–M5 based on the thresholds adopted in Figure 20.

7.5.3. σ Ori

For the σ Ori cluster ($\tau \sim 3$ Myr, Hernández et al. 2007a, references therein), we have adopted the membership list that was compiled by Luhman et al. (2008b). The colors measured in that study and by 2MASS for K5–M2 and M3–M5 stars are plotted in Figure 21. We have not corrected the colors for extinction since the cluster exhibits little reddening. Since many members of σ Ori have not been spectroscopically classified, we assume that stars with $2.1 < V - J < 3.5$ and $3.5 \leq V - J < 5.7$ have types of K5–M2 and M3–M5, respectively. For stars that lack V-band measurements, we apply criteria of $J - K_s > 0.7$ and $J < 11.7$ for K5–M2 and $J - K_s > 0.7$ and $11.7 \leq J < 14.5$ for M3–M5. We adopt measurements of V and J from Hernández et al. (2007a) and 2MASS, respectively.

The distribution of colors in Figure 21 for σ Ori is similar to that of Taurus, showing a prominent gap between stellar photospheres and the main population of disks. Our classifications of transitional and evolved disks differ from those of Hernández et al. (2007a) in only a few cases. Hernández et al. (2007a) classified sources 540 and 1156 from their study as class II while we identify them as possible transitional disks based on Figure 21. Inspection of the SEDs of these stars from Hernández et al. (2007a) tends to confirm our designations. Sources 615, 818, and 1267 appear above our adopted thresholds in Figure 21 but were listed as evolved or transitional systems by Hernández et al. (2007a). The latter two stars exhibit color excesses in all of the IRAC bands relative to the K_s but not in $[3.6] - [4.5]$ and $[4.5] - [5.8]$, which can be explained by variability between the 2MASS and $Spitzer$ observations. Thus, these two stars probably do have transitional disks as found by Hernández et al. (2007a).

7.5.4. Tr 37

For Trumpler 37 (Tr 37, $\tau \sim 4$ Myr, Sicilia-Aguilar et al. 2005), we have adopted the membership list, extinction estimates, and spectral types that were presented by Sicilia-Aguilar et al. (2005), the $Spitzer$ photometry measured by Sicilia-Aguilar et al. (2006), and the K_s data from 2MASS. The dereddened colors for K5–M2 members of Tr 37 are shown in Figure 22. We have omitted stars for which extinctions were not estimated by Sicilia-Aguilar et al. (2005).

The data in Figure 22 are incomplete at bluer colors because of the detection limit of the 24 μm image, which does not reach stellar photospheres between K5 and M2. Nevertheless, the available colors are consistent with a gap between primordial disks and photospheres that is similar to the one in Taurus. Sicilia-Aguilar et al. (2006) suggested that the median SED for stars with disks in Tr 37 exhibits less excess emission than the median SED in Taurus. However, we find that the median SEDs do not differ significantly when we utilize our photometry in Taurus. For instance, the dereddened colors for class II K5–M2 stars have median values of $K_s - [5.8] = 1.38$ and

1.50, $K_s - [8.0] = 2.20$ and 2.06, and $K_s - [24] = 5.16$ and 5.11 for Taurus and Tr 37, respectively.

Sicilia-Aguilar et al. (2006) defined transitional objects as stars that have photospheric colors at $\lambda \leq 4.5$ μm and excess emission at longer wavelengths. They identified as many as 14 sources of this kind in Tr 37. Eleven of these stars were not detected at 24 μm and one additional star is outside of the range of spectral types that we are considering. As a result, these 12 sources are absent from Figure 22. Among the remaining two candidate transitional disks from Sicilia-Aguilar et al. (2006), we classify one as a primordial disk (14-11) and the other as a transitional disk (13-52) based on our adopted criteria.

7.5.5. NGC 2362

For NGC 2362 ($\tau \sim 5$ Myr, Balona & Laney 1996; Moitinho et al. 2001; Dahm 2005; Mayne & Naylor 2008), we have used the spectral types measured by Dahm (2005) and estimated from colors by Currie et al. (2009a), the IRAC and MIPS photometry from Currie et al. (2009a), and the K_s photometry from 2MASS. The IRAC data from Currie et al. (2009a) are similar to those measured from the same images by Dahm & Hillenbrand (2007). Before using these data for our color-color diagrams, we inspected the 24 μm images from MIPS for the faintest detections that were presented by Currie et al. (2009a). In contrast to Currie et al. (2009a), we find that source 1091 from Irwin et al. (2008) was not detected in the MIPS images. The nearest intensity peak in the MIPS data is $\sim 3\farcs5$ from the optical and IRAC coordinates of 1091, which is too far to correspond to a 24 μm counterpart. We also find that source 663 from Irwin et al. (2008) was not detected by MIPS. Sources 809 and 931 from Irwin et al. (2008) and sources 41 and 63 from Dahm & Hillenbrand (2007) were detected with signal-to-noise ratios of $\lesssim 2$–3, which is too low for useful photometry. We exclude from our analysis the 24 μm measurements for these six stars that were reported by Currie et al. (2009a). After doing so, there remain 29 stars that were found to have disks by Dahm & Hillenbrand (2007) and Currie et al. (2009a) and that have 24 μm photometry. The colors of the 25 stars between K5 and M2 are plotted in Figure 22. We have not corrected the colors for reddening since little extinction is present in NGC 2362 ($A_V < 1$, Moitinho et al. 2001). The four disk-bearing stars outside of the range K5–M2 consist of one K3 star and three M3 stars. We classify the former as a transitional disk and the latter stars as primordial disks with our criteria developed for Taurus. We include the classifications of these four stars with those of the K5–M2 stars in the statistics that we are about to describe.

Sixteen of the 47 disk-bearing stars that were identified by Dahm & Hillenbrand (2007) have 24 μm photometry. These MIPS-detected sources consist of 11 primordial disks and five weak (evolved) disks according to the criteria adopted by Dahm & Hillenbrand (2007). Currie et al. (2009a) classified only four of the 16 disks as primordial, suggesting that Dahm & Hillenbrand (2007) overestimated the number of primordial disks. In comparison, we classify 15 of these disks as primordial since they appear above the boundaries indicated in Figure 22 and thus fall within the region inhabited by the main

population of disks in Taurus.

Currie et al. (2009a) presented a sample of 35 stars with MIPS photometry and detections of disks, which they classified as six primordial disks, 17 homologously-depleted (evolved) disks, and 12 transitional disks. Among the latter two categories, we find that six stars have unreliable MIPS photometry (see above) and nine stars appear above both of our thresholds for primordial disks in Figure 22. Currie et al. (2009a) underestimated the number of primordial disks because they defined these disks to be close to the median SED of disks in Taurus without accounting for the spread in the colors of the Taurus disks.

As seen in a comparison of Figures 18 and 22, the primordial disk population in NGC 2362 is weighted more heavily toward bluer colors, or flatter disks, than the primordial disks in Taurus. This feature suggests the youngest members of NGC 2362 are old enough that most of them have already evolved from flared disks to settled disks. In other words, if the reddest (and youngest) primordial disks in Taurus were removed from Figure 18, the resulting distribution of colors would resemble the distribution in NGC 2362. The similarity in those distributions of colors extends to the evolved and transitional regime. For instance, the ratio of the number of evolved and transitional disks to the number of flat primordial disks ($K_s - [8.0] < 2$, $K_s - [5.8] < 1.4$) in NGC 2362 (7/16) does not differ significantly from the value in Taurus (7/22) for the range of spectral types in the NGC 2362 sample of disks (K4.5–M3).

Currie et al. (2009a) concluded that the ratio of evolved and transitional disks to all primordial disks is much higher in NGC 2362 than in Taurus, which they interpreted as evidence for a long timescale for the evolved/transitional phases (§ 7.6). However, that ratio is only meaningful if the rate of star formation has been roughly constant from the earliest point at which stars enter the class II stage (reddest and most flared disks) through the evolved and transitional stages. In other words, without ongoing star formation in a cluster, the ratio of evolved/transitional disks to primordial disks will naturally increase over time as the supply of primordial disks is exhausted. It is clear that star formation is not continuing at a constant rate in NGC 2362 based on the paucity of red primordial disks in Figure 22 and the positions of cluster members on the color-magnitude diagram from Moitinho et al. (2001). The appropriate metric for comparing two clusters with different star formation histories is the number ratio of evolved/transitional disks to stars in the stage immediately preceding stage, i.e., primordial disks that have experienced large degrees of dust settling, which is the ratio that we employed in the previous paragraph. In addition, Currie et al. (2009a) counted as evolved/transitional disks the six stars that we excluded because of questionable MIPS detections, and they did not apply the same observational criteria for evolved, transitional, and primordial disks to both NGC 2362 and Taurus, making their comparison of the two populations less reliable.

7.5.6. γ Velorum, 25 Ori, and Orion OB1b

For the γ Velorum, 25 Ori, and Orion OB1b stellar populations ($\tau \sim 5$, 7–10, and 5 Myr, Briceño et al. 2007; Hernández et al. 2008), we have adopted the *Spitzer* pho-

tometry from Hernández et al. (2007b, 2008) and the K_s data from 2MASS. We have used the spectral types measured by Briceño et al. (2005, 2007) and Downes et al. (2008) when possible, and otherwise estimated them from $V - J$ using V data from Hernández et al. (2007b, 2008) and J photometry from 2MASS. The colors for K5–M2 and M3–M5 members of the three populations are presented in Figures 23 and 24. We have not dereddened the colors since these stars exhibit little extinction ($A_V < 1$, Pozzo et al. 2000; Briceño et al. 2005; Hernández et al. 2006).

Like NGC 2362, the primordial disks in γ Velorum are dominated by bluer, flatter disks. The number ratio of transitional and evolved disks to those flatter disks (4/7) is consistent with the one described in § 7.5.5 for Taurus. The classifications based on our adopted criteria agree with those of Hernández et al. (2008) with the exception of sources 115 and 414 from that study. These stars appear on or above the lower boundaries for primordial disks in Figure 23 while Hernández et al. (2008) classified them as evolved disks.

The samples of disks in 25 Ori and OB1b are too small for quantitative comparisons to Taurus. In both samples, a majority of the disks are primordial. We classify source 905 from Hernández et al. (2007b) as a primordial disk since it is slightly above the boundaries in Figure 23 while Hernández et al. (2007b) classified it as an evolved disk. Similarly, source 585 was listed as a transitional disk by Hernández et al. (2007b), but its 5.8 μm excess is slightly too large to satisfy our adopted criteria for this category. Our remaining classifications in 25 Ori and OB1b agree with those of Hernández et al. (2007b). One of the transitional disks in 25 Ori, source 1200 from Hernández et al. (2007b), has been studied in detail through IRS and Hα spectroscopy and a comparison of its SED to the predictions of disk models (Espaillat et al. 2008b).

7.5.7. η Cha

For the η Cha association ($\tau \sim 6$ Myr, Mamajek et al. 1999; Lawson et al. 2001; Luhman & Steeghs 2004), we have adopted the spectral types from Luhman & Steeghs (2004), the IRAC photometry from Megeath et al. (2005), and the K_s photometry from 2MASS. Gautier et al. (2008) and Sicilia-Aguilar et al. (2009) presented 24 μm photometry based on the same MIPS images of η Cha. Sicilia-Aguilar et al. (2009) noted a systematic difference between the data from the two studies. After reducing those images with the methods that were employed for Taurus, we arrive at photometry that is an average of 0.1 mag brighter and 0.05 mag fainter than the measurements from Gautier et al. (2008) and Sicilia-Aguilar et al. (2009), respectively. In addition, we have measured photometry from all other MIPS images of η Cha, which were obtained through *Spitzer* programs PID=40, 84, 173, and 50316. We present our 24 μm measurements in § A and adopt them for our analysis of η Cha, using the weighed average for each star that was observed more than once. The colors for K5–M2 and M3–M5 members of the association are shown in Figure 24. No correction for reddening has been applied to these data ($A_V < 1$, Luhman & Steeghs 2004). Because of their close proximity to the Sun ($d \sim 100$ pc, Mamajek et al. 1999), all of the members of η Cha that

were within the 24 μm images were detected in those data. As a result, the distributions of colors in Figure 24 do not suffer from incompleteness among the stellar photospheres, although they are poorly sampled because of the small size of the association.

Through analysis of their IRAC data, Megeath et al. (2005) found that six members of η Cha have excess emission at 8 μm. Four of these stars (M4–M5.75) exhibit little or no excess at $\lambda < 6$ μm, which Megeath et al. (2005) interpreted as evidence of inner holes. The resulting number ratio of transitional disks to all disks with 8 μm excesses (4/6) appeared to differ significantly from that in Taurus. However, through our full census of disks in Taurus, we find that three of the four stars cited as transitional disks in η Cha have colors that fall within the main population of disks in Taurus, as demonstrated by a comparison of Figures 18 and 24, and that can be explained in terms of optically thick disks with large degrees of dust settling (§ 7.3, Ercolano et al. 2009). Only one of these stars, RECX-5, qualifies as a transitional disk based on our adopted criteria.

Sicilia-Aguilar et al. (2009) studied the disk population in η Cha by combining the IRAC data with MIPS photometry and IRS spectroscopy. They identified four stars (M1.75–M4.5) that have photospheric colors at $\lambda < 6$ μm and excess emission at longer wavelengths. Two of these disks were classified as transitional by Megeath et al. (2005) while the remaining two stars lack excesses in any of the IRAC bands. For low-mass stars, Sicilia-Aguilar et al. (2009) suggested that the absence of excess emission at $\lambda < 6$ μm indicates that the disk has an inner hole, or perhaps is relatively flat (Ercolano et al. 2009). In either case, Sicilia-Aguilar et al. (2009) advocated for the classification of these disks as transitional. The resulting number ratio of transitional disks to all disks with 24 μm excesses (4/8) appeared to be much larger than the value in Taurus. As a result, Sicilia-Aguilar et al. (2009) concluded that the transitional phase is not rapid relative to the lifetimes of primordial disks.

As discussed in § 7.1, transitional objects were originally defined as stars whose colors appear within a gap between stellar photospheres and most stars with disks in Taurus. These sources were interpreted as disks in which the dust in the inner regions is optically thin or completely cleared. The criterion for transitional disks proposed by Sicilia-Aguilar et al. (2009) for low-mass stars — an absence of excess emission at $\lambda < 6$ μm — does not satisfy either of these observational and theoretical definitions since it encompasses stars that are within the main population of disks in Taurus in terms of their IR colors, and since those colors can be explained with optically disks, as shown in § 7.3 and Figures 12–14. Furthermore, because the definition of transitional disks from Sicilia-Aguilar et al. (2009) included flat optically thick disks, it does not provide a measurement of the timescale of inner disk clearing.

When we apply our classification criteria to the data for η Cha in Figure 24, we find that the association contains five primordial disks, one transitional disk, and two stars that have weak excess emission at 24 μm, indicating the presence of either evolved transitional disks or debris disks. As done for NGC 2362 (§ 7.5.5), we compare η Cha to Taurus in terms of their number ratios of

evolved and transitional disks to the bluest and flattest of the primordial disks. For spectral types of K5 to M5, this ratio is (1–3)/4 for η Cha and (11–15)/43 for Taurus, where the range of values for each numerator corresponds to the uncertainty in the nature of the disks with weak 24 μm emission. These ratios are consistent with each other within the statistical uncertainties.

7.5.8. *Upper Sco*

For the Upper Sco association ($\tau \sim 5$ Myr, Preibisch & Mamajek 2008), we have adopted the *Spitzer* photometry from Carpenter et al. (2006, 2009), the K_s data from 2MASS, and the compilation of spectral types and extinctions from Carpenter et al. (2009). The *Spitzer* observations were performed at 4.5, 8.0, and 24 μm and did not include 3.6 and 4.5 μm. The dereddened values of $K_s - [8.0]$ and $K_s - [24]$ for K5–M2 and M3–M5 members of Upper Sco are plotted in Figure 25. We have omitted sources that have questionable 24 μm data according to Carpenter et al. (2009).

Because of the close proximity of Upper Sco ($d \sim 145$ pc, Preibisch & Mamajek 2008), the 24 μm images were able to detect the stellar photospheres of a large number of low-mass stars. Like Taurus and the other young populations that we have examined, Upper Sco exhibits a distinct gap between stellar photospheres and redder sources. Our classification criteria suggest that the following seven stars between K5 and M5 have disks that are evolved or transitional: [PBB2002] USco J155729.9−225843, [PBB2002] USco J160525.5−203539, [PBB2002] USco J160600.6−195711, [PBB2002] USco J160622.8−201124, [PBB2002] USco J160643.8−190805, [PBB2002] USco J160827.5−194904, and ScoPMS 31. Carpenter et al. (2009) identified 10 additional K5–M5 stars with smaller 24 μm excesses that are candidates for debris disks (see Figure 25). Given that the excesses in these latter sources could also arise from evolved transitional disks, the ratio of the number of evolved and transitional disks to the number of relatively flat primordial disks ($K_s - [8.0] < 2$, § 7.5.5) is 7–17/12. This ratio is higher than the value of 11–15/43 for Taurus, although they are consistent within the statistical errors. A higher ratio in Upper Sco could be explained by a star formation history that is not uniform across the phases represented in the numerator and denominator (§ 7.5.5). In other words, if the youngest members of Upper Sco are old enough to have begun clearing their disks, then one would expect a ratio of transitional/evolved disks to primordial disks that is larger than that in Taurus.

7.6. *Timescale of Disk Clearing*

The frequency of evolved and transitional disks provides a constraint on the timescale of the clearing of optically thick disks. Based on the small number of transitional disks in Taurus, Skrutskie et al. (1990) concluded that this process occurs rapidly. By combining a value of 3/30 for the number ratio of transitional disks to primordial disks with an average lifetime of ~ 3 Myr for primordial disks, they estimated a timescale of ~ 0.3 Myr for the transitional phase. Other studies of Taurus have arrived at even shorter timescales ($\tau \lesssim 0.1$ Myr, Simon & Prato 1995; Wolk & Walter 1996). Using our classifications of the *Spitzer* data in Taurus, we find that the number ratio of evolved and transitional disks to primordial disks

is 15/98 for spectral types of K5–M5. Thus, we derive a somewhat longer timescale of ~ 0.45 Myr, assuming a primordial disk lifetime of 3 Myr. We have overestimated this timescale if some of the stars with weak 24 μm emission have debris disks rather than evolved transitional disks, or if stellar companions are responsible for the inner holes in some of the transitional disks (CoKu Tau/4, Ireland & Kraus 2008).

The timescale of disk clearing has been investigated further through the *Spitzer* observations of older clusters that were described in § 7.5. Some of those studies have concluded that the frequency of evolved and transitional disks is much higher in older clusters than in Taurus, implying a timescale for this phase that is longer than previous estimates (Currie et al. 2009a; Sicilia-Aguilar et al. 2009). However, in our analysis of the two clusters in question, NGC 2362 and η Cha (§ 7.5.5, § 7.5.7), we found that Currie et al. (2009a) and Sicilia-Aguilar et al. (2009) overestimated the number of evolved and transitional disks because they adopted criteria that encompassed optically thick disks that are relatively flat. In addition, when computing the frequencies of evolved and transitional disks in NGC 2362 and η Cha for comparison to Taurus, Currie et al. (2009a) and Sicilia-Aguilar et al. (2009) divided by the number of all primordial disks, whereas only the flatter primordial disks should have been counted given that star formation is no longer occurring in these clusters. In § 7.5.5 and § 7.5.7, we addressed these issues by applying classification criteria that exclude flat optically thick disks from the transitional stage, and by comparing the populations in terms of the ratio of evolved and transitional disks to flatter primordial disks. By doing so, we found that the frequencies of evolved and transitional disks in NGC 2362 and η Cha do not differ significantly from the value in Taurus. The other clusters that were examined in § 7.5 also exhibit distributions of color excesses that are consistent with the same timescale of disk clearing that is implied by the data in Taurus.

Based on the large frequency of evolved and transitional disks that they measured in NGC 2362, Currie et al. (2009a) concluded that the timescale of these phases may be comparable to the lifetime of primordial disks. Currie et al. (2009a) attempted to explain how the low number of evolved and transitional disks in Taurus (i.e., the gap in IR colors) is consistent with such a long lifetime for those disks. They suggested that Taurus contains few evolved and transitional disks because most disks in Taurus are too young to have evolved beyond the primordial stage. However, that hypothesis is inconsistent with the fact that a large fraction of the stellar population in Taurus (40%) has already fully cleared their disks and become class III stars (Table 8). If Taurus is old enough to have a significant number of diskless stars, then the evolved and transitional phases should be heavily populated as well if they have a long timescale.

To account for the existence of class III stars in Taurus, Currie et al. (2009a) contended that the bulk of these stars may have lost their disks through interactions with stellar companions rather than mechanisms associated with the dispersal of disks during the evolved and transitional phases. However, if disruption by companions has been the dominant mechanism for disk removal in Taurus, then the disk fraction as a function

of stellar mass should be anti-correlated with binary frequency, but this is not observed in Taurus (Figure 7; Kraus, White, & Hillenbrand 2006; Luhman et al. 2007b). In addition, according to the scenario proposed by Currie et al. (2009a), class III stars should have the same ages as class II sources in Taurus. However, class III stars are more widely distributed than members with disks (§ 5), which indicates that they are older on average. In other words, if the fundamental difference between class II and III sources is the absence or presence of tight binaries, then they should share the same spatial distribution. Overall, the suggestion that the lifetime of evolved and transitional disks is comparable to that of primordial disks is incompatible with the observed properties of stars and disks in Taurus. The same conclusion applies to other clusters that also exhibit clear evidence of a paucity of evolved and transitional disks (e.g., Chamaeleon I).

8. CONCLUSIONS

We have performed a census of the circumstellar disk population of the Taurus star-forming region ($\tau \sim 1$ Myr) using mid-IR images obtained with the *Spitzer Space Telescope*. The results of this study are summarized as follows:

1. We have analyzed nearly all images of the Taurus cloud complex at 3.6, 4.5, 5.8, 8.0, and 24 μm that were collected by *Spitzer* during its cryogen mission. The IRAC and MIPS cameras on board *Spitzer* each covered a total area 46 deg^2 and encompassed 346 and 299 members of Taurus, respectively, corresponding to 99% of the known stellar population. We have presented photometry for all members that were detected in these images.

2. We have used our mid-IR photometry in conjunction with other available observations to determine the likely evolutionary stages of all members of Taurus (classes 0–III). Stars that exhibit evidence of circumstellar envelopes in previous measurements (e.g., IRS spectra) are assigned to classes 0 and I. We have classified the remaining members of Taurus using their mid-IR SEDs, or Hα emission for the few stars that lack *Spitzer* data.

3. Based on our classifications, the disk fraction in Taurus, N(II)/N(II+III), is $\sim 75\%$ for solar-mass stars and declines to $\sim 45\%$ for low-mass stars and brown dwarfs (0.01–0.3 $M_\odot$). A similar dependence on stellar mass has been observed in Chamaeleon I (Luhman et al. 2008a). In contrast to Taurus and Chamaeleon I, IC 348 exhibits a disk fraction of only $\sim 20\%$ for solar-mass stars (Lada et al. 2006; Muench et al. 2007; Luhman et al. 2005). Given that IC 348 is roughly coeval with Chamaeleon I ($\tau \sim 2$–3 Myr), the comparison of these three regions suggests that disk lifetimes for solar-mass stars are longer in star-forming regions like Taurus and Chamaeleon I that have lower stellar densities.

4. As previously observed in Taurus (Hartmann 2002), we find that the positions of the class I and II members closely follow the distribution of

dense gas while the class III stars are more widely distributed. An analysis of the nearest neighbor distances also suggests that class II sources may have a wider distribution than class I sources, although this difference is only marginally significant. The median of the nearest neighbor distances for classes I and II is 0.15 pc, which is twice the average value in nearby star-forming clusters (Gutermuth et al. 2009).

5. Our study has produced multiple epochs of mid-IR photometry for ~ 200 members of Taurus. In these data, the mid-IR variability of class I/II sources is much greater than that of class III stars, which agrees with similar measurements with *Spitzer* in Chamaeleon I (Luhman et al. 2008a). The fraction of disk-bearing stars that are variable is higher in Taurus than in Chamaeleon I, indicating that the variability of disks decreases with age.

6. We have used our *Spitzer* photometry for the disk population in Taurus to refine the observational criteria for the evolutionary phases of disks. When plotted in terms of $K_s - [5.8]$, $K_s - [8.0]$, and $K_s - [24]$, the members of Taurus appear predominantly within two distinct groups that are well-separated from each other, as found in early mid-IR studies of Taurus (Skrutskie et al. 1990). The colors of the stars in the bluer group are consistent with stellar photospheres. We have defined the large, continuous population of much redder sources as primordial disks. Using our models of accretion disks, we have demonstrated that the colors of these primordial disks can be explained in terms of optically thick disks. The sources that fall within the gap between primordial disks and stellar photospheres are defined as evolved disks (weak excess in all bands), transitional disks (weak or no excess at $\lambda < 10$ μm, large excess at longer λ), and evolved transitional disks or debris disks (only weak 24 μm excess). We have identified 19 members of

Taurus that are candidates for disks in these later stages of disk evolution, 11 of which have not been previously recognized as such.

7. We have applied our classification criteria for disks to nearby clusters and associations with ages of 2–10 Myr that have been observed with *Spitzer*. We find that the number of evolved and transitional disks in those regions is consistent with the paucity of such disks in Taurus. Some of the sources that have been classified as evolved and transitional disks in previous *Spitzer* studies have colors that are similar to those of the bluer primordial disks in Taurus (i.e., flatter optically thick disks). The number ratio of evolved and transitional disks to primordial disks in Taurus is 15/98 for spectral types of K5–M5, indicating a timescale of inner disk clearing that is $\sim 15\%$ of the lifetime of primordial disks (~ 3 Myr). The data in Taurus and the older populations that we have examined are inconsistent with notion that the lifetime of the evolved and transitional phases (i.e., disk clearing timescale) is comparable to that of primordial disks.

APPENDIX

INFRARED COLORS OF YOUNG STELLAR PHOTOSPHERES

We have estimated the intrinsic IR colors of young stellar photospheres as a function of spectral type from K4 to L0 ($M \sim 0.01$–1 $M_\odot$). For this analysis, we examined the colors of probable members of the η Cha, ϵ Cha, and TW Hya associations (TWA, Mamajek et al. 1999; Webb et al. 1999; Lawson et al. 2002; Gizis 2002; Feigelson et al. 2003; Luhman & Steeghs 2004; Luhman 2004a; Lyo et al. 2004; Song et al. 2004; Zuckerman & Song 2004; Mamajek 2005; Scholz et al. 2005; Looper et al. 2007; Luhman et al. 2008a; Kastner et al. 2008) and young late-type dwarfs in the solar neighborhood (Kirkpatrick et al. 2006, 2008; Cruz et al. 2007, 2009). These sources should have negligible extinction ($A_V < 1$) since they are relatively nearby ($d \lesssim 100$ pc) and are not associated with molecular clouds. As a result, their observed colors should not depart from the intrinsic photospheric values unless emission from circumstellar disks is present. Although the members of embedded clusters are subject to both reddening and excess emission from disks, the bluest sources provide useful constraints on the intrinsic colors of photospheres. Taurus and Chamaeleon I are the best star-forming regions for this purpose since accurate spectral types and *Spitzer* photometry have been measured for most of their members and the census of each population is large and reaches the end of the M spectral sequence (Luhman 2007; Luhman & Muench 2008; Luhman et al. 2009b, references therein).

We have adopted measurements of J, H, and K_s from the 2MASS Point Source Catalog when they are available. For the faintest members of Chamaeleon I, we used photometry measured from deeper near-IR images that were calibrated with 2MASS sources (Luhman 2007). In the *Spitzer* bands between 3.6 and 24 μm, we have used our photometry in Taurus and our previous measurements for Chamaeleon I (Luhman et al. 2008a; Luhman & Muench 2008), ϵ Cha (Luhman et al. 2008a), and young late-type dwarfs (Luhman et al. 2009b). We have analyzed all *Spitzer* images of η Cha, TWA, and additional members of ϵ Cha with the same methods that we have applied to Taurus. The resulting photometry for the members of these associations is presented in Tables 9–12. Stars that were not observed by either

IRAC or MIPS are excluded from these tabulations.

The IR colors for Taurus, Chamaeleon I, η Cha, ϵ Cha, TWA, and young dwarfs are plotted as a function of spectral type in Figure 26. The limits of these diagrams encompass only the bluest colors since we wish to examine the colors of the stellar photospheres. As a result, many of the stars with disks are too red to appear in Figure 26, particularly in the colors at longer wavelengths. The spectral types that we have measured in TWA from unpublished spectra are a few subclasses later than some of the classifications from previous studies. Therefore, we have plotted only the TWA members for which we have measured types, or that have been classified with similar methods (Looper et al. 2007; Herczeg et al. 2009). We also have excluded measurements that have photometric uncertainties greater than 0.1 mag. Few of the class III sources at the latest types have accurate 24 μm data. To help constrain the photospheric colors at those types, we have measured IRAC and MIPS photometry for field dwarfs from M9–L0 and have included them in the diagram for $[8.0] - [24]$. These stars consist of BRI 0021$-$0214, LHS 2065, LP944$-$20, LHS 2924, and 2MASS J07464256+2000321. The $[8.0] - [24]$ color of the TWA brown dwarf 2MASSW J1139511$-$315921 (M8.5) is similar to colors of these fields dwarfs, which illustrates the absence of 24 μm excess emission from this object that was discussed by Morrow et al. (2008).

For each IR color, we have estimated the photospheric values as a function of spectral type by performing a fit to the sequence of class III objects from the young associations and the solar neighborhood. This fit was also constrained to agree with the blue envelope of colors from Taurus and Chamaeleon I. These color relations are plotted in Figure 26 and are presented in Table 13.

<div align="center">REFERENCES</div>

Adams, F. C., Lada, C. J., & Shu, F. H. 1987, ApJ, 571, 378

Allen, L. E., et al. 2004, ApJS, 154, 363

André, P., Motte, F., Bacmann, A. 1999, ApJ, 513, L57

André, P., Ward-Thompson, D., & Barsony, M. 1993, ApJ, 406, 122

Andrews, S. M., & Williams, J. P. 2005, ApJ, 631, 1134

Backman, D., & Paresce, F. 1993, Protostars and Planets III, ed. E. H. Levy, J. I. Lunine (Tucson, AZ: Univ. Arizona Press), 1253

Balona, L. A., & Laney, C. D. 1996, MNRAS, 281, 1341

Baraffe, I., Chabrier, G., Allard, F., & Hauschildt, P. H. 1998, A&A, 337, 403

Barrado y Navascués, D., et al. 2007, ApJ, 664, 481

Beck, T. L. 2007, AJ, 133, 1673

Beichman, C. A., Myers, P. C., Emerson, J. P., Harris, S., Mathieu, R., Benson, P. J., & Jennings, R. E. 1986, ApJ, 307, 337

Bontemps, S., André, P., Terebey, S., & Cabrit, S. 1996, A&A, 311, 858

Bourke, T. L., et al. 2006, ApJ, 649, L37

Briceño, C., Calvet, N., Hernández, J., Vivas, A. K., Hartmann, L., Downes, J. J., & Berlind P. 2005, AJ, 129, 907

Briceño, C., Hartmann, L., Hernandez, J., Calvet, N., Katherina Vivas, A., Furesz, G., & Szentgyorgyi, A. 2007, ApJ, 661, 1119

Briceño, C., Hartmann, L., Stauffer, J., & Martín, E. L., 1998, AJ, 115, 2074

Briceño, C., Luhman, K. L., Hartmann, L., Stauffer, J. R., & Kirkpatrick, J. D. 2002, ApJ, 580, 317

Brown, J. M., Blake, G. A., Qi, C., Dullemond, C. P., & Wilner, D. J. 2008, ApJ, 675, L109

Burgasser, A. J., Kirkpatrick, J. D., Reid, I. N., Brown, M. E., Miskey, C. L., & Gizis, J. E. 2003, ApJ, 586, 512

Calvet, N., et al. 2005, ApJ, 630, L185

Carpenter, J. M., Mamajek, E. E., Hillenbrand, L. A., & Meyer, M. R. 2006, ApJ, 651, L49

Carpenter, J. M., Mamajek, E. E., Hillenbrand, L. A., & Meyer, M. R. 2009, ApJ, 705, 1646

Chabrier, G., Baraffe, I., Allard, F., & Hauschildt, P. 2000, ApJ, 542, L119

Chen, H., Myers, P. C., Ladd, E. F., & Wood, D. O. S. 1995, ApJ, 445, 377

Covino, E., Alcalá, J. M., Allain, S., Bouvier, J., Terranegra, L., & Krautter, J. 1997, A&A, 328, 187

Cowley, A. 1972, AJ, 77, 750

Cruz, K. L., Kirkpatrick, J. D., & Burgasser, A. J. 2009, AJ, 137, 3345

Cruz, K. L., et al. 2007, AJ, 133, 439

Currie, T., & Kenyon, S. J. 2009b, AJ, 138, 703

Currie, T., Kenyon, S. J., Balog, Z., Rieke, G., Bragg, A., & Bromley, B. 2008, ApJ, 672, 558

Currie, T., Lada, C. J., Plavchan, P., Robitaille, T. P., Irwin, J., & Kenyon, S. J. 2009a, ApJ, 698, 1

Dahm, S. E. 2005, AJ, 130, 1805

Dahm, S. E., & Hillenbrand, L. A. 2007, AJ, 133, 2072

D'Alessio, P., Calvet, N., Hartmann, L., Franco-Hernández, R., & Servín, H. 2006, ApJ, 638, 314

D'Alessio, P., et al. 2005, ApJ, 621, 461

Damjanov, I., Jayawardhana, R., Scholz, A., Ahmic, M., Nguyen, D. C., et al. 2007, ApJ, 670, 1337

Dobashi, K., Uehara, H., Kandori, R., Sakurai, T., Kaiden, M., Umemoto, T., & Sato, F. 2005, PASJ, 57, 1

Downes, J. J., Briceño, C., Hernández, J., Calvet, N., Hartmann, L., & Balaguer, E. P. 2008, AJ, 136, 51

Draine, B. T. & Lee, H. M. 1984, ApJ, 285, 89

Duchêne, G., Bouvier, J., Bontemps, S., André, P., & Motte, F. 2004, A&A, 427, 651

Duchêne, G., Monin, J.-L., Bouvier, J., & Ménard, F. 1999, A&A, 351, 954

Dunham, M. M., et al. 2006, ApJ, 651, 945

Dutrey, A., et al. 2008, A&A, 490, L15

Engelbracht, C. W., et al. 2007, PASP, 119, 994

Ercolano, B., Clarke, C. J., & Robitaille, T. P. 2009, MNRAS, 394, L141

Espaillat, C., Calvet, N., Luhman, K. L., Muzerolle, J., & D'Alessio, P. 2008a, ApJ, 682, L125

Espaillat, C., et al. 2007a, ApJ, 664, L111

Espaillat, C., et al. 2007b, ApJ, 670, L135

Espaillat, C., et al. 2008b, ApJ, 689, L145

Evans, N. J., II, et al. 2009, ApJS, 181, 321

Fazio, G. G., et al. 2004, ApJS, 154, 10

Feigelson, E. D., Lawson, W. A., & Garmire, G. P. 2003, ApJ, 599, 1207

Flaherty, K. M., Pipher, J. L., Megeath, S. T., Winston, E. M., Gutermuth, R. A., Muzerolle, J., Allen, L. E., & Fazio, G. G. 2007, ApJ, 663, 1069

Forrest, W. J., et al. 2004, ApJS, 154, 443

Furlan, E., et al. 2006, ApJS, 165, 568

Furlan, E., et al. 2008, ApJS, 176, 184

Furlan, E., et al. 2009, ApJ, 706, 1194

Gautier, T. N., III, Rebull, L. M., Stapelfeldt, K. R., & Mainzer, A. 2008, ApJ, 683, 813

Gizis, J. E. 2002, ApJ, 575, 484

Greene, T. P., Wilking, B. A., André, P., Young, E. T., & Lada, C. J. 1994, ApJ, 434, 614

Güdel, M., et al. 2007, A&A, 468, 353

Guenther, E., Esposito, M., Mundt, R., Covino, E., Alcalá, J. M., et al. 2007, A&A, 467, 1147

Guieu, S., Dougados, C., Monin, J.-L., Magnier, E. & Martín, E. L. 2006, A&A, 446, 485

Guieu, S., et al. 2007, A&A, 465, 855

Gutermuth, R. A., et al. 2008, ApJ, 674, 336

Gutermuth, R. A., et al. 2009, ApJS, 184, 18

Haisch, K. E., Lada, E. A., & Lada, C. J. 2001, ApJ, 553, L153

Hartigan, P., & Kenyon, S. J. 2003, ApJ, 583, 334

Hartigan, P., Strom, K. M., & Strom, S. E. 1994, ApJ, 427, 961

Hartmann, L. 2002, ApJ, 578, 914

Hartmann, L., Megeath, S. T., Allen, L., Luhman, K., Calvet, N., D'Alessio, P., Franco-Hernandez, R., & Fazio, G. 2005, ApJ, 629, 881

Herczeg, G. J., Cruz, K. L., & Hillenbrand, L. A. 2009, ApJ, 696, 1589

Hernández, J., Briceño, C., Calvet, N., Hartmann, L., Muzerolle, J., & Quintero, A. 2006, ApJ, 652, 472

Hernández, J., et al. 2007a, ApJ, 662, 1067

Hernández, J., et al. 2007b, ApJ, 671, 1784

Hernández, J., Hartmann, L., Calvet, N., Jeffries, R. D., Gutermuth, R., Muzerolle, J., & Stauffer, J. 2008, ApJ, 686, 1195

Hughes, A. M., Wilner, D. J., Calvet, N., D'Alessio, P., Claussen, M. J., & Hogerheijde, M. R. 2007, ApJ, 664, 536

Hughes, A. M., et al. 2009, ApJ, 698, 131

Ireland, M. J., & Kraus, A. L. 2008, ApJ, 678, L59

Irwin, J., et al. 2008, MNRAS, 384, 675

Kastner, J. H., Zuckerman, B., & Bessell, M. 2008, A&A, 491, 829

Kenyon, S. J., & Bromley, B. C. 2005, ApJ, 130, 269

Kenyon, S. J., Brown, D. I., Tout, C. A., & Berlind, P. 1998, AJ, 115, 2491

Kenyon, S. J., Gómez, M., Marzke, R. O., & Hartmann, L. 1994, AJ, 108, 251

Kenyon, S. J., Gómez, M., & Whitney, B. A. 2008, in Handbook of Star Forming Regions, Vol. 1, The Northern Sky, ASP Monograph Series 4, ed. B. Reipurth (San Francisco, CA: ASP), 405

Kenyon, S. J., & Hartmann, L. 1995, ApJS, 101, 117

Kenyon, S. J., Hartmann, L. W., Strom, K. M., & Strom, S. E. 1990, AJ, 99, 869

Kim, K. H., et al. 2009, ApJ, 700, 1017

Kirkpatrick, J. D., et al. 2006, ApJ, 639, 1120

Kirkpatrick, J. D., et al. 2008, ApJ, 689, 1295

Kraus, A. L., White, R. J., & Hillenbrand, L. A. 2006, ApJ, 649, 306

Lada, C. J. 1987, in IAU Symp. 115, Star Forming Regions, ed. M. Peimbert & J. Jugaku (Dordrecht: Reidel), 1

Lada, C. J., & Wilking, B. A. 1984, ApJ, 287, 610

Lada, C. J., et al. 2006, AJ, 131, 1574

Lawson, W. A., Crause, L. A., Mamajek, E. E., & Feigelson, E. D. 2001, MNRAS, 321, 57

Lawson, W. A., Crause, L. A., Mamajek, E. E., & Feigelson, E. D. 2002, MNRAS, 329, L29

Looper, D. L., Burgasser, A. J., Kirkpatrick, J. D., & Swift, B. J. 2007, ApJ, 669, L97

Luhman, K. L. 2004a, ApJ, 616, 1033

Luhman, K. L. 2004b, ApJ, 617, 1216

Luhman, K. L. 2006, ApJ, 645, 676

Luhman, K. L. 2007, ApJS, 173, 104

Luhman, K. L., Briceño, C., Stauffer, J. R., Hartmann, L., Barrado y Navascués, D., & Nelson, C. 2003a, ApJ, 590, 348

Luhman, K. L., Hernández, J., Downes, J. J., Hartmann, L., & Briceño, C. 2008b, ApJ, 688, 362

Luhman, K. L., Joergens, V., Lada, C., Muzerolle, J., Pascucci, I., & White, R. 2007b, Protostars and Planets V, B. Reipurth, D. Jewitt, and K. Keil (eds.), University of Arizona Press, Tucson, 443

Luhman, K. L., Mamajek, E. E., Allen, P. R., Muench, A. A., & Finkbeiner, D. P. 2009a, ApJ, 691, 1265

Luhman, K. L., Mamajek, E. E., Cruz, K. L., & Allen, P. R. 2009b, ApJ, 703, 399

Luhman, K. L., & Muench, A. A. 2008, ApJ, 684, 654

Luhman, K. L., & Rieke, G. H. 1998, ApJ, 497, 354

Luhman, K. L., Stauffer, J. R., Muench, A. A., Rieke, G. H., Lada, E. A., Bouvier, J., & Lada, C. J. 2003b, ApJ, 593, 1093

Luhman, K. L., & Steeghs, D. 2004, ApJ, 609, 917

Luhman, K. L., Whitney, B. A., Meade, M. R., Babler, B. L., Indebetouw, R., Bracker, S., & Churchwell, E. B. 2006, ApJ, 647, 1180

Luhman, K. L., et al. 2005, ApJ, 631, L69

Luhman, K. L., et al. 2007a, ApJ, 666, 1219

Luhman, K. L., et al. 2008a, ApJ, 675, 1375

Lyo, A.-R, Lawson, W. A., Feigelson, E. D., & Crause, L. A. 2004, MNRAS, 347, 246

Malfait, K., Bogaert, E., & Waelkens, C. 1998, A&A, 331, 211

Mamajek, E. E. 2005, ApJ, 634, 1385

Mamajek, E., Lawson, W. A., & Feigelson, E. D. 1999, ApJ, 516, 77

Mannings, V., Koerner, D. W., & Sargent, A. J. 1997, Nature, 388, 555

Mayne, N. J., & Naylor, T. 2008, MNRAS, 386, 261

Marengo, M., Megeath, S. T., Fazio, G. G., Stapelfeldt, K. R., Werner, M. W., Backman, D. E. 2006, ApJ, 647, 1437

Martín, E. L. 2000, AJ, 120, 2114

Martín, E. L., Dougados, C., Magnier, E., Ménard, F., Magazzù, A., Cuilandre, J.-C., & Delfosse, X. 2001, ApJ, 561, L195

Massarotti, A., Latham, D. W., Torres, G., Brown, R. A., & Oppenheimer, B. D. 2005, AJ, 129, 2294

Megeath, S. T., Hartmann, L., Luhman, K. L., & Fazio, G. G. 2005, ApJ, 634, L113

Megeath, S. T., et al. 2004, ApJS, 154, 367

Moitinho, A., Alves, J., Huelamo, N., & Lada, C. J. 2001, ApJ, 563, L73

Moriarty-Schieven, G. H., Butner, H. M., & Wannier, P. G. 1995, ApJ, 445, L55

Moriarty-Schieven, G. H., Wannier, P. G., Tamura, M., & Keene, J. 1992, ApJ, 400, 260

Morrow, A. L., et al. 2008, ApJ, 676, L143

Motte, F. 1998, Ph.D. Thesis, Univeristy Paris XI

Motte, F., & André, P. 2001, A&A, 365, 440

Motte, F., André, P., & Neri, R. 1998, A&A, 336, 150

Muench, A. A., Lada, C. J., Luhman, K. L., Muzerolle, J., & Young, E. 2007, AJ, 134, 411

Muzerolle, J., Hillenbrand, L., Calvet, N., Briceño, C., & Hartmann, L. 2003, ApJ, 592, 266

Najita, J. R., Strom, S. E., & Muzerolle, J. 2007, MNRAS, 378, 369

Pozzo, M., Jeffries, R. D., Naylor, T., Totten, E. J., Harmer, S., & Kenyon, M. 2000, MNRAS, 313, L23

Prato, L., Lockhart, K. E., Johns-Krull, C. M., & Rayner, J. T. 2009, AJ, 137, 3931

Preibisch, T., Brown, A. G. A., Bridges, T., Guenther, E., & Zinnecker, H., 2002, AJ, 124, 404

Preibisch, T., & Mamajek, E. 2008, in Handbook of Star Forming Regions, Vol. 2, The Southern Sky, ASP Monograph Series 5, ed. B. Reipurth (San Francisco, CA: ASP), 235

Prusti, T., Clark, F. O., Laureijs, R. J., Wakker, B. P., & Wesselius, P. R. 1992, A&A, 259, 537

Quillen, A. C., Blackman, E. G., Frank, A., & Varni'ere, P., 2004, ApJ, 612, L137

Rebull, L. M., et al. 2010, ApJS, in press

Reach, W. T., et al. 2005, PASP, 117, 978

Rice, W. K. M., Wood, K., Armitage, P. J., Whitney, B. A., & Bjorkman, J. E. 2003, MNRAS, 342, 79

Rieke, G. H., & Lebofsky, M. J. 1985, ApJ, 288, 618

Rieke, G. H., et al. 2004, ApJS, 154, 25

Rieke, G. H., et al. 2005, ApJ, 620, 1010

Scholz, R.-D., McCaughrean, M. J., Zinnecker, H., & Lodieu, N. 2005, A&A, 430, L49

Skrutskie, M. F., Dutkevitch, D., Strom, S. E., Edwards, S., Strom, K. M., & Shure, M. A. 1990, AJ, 99, 1187

Skrutskie, M., et al 2006, AJ, 131, 1163

Slesnick, C. L., Carpenter, J. M., Hillenbrand, L. A., & Mamajek, E. E. 2006, AJ, 132, 2665

Sicilia-Aguilar, A., Hartmann, L. W., Hernández, J., Briceño, C., & Calvet, N. 2005, AJ, 130, 188

Sicilia-Aguilar, A., et al. 2006, ApJ, 638, 897

Sicilia-Aguilar, A., et al. 2009, ApJ, 701, 1188

Simon, M., & Prato, L. 1995, ApJ, 450, 824

Song, I., Zuckerman, B., & Bessell, M. S. 2004, ApJ, 600, 1016

Steffen, A. T., et al. 2001, AJ, 122, 997

Strom, K. M., & Strom, S. E. 1994, ApJ, 424, 237

Strom, K. M., Strom, S. E., Edwards, S., Cabrit, S., & Skrutskie, M. F. 1989, AJ, 97, 1451

Takami, M., Bailey, J., & Chrysostomou, A. 2003, A&A, 397, 675

Tamura, M., Gatley, I., Waller, W., & Werner, M. W. 1991, ApJ, 374, L25

Torres, C. A. O., Quast, G., de La Reza, R., Gregorio-Hetem, J., Lepine, J. R. D. 1995, AJ, 109, 2146

Walter, F. M., Beck, T. L., Morse, J. A., & Wolk, S. J. 2003, AJ, 125, 2123

Watson, D. M., et al. 2004, ApJS, 154, 391

Webb, R. A., Zuckerman, B., Platais, I., Patience, J., White, R.
    J., Schwartz, M. J., & McCarthy, C. 1999, ApJ, 512, L63
Werner, M. W., et al. 2004, ApJS, 154, 1
White, R. J., & Basri, G. 2003, ApJ, 582, 1109
White, R. J., & Ghez, A. M. 2001, ApJ, 556, 265
White, R. J., Ghez, A. M., Reid, I. N., & Schultz, G. 1999, ApJ,
    520, 811

Wichmann, R., et al. 1996, A&A, 312, 439
Wolk, S. J., & Walter, F. M. 1996, AJ, 111, 2066
Zasowski, G., Kemper, F., Watson, D. M., Furlan, E., Bohac, C.
    J., Hull, C., & Green, J. D. 2009, ApJ, 694, 459
Zuckerman, B., & Song, I. 2004, ARA&A, 42, 685

TABLE 1
IRAC Observing Log

AOR	PID	Date (UT)	3.6/5.8 Center (J2000)	4.5/8.0 Center (J2000)	Dimensions (arcmin)	Angle[a] (deg)	Exp Time[b] (s)
3963904	37	2004 Feb 9	04 46 42.3 +24 58 58	04 46 42.3 +24 58 58	5.3×5.3	85.0	31.2 HDR
			04 46 46.6 +24 52 21	04 46 38.5 +25 05 43	5.3×5.3	85.0	31.2 HDR
			04 44 31.0 +25 12 21	04 44 31.0 +25 12 21	5.3×5.3	85.0	31.2 HDR
			04 44 34.9 +25 05 50	04 44 27.2 +25 19 06	5.3×5.3	85.0	31.2 HDR
			04 43 03.4 +25 20 10	04 43 03.4 +25 20 10	5.3×5.3	85.0	31.2 HDR
			04 43 07.2 +25 13 44	04 43 00.0 +25 26 56	5.3×5.3	85.0	31.2 HDR
			04 42 38.0 +25 15 29	04 42 38.0 +25 15 29	5.3×5.3	85.0	31.2 HDR
			04 42 41.4 +25 08 54	04 42 34.1 +25 22 14	5.3×5.3	85.0	31.2 HDR
			04 42 21.5 +25 20 26	04 42 21.5 +25 20 26	5.3×5.3	85.0	31.2 HDR
			04 42 24.8 +25 13 53	04 42 17.7 +25 27 11	5.3×5.3	85.0	31.2 HDR
			04 42 07.6 +25 22 53	04 42 07.6 +25 22 53	5.3×5.3	85.0	31.2 HDR
			04 42 11.2 +25 16 21	04 42 03.8 +25 29 38	5.3×5.3	85.0	31.2 HDR
			04 41 04.5 +24 51 02	04 41 04.5 +24 51 02	5.3×5.3	85.0	31.2 HDR
			04 41 08.7 +24 44 22	04 41 00.5 +24 57 46	5.3×5.3	85.0	31.2 HDR
			04 41 39.7 +25 56 17	04 41 39.7 +25 56 17	5.3×5.3	85.0	31.2 HDR
			04 41 42.4 +25 49 48	04 41 35.9 +26 03 01	5.3×5.3	85.0	31.2 HDR
			04 41 12.8 +25 46 38	04 41 12.8 +25 46 38	5.3×5.3	85.0	31.2 HDR
			04 41 17.0 +25 39 51	04 41 09.0 +25 53 22	5.3×5.3	85.0	31.2 HDR
			04 40 50.0 +25 51 18	04 40 50.0 +25 51 18	5.3×5.3	85.0	31.2 HDR
			04 40 53.4 +25 44 36	04 40 46.1 +25 58 02	5.3×5.3	85.0	31.2 HDR
3965440	37	2004 Feb 9	04 47 49.0 +29 25 09	04 47 49.0 +29 25 09	5.3×5.3	87.0	31.2 HDR
			04 47 51.2 +29 18 26	04 47 46.6 +29 31 56	5.3×5.3	87.0	31.2 HDR
			04 43 20.4 +29 40 08	04 43 20.4 +29 40 08	5.3×5.3	87.0	31.2 HDR
			04 43 23.6 +29 33 19	04 43 17.6 +29 46 54	5.3×5.3	87.0	31.2 HDR
			04 41 17.7 +28 39 50	04 41 17.7 +28 39 50	5.3×5.3	87.0	31.2 HDR
			04 41 19.7 +28 33 18	04 41 14.5 +28 46 37	5.3×5.3	87.0	31.2 HDR
3967488	37	2004 Feb 10	04 14 47.7 +26 47 22	04 14 47.7 +26 47 22	5.3×5.3	82.0	31.2 HDR
			04 14 53.2 +26 40 38	04 14 42.6 +26 54 05	5.3×5.3	82.0	31.2 HDR
3967232	37	2004 Feb 11	04 04 39.4 +21 58 22	04 04 39.4 +21 58 22	5.3×5.3	80.0	31.2 HDR
			04 04 45.9 +21 51 41	04 04 33.4 +22 05 00	5.3×5.3	80.0	31.2 HDR
3966464	37	2004 Feb 12	05 07 49.7 +30 24 07	05 07 49.7 +30 24 07	5.3×5.3	89.5	31.2 HDR
			05 07 51.3 +30 17 17	05 07 48.5 +30 30 55	5.3×5.3	89.5	31.2 HDR
3964928	37	2004 Feb 14	05 07 55.1 +25 00 03	05 07 55.1 +25 00 03	5.3×5.3	86.0	31.2 HDR
			05 07 57.7 +24 53 31	05 07 52.4 +25 06 51	5.3×5.3	86.0	31.2 HDR
			05 07 12.4 +24 37 08	05 07 12.4 +24 37 08	5.3×5.3	86.0	31.2 HDR
			05 07 15.2 +24 30 40	05 07 09.5 +24 43 54	5.3×5.3	86.0	31.2 HDR
			05 06 23.8 +24 32 17	05 06 23.8 +24 32 17	5.3×5.3	86.0	31.2 HDR
			05 06 26.4 +24 25 35	05 06 20.9 +24 39 04	5.3×5.3	86.0	31.2 HDR
			05 06 17.3 +24 46 02	05 06 17.3 +24 46 02	5.3×5.3	86.0	31.2 HDR
			05 06 19.6 +24 39 27	05 06 14.4 +24 52 48	5.3×5.3	86.0	31.2 HDR
			05 05 23.0 +25 31 34	05 05 23.0 +25 31 34	5.3×5.3	86.0	31.2 HDR
			05 05 26.1 +25 24 45	05 05 20.3 +25 38 21	5.3×5.3	86.0	31.2 HDR
			05 04 42.2 +25 09 44	05 04 42.2 +25 09 44	5.3×5.3	86.0	31.2 HDR
			05 04 44.0 +25 03 13	05 04 39.4 +25 16 30	5.3×5.3	86.0	31.2 HDR
3965696	37	2004 Feb 14	04 56 00.0 +30 33 50	04 56 00.0 +30 33 50	5.3×5.3	88.0	31.2 HDR
			04 56 01.5 +30 27 17	04 55 57.6 +30 40 37	5.3×5.3	88.0	31.2 HDR
			04 55 46.3 +30 33 03	04 55 46.3 +30 33 03	5.3×5.3	88.0	31.2 HDR
			04 55 47.9 +30 26 19	04 55 44.1 +30 39 51	5.3×5.3	88.0	31.2 HDR
			04 56 02.3 +30 20 56	04 56 02.3 +30 20 56	5.3×5.3	88.0	31.2 HDR
			04 56 03.9 +30 14 19	04 56 00.2 +30 27 44	5.3×5.3	88.0	31.2 HDR
			04 55 37.3 +30 17 47	04 55 37.3 +30 17 47	5.3×5.3	88.0	31.2 HDR
			04 55 39.6 +30 11 18	04 55 35.2 +30 24 35	5.3×5.3	88.0	31.2 HDR
			04 55 11.5 +30 21 50	04 55 11.5 +30 21 50	5.3×5.3	88.0	31.2 HDR
			04 55 13.2 +30 15 15	04 55 09.4 +30 28 38	5.3×5.3	88.0	31.2 HDR
			04 52 06.7 +30 47 20	04 52 06.7 +30 47 20	5.3×5.3	88.0	31.2 HDR
			04 52 09.3 +30 40 29	04 52 04.6 +30 54 07	5.3×5.3	88.0	31.2 HDR
			04 51 48.0 +30 47 03	04 51 48.0 +30 47 03	5.3×5.3	88.0	31.2 HDR
			04 51 49.5 +30 40 31	04 51 45.8 +30 53 50	5.3×5.3	88.0	31.2 HDR
4915200	94	2004 Feb 14	04 55 03.5 +30 31 26	04 55 01.3 +30 38 13	14.3×19.0	177.5	52 HDR
4916992	94	2004 Feb 14	05 04 24.7 +25 08 16	05 04 21.9 +25 15 02	10.3×15.0	176.0	52 HDR
4915456	94	2004 Feb 15	04 55 03.5 +30 31 26	04 55 01.3 +30 38 13	14.3×19.0	177.5	52 HDR
4917248	94	2004 Feb 16	05 04 24.7 +25 08 16	05 04 21.9 +25 15 02	10.3×15.0	176.0	52 HDR
3966720	37	2004 Mar 6	04 46 59.6 +17 00 42	04 46 59.6 +17 00 42	5.3×5.3	83.5	31.2 HDR
			04 47 04.0 +16 53 56	04 46 55.6 +17 07 27	5.3×5.3	83.5	31.2 HDR
3963392	37	2004 Mar 7	04 30 57.0 +25 56 37	04 30 57.0 +25 56 37	5.3×5.3	82.0	31.2 HDR
			04 31 02.2 +25 49 57	04 30 51.9 +26 03 18	5.3×5.3	82.0	31.2 HDR
			04 30 44.2 +26 01 23	04 30 44.2 +26 01 23	5.3×5.3	82.0	31.2 HDR
			04 30 49.5 +25 54 53	04 30 39.2 +26 08 05	5.3×5.3	82.0	31.2 HDR
			04 30 07.4 +26 08 23	04 30 07.4 +26 08 23	5.3×5.3	82.0	31.2 HDR
			04 30 12.7 +26 01 34	04 30 02.2 +26 15 05	5.3×5.3	82.0	31.2 HDR
			04 29 51.4 +26 06 41	04 29 51.4 +26 06 41	5.3×5.3	82.0	31.2 HDR
			04 29 56.7 +26 00 02	04 29 46.1 +26 13 23	5.3×5.3	82.0	31.2 HDR
			04 29 30.1 +26 16 45	04 29 30.1 +26 16 45	5.3×5.3	82.0	31.2 HDR
			04 29 35.2 +26 10 20	04 29 24.9 +26 23 26	5.3×5.3	82.0	31.2 HDR

Luhman et al.

TABLE 1 — *Continued*

AOR	PID	Date (UT)	3.6/5.8 Center (J2000)	4.5/8.0 Center (J2000)	Dimensions (arcmin)	Angle[a] (deg)	Exp Time[b] (s)
			04 29 44.1 +26 31 44	04 29 44.1 +26 31 44	5.3×5.3	82.0	31.2 HDR
			04 29 48.8 +26 25 13	04 29 38.9 +26 38 27	5.3×5.3	82.0	31.2 HDR
			04 29 20.9 +26 33 39	04 29 20.9 +26 33 39	5.3×5.3	82.0	31.2 HDR
			04 29 25.5 +26 27 00	04 29 15.7 +26 40 20	5.3×5.3	82.0	31.2 HDR
			04 29 05.1 +26 49 10	04 29 05.1 +26 49 10	5.3×5.3	82.0	31.2 HDR
			04 29 10.7 +26 42 25	04 29 00.0 +26 55 52	5.3×5.3	82.0	31.2 HDR
			04 31 14.6 +27 10 21	04 31 14.6 +27 10 21	5.3×5.3	82.0	31.2 HDR
			04 31 19.7 +27 03 37	04 31 09.5 +27 17 05	5.3×5.3	82.0	31.2 HDR
			04 27 03.1 +25 42 15	04 27 03.1 +25 42 15	5.3×5.3	82.0	31.2 HDR
			04 27 07.9 +25 35 43	04 26 57.8 +25 48 58	5.3×5.3	82.0	31.2 HDR
			04 26 59.3 +26 06 24	04 26 59.3 +26 06 24	5.3×5.3	82.0	31.2 HDR
			04 27 04.2 +25 59 57	04 26 53.9 +26 13 07	5.3×5.3	82.0	31.2 HDR
			04 27 27.7 +26 12 02	04 27 27.7 +26 12 02	5.3×5.3	82.0	31.2 HDR
			04 27 33.4 +26 05 26	04 27 22.4 +26 18 46	5.3×5.3	82.0	31.2 HDR
			04 27 58.2 +26 19 10	04 27 58.2 +26 19 10	5.3×5.3	82.0	31.2 HDR
			04 28 02.2 +26 12 41	04 27 53.0 +26 25 52	5.3×5.3	82.0	31.2 HDR
			04 26 29.4 +26 24 04	04 26 29.4 +26 24 04	5.3×5.3	82.0	31.2 HDR
			04 26 34.7 +26 17 36	04 26 24.0 +26 30 48	5.3×5.3	82.0	31.2 HDR
			04 25 17.3 +26 17 45	04 25 17.3 +26 17 45	5.3×5.3	82.0	31.2 HDR
			04 25 23.3 +26 11 12	04 25 11.9 +26 24 26	5.3×5.3	82.0	31.2 HDR
			04 24 45.1 +26 10 12	04 24 45.1 +26 10 12	5.3×5.3	82.0	31.2 HDR
			04 24 50.1 +26 03 34	04 24 39.5 +26 16 57	5.3×5.3	82.0	31.2 HDR
3963648	37	2004 Mar 7	04 40 09.7 +26 05 15	04 40 09.7 +26 05 15	5.3×5.3	82.5	31.2 HDR
			04 40 13.8 +25 58 45	04 40 05.2 +26 11 58	5.3×5.3	82.5	31.2 HDR
			04 39 50.6 +26 02 25	04 39 50.6 +26 02 25	5.3×5.3	82.5	31.2 HDR
			04 39 55.6 +25 55 40	04 39 46.0 +26 09 08	5.3×5.3	82.5	31.2 HDR
			04 39 13.7 +25 53 17	04 39 13.7 +25 53 17	5.3×5.3	82.5	31.2 HDR
			04 39 18.4 +25 46 38	04 39 09.1 +26 00 00	5.3×5.3	82.5	31.2 HDR
			04 39 21.4 +25 44 53	04 39 21.4 +25 44 53	5.3×5.3	82.5	31.2 HDR
			04 39 25.5 +25 38 21	04 39 16.9 +25 51 36	5.3×5.3	82.5	31.2 HDR
			04 39 36.0 +25 41 36	04 39 36.0 +25 41 36	5.3×5.3	82.5	31.2 HDR
			04 39 39.4 +25 35 06	04 39 31.5 +25 48 18	5.3×5.3	82.5	31.2 HDR
			04 39 56.0 +25 44 54	04 39 56.0 +25 44 54	5.3×5.3	82.5	31.2 HDR
			04 40 00.6 +25 38 28	04 39 51.5 +25 51 37	5.3×5.3	82.5	31.2 HDR
			04 38 28.7 +26 10 00	04 38 28.7 +26 10 00	5.3×5.3	82.5	31.2 HDR
			04 38 33.0 +26 03 20	04 38 24.1 +26 16 44	5.3×5.3	82.5	31.2 HDR
			04 36 19.3 +25 42 51	04 36 19.3 +25 42 51	5.3×5.3	82.5	31.2 HDR
			04 36 23.6 +25 36 19	04 36 14.6 +25 49 33	5.3×5.3	82.5	31.2 HDR
			04 33 39.0 +25 20 30	04 33 39.0 +25 20 30	5.3×5.3	82.5	31.2 HDR
			04 33 43.9 +25 13 58	04 33 34.2 +25 27 13	5.3×5.3	82.5	31.2 HDR
			04 33 54.7 +26 13 25	04 33 54.7 +26 13 25	5.3×5.3	82.5	31.2 HDR
			04 34 00.0 +26 06 55	04 33 49.8 +26 20 06	5.3×5.3	82.5	31.2 HDR
			04 33 36.5 +26 09 43	04 33 36.5 +26 09 43	5.3×5.3	82.5	31.2 HDR
			04 33 41.8 +26 03 09	04 33 31.4 +26 16 26	5.3×5.3	82.5	31.2 HDR
			04 33 14.2 +26 14 20	04 33 14.2 +26 14 20	5.3×5.3	82.5	31.2 HDR
			04 33 19.3 +26 07 40	04 33 09.2 +26 21 02	5.3×5.3	82.5	31.2 HDR
			04 32 43.2 +25 52 30	04 32 43.2 +25 52 30	5.3×5.3	82.5	31.2 HDR
			04 32 47.6 +25 45 49	04 32 38.2 +25 59 12	5.3×5.3	82.5	31.2 HDR
			04 31 58.1 +25 43 26	04 31 58.1 +25 43 26	5.3×5.3	82.5	31.2 HDR
			04 32 03.5 +25 36 50	04 31 53.1 +25 50 08	5.3×5.3	82.5	31.2 HDR
3966208	37	2004 Mar 8	04 20 52.8 +17 46 43	04 20 52.8 +17 46 43	5.3×5.3	81.5	31.2 HDR
			04 20 58.1 +17 39 59	04 20 47.8 +17 53 26	5.3×5.3	81.5	31.2 HDR
			04 18 22.3 +16 58 35	04 18 22.3 +16 58 35	5.3×5.3	81.5	31.2 HDR
			04 18 26.1 +16 52 08	04 18 17.3 +17 05 17	5.3×5.3	81.5	31.2 HDR
3967744	37	2004 Mar 9	04 39 16.0 +30 32 10	04 39 16.0 +30 32 10	5.3×5.3	83.0	31.2 HDR
			04 39 21.4 +30 25 26	04 39 11.0 +30 38 53	5.3×5.3	83.0	31.2 HDR
4913152	94	2004 Mar 9	04 34 09.3 +24 06 27	04 34 04.5 +24 13 09	10.3×19.0	172.3	52 HDR
4913664	94	2004 Mar 9	04 36 14.5 +24 40 47	04 36 09.8 +24 47 30	10.3×15.0	172.4	52 HDR
4914176	94	2004 Mar 9	04 40 41.0 +29 50 28	04 40 36.1 +29 57 12	6.3×15.0	172.5	52 HDR
4914688	94	2004 Mar 9	04 43 32.7 +29 36 43	04 43 28.0 +29 43 25	6.3×15.0	173.0	52 HDR
4913920	94	2004 Mar 11	04 36 14.5 +24 40 47	04 36 09.8 +24 47 30	10.3×15.0	172.4	52 HDR
4914432	94	2004 Mar 11	04 40 41.0 +29 50 28	04 40 36.1 +29 57 12	6.3×15.0	172.5	52 HDR
4914944	94	2004 Mar 11	04 43 32.7 +29 36 43	04 43 28.0 +29 43 25	6.3×15.0	173.0	52 HDR
4913408	94	2004 Mar 12	04 34 09.3 +24 06 27	04 34 09.3 +24 06 27	10.3×19.0	172.3	52 HDR
5075712	139	2004 Sep 7	04 28 35.6 +26 55 46	04 28 40.7 +26 49 03	5.3×15.0	172.0	20.8
5076736	139	2004 Sep 7	04 29 34.7 +26 58 55	04 29 34.7 +26 58 55	5.3×5.3	82.0	20.8
			04 29 30.4 +27 05 34	04 29 39.9 +26 52 12	5.3×5.3	82.0	20.8
5086464	139	2004 Sep 7	04 42 36.0 +29 47 12	04 42 40.5 +29 40 28	5.3×19.7	173.3	20.8
5657856	173	2004 Sep 7	04 09 22.3 +17 16 38	04 09 15.6 +17 15 40	5.6×5.6	80.5	20.8 HDR
			04 09 10.4 +17 22 22	04 09 27.5 +17 09 57	5.6×5.6	80.5	20.8 HDR
5658368	173	2004 Sep 7	04 18 56.7 +17 23 45	04 18 50.1 +17 22 48	5.6×5.6	81.5	20.8 HDR
			04 18 45.0 +17 29 30	04 19 01.8 +17 17 03	5.6×5.6	81.5	20.8 HDR
5658624	173	2004 Sep 7	04 20 29.9 +31 23 55	04 20 22.7 +31 22 56	5.6×5.6	81.0	20.8 HDR
			04 20 16.7 +31 29 37	04 20 35.9 +31 17 13	5.6×5.6	81.0	20.8 HDR
5658880	173	2004 Sep 7	04 24 54.1 +26 43 42	04 24 47.1 +26 42 45	5.6×5.6	82.0	20.8 HDR

TABLE 1 — *Continued*

AOR	PID	Date (UT)	3.6/5.8 Center (J2000)	4.5/8.0 Center (J2000)	Dimensions (arcmin)	Angle[a] (deg)	Exp Time[b] (s)
			04 24 41.6 +26 49 27	04 24 59.5 +26 37 02	5.6×5.6	82.0	20.8 HDR
5659136	173	2004 Sep 7	04 34 40.0 +25 01 20	04 34 39.4 +25 00 31	5.6×5.6	82.0	20.8 HDR
			04 34 34.8 +25 07 15	04 34 44.8 +24 54 38	5.6×5.6	82.0	20.8 HDR
			04 36 01.9 +23 52 33	04 35 55.3 +23 51 38	5.6×5.6	82.0	20.8 HDR
			04 35 50.8 +23 58 23	04 36 06.8 +23 45 47	5.6×5.6	82.0	20.8 HDR
			04 29 26.6 +24 39 51	04 29 28.9 +24 40 16	5.6×5.6	82.0	20.8 HDR
			04 29 24.0 +24 46 58	04 29 31.8 +24 33 09	5.6×5.6	82.0	20.8 HDR
5659392	173	2004 Sep 7	04 38 13.7 +20 22 59	04 38 13.5 +20 22 10	5.6×5.6	83.0	20.8 HDR
			04 38 08.9 +20 28 55	04 38 18.0 +20 16 28	5.6×5.6	83.0	20.8 HDR
			04 37 32.2 +18 51 54	04 37 25.4 +18 51 00	5.6×5.6	83.0	20.8 HDR
			04 37 20.8 +18 57 42	04 37 36.3 +18 45 11	5.6×5.6	83.0	20.8 HDR
5659648	173	2004 Sep 7	04 45 52.0 +15 56 04	04 45 51.6 +15 55 21	5.6×5.6	83.5	20.8 HDR
			04 45 47.5 +16 02 07	04 45 55.9 +15 49 29	5.6×5.6	83.5	20.8 HDR
			04 38 43.9 +15 46 41	04 38 37.5 +15 45 46	5.6×5.6	83.5	20.8 HDR
			04 38 33.2 +15 52 30	04 38 48.2 +15 39 59	5.6×5.6	83.5	20.8 HDR
5660416	173	2004 Sep 7	04 52 35.9 +17 30 50	04 52 29.3 +17 30 00	5.6×5.6	84.0	20.8 HDR
			04 52 25.4 +17 36 45	04 52 39.9 +17 24 05	5.6×5.6	84.0	20.8 HDR
			04 52 50.9 +16 22 31	04 52 50.2 +16 21 42	5.6×5.6	84.0	20.8 HDR
			04 52 46.4 +16 28 21	04 52 54.7 +16 15 49	5.6×5.6	84.0	20.8 HDR
5660928	173	2004 Sep 7	04 58 40.7 +20 46 52	04 58 40.0 +20 46 15	5.6×5.6	84.5	20.8 HDR
			04 58 36.4 +20 53 01	04 58 44.0 +20 40 16	5.6×5.6	84.5	20.8 HDR
			04 57 35.7 +20 14 55	04 57 29.0 +20 14 03	5.6×5.6	84.5	20.8 HDR
			04 57 25.4 +20 20 48	04 57 39.4 +20 08 09	5.6×5.6	84.5	20.8 HDR
5661184	173	2004 Sep 7	05 03 12.1 +25 23 44	05 03 04.9 +25 22 55	5.6×5.6	85.5	20.8 HDR
			05 03 01.7 +25 29 40	05 03 15.2 +25 17 00	5.6×5.6	85.5	20.8 HDR
5672960	173	2004 Sep 7	04 12 51.2 +19 37 27	04 12 51.1 +19 36 31	5.6×5.6	81.0	20.8 HDR
			04 12 45.7 +19 43 03	04 12 56.7 +19 30 48	5.6×5.6	81.0	20.8 HDR
			04 05 24.7 +20 09 53	04 05 18.2 +20 08 58	5.6×5.6	81.0	20.8 HDR
			04 05 12.4 +20 15 37	04 05 30.4 +20 03 17	5.6×5.6	81.0	20.8 HDR
5710336	173	2004 Sep 7	04 32 58.3 +17 36 01	04 32 51.7 +17 35 08	5.6×5.6	82.5	20.8 HDR
			04 32 47.1 +17 41 50	04 33 03.0 +17 29 19	5.6×5.6	82.5	20.8 HDR
5073920	139	2004 Sep 8	04 21 56.4 +15 29 49	04 21 56.4 +15 29 49	5.3×5.3	82.0	20.8 HDR
			04 21 52.4 +15 36 27	04 22 01.1 +15 23 06	5.3×5.3	82.0	20.8 HDR
5658112	173	2004 Sep 8	04 09 56.4 +24 46 52	04 09 49.7 +24 45 55	5.6×5.6	80.0	20.8 HDR
			04 09 43.6 +24 52 34	04 10 02.6 +24 40 14	5.6×5.6	80.0	20.8 HDR
5660160	173	2004 Sep 8	04 41 13.9 +25 56 35	04 41 06.8 +25 55 40	5.6×5.6	83.5	20.8 HDR
			04 41 02.5 +26 02 27	04 41 18.4 +25 49 50	5.6×5.6	83.5	20.8 HDR
5076224	139	2004 Sep 9	04 28 35.6 +26 55 46	04 28 40.7 +26 49 03	5.3×15.0	172.0	20.8
5077248	139	2004 Sep 9	04 29 34.7 +26 58 55	04 29 34.7 +26 58 55	5.3×5.3	82.0	20.8
			04 29 30.4 +27 05 34	04 29 39.9 +26 52 12	5.3×5.3	82.0	20.8
5074432	139	2004 Sep 10	04 21 56.4 +15 29 49	04 21 56.4 +15 29 49	5.3×5.3	82.0	20.8 HDR
			04 21 52.4 +15 36 27	04 22 01.1 +15 23 06	5.3×5.3	82.0	20.8 HDR
5086976	139	2004 Sep 10	04 42 36.0 +29 47 12	04 42 40.5 +29 40 28	5.3×19.7	173.3	20.8
5074688	139	2004 Oct 5	04 23 36.4 +26 40 07	04 23 36.4 +26 40 07	5.3×5.3	79.5	20.8
			04 23 30.6 +26 46 46	04 23 42.9 +26 33 29	5.3×5.3	79.5	20.8
5077760	139	2004 Oct 5	04 30 06.4 +24 25 55	04 30 06.4 +24 25 55	5.3×5.3	81.5	20.8
			04 30 01.7 +24 32 34	04 30 11.8 +24 19 13	5.3×5.3	81.5	20.8
5078784	139	2004 Oct 5	04 31 53.3 +24 36 11	04 31 58.4 +24 29 28	10.0×15.0	171.5	20.8
5079808	139	2004 Oct 5	04 32 36.1 +24 52 05	04 32 36.1 +24 52 05	5.3×5.3	81.5	20.8
			04 32 31.5 +24 58 45	04 32 41.5 +24 45 24	5.3×5.3	81.5	20.8
5080832	139	2004 Oct 5	04 32 45.6 +24 27 38	04 32 50.9 +24 20 55	10.0×15.0	171.5	20.8
5081856	139	2004 Oct 5	04 35 52.4 +24 09 33	04 35 53.2 +24 09 30	5.3×5.3	82.0	20.8
			04 35 48.2 +24 16 12	04 35 57.3 +24 02 51	5.3×5.3	82.0	20.8
3653120	6	2004 Oct 7	04 31 38.0 +18 14 20	04 31 41.3 +18 07 35	28.5×33.2	175.0	20.8 HDR
5075200	139	2004 Oct 7	04 23 36.4 +26 40 07	04 23 36.4 +26 40 07	5.3×5.3	79.5	20.8
			04 23 30.6 +26 46 46	04 23 42.9 +26 33 29	5.3×5.3	79.5	20.8
5078272	139	2004 Oct 7	04 30 06.4 +24 25 55	04 30 06.4 +24 25 55	5.3×5.3	81.5	20.8
			04 30 01.7 +24 32 34	04 30 11.8 +24 19 13	5.3×5.3	81.5	20.8
5079296	139	2004 Oct 7	04 31 53.3 +24 36 11	04 31 58.4 +24 29 28	10.0×15.0	171.5	20.8
5080320	139	2004 Oct 7	04 32 36.1 +24 52 05	04 32 36.1 +24 52 05	5.3×5.3	81.5	20.8
			04 32 31.5 +24 58 45	04 32 41.5 +24 45 24	5.3×5.3	81.5	20.8
5081344	139	2004 Oct 7	04 32 45.6 +24 27 38	04 32 50.9 +24 20 55	10.0×15.0	171.5	20.8
5082368	139	2004 Oct 7	04 35 52.4 +24 09 33	04 35 53.2 +24 09 30	5.3×5.3	82.0	20.8
			04 35 48.2 +24 16 12	04 35 57.3 +24 02 51	5.3×5.3	82.0	20.8
5082880	139	2004 Oct 8	04 40 54.8 +26 13 24	04 40 59.8 +26 06 44	10.0×19.5	171.5	20.8
5083392	139	2004 Oct 8	04 40 54.8 +26 13 24	04 40 59.8 +26 06 44	10.0×19.5	171.5	20.8
5084416	139	2004 Oct 8	04 41 29.8 +26 04 12	04 41 34.8 +25 57 28	10.0×24.0	171.6	20.8 HDR
5084928	139	2004 Oct 8	04 41 29.8 +26 04 12	04 41 34.8 +25 57 28	10.0×24.0	171.6	20.8 HDR
5085440	139	2004 Oct 8	04 41 41.0 +25 45 47	04 41 46.1 +25 39 05	10.0×19.5	171.8	20.8
5085952	139	2004 Oct 8	04 41 41.0 +25 45 47	04 41 46.1 +25 39 05	10.0×19.5	171.8	20.8
6634752	139	2004 Oct 8	04 40 57.1 +25 57 27	04 41 02.1 +25 50 46	10.0×19.5	171.6	20.8
6635008	139	2004 Oct 8	04 40 57.1 +25 57 27	04 41 02.1 +25 50 46	10.0×19.5	171.6	20.8
4912640	94	2005 Feb 18	04 10 55.7 +25 05 43	04 10 50.1 +25 12 24	10.4×23.0	170.9	52 HDR
3653888	6	2005 Feb 19	04 14 28.7 +28 12 19	04 14 23.8 +28 19 02	28.6×33.2	172.3	20.8 HDR
3965184	37	2005 Feb 19	04 31 27.5 +17 06 24	04 31 27.5 +17 06 24	5.3×5.3	80.0	31.2 HDR

Luhman et al.

TABLE 1 — *Continued*

AOR	PID	Date (UT)	3.6/5.8 Center (J2000)	4.5/8.0 Center (J2000)	Dimensions (arcmin)	Angle[a] (deg)	Exp Time[b] (s)
			04 31 32.3 +16 59 43	04 31 21.9 +17 13 04	5.3×5.3	80.0	31.2 HDR
			04 32 30.4 +17 31 38	04 32 30.4 +17 31 38	5.3×5.3	80.0	31.2 HDR
			04 32 36.0 +17 24 53	04 32 24.8 +17 38 18	5.3×5.3	80.0	31.2 HDR
			04 33 39.5 +17 51 48	04 33 39.5 +17 51 48	5.3×5.3	80.0	31.2 HDR
			04 33 45.1 +17 45 14	04 33 34.0 +17 58 29	5.3×5.3	80.0	31.2 HDR
			04 35 24.3 +17 51 38	04 35 24.3 +17 51 38	5.3×5.3	80.0	31.2 HDR
			04 35 30.0 +17 45 05	04 35 18.9 +17 58 19	5.3×5.3	80.0	31.2 HDR
			04 32 09.4 +17 57 19	04 32 09.4 +17 57 19	5.3×5.3	80.0	31.2 HDR
			04 32 14.4 +17 50 44	04 32 03.9 +18 03 59	5.3×5.3	80.0	31.2 HDR
			04 32 44.0 +18 03 03	04 32 44.0 +18 03 03	5.3×5.3	80.0	31.2 HDR
			04 32 49.0 +17 56 17	04 32 38.5 +18 09 44	5.3×5.3	80.0	31.2 HDR
			04 33 48.6 +18 10 09	04 33 48.6 +18 10 09	5.3×5.3	80.0	31.2 HDR
			04 33 54.9 +18 03 23	04 33 43.1 +18 16 51	5.3×5.3	80.0	31.2 HDR
			04 34 17.9 +18 30 02	04 34 17.9 +18 30 02	5.3×5.3	80.0	31.2 HDR
			04 34 23.6 +18 23 22	04 34 12.6 +18 36 44	5.3×5.3	80.0	31.2 HDR
			04 33 55.8 +18 38 44	04 33 55.8 +18 38 44	5.3×5.3	80.0	31.2 HDR
			04 34 01.1 +18 31 54	04 33 50.6 +18 45 25	5.3×5.3	80.0	31.2 HDR
			04 32 22.2 +18 27 32	04 32 22.2 +18 27 32	5.3×5.3	80.0	31.2 HDR
			04 32 27.9 +18 20 52	04 32 16.8 +18 34 14	5.3×5.3	80.0	31.2 HDR
			04 30 04.6 +18 13 45	04 30 04.6 +18 13 45	5.3×5.3	80.0	31.2 HDR
			04 30 09.5 +18 07 15	04 29 59.1 +18 20 25	5.3×5.3	80.0	31.2 HDR
			04 27 10.7 +17 50 40	04 27 10.7 +17 50 40	5.3×5.3	80.0	31.2 HDR
			04 27 16.1 +17 43 58	04 27 05.0 +17 57 21	5.3×5.3	80.0	31.2 HDR
3962880	37	2005 Feb 20	04 19 01.4 +28 02 44	04 19 01.4 +28 02 44	5.3×5.3	83.0	31.2 HDR
			04 19 05.7 +27 56 07	04 18 56.5 +28 09 28	5.3×5.3	83.0	31.2 HDR
			04 17 38.9 +28 32 59	04 17 38.9 +28 32 59	5.3×5.3	83.0	31.2 HDR
			04 17 44.2 +28 26 13	04 17 34.1 +28 39 41	5.3×5.3	83.0	31.2 HDR
			04 19 15.7 +29 06 27	04 19 15.7 +29 06 27	5.3×5.3	83.0	31.2 HDR
			04 19 21.2 +28 59 38	04 19 11.0 +29 13 10	5.3×5.3	83.0	31.2 HDR
			04 15 14.6 +28 00 08	04 15 14.6 +28 00 08	5.3×5.3	83.0	31.2 HDR
			04 15 19.9 +27 53 23	04 15 09.5 +28 06 51	5.3×5.3	83.0	31.2 HDR
			04 14 48.4 +27 52 40	04 14 48.4 +27 52 40	5.3×5.3	83.0	31.2 HDR
			04 14 53.2 +27 45 48	04 14 43.3 +27 59 24	5.3×5.3	83.0	31.2 HDR
			04 13 27.3 +28 16 23	04 13 27.3 +28 16 23	5.3×5.3	83.0	31.2 HDR
			04 13 32.4 +28 09 37	04 13 22.3 +28 23 06	5.3×5.3	83.0	31.2 HDR
			04 13 14.3 +28 19 09	04 13 14.3 +28 19 09	5.3×5.3	83.0	31.2 HDR
			04 13 19.5 +28 12 33	04 13 09.2 +28 25 52	5.3×5.3	83.0	31.2 HDR
			04 13 58.1 +29 18 16	04 13 58.1 +29 18 16	5.3×5.3	83.0	31.2 HDR
			04 14 02.4 +29 11 43	04 13 53.1 +29 24 58	5.3×5.3	83.0	31.2 HDR
3963136	37	2005 Feb 20	04 24 44.8 +27 01 41	04 24 44.8 +27 01 41	5.3×5.3	83.5	31.2 HDR
			04 24 49.8 +26 55 03	04 24 40.2 +27 08 25	5.3×5.3	83.5	31.2 HDR
			04 24 57.0 +27 11 54	04 24 57.0 +27 11 54	5.3×5.3	83.5	31.2 HDR
			04 25 01.9 +27 05 10	04 24 52.4 +27 18 38	5.3×5.3	83.5	31.2 HDR
			04 22 02.6 +26 57 36	04 22 02.6 +26 57 36	5.3×5.3	83.5	31.2 HDR
			04 22 07.1 +26 50 44	04 21 57.8 +27 04 20	5.3×5.3	83.5	31.2 HDR
			04 21 10.2 +27 01 39	04 21 10.2 +27 01 39	5.3×5.3	83.5	31.2 HDR
			04 21 15.2 +26 55 02	04 21 05.4 +27 08 22	5.3×5.3	83.5	31.2 HDR
			04 19 58.2 +27 09 58	04 19 58.2 +27 09 58	5.3×5.3	83.5	31.2 HDR
			04 20 04.5 +27 03 09	04 19 53.4 +27 16 39	5.3×5.3	83.5	31.2 HDR
			04 19 43.6 +27 13 30	04 19 43.6 +27 13 30	5.3×5.3	83.5	31.2 HDR
			04 19 47.8 +27 06 59	04 19 38.8 +27 20 14	5.3×5.3	83.5	31.2 HDR
			04 19 41.5 +27 49 48	04 19 41.5 +27 49 48	5.3×5.3	83.5	31.2 HDR
			04 19 45.6 +27 43 04	04 19 36.8 +27 56 29	5.3×5.3	83.5	31.2 HDR
			04 21 55.7 +27 55 03	04 21 55.7 +27 55 03	5.3×5.3	83.5	31.2 HDR
			04 22 00.4 +27 48 17	04 21 51.0 +28 01 48	5.3×5.3	83.5	31.2 HDR
			04 23 11.7 +28 05 59	04 23 11.7 +28 05 59	5.3×5.3	83.5	31.2 HDR
			04 23 16.6 +27 59 14	04 23 07.1 +28 12 44	5.3×5.3	83.5	31.2 HDR
			04 21 59.1 +28 18 13	04 21 59.1 +28 18 13	5.3×5.3	83.5	31.2 HDR
			04 22 03.4 +28 11 27	04 21 54.4 +28 24 58	5.3×5.3	83.5	31.2 HDR
			04 22 00.4 +28 26 04	04 22 00.4 +28 26 04	5.3×5.3	83.5	31.2 HDR
			04 22 04.6 +28 19 26	04 21 55.8 +28 32 49	5.3×5.3	83.5	31.2 HDR
3964160	37	2005 Feb 20	04 39 17.9 +22 20 58	04 39 17.9 +22 20 58	5.3×5.3	83.0	31.2 HDR
			04 39 22.0 +22 14 23	04 39 13.3 +22 27 42	5.3×5.3	83.0	31.2 HDR
			04 39 17.8 +22 47 45	04 39 17.8 +22 47 45	5.3×5.3	83.0	31.2 HDR
			04 39 21.9 +22 41 19	04 39 13.3 +22 54 28	5.3×5.3	83.0	31.2 HDR
			04 35 20.3 +22 32 10	04 35 20.3 +22 32 10	5.3×5.3	83.0	31.2 HDR
			04 35 24.7 +22 25 31	04 35 15.6 +22 38 53	5.3×5.3	83.0	31.2 HDR
			04 35 42.2 +22 34 09	04 35 42.2 +22 34 09	5.3×5.3	83.0	31.2 HDR
			04 35 46.1 +22 27 28	04 35 37.4 +22 40 54	5.3×5.3	83.0	31.2 HDR
			04 36 39.1 +22 58 10	04 36 39.1 +22 58 10	5.3×5.3	83.0	31.2 HDR
			04 36 43.1 +22 51 30	04 36 34.6 +23 04 54	5.3×5.3	83.0	31.2 HDR
			04 36 10.4 +22 59 56	04 36 10.4 +22 59 56	5.3×5.3	83.0	31.2 HDR
			04 36 14.9 +22 53 10	04 36 05.8 +23 06 37	5.3×5.3	83.0	31.2 HDR
			04 35 52.7 +22 54 21	04 35 52.7 +22 54 21	5.3×5.3	83.0	31.2 HDR
			04 35 57.5 +22 47 37	04 35 48.1 +23 01 04	5.3×5.3	83.0	31.2 HDR

TABLE 1 — *Continued*

AOR	PID	Date (UT)	3.6/5.8 Center (J2000)	4.5/8.0 Center (J2000)	Dimensions (arcmin)	Angle[a] (deg)	Exp Time[b] (s)
			04 35 51.1 +22 49 09	04 35 51.1 +22 49 09	5.3×5.3	83.0	31.2 HDR
			04 35 56.2 +22 42 31	04 35 46.6 +22 55 52	5.3×5.3	83.0	31.2 HDR
			04 35 21.1 +22 54 23	04 35 21.1 +22 54 23	5.3×5.3	83.0	31.2 HDR
			04 35 25.9 +22 47 44	04 35 16.4 +23 01 05	5.3×5.3	83.0	31.2 HDR
			04 34 13.4 +22 51 13	04 34 13.4 +22 51 13	5.3×5.3	83.0	31.2 HDR
			04 34 18.1 +22 44 27	04 34 08.6 +22 57 56	5.3×5.3	83.0	31.2 HDR
			04 33 52.5 +22 50 36	04 33 52.5 +22 50 36	5.3×5.3	83.0	31.2 HDR
			04 33 56.9 +22 43 43	04 33 47.6 +22 57 18	5.3×5.3	83.0	31.2 HDR
			04 33 16.2 +22 53 23	04 33 16.2 +22 53 23	5.3×5.3	83.0	31.2 HDR
			04 33 21.7 +22 46 31	04 33 11.6 +23 00 04	5.3×5.3	83.0	31.2 HDR
			04 33 19.1 +22 46 36	04 33 19.1 +22 46 36	5.3×5.3	83.0	31.2 HDR
			04 33 24.2 +22 39 46	04 33 14.5 +22 53 15	5.3×5.3	83.0	31.2 HDR
			04 32 49.2 +22 53 01	04 32 49.2 +22 53 01	5.3×5.3	83.0	31.2 HDR
			04 32 54.0 +22 46 13	04 32 45.7 +22 59 49	5.3×5.3	83.0	31.2 HDR
			04 32 32.6 +22 57 23	04 32 32.6 +22 57 23	5.3×5.3	83.0	31.2 HDR
			04 32 36.8 +22 50 51	04 32 27.9 +23 04 06	5.3×5.3	83.0	31.2 HDR
3964416	37	2005 Feb 20	04 30 50.4 +22 59 57	04 30 50.4 +22 59 57	5.3×5.3	82.5	31.2 HDR
			04 30 54.9 +22 53 31	04 30 45.4 +23 06 41	5.3×5.3	82.5	31.2 HDR
			04 35 40.7 +24 11 05	04 35 40.7 +24 11 05	5.3×5.3	82.5	31.2 HDR
			04 35 45.4 +24 04 28	04 35 36.2 +24 17 49	5.3×5.3	82.5	31.2 HDR
			04 35 36.0 +24 08 12	04 35 36.0 +24 08 12	5.3×5.3	82.5	31.2 HDR
			04 35 39.9 +24 01 44	04 35 31.5 +24 14 56	5.3×5.3	82.5	31.2 HDR
			04 35 27.7 +24 14 57	04 35 27.7 +24 14 57	5.3×5.3	82.5	31.2 HDR
			04 35 31.5 +24 08 18	04 35 23.2 +24 21 40	5.3×5.3	82.5	31.2 HDR
			04 34 55.7 +24 29 00	04 34 55.7 +24 29 00	5.3×5.3	82.5	31.2 HDR
			04 35 00.0 +24 22 11	04 34 51.2 +24 35 45	5.3×5.3	82.5	31.2 HDR
			04 33 06.4 +24 09 30	04 33 06.4 +24 09 30	5.3×5.3	82.5	31.2 HDR
			04 33 10.5 +24 02 52	04 33 01.8 +24 16 11	5.3×5.3	82.5	31.2 HDR
			04 33 10.1 +24 33 43	04 33 10.1 +24 33 43	5.3×5.3	82.5	31.2 HDR
			04 33 14.4 +24 26 57	04 33 05.6 +24 40 25	5.3×5.3	82.5	31.2 HDR
			04 33 34.5 +24 21 03	04 33 34.5 +24 21 03	5.3×5.3	82.5	31.2 HDR
			04 33 39.3 +24 14 19	04 33 30.1 +24 27 47	5.3×5.3	82.5	31.2 HDR
			04 33 02.4 +24 21 06	04 33 02.4 +24 21 06	5.3×5.3	82.5	31.2 HDR
			04 33 06.7 +24 14 13	04 32 57.9 +24 27 48	5.3×5.3	82.5	31.2 HDR
			04 32 31.9 +24 19 58	04 32 31.9 +24 19 58	5.3×5.3	82.5	31.2 HDR
			04 32 36.7 +24 13 15	04 32 27.5 +24 26 43	5.3×5.3	82.5	31.2 HDR
			04 32 15.7 +24 28 58	04 32 15.7 +24 28 58	5.3×5.3	82.5	31.2 HDR
			04 32 20.0 +24 22 18	04 32 11.0 +24 35 40	5.3×5.3	82.5	31.2 HDR
			04 32 18.7 +24 22 26	04 32 18.7 +24 22 26	5.3×5.3	82.5	31.2 HDR
			04 32 22.9 +24 15 44	04 32 14.2 +24 29 09	5.3×5.3	82.5	31.2 HDR
			04 31 50.5 +24 24 19	04 31 50.5 +24 24 19	5.3×5.3	82.5	31.2 HDR
			04 31 55.9 +24 17 31	04 31 45.9 +24 31 04	5.3×5.3	82.5	31.2 HDR
			04 31 23.9 +24 10 49	04 31 23.9 +24 10 49	5.3×5.3	82.5	31.2 HDR
			04 31 28.1 +24 04 11	04 31 19.2 +24 17 31	5.3×5.3	82.5	31.2 HDR
			04 30 29.8 +24 26 43	04 30 29.8 +24 26 43	5.3×5.3	82.5	31.2 HDR
			04 30 34.4 +24 19 55	04 30 25.1 +24 33 25	5.3×5.3	82.5	31.2 HDR
3965952	37	2005 Feb 20	04 22 00.1 +19 32 02	04 22 00.1 +19 32 02	5.3×5.3	80.5	31.2 HDR
			04 22 05.0 +19 25 33	04 21 54.5 +19 38 42	5.3×5.3	80.5	31.2 HDR
			04 21 43.0 +19 34 14	04 21 43.0 +19 34 14	5.3×5.3	80.5	31.2 HDR
			04 21 49.5 +19 27 29	04 21 37.5 +19 40 54	5.3×5.3	80.5	31.2 HDR
3966976	37	2005 Feb 20	04 04 43.6 +26 18 52	04 04 43.6 +26 18 52	5.3×5.3	80.5	31.2 HDR
			04 04 48.6 +26 12 23	04 04 37.8 +26 25 34	5.3×5.3	80.5	31.2 HDR
			04 03 50.7 +26 10 56	04 03 50.7 +26 10 56	5.3×5.3	80.5	31.2 HDR
			04 03 57.4 +26 04 10	04 03 44.9 +26 17 35	5.3×5.3	80.5	31.2 HDR
			04 03 14.1 +25 52 58	04 03 14.1 +25 52 58	5.3×5.3	80.5	31.2 HDR
			04 03 20.1 +25 46 23	04 03 08.2 +25 59 37	5.3×5.3	80.5	31.2 HDR
4912896	94	2005 Feb 20	04 10 55.7 +25 05 43	04 10 50.1 +25 12 24	10.4×23.0	170.9	52 HDR
11233024	3584	2005 Feb 20	04 28 07.7 +24 14 06	04 28 03.2 +24 20 49	34.2×184.2	172.8	10.4 HDR
11233536	3584	2005 Feb 20	04 25 34.4 +24 09 36	04 25 29.4 +24 16 19	34.2×184.0	172.6	10.4 HDR
11236864	3584	2005 Feb 20	04 28 07.7 +24 14 06	04 28 03.2 +24 20 49	34.2×184.2	172.8	10.4 HDR
11237376	3584	2005 Feb 20	04 25 34.4 +24 09 36	04 25 29.4 +24 16 19	34.2×184.0	172.6	10.4 HDR
11237632	3584	2005 Feb 20	04 19 22.5 +27 47 24	04 19 17.9 +27 54 11	63.3×82.5	172.4	10.4 HDR
12663552	37	2005 Feb 20	04 57 48.9 +30 15 17	04 57 48.9 +30 15 17	5.3×5.3	88.0	31.2
			04 57 51.2 +30 08 28	04 57 46.8 +30 22 04	5.3×5.3	88.0	31.2
			04 55 52.7 +30 06 51	04 55 52.7 +30 06 51	5.3×5.3	88.0	31.2
			04 55 55.8 +30 00 00	04 55 50.3 +30 13 39	5.3×5.3	88.0	31.2
			04 55 45.3 +30 19 35	04 55 45.3 +30 19 35	5.3×5.3	88.0	31.2
			04 55 48.1 +30 12 47	04 55 43.3 +30 26 19	5.3×5.3	88.0	31.2
			04 55 48.7 +30 28 01	04 55 48.7 +30 28 01	5.3×5.3	88.0	31.2
			04 55 50.2 +30 21 26	04 55 46.6 +30 34 46	5.3×5.3	88.0	31.2
			04 55 23.5 +30 27 32	04 55 23.5 +30 27 32	5.3×5.3	88.0	31.2
			04 55 25.4 +30 20 42	04 55 21.4 +30 34 21	5.3×5.3	88.0	31.2
			04 55 40.7 +30 39 04	04 55 40.7 +30 39 04	5.3×5.3	88.0	31.2
			04 55 42.9 +30 32 25	04 55 38.6 +30 45 50	5.3×5.3	88.0	31.2
			04 55 56.8 +30 49 41	04 55 56.8 +30 49 41	5.3×5.3	88.0	31.2

TABLE 1 — *Continued*

AOR	PID	Date (UT)	3.6/5.8 Center (J2000)	4.5/8.0 Center (J2000)	Dimensions (arcmin)	Angle[a] (deg)	Exp Time[b] (s)
			04 55 58.7 +30 42 45	04 55 54.8 +30 56 29	5.3×5.3	88.0	31.2
12914944	3584	2005 Feb 20	04 33 09.7 +28 56 14	04 33 05.8 +29 02 57	53.7×121.3	174.4	10.4 HDR
12915712	3584	2005 Feb 20	04 33 09.7 +28 56 14	04 33 05.8 +29 02 57	53.7×121.3	174.4	10.4 HDR
11231488	3584	2005 Feb 21	04 36 21.8 +24 05 29	04 36 18.2 +24 12 08	39.1×150.4	173.4	10.4 HDR
11232000	3584	2005 Feb 21	04 33 15.1 +24 22 30	04 33 10.8 +24 29 15	39.0×184.2	173.0	10.4 HDR
11233280	3584	2005 Feb 21	04 23 49.0 +27 07 42	04 23 43.6 +27 14 24	34.2×184.0	172.1	10.4 HDR
11233792	3584	2005 Feb 21	04 19 22.5 +27 47 24	04 19 17.9 +27 54 11	63.3×82.5	172.4	10.4 HDR
11235328	3584	2005 Feb 21	04 36 21.8 +24 05 29	04 36 18.2 +24 12 08	39.1×150.4	173.4	10.4 HDR
11235840	3584	2005 Feb 21	04 33 15.1 +24 22 30	04 33 10.8 +24 29 15	39.0×184.2	173.0	10.4 HDR
11237120	3584	2005 Feb 21	04 23 49.0 +27 07 42	04 23 43.6 +27 14 24	34.2×184.0	172.1	10.4 HDR
3653376	6	2005 Feb 22	04 18 40.7 +28 16 42	04 18 35.9 +28 23 24	28.6×33.2	171.8	20.8 HDR
3653632	6	2005 Feb 22	04 16 36.8 +28 14 27	04 16 31.7 +28 21 09	28.6×33.2	171.8	20.8 HDR
5657600	173	2005 Feb 22	04 05 25.7 +21 50 40	04 05 32.3 +21 51 39	5.6×5.6	80.0	20.8 HDR
			04 05 38.2 +21 44 57	04 05 19.6 +21 57 21	5.6×5.6	80.0	20.8 HDR
11230720	3584	2005 Feb 22	04 39 18.8 +24 31 41	04 39 14.7 +24 38 23	48.7×121.4	173.3	10.4 HDR
11231232	3584	2005 Feb 22	04 35 07.1 +26 34 29	04 35 02.8 +26 41 11	39.1×155.1	173.2	10.4 HDR
11232768	3584	2005 Feb 22	04 26 25.5 +27 12 14	04 26 20.6 +27 18 54	34.2×184.2	172.4	10.4 HDR
11234560	3584	2005 Feb 22	04 39 18.8 +24 31 41	04 39 14.7 +24 38 23	48.7×121.4	173.3	10.4 HDR
11235072	3584	2005 Feb 22	04 35 07.1 +26 34 29	04 35 02.8 +26 41 11	39.1×155.1	173.2	10.4 HDR
11236608	3584	2005 Feb 22	04 26 25.5 +27 12 14	04 26 20.6 +27 18 54	34.2×184.2	172.4	10.4 HDR
3964672	37	2005 Feb 23	04 30 51.5 +24 42 20	04 30 51.5 +24 42 20	5.3×5.3	82.0	31.2 HDR
			04 30 56.4 +24 35 42	04 30 46.9 +24 49 03	5.3×5.3	82.0	31.2 HDR
			04 29 07.5 +24 43 49	04 29 07.5 +24 43 49	5.3×5.3	82.0	31.2 HDR
			04 29 13.2 +24 37 01	04 29 02.8 +24 50 32	5.3×5.3	82.0	31.2 HDR
			04 29 24.4 +24 32 56	04 29 24.4 +24 32 56	5.3×5.3	82.0	31.2 HDR
			04 29 28.4 +24 26 24	04 29 19.6 +24 39 38	5.3×5.3	82.0	31.2 HDR
			04 26 56.4 +24 43 34	04 26 56.4 +24 43 34	5.3×5.3	82.0	31.2 HDR
			04 27 01.2 +24 36 47	04 26 51.6 +24 50 16	5.3×5.3	82.0	31.2 HDR
			04 23 39.3 +24 56 13	04 23 39.3 +24 56 13	5.3×5.3	82.0	31.2 HDR
			04 23 44.5 +24 49 27	04 23 34.3 +25 02 55	5.3×5.3	82.0	31.2 HDR
11230208	3584	2005 Feb 23	04 47 59.0 +24 58 48	04 47 55.6 +25 05 32	63.3×174.3	174.6	10.4 HDR
11230464	3584	2005 Feb 23	04 43 18.2 +25 07 31	04 43 14.5 +25 14 13	58.5×174.4	174.0	10.4 HDR
11230976	3584	2005 Feb 23	04 38 21.2 +26 30 59	04 38 17.1 +26 37 42	48.7×121.3	173.1	10.4 HDR
11232256	3584	2005 Feb 23	04 29 01.8 +27 16 37	04 28 57.2 +27 23 25	34.2×189.0	172.6	10.4 HDR
11234304	3584	2005 Feb 23	04 43 18.2 +25 07 31	04 43 14.5 +25 14 13	58.5×174.4	174.0	10.4 HDR
11234816	3584	2005 Feb 23	04 38 21.2 +26 30 59	04 38 17.1 +26 37 42	48.7×121.3	173.1	10.4 HDR
11231744	3584	2005 Feb 24	04 31 39.4 +27 20 58	04 31 34.8 +27 27 43	39.1×198.8	172.6	10.4 HDR
11232512	3584	2005 Feb 24	04 30 43.1 +24 18 04	04 30 38.4 +24 24 47	34.4×184.2	172.9	10.4 HDR
11234048	3584	2005 Feb 24	04 47 59.0 +24 58 48	04 47 55.6 +25 05 32	63.3×174.3	174.6	10.4 HDR
11235584	3584	2005 Feb 24	04 31 39.4 +27 20 58	04 31 34.8 +27 27 43	39.1×198.8	172.6	10.4 HDR
11236096	3584	2005 Feb 24	04 29 01.8 +27 16 37	04 28 57.2 +27 23 25	34.2×189.0	172.6	10.4 HDR
11236352	3584	2005 Feb 24	04 30 43.1 +24 18 04	04 30 38.4 +24 24 47	34.4×184.2	172.9	10.4 HDR
14604544	20386	2005 Sep 16	04 23 36.8 +26 40 12	04 23 36.8 +26 40 12	5.3×5.3	81.0	214.4 HDR
			04 23 31.1 +26 46 51	04 23 42.3 +26 33 31	5.3×5.3	81.0	214.4 HDR
14604800	20386	2005 Sep 17	04 23 36.8 +26 40 12	04 23 36.8 +26 40 12	5.3×5.3	81.0	214.4 HDR
			04 23 31.1 +26 46 51	04 23 42.3 +26 33 31	5.3×5.3	81.0	214.4 HDR
14617856	20386	2005 Sep 17	04 21 56.7 +15 29 54	04 21 56.7 +15 29 54	5.3×5.3	82.0	214.4 HDR
			04 21 52.0 +15 36 33	04 22 01.4 +15 23 09	5.3×5.3	82.0	214.4 HDR
14618112	20386	2005 Sep 17	04 21 56.7 +15 29 54	04 21 56.7 +15 29 54	5.3×5.3	82.0	214.4 HDR
			04 21 52.0 +15 36 33	04 22 01.4 +15 23 09	5.3×5.3	82.0	214.4 HDR
15123456	20762	2006 Mar 23	04 31 10.0 +18 12 36	04 31 10.0 +18 12 36	5.5×5.5	82.7	241.2
			04 31 14.5 +18 05 57	04 31 05.7 +18 19 19	5.5×5.5	82.7	241.2
14605568	20386	2006 Mar 24	04 28 39.2 +26 51 39	04 28 39.2 +26 51 39	5.3×5.3	81.5	214.4 HDR
			04 28 44.6 +26 45 01	04 28 33.8 +26 58 22	5.3×5.3	81.5	214.4 HDR
14609920	20386	2006 Mar 24	04 29 21.3 +26 14 25	04 29 21.3 +26 14 25	5.3×5.3	81.5	214.4 HDR
			04 29 26.5 +26 07 46	04 29 16.0 +26 21 07	5.3×5.3	81.5	214.4 HDR
14511616	20302	2006 Mar 25	04 35 09.5 +24 05 44	04 35 04.7 +24 12 28	20.3×32.6	172.7	72.8
14605824	20386	2006 Mar 25	04 28 39.2 +26 51 39	04 28 39.2 +26 51 39	5.3×5.3	81.5	214.4 HDR
			04 28 44.6 +26 45 01	04 28 33.8 +26 58 22	5.3×5.3	81.5	214.4 HDR
14610176	20386	2006 Mar 25	04 29 21.3 +26 14 25	04 29 21.3 +26 14 25	5.3×5.3	81.5	214.4 HDR
			04 29 26.5 +26 07 46	04 29 16.0 +26 21 07	5.3×5.3	81.5	214.4 HDR
14611968	20386	2006 Mar 25	04 32 49.0 +24 25 18	04 32 49.0 +24 25 18	5.3×5.3	82.4	214.4 HDR
			04 32 53.8 +24 18 35	04 32 44.0 +24 31 59	5.3×5.3	82.4	214.4 HDR
14612224	20386	2006 Mar 26	04 32 49.0 +24 25 18	04 32 49.0 +24 25 18	5.3×5.3	82.4	214.4 HDR
			04 32 53.8 +24 18 35	04 32 44.0 +24 31 59	5.3×5.3	82.4	214.4 HDR
14610432	20386	2006 Mar 29	05 04 16.8 +25 10 53	05 04 16.8 +25 10 53	5.3×5.3	85.5	214.4 HDR
			05 04 20.1 +25 04 09	05 04 13.6 +25 17 40	5.3×5.3	85.5	214.4 HDR
14610688	20386	2006 Mar 29	05 04 16.8 +25 10 53	05 04 16.8 +25 10 53	5.3×5.3	85.5	214.4 HDR
			05 04 20.1 +25 04 09	05 04 13.6 +25 17 40	5.3×5.3	85.5	214.4 HDR
18365440	30540	2006 Sep 28	04 22 16.0 +25 49 13	04 22 16.0 +25 49 13	5.5×5.5	81.0	52
			04 22 10.5 +25 55 49	04 22 21.6 +25 42 33	5.5×5.5	81.0	52
18365696	30540	2006 Sep 28	04 15 23.7 +29 10 46	04 15 23.7 +29 10 46	5.5×5.5	79.5	134
			04 15 17.3 +29 17 19	04 15 30.1 +29 04 05	5.5×5.5	79.5	134
18363648	30540	2006 Oct 26	04 57 48.5 +30 15 20	04 57 48.5 +30 15 20	5.5×5.5	81.5	134
			04 57 43.3 +30 22 00	04 57 53.9 +30 08 40	5.5×5.5	81.5	134

TABLE 1 — *Continued*

AOR	PID	Date (UT)	3.6/5.8 Center (J2000)	4.5/8.0 Center (J2000)	Dimensions (arcmin)	Angle[a] (deg)	Exp Time[b] (s)
18365952	30540	2006 Oct 26	04 48 41.5 +17 03 41	04 48 41.5 +17 03 41	5.5×5.5	87.5	134
			04 48 39.5 +17 10 22	04 48 43.5 +16 56 50	5.5×5.5	87.5	134
18363904	30540	2007 Mar 28	04 26 30.8 +24 43 59	04 26 30.8 +24 43 59	5.5×5.5	81.5	134
			04 26 36.1 +24 37 18	04 26 25.8 +24 50 36	5.5×5.5	81.5	134
18364160	30540	2007 Mar 28	04 41 45.2 +23 01 50	04 41 45.2 +23 01 50	5.5×5.5	83.3	134
			04 41 49.5 +22 55 13	04 41 40.9 +23 08 36	5.5×5.5	83.3	134
18364416	30540	2007 Mar 28	04 21 54.9 +26 52 34	04 21 54.9 +26 52 34	5.5×5.5	81.0	134
			04 22 00.5 +26 45 56	04 21 49.3 +26 59 12	5.5×5.5	81.0	134
18364672	30540	2007 Mar 28	04 36 10.7 +21 59 36	04 36 10.7 +21 59 36	5.5×5.5	82.5	134
			04 36 15.2 +21 52 57	04 36 06.2 +22 06 18	5.5×5.5	82.5	134
18364928	30540	2007 Mar 28	04 14 33.5 +30 33 41	04 14 33.5 +30 33 41	5.5×5.5	80.0	134
			04 14 39.8 +30 27 08	04 14 27.0 +30 40 20	5.5×5.5	80.0	134
19030528	30816	2007 Mar 28	04 18 49.9 +25 02 50	04 18 43.8 +25 09 31	36.7×185.0	170.3	10.4 HDR
18365184	30540	2007 Mar 29	04 22 13.7 +19 34 42	04 22 13.7 +19 34 42	5.5×5.5	81.5	52
			04 22 18.7 +19 28 03	04 22 08.8 +19 41 22	5.5×5.5	81.5	52
18366208	30540	2007 Mar 29	04 55 23.7 +30 27 38	04 55 23.7 +30 27 38	5.5×5.5	85.0	52
			04 55 27.3 +30 20 56	04 55 20.1 +30 34 23	5.5×5.5	85.0	52
18366464	30540	2007 Mar 29	04 33 09.9 +22 46 49	04 33 09.9 +22 46 49	5.5×5.5	82.5	52
			04 33 14.4 +22 40 12	04 33 05.1 +22 53 33	5.5×5.5	82.5	52
19027712	30816	2007 Mar 29	04 19 08.8 +29 07 47	04 19 02.9 +29 14 26	51.2×80.2	170.2	10.4 HDR
19027968	30816	2007 Mar 29	04 19 08.8 +29 07 47	04 19 02.9 +29 14 26	51.2×80.2	170.2	10.4 HDR
19028736	30816	2007 Mar 29	04 23 03.9 +23 34 20	04 22 58.6 +23 41 01	51.2×118.3	170.9	10.4 HDR
19030784	30816	2007 Mar 29	04 13 46.3 +28 11 03	04 13 39.8 +28 17 42	36.7×186.7	169.9	10.4 HDR
19031040	30816	2007 Mar 29	04 16 05.7 +25 12 53	04 16 00.0 +25 19 34	36.7×185.0	170.2	10.4 HDR
19034112	30816	2007 Mar 29	04 18 49.9 +25 02 50	04 18 43.8 +25 09 31	36.7×185.0	170.3	10.4 HDR
19034368	30816	2007 Mar 29	04 13 46.3 +28 11 03	04 13 39.8 +28 17 42	36.7×186.7	169.9	10.4 HDR
19028224	30816	2007 Mar 30	04 21 42.1 +25 32 21	04 21 36.6 +25 39 01	51.2×117.3	170.8	10.4 HDR
19028480	30816	2007 Mar 30	04 21 42.1 +25 32 21	04 21 36.6 +25 39 01	51.2×117.3	170.8	10.4 HDR
19028992	30816	2007 Mar 30	04 23 03.9 +23 34 20	04 22 58.6 +23 41 01	51.2×118.3	170.9	10.4 HDR
19030272	30816	2007 Mar 30	04 16 35.2 +28 01 08	04 16 28.8 +28 07 50	36.7×186.7	169.9	10.4 HDR
19034624	30816	2007 Mar 30	04 16 05.7 +25 12 53	04 16 00.0 +25 19 34	36.7×185.0	170.2	10.4 HDR
19033856	30816	2007 Mar 31	04 16 35.2 +28 01 08	04 16 28.8 +28 07 50	36.7×186.7	169.9	10.4 HDR
19032576	30816	2007 Apr 2	04 35 36.6 +22 14 56	04 35 32.2 +22 21 40	94.7×109.3	82.2	10.4 HDR
19036160	30816	2007 Apr 3	04 35 36.6 +22 14 56	04 35 32.2 +22 21 40	94.7×109.3	82.2	10.4 HDR
21916416	40302	2007 Oct 16	04 20 24.9 +27 00 38	04 20 24.9 +27 00 38	5.5×5.5	79.5	52
			04 20 18.8 +27 07 13	04 20 31.3 +26 53 58	5.5×5.5	79.5	52
24242688	462	2007 Oct 16	04 22 16.8 +24 33 25	04 22 22.4 +24 26 44	5.2×51.0	81.0	20.8 HDR
24243200	462	2007 Oct 16	04 20 42.5 +26 55 59	04 20 49.0 +26 49 22	56.0×56.0	79.9	10.4 HDR
24243456	462	2007 Oct 16	04 20 42.5 +26 55 59	04 20 49.0 +26 49 22	56.0×56.0	79.9	10.4 HDR
24243712	462	2007 Oct 16	04 45 27.0 +25 13 43	04 45 31.3 +25 07 00	5.2×162.4	173.0	20.8 HDR
24243968	462	2007 Oct 16	04 41 13.5 +24 33 10	04 41 18.1 +24 26 27	5.2×87.3	172.8	20.8 HDR
24244224	462	2007 Oct 16	04 40 33.0 +26 00 09	04 40 37.7 +25 53 27	5.2×87.3	172.3	20.8 HDR
24244480	462	2007 Oct 16	04 34 10.9 +28 07 23	04 34 16.4 +28 00 42	10.0×41.4	80.9	20.8 HDR
24244736	462	2007 Oct 16	04 34 39.0 +24 29 25	04 34 44.0 +24 22 43	5.2×152.7	172.0	20.8 HDR
24244992	462	2007 Oct 16	04 33 22.5 +26 55 39	04 33 27.8 +26 48 58	5.2×152.7	171.2	20.8 HDR
24245248	462	2007 Oct 16	04 29 17.2 +24 27 51	04 29 22.5 +24 21 10	5.2×181.7	171.4	20.8 HDR
24245504	462	2007 Oct 16	04 27 39.0 +27 20 10	04 27 44.8 +27 13 30	5.2×181.7	170.4	20.8 HDR
24245760	462	2007 Oct 16	04 26 41.6 +24 24 58	04 26 47.0 +24 18 17	5.2×181.7	171.1	20.8 HDR
24246016	462	2007 Oct 16	04 24 57.8 +27 22 29	04 25 04.0 +27 15 49	5.2×181.7	170.0	20.8 HDR
24246272	462	2007 Oct 16	04 21 57.7 +27 39 52	04 22 04.0 +27 33 11	5.2×46.2	169.7	20.8 HDR
24246528	462	2007 Oct 16	04 21 32.2 +28 24 39	04 21 38.8 +28 18 00	5.2×46.2	169.3	20.8 HDR
24246784	462	2007 Oct 16	04 34 18.8 +27 53 56	04 34 24.4 +27 47 14	10.0×41.4	81.1	20.8 HDR
24242944	462	2007 Oct 23	04 22 07.1 +24 47 19	04 22 12.9 +24 40 38	5.2×51.0	80.5	20.8 HDR
26472448	50584	2008 Oct 31	04 16 27.1 +20 52 57	04 16 27.1 +20 52 57	6.0×6.0	81.3	41.6 HDR
			04 16 23.9 +20 59 57	04 16 32.3 +20 46 20	6.0×6.0	81.3	41.6 HDR
26475008	50584	2008 Oct 31	04 27 07.2 +22 14 55	04 27 07.2 +22 14 55	6.0×6.0	82.0	41.6 HDR
			04 27 00.0 +22 21 55	04 27 12.4 +22 08 10	6.0×6.0	82.0	41.6 HDR
			04 26 44.9 +21 31 52	04 26 44.9 +21 31 52	6.0×6.0	82.0	41.6 HDR
			04 27 12.4 +22 08 10	04 26 49.6 +21 25 10	6.0×6.0	82.0	41.6 HDR
26476800	50584	2008 Oct 31	05 02 37.4 +21 54 18	05 02 37.4 +21 54 18	6.0×6.0	86.0	41.6 HDR
			05 02 36.6 +22 00 56	05 02 40.5 +21 47 28	6.0×6.0	86.0	41.6 HDR
			05 06 46.5 +21 04 20	05 06 46.5 +21 04 20	6.0×6.0	86.0	41.6 HDR
			05 06 41.6 +21 11 39	05 06 49.4 +20 57 24	6.0×6.0	86.0	41.6 HDR
26476544	50584	2008 Nov 1	04 55 45.1 +30 36 10	04 55 49.7 +30 29 38	18.0×9.5	82.5	41.6 HDR
26472960	50584	2008 Nov 2	04 16 55.8 +31 40 49	04 16 55.8 +31 40 49	6.0×6.0	77.0	41.6 HDR
			04 16 47.4 +31 47 10	04 17 04.2 +31 34 16	6.0×6.0	77.0	41.6 HDR
			04 24 27.7 +31 03 40	04 24 27.7 +31 03 40	6.0×6.0	77.0	41.6 HDR
			04 24 21.2 +31 10 09	04 24 35.5 +30 57 08	6.0×6.0	77.0	41.6 HDR
			04 21 17.3 +30 51 50	04 21 17.3 +30 51 50	6.0×6.0	77.0	41.6 HDR
			04 24 35.5 +30 57 08	04 21 25.1 +30 45 23	6.0×6.0	77.0	41.6 HDR
			04 16 30.5 +30 37 15	04 16 30.5 +30 37 15	6.0×6.0	77.0	41.6 HDR
			04 21 25.1 +30 45 23	04 16 38.3 +30 30 42	6.0×6.0	77.0	41.6 HDR
26475520	50584	2008 Nov 2	04 40 53.4 +20 55 44	04 40 53.4 +20 55 44	6.0×6.0	84.0	41.6 HDR
			04 40 51.6 +21 02 39	04 40 57.0 +20 49 04	6.0×6.0	84.0	41.6 HDR

TABLE 1 — *Continued*

AOR	PID	Date (UT)	3.6/5.8 Center (J2000)	4.5/8.0 Center (J2000)	Dimensions (arcmin)	Angle[a] (deg)	Exp Time[b] (s)

[a] Position angle of the long axis of the map.
[b] Total exposure time for each position and filter. "HDR" indicates that 0.4 s exposures were also obtained.

TABLE 2
MIPS 24 μm Observing Log

AOR	PID	Date (UT)	Center (J2000)	Dimensions (arcmin)	Angle[a] (deg)	Exp Time (s)
3662080	6	2004 Feb 20	04 31 40.6 +18 08 45	30.5×54	170.7	40
5675776	173	2004 Sep 18	04 20 24.3 +31 23 26	7.4×8.2	167.9	277
			04 20 07.3 +31 35 21	5.6×8	167.9	357
5680384	173	2004 Sep 18	04 33 34.6 +24 21 09	7.4×8.2	171.0	36
			04 33 21.6 +24 33 15	5.6×8	171.0	31
5675264	173	2004 Sep 19	04 17 39.0 +28 33 03	7.4×8.2	168.2	73
			04 17 22.8 +28 45 00	5.6×8	168.2	357
5676032	173	2004 Sep 19	04 21 58.9 +28 18 07	7.4×8.2	168.8	36
			04 21 43.3 +28 30 06	5.6×8	168.8	344
5676288	173	2004 Sep 19	04 22 03.2 +28 25 40	7.4×8.2	168.8	34
			04 21 47.6 +28 37 39	5.6×8	168.8	357
9426432	139	2004 Sep 19	04 23 34.7 +26 37 32	5.6×10.8	169.3	26
			04 23 17.5 +26 51 59	6×10	169.3	80
5673728	173	2004 Sep 22	04 05 19.7 +20 09 26	7.4×8.2	169.3	36
			04 05 05.5 +20 21 27	5.6×8	169.3	357
5674240	173	2004 Sep 22	04 09 17.2 +17 16 10	7.4×8.2	170.7	73
			04 09 04.5 +17 28 14	5.6×8	170.7	357
9422848	139	2004 Sep 22	04 23 43.5 +26 37 48	5.6×10.8	169.2	26
			04 23 26.1 +26 52 15	6×10	169.2	80
3662336	6	2004 Sep 23	04 18 37.0 +28 22 13	32.5×56	168.5	80
3662592	6	2004 Sep 23	04 16 32.9 +28 19 58	32.5×54	168.3	80
5678848	173	2004 Sep 23	04 32 09.4 +17 57 24	7.4×8.2	172.6	110
			04 31 58.3 +18 09 35	5.6×8	172.6	357
			04 35 34.2 +17 51 42	7.4×8.2	172.9	110
			04 35 23.5 +18 03 54	5.6×8	172.9	357
12026368	53	2004 Sep 23	04 43 27.5 +29 42 54	13.4×55.0	171.4	161
12026624	53	2004 Sep 23	04 10 49.6 +25 11 53	16.0×55.0	168.5	161
9409536	139	2004 Sep 24	04 29 32.9 +26 56 19	5.6×10.8	169.6	26
			04 29 16.0 +27 10 47	6×10	169.6	80
9415168	139	2004 Sep 24	04 40 53.6 +26 09 03	7.4×18.2	171.2	36
			04 40 40.6 +26 21 10	5.6×13	171.2	200
9416448	139	2004 Sep 24	04 42 38.0 +29 45 10	7.4×18.2	170.6	36
			04 42 23.9 +29 57 14	5.6×13	170.6	200
9431040	139	2004 Sep 24	04 28 34.9 +26 52 15	7.4×18.2	169.5	36
			04 28 20.2 +27 04 16	5.6×13	169.5	200
5673984	173	2004 Sep 25	04 05 31.0 +21 51 12	7.4×8.2	168.7	415
			04 05 16.1 +22 03 10	5.6×8	168.7	357
5674752	173	2004 Sep 25	04 12 50.8 +19 36 59	7.4×8.2	170.4	110
			04 12 37.6 +19 49 03	5.6×8	170.4	357
5675520	173	2004 Sep 25	04 18 51.7 +17 23 16	7.4×8.2	171.8	110
			04 18 40.0 +17 35 25	5.6×8	171.8	357
5676544	173	2004 Sep 25	04 24 48.7 +26 43 14	7.4×8.2	169.1	36
			04 24 33.6 +26 55 14	5.6×8	169.1	119
5676800	173	2004 Sep 25	04 27 10.7 +17 50 43	7.4×8.2	172.4	36
			04 26 59.4 +18 02 53	5.6×8	172.4	357
5677056	173	2004 Sep 25	04 29 42.1 +26 32 56	7.4×8.2	169.8	36
			04 29 27.7 +26 44 57	5.6×8	169.8	119
5677312	173	2004 Sep 25	04 30 04.1 +18 13 50	7.4×8.2	172.5	36
			04 29 52.9 +18 26 00	5.6×8	172.5	357
5677824	173	2004 Sep 25	04 30 51.5 +24 42 24	7.4×8.2	170.5	73
			04 30 37.9 +24 54 28	5.6×8	170.5	94
5678080	173	2004 Sep 25	04 31 22.6 +24 10 56	7.4×8.2	170.7	73
			04 31 09.3 +24 23 00	5.6×8	170.7	357
5678336	173	2004 Sep 25	04 31 27.3 +17 06 26	7.4×8.2	173.0	277
			04 31 16.6 +17 18 38	5.6×8	173.0	357
5678592	173	2004 Sep 25	04 31 57.8 +18 21 38	7.4×8.2	172.6	219
			04 31 50.7 +18 23 57	5.6×8	172.6	312
5679104	173	2004 Sep 25	04 32 18.9 +24 22 29	7.4×8.2	170.7	36
			04 32 05.6 +24 34 34	5.6×8	170.7	357
5679360	173	2004 Sep 25	04 32 43.9 +18 02 59	7.4×8.2	172.8	139
			04 32 33.0 +18 15 10	5.6×8	172.8	357
5679616	173	2004 Sep 25	04 32 53.4 +17 35 35	7.4×8.2	172.9	73
			04 32 42.7 +17 47 47	5.6×8	172.9	357
5680896	173	2004 Sep 25	04 36 19.2 +25 43 00	7.4×8.2	170.8	73
			04 36 05.8 +25 55 06	5.6×8	170.8	357

TABLE 2 — *Continued*

AOR	PID	Date (UT)	Center (J2000)	Dimensions (arcmin)	Angle[a] (deg)	Exp Time (s)
5682432	173	2004 Sep 25	04 42 05.6 +25 22 58	7.4×8.2	171.6	36
			04 41 53.0 +25 35 06	5.6×8	171.6	357
5683200	173	2004 Sep 25	04 56 02.3 +30 21 04	7.4×8.2	172.1	36
			04 55 49.6 +30 33 13	5.6×8	172.1	357
5684480	173	2004 Sep 25	05 03 06.7 +25 23 21	7.4×8.2	173.9	73
			05 02 56.3 +25 35 35	5.6×8	173.9	357
9413376	139	2004 Sep 25	04 41 36.6 +26 01 29	7.4×18.2	171.3	36
			04 41 23.7 +26 13 36	5.6×13	171.3	200
9413888	139	2004 Sep 25	04 29 41.7 +26 56 35	5.6×10.8	169.6	26
			04 29 24.8 +27 11 03	6×10	169.6	80
9414144	139	2004 Sep 25	04 32 42.9 +24 49 47	5.6×10.8	170.6	26
			04 32 27.4 +25 04 19	6×10	170.6	80
9415424	139	2004 Sep 25	04 41 29.6 +26 01 18	7.4×18.2	171.3	36
			04 41 16.7 +26 13 24	5.6×13	171.3	200
9417984	139	2004 Sep 25	04 41 47.6 +25 42 29	7.4×18.2	171.4	36
			04 41 34.8 +25 54 36	5.6×13	171.4	200
9419776	139	2004 Sep 25	04 28 42.1 +26 52 28	7.4×18.2	169.5	36
			04 28 27.4 +27 04 29	5.6×13	169.5	200
9425152	139	2004 Sep 25	04 41 00.6 +26 09 16	7.4×18.2	171.2	36
			04 40 47.6 +26 21 22	5.6×13	171.2	200
9425920	139	2004 Sep 25	04 30 04.4 +24 23 18	5.6×10.8	170.5	26
			04 29 48.8 +24 37 50	6×10	170.5	80
9427712	139	2004 Sep 25	04 32 45.3 +24 24 07	7.4×18.2	170.8	36
9428992	139	2004 Sep 25	04 41 13.6 +25 49 35	7.4×18.2	171.3	36
			04 41 00.7 +26 01 42	5.6×13	171.3	200
9430528	139	2004 Sep 25	04 42 39.4 +29 42 23	7.4×18.2	170.5	36
			04 42 25.2 +29 54 27	5.6×13	170.5	200
9432832	139	2004 Sep 25	04 32 52.3 +24 24 20	7.4×18.2	170.8	36
			04 32 39.1 +24 36 25	5.6×13	170.8	200
9434624	139	2004 Sep 25	04 41 06.6 +25 49 24	7.4×18.2	171.3	36
			04 40 53.7 +26 01 30	5.6×13	171.3	200
9434880	139	2004 Sep 25	04 32 34.1 +24 49 30	5.6×10.8	170.6	26
			04 32 18.6 +25 04 02	6×10	170.6	80
9435136	139	2004 Sep 25	04 41 40.6 +25 42 18	7.4×18.2	171.4	36
			04 41 27.8 +25 54 25	5.6×13	171.4	200
9435392	139	2004 Sep 25	04 31 52.8 +24 32 39	7.4×18.2	170.6	36
			04 31 39.4 +24 44 43	5.6×13	170.6	200
9439488	139	2004 Sep 25	04 31 59.8 +24 32 52	7.4×18.2	170.6	36
			04 31 46.4 +24 44 56	5.6×13	170.6	200
9410816	139	2004 Sep 26	04 30 13.2 +24 23 35	5.6×10.8	170.5	26
			04 29 57.6 +24 38 06	6×10	170.5	80
5682944	173	2004 Oct 12	04 55 37.1 +30 17 56	7.4×8.2	169.9	36
			04 55 22.3 +30 29 58	5.6×8	169.9	357
5683712	173	2004 Oct 13	04 57 30.7 +20 14 30	7.4×8.2	175.6	73
			04 57 22.2 +20 26 48	5.6×8	175.6	357
5683968	173	2004 Oct 13	04 58 39.9 +20 46 45	7.4×8.2	175.4	400
			04 58 31.2 +20 59 02	5.6×8	175.4	357
5681152	173	2005 Feb 25	04 37 26.7 +18 51 24	7.4×8.2	170.6	73
			04 37 39.6 +18 39 20	5.6×8	170.6	357
5705984	173	2005 Feb 25	04 38 12.9 +20 22 45	7.4×8.2	171.0	139
			04 38 25.5 +20 10 40	5.6×8	171.0	357
5673472	173	2005 Feb 26	04 03 49.1 +26 10 52	7.4×8.2	168.9	139
			04 04 04.2 +25 58 54	5.6×8	168.9	357
5675008	173	2005 Feb 26	04 14 47.9 +27 52 33	7.4×8.2	170.4	36
			04 15 01.9 +27 40 30	5.6×8	170.4	357
			04 13 14.0 +28 19 09	7.4×8.2	170.3	36
			04 13 28.2 +28 07 06	5.6×8	170.3	357
			04 19 41.2 +27 49 38	7.4×8.2	170.9	36
			04 19 54.7 +27 37 32	5.6×8	170.9	357
5677568	173	2005 Feb 26	04 30 29.5 +24 26 44	7.4×8.2	171.3	292
			04 30 37.2 +24 24 28	5.6×8	171.3	312
5679872	173	2005 Feb 26	04 33 06.5 +24 09 44	7.4×8.2	171.5	36
			04 33 19.0 +23 57 36	5.6×8	171.5	357
5680128	173	2005 Feb 26	04 33 09.9 +24 33 42	7.4×8.2	171.6	36
			04 33 22.4 +24 21 34	5.6×8	171.6	357
			04 34 39.2 +25 01 00	7.4×8.2	171.9	36
			04 34 51.5 +24 48 51	5.6×8	171.9	357
5680640	173	2005 Feb 26	04 35 56.8 +23 52 04	7.4×8.2	171.7	73
			04 36 09.1 +23 39 56	5.6×8	171.7	357
5681920	173	2005 Feb 26	04 41 04.6 +24 51 06	7.4×8.2	172.5	36
			04 41 16.3 +24 38 56	5.6×8	172.5	357
5682176	173	2005 Feb 26	04 41 08.3 +25 56 06	7.4×8.2	172.7	73
			04 41 19.8 +25 43 55	5.6×8	172.7	110
			04 38 35.1 +26 10 38	7.4×8.2	172.5	73
			04 38 46.9 +25 58 27	5.6×8	172.5	120
5682688	173	2005 Feb 26	04 52 30.7 +17 30 25	7.4×8.2	171.3	36

Luhman et al.

TABLE 2 — *Continued*

AOR	PID	Date (UT)	Center (J2000)	Dimensions (arcmin)	Angle[a] (deg)	Exp Time (s)
			04 52 42.8 +17 18 18	5.6×8	171.3	357
			04 52 50.1 +16 22 09	7.4×8.2	171.0	36
			04 53 02.4 +16 10 03	5.6×8	171.0	357
9412096	139	2005 Feb 26	04 35 55.7 +24 12 07	5.6×10.8	171.8	26
			04 36 09.8 +23 57 31	6×10	171.8	80
9433856	139	2005 Feb 26	04 35 47.1 +24 11 51	5.6×10.8	171.8	26
			04 36 01.2 +23 57 15	6×10	171.8	80
11229184	3584	2005 Feb 27	04 24 44.8 +25 37 18	35.6×385.3	171.7	15.5
11229440	3584	2005 Feb 27	04 24 33.3 +25 36 36	35.6×385.3	171.7	15.5
12915200	3584	2005 Feb 27	04 33 11.0 +28 57 12	55.8×85.2	173.3	15.5
12915456	3584	2005 Feb 27	04 32 56.3 +29 03 13	55.8×85.2	173.3	15.5
11225600	3584	2005 Feb 28	04 48 00.4 +25 01 29	65.8×186.3	174.0	15.5
11225856	3584	2005 Feb 28	04 47 50.6 +25 00 50	65.8×186.3	174.0	15.5
11226112	3584	2005 Feb 28	04 43 18.9 +25 09 17	65.8×186.3	173.5	15.5
11226368	3584	2005 Feb 28	04 43 09.5 +25 09 03	65.8×186.3	173.5	15.5
11228672	3584	2005 Feb 28	04 27 18.4 +25 42 06	35.6×385.3	171.9	15.5
11229696	3584	2005 Feb 28	04 19 46.7 +27 49 16	60.7×85.2	171.5	15.5
11229952	3584	2005 Feb 28	04 19 57.8 +27 49 22	60.7×85.2	171.5	15.5
3662848	6	2005 Mar 1	04 14 28.6 +28 13 09	32.5×54	170.8	80
11227136	3584	2005 Mar 1	04 35 39.5 +25 20 26	40.6×311.3	172.7	15.5
11227392	3584	2005 Mar 1	04 35 28.4 +25 19 50	40.6×311.3	172.7	15.5
11227648	3584	2005 Mar 1	04 32 27.8 +25 51 48	35.6×385.3	172.4	15.5
11228928	3584	2005 Mar 1	04 27 08.0 +25 41 27	35.6×385.3	171.9	15.5
11227904	3584	2005 Mar 2	04 32 17.7 +25 51 07	35.6×385.3	172.4	15.5
11228160	3584	2005 Mar 2	04 29 53.7 +25 46 57	35.6×385.3	172.1	15.5
11228416	3584	2005 Mar 2	04 29 43.2 +25 46 17	35.6×385.3	172.1	15.5
5681408	173	2005 Mar 3	04 38 38.9 +15 46 13	7.4×8.2	170.6	34
			04 38 51.6 +15 34 08	5.6×8	170.6	357
			04 45 51.2 +15 55 49	7.4×8.2	171.1	36
			04 46 03.5 +15 43 43	5.6×8	171.1	357
11226624	3584	2005 Mar 4	04 38 51.4 +25 32 39	50.7×253.8	172.9	15.5
11226880	3584	2005 Mar 5	04 38 40.0 +25 32 02	50.7×253.8	172.9	15.5
12662784	37	2005 Mar 5	04 55 35.8 +30 35 05	17.8×56.0	175.5	80
12663296	37	2005 Mar 6	04 04 42.9 +26 18 53	7.4×8.2	168.4	36
			04 04 58.4 +26 06 56	5.6×8.0	168.4	31
			04 03 50.8 +26 10 50	7.4×8.2	168.4	36
			04 04 06.5 +25 58 55	5.6×8.0	168.4	31
			04 03 13.9 +25 52 56	7.4×8.2	168.4	36
			04 03 29.6 +25 41 01	5.6×8.0	168.4	31
14614016	20386	2005 Sep 25	04 30 08.8 +24 23 29	5.6×10.8	170.6	292
14617344	20386	2005 Sep 25	04 32 50.4 +24 22 47	5.6×10.8	171.0	292
14613760	20386	2005 Sep 26	04 23 39.1 +26 37 42	5.6×10.8	169.5	292
14618368	20386	2005 Sep 26	04 21 58.4 +15 27 20	5.6×10.8	172.0	297
14618624	20386	2005 Sep 26	04 21 58.4 +15 27 30	5.6×10.8	172.0	297
12615168	6	2006 Feb 19	04 31 40.9 +18 08 44	32.5×56.0	169.3	80
14511872	20302	2006 Feb 26	04 35 09.4 +24 06 46	25.7×56.0	172.5	200
18966528	30765	2006 Oct 9	04 31 37.3 +24 36 23	5.6×8.0	170.7	950
19026944	30816	2007 Feb 23	04 19 13.5 +29 07 36	50.7×85.2	174.2	15.5
19027456	30816	2007 Feb 23	04 19 02.3 +29 07 05	50.7×85.2	174.1	15.5
19029248	30816	2007 Feb 23	04 17 48.1 +26 32 11	35.6×385.3	172.6	15.5
19032832	30816	2007 Feb 23	04 17 37.2 +26 31 36	35.6×385.3	172.5	15.5
14510592	20302	2007 Feb 24	04 29 16.9 +26 11 41	25.7×56.0	173.4	200
19029504	30816	2007 Feb 26	04 15 01.2 +26 42 11	35.6×385.3	172.1	15.5
19032320	30816	2007 Feb 26	04 35 41.8 +22 14 49	111×85.2	171.7	15.5
19033088	30816	2007 Feb 27	04 14 50.3 +26 41 35	35.6×385.3	172.0	15.5
19035904	30816	2007 Feb 27	04 35 31.3 +22 14 12	111×85.2	171.7	15.5
19026688	30816	2007 Feb 28	04 22 20.6 +24 43 29	50.7×253.8	171.9	15.5
19027200	30816	2007 Feb 28	04 22 03.6 +24 52 49	50.7×253.8	171.8	15.5
18152960	30384	2007 Sep 23	04 21 55.3 +15 32 11	14.7×56.0	170.4	161
18153728	30384	2007 Sep 23	04 23 35.3 +26 42 31	14.7×56.0	171.3	161
18153984	30384	2007 Sep 23	04 30 04.2 +24 27 38	14.7×56.0	171.8	161
18154240	30384	2007 Sep 23	04 31 56.2 +24 34 53	14.7×56.0	172.0	161
18154496	30384	2007 Sep 24	04 32 37.6 +24 25 52	14.7×56.0	172.0	161
18155264	30384	2007 Sep 24	04 41 08.8 +25 45 55	14.7×56.0	173.0	161
18153216	30384	2007 Sep 25	04 28 38.4 +26 54 00	14.7×56.0	171.7	161
18155008	30384	2007 Sep 25	04 41 51.4 +25 50 15	14.7×56.0	173.1	161
18155520	30384	2007 Sep 25	04 42 37.4 +29 46 10	14.7×56.0	173.6	161
24248064	462	2007 Sep 27	04 34 01.6 +28 00 12	40.6×85.2	172.3	15.5
24248320	462	2007 Sep 27	04 34 12.8 +28 00 17	40.6×85.2	172.3	15.5
24247552	462	2007 Sep 29	04 20 06.0 +24 56 09	10.5×186.3	170.6	15.5
24247808	462	2007 Sep 29	04 20 06.2 +24 55 53	10.5×186.3	170.6	15.5
24248576	462	2007 Oct 27	04 33 57.1 +25 09 21	7.8×253.8	171.0	15.5
24247040	462	2007 Oct 28	04 20 29.2 +27 15 22	60.7×85.2	168.1	15.5
24247296	462	2007 Oct 28	04 20 40.3 +27 15 36	60.7×85.2	168.1	15.5
23273728	40844	2007 Oct 29	04 19 58.6 +28 33 24	5.6×8.0	167.7	594
23273984	40844	2007 Oct 29	04 20 08.3 +28 31 15	5.6×8.0	166.7	475

TABLE 2 — *Continued*

AOR	PID	Date (UT)	Center (J2000)	Dimensions (arcmin)	Angle[a] (deg)	Exp Time (s)
23274240	40844	2007 Oct 29	04 20 08.8 +28 16 01	5.6×8.0	166.8	475
23276544	40844	2007 Oct 29	04 25 16.3 +28 33 18	5.6×8.0	167.4	594
23277056	40844	2007 Oct 29	04 26 18.3 +28 27 40	5.6×8.0	167.6	594
18155776	30384	2008 Apr 17	05 04 17.4 +25 08 26	14.7×56.0	174.9	161

[a] Position angle of the long axis of the map.

TABLE 3
IRAC Aperture Corrections

Band	2/14/15[a]	3/3/4[a]	4/4/5[a]	4/4/10[a]
[3.6]	0.450	0.270	0.180[b]	⋯
[4.5]	0.485	0.300	0.170[b]	⋯
[5.8]	0.645	0.515	⋯	0.165[b]
[8.0]	0.750	0.735	⋯	0.260[b]

[a] Aperture radius and inner and outer radii of the sky annulus in pixels (1 pixel = 0″.86).
[b] Default aperture and sky annulus.

TABLE 4
IRAC Photometry for Members of Taurus

2MASS[a]	Name	[3.6]	[4.5]	[5.8]	[8.0]	Date
J04034930+2610520	HBC 358 A+B+C	9.15±0.02	9.11±0.02	9.05±0.03	9.05±0.03	2005 Feb 20
J04034997+2620382	XEST 06-006	out	out	out	out	⋯
J04035084+2610531	HBC 359	9.33±0.02	9.26±0.02	9.23±0.03	9.23±0.03	2005 Feb 20
J04043936+2158186	HBC 360	9.71±0.02	9.69±0.02	9.62±0.03	9.62±0.03	2004 Feb 11
J04043984+2158215	HBC 361	9.87±0.02	9.81±0.02	9.76±0.03	9.76±0.03	2004 Feb 11
J04044307+2618563	IRAS 04016+2610	6.76±0.02	5.46±0.02	4.42±0.03	3.56±0.03	2005 Feb 20
J04053087+2151106	HBC 362	9.83±0.02	9.82±0.02	9.76±0.03	9.75±0.03	2005 Feb 22
J04080782+2807280	⋯	out	out	out	out	⋯
J04131414+2819108	LkCa 1	8.47±0.02	8.47±0.02	8.40±0.03	8.40±0.03	2005 Feb 20
		8.52±0.02	8.45±0.02	8.39±0.03	8.44±0.03	2007 Mar 29
J04132722+2816247	Anon 1	7.18±0.02	7.16±0.02	7.13±0.03	7.07±0.03	2005 Feb 19
		7.23±0.02	7.18±0.02	7.10±0.03	7.07±0.03	2005 Feb 20
		7.22±0.02	7.18±0.02	7.10±0.03	7.07±0.03	2007 Mar 29
J04135328+2811233	IRAS 04108+2803 A	8.98±0.02	8.34±0.02	7.75±0.03	6.70±0.03	2005 Feb 19
		8.97±0.02	8.34±0.02	7.62±0.03	6.52±0.03	2007 Mar 29
J04135471+2811328	IRAS 04108+2803 B	9.28±0.02	7.94±0.02	6.81±0.03	5.81±0.03	2005 Feb 19
		9.32±0.02	8.02±0.02	7.08±0.03	5.87±0.03	2007 Mar 29
J04135737+2918193	IRAS 04108+2910	7.90±0.02	7.26±0.02	6.70±0.03	5.96±0.03	2005 Feb 20
		7.46±0.02	6.74±0.02	6.22±0.03	5.49±0.03	2007 Mar 29
J04141188+2811535	⋯	10.82±0.02	10.27±0.02	9.80±0.03	8.89±0.03	2005 Feb 19
		11.01±0.02	10.35±0.02	9.88±0.03	8.99±0.03	2007 Mar 29
⋯	IRAS 04111+2800G	13.02±0.02	11.82±0.02	11.20±0.03	10.49±0.03	2005 Feb 19
		13.15±0.02	11.84±0.02	11.10±0.03	10.36±0.03	2007 Mar 29
J04141291+2812124	V773 Tau A+B	6.00±0.02	5.53±0.02	5.08±0.03	4.41±0.03	2005 Feb 19
		6.00±0.02	5.55±0.02	5.05±0.03	4.36±0.03	2007 Mar 29
J04141358+2812492	FM Tau	7.82±0.02	7.40±0.02	7.13±0.03	6.22±0.03	2005 Feb 19
		8.10±0.02	7.63±0.02	7.28±0.03	6.39±0.03	2007 Mar 29
J04141458+2827580	FN Tau	7.46±0.02	6.97±0.02	6.53±0.03	5.57±0.03	2005 Feb 19
		7.55±0.02	7.11±0.02	6.64±0.03	5.84±0.03	2007 Mar 29
J04141700+2810578	CW Tau	sat	5.23±0.02	4.79±0.03	4.31±0.03	2005 Feb 19
		5.86±0.02	5.38±0.02	4.98±0.03	4.39±0.03	2007 Mar 29
J04141760+2806096	CIDA 1	8.48±0.02	7.84±0.02	7.40±0.03	6.53±0.03	2005 Feb 19
		8.64±0.02	8.10±0.02	7.59±0.03	6.57±0.03	2007 Mar 29
J04142626+2806032	MHO 1	6.63±0.05	5.78±0.05	5.20±0.05	4.52±0.05	2005 Feb 19
		6.00±0.05	5.18±0.05	4.63±0.05	3.90±0.05	2007 Mar 29
J04142639+2805597	MHO 2	7.21±0.05	6.49±0.05	5.87±0.05	5.02±0.05	2005 Feb 19
		7.50±0.05	6.61±0.05	5.92±0.05	4.99±0.05	2007 Mar 29
J04143054+2805147	MHO 3	7.40±0.02	6.84±0.02	6.26±0.03	5.11±0.03	2005 Feb 19
		7.21±0.02	6.44±0.02	5.69±0.03	4.57±0.03	2007 Mar 29
J04144730+2646264	FP Tau	8.47±0.02	8.25±0.02	7.86±0.03	7.25±0.03	2004 Feb 10
		8.07±0.02	7.78±0.02	7.58±0.03	7.28±0.03	2007 Mar 29
J04144739+2803055	XEST 20-066	9.78±0.02	9.55±0.02	9.59±0.03	9.53±0.03	2005 Feb 19
		9.61±0.02	9.58±0.02	9.50±0.03	9.50±0.03	2007 Mar 29
J04144786+2648110	CX Tau	8.41±0.02	8.06±0.02	7.62±0.03	6.64±0.03	2004 Feb 10
		8.51±0.02	8.01±0.02	7.64±0.03	6.62±0.03	2007 Mar 29

TABLE 4 — *Continued*

2MASS[a]	Name	[3.6]	[4.5]	[5.8]	[8.0]	Date
J04144797+2752346	LkCa 3 A+B	7.35±0.02	7.28±0.02	7.24±0.03	7.23±0.03	2005 Feb 20
		7.26±0.02	7.28±0.02	7.22±0.03	7.22±0.03	2007 Mar 29
J04144928+2812305	FO Tau A+B	7.66±0.02	7.12±0.02	6.81±0.03	5.84±0.03	2005 Feb 19
		7.47±0.02	7.09±0.02	6.72±0.03	5.88±0.03	2007 Mar 29
J04145234+2805598	XEST 20-071	7.41±0.02	7.34±0.02	7.28±0.03	7.24±0.03	2005 Feb 19
		7.40±0.02	7.36±0.02	7.24±0.03	7.21±0.03	2007 Mar 29
J04150515+2808462	CIDA 2	8.83±0.02	8.74±0.02	8.68±0.03	8.70±0.03	2005 Feb 19
		out	8.73±0.02	out	8.64±0.03	2005 Feb 20
		8.83±0.02	8.69±0.02	8.67±0.03	8.78±0.03	2007 Mar 29
J04151471+2800096	KPNO 1	13.21±0.02	out	13.03±0.05	out	2005 Feb 19
		13.19±0.02	13.06±0.02	13.10±0.04	12.81±0.06	2005 Feb 20
		13.18±0.02	13.04±0.02	13.09±0.05	13.09±0.07	2007 Mar 29
J04152409+2910434	⋯	11.85±0.02	11.71±0.02	11.65±0.03	11.60±0.03	2006 Sep 28
		11.81±0.02	11.71±0.02	11.62±0.03	11.50±0.04	2007 Mar 29
J04153916+2818586	⋯	8.67±0.02	8.38±0.02	8.45±0.03	7.53±0.03	2005 Feb 19
		8.73±0.02	8.43±0.02	8.23±0.03	7.53±0.03	2007 Mar 29
J04154278+2909597	IRAS 04125+2902	9.09±0.02	9.06±0.02	8.97±0.03	9.05±0.03	2007 Mar 29
J04155799+2746175	⋯	9.71±0.02	9.37±0.02	9.04±0.03	8.36±0.03	2007 Mar 29
J04161210+2756385	⋯	9.35±0.02	8.99±0.02	8.69±0.03	8.29±0.03	2007 Mar 29
J04161885+2752155	⋯	10.92±0.02	10.74±0.02	10.64±0.03	10.68±0.03	2007 Mar 29
J04162725+2053091	⋯	10.77±0.02	10.67±0.02	10.65±0.03	10.59±0.03	2008 Oct 31
J04162810+2807358	LkCa 4	8.26±0.02	8.06±0.02	8.04±0.03	7.97±0.03	2005 Feb 19
		8.19±0.02	8.17±0.02	7.99±0.03	8.03±0.03	2007 Mar 29
J04163048+3037053	⋯	12.29±0.02	12.17±0.02	12.16±0.03	12.23±0.04	2008 Nov 2
J04163911+2858491	⋯	10.46±0.02	10.07±0.02	9.82±0.03	9.41±0.03	2007 Mar 29
J04173372+2820468	CY Tau	7.96±0.02	7.62±0.02	7.30±0.03	6.74±0.03	2005 Feb 19
		7.94±0.02	7.71±0.02	7.25±0.03	6.69±0.03	2005 Feb 21
		7.63±0.02	7.25±0.02	7.02±0.03	6.48±0.03	2007 Mar 29
J04173893+2833005	LkCa 5	out	8.85±0.02	out	8.76±0.03	2005 Feb 19
		8.88±0.02	8.84±0.02	8.80±0.03	8.76±0.03	2005 Feb 20
		8.90±0.02	out	8.78±0.03	out	2007 Mar 29
J04174955+2813318	KPNO 10	10.79±0.02	10.32±0.02	9.80±0.03	8.84±0.03	2005 Feb 19
		10.79±0.02	10.29±0.02	9.88±0.03	8.81±0.03	2005 Feb 21
		10.80±0.02	out	out	out	2007 Mar 29
J04174965+2829362	V410 X-ray 1	8.17±0.02	7.73±0.02	7.25±0.03	6.42±0.03	2005 Feb 19
		out	7.76±0.02	out	6.42±0.03	2005 Feb 21
		8.41±0.02	out	7.39±0.03	out	2007 Mar 29
J04180796+2826036	V410 X-ray 3	9.99±0.02	9.85±0.02	9.86±0.03	9.82±0.03	2005 Feb 19
		9.96±0.02	9.91±0.02	9.88±0.03	9.81±0.03	2005 Feb 21
		9.99±0.02	out	9.78±0.03	out	2007 Mar 29
J04181078+2519574	V409 Tau	8.05±0.02	7.70±0.02	7.25±0.03	6.30±0.03	2007 Mar 30
J04181710+2828419	V410 Anon 13	10.24±0.02	9.81±0.02	9.46±0.03	8.81±0.03	2005 Feb 19
		out	9.92±0.02	out	8.80±0.03	2005 Feb 21
		10.20±0.02	out	9.47±0.03	out	2007 Mar 29
J04182147+1658470	HBC 372	10.39±0.02	10.39±0.02	10.40±0.03	10.33±0.03	2004 Mar 8
J04182909+2826191	V410 Anon 25	8.87±0.02	8.58±0.02	8.38±0.03	8.40±0.03	2005 Feb 19
		8.89±0.02	8.56±0.02	8.41±0.03	8.37±0.03	2005 Feb 21
		8.92±0.02	out	8.31±0.03	out	2007 Mar 29
J04183030+2743208	KPNO 11	10.66±0.02	10.54±0.02	10.55±0.03	10.49±0.03	2005 Feb 21
J04183110+2827162	V410 Tau A+B+C	7.40±0.02	7.29±0.02	7.31±0.03	7.20±0.03	2005 Feb 19
		7.31±0.02	7.31±0.02	7.34±0.03	7.24±0.03	2005 Feb 21
		7.37±0.02	out	7.29±0.03	out	2007 Mar 29
J04183112+2816290	DD Tau A+B	6.54±0.02	5.72±0.02	5.19±0.03	4.41±0.03	2005 Feb 19
		6.45±0.02	5.78±0.02	5.23±0.03	4.42±0.03	2005 Feb 21
J04183158+2816585	CZ Tau A+B	8.47±0.02	7.60±0.02	6.57±0.03	5.00±0.03	2005 Feb 19
		8.46±0.02	7.55±0.02	6.63±0.03	4.95±0.03	2005 Feb 21
J04183203+2831153	IRAS 04154+2823	7.89±0.02	7.03±0.02	6.31±0.03	5.51±0.03	2005 Feb 19
		out	6.99±0.02	out	5.47±0.03	2005 Feb 21
		7.55±0.02	out	6.06±0.03	out	2007 Mar 29
J04183444+2830302	V410 X-ray 2	8.22±0.02	8.06±0.02	7.84±0.03	7.50±0.03	2005 Feb 19
		out	8.04±0.02	out	7.66±0.03	2005 Feb 21
		8.30±0.02	out	7.77±0.03	out	2007 Mar 29
J04184023+2824245	V410 X-ray 4	8.83±0.02	8.64±0.02	8.47±0.03	8.41±0.03	2005 Feb 19
		8.85±0.02	8.58±0.02	8.55±0.03	8.41±0.03	2005 Feb 21
J04184061+2819155	V892 Tau	sat	sat	3.56±0.03	sat	2005 Feb 19
		sat	sat	3.56±0.03	sat	2005 Feb 21
J04184133+2827250	LR1	9.38±0.02	8.86±0.02	8.40±0.03	7.95±0.03	2005 Feb 19
		9.45±0.02	8.82±0.02	8.42±0.03	7.97±0.03	2005 Feb 21
		9.38±0.02	out	8.35±0.03	out	2007 Mar 29
J04184250+2818498	V410 X-ray 7	8.74±0.02	8.59±0.02	8.38±0.03	8.08±0.04	2005 Feb 19
		8.86±0.02	8.56±0.02	8.37±0.03	8.04±0.04	2005 Feb 21
J04184703+2820073	Hubble 4	7.16±0.02	7.08±0.02	6.94±0.03	6.92±0.03	2005 Feb 19
		7.11±0.02	7.01±0.02	6.98±0.03	6.94±0.03	2005 Feb 21
J04185115+2814332	KPNO 2	12.19±0.02	12.09±0.02	12.04±0.04	12.02±0.04	2005 Feb 19
		12.21±0.02	12.07±0.02	11.96±0.04	11.76±0.04	2005 Feb 21
J04185147+2820264	CoKu Tau/1	10.07±0.02	8.85±0.02	7.56±0.03	5.71±0.03	2005 Feb 19
		10.19±0.02	8.96±0.02	7.72±0.03	5.84±0.03	2005 Feb 21

TABLE 4 — *Continued*

2MASS[a]	Name	[3.6]	[4.5]	[5.8]	[8.0]	Date
J04185170+1723165	HBC 376	9.24±0.02	9.20±0.02	9.16±0.03	9.13±0.03	2004 Sep 7
J04185813+2812234	IRAS 04158+2805	9.21±0.02	8.46±0.02	7.74±0.03	6.83±0.03	2005 Feb 19
		9.26±0.02	8.43±0.02	7.78±0.03	6.92±0.03	2005 Feb 21
J04190110+2819420	V410 X-ray 6	8.73±0.02	8.60±0.02	8.53±0.03	8.25±0.03	2005 Feb 19
		8.85±0.02	8.59±0.02	8.49±0.03	8.25±0.03	2005 Feb 21
J04190126+2802487	KPNO 12	13.89±0.02	out	13.05±0.05	out	2005 Feb 19
		13.94±0.02	13.49±0.04	13.11±0.04	12.56±0.05	2005 Feb 20
		13.93±0.02	13.54±0.03	13.17±0.05	12.66±0.05	2005 Feb 21
J04190197+2822332	V410 X-ray 5a	9.64±0.02	9.50±0.02	9.48±0.03	9.40±0.03	2005 Feb 19
		9.65±0.02	9.58±0.02	bad	9.48±0.03	2005 Feb 21
J04191281+2829330	FQ Tau A+B	8.69±0.02	8.34±0.02	8.03±0.03	7.39±0.03	2005 Feb 19
		out	8.35±0.02	out	7.42±0.03	2005 Feb 21
		8.72±0.02	out	8.09±0.03	out	2007 Mar 29
J04191583+2906269	BP Tau	7.33±0.02	6.97±0.02	6.67±0.03	5.66±0.03	2005 Feb 20
		7.23±0.02	6.84±0.02	6.61±0.03	5.66±0.03	2007 Mar 29
J04192625+2826142	V819 Tau	8.19±0.02	8.16±0.02	8.06±0.03	8.06±0.03	2005 Feb 19
		8.20±0.02	8.24±0.02	8.13±0.03	8.04±0.03	2005 Feb 21
J04193545+2827218	FR Tau	9.39±0.02	8.84±0.02	8.23±0.03	7.25±0.03	2005 Feb 19
		9.43±0.02	8.87±0.02	8.32±0.03	7.26±0.03	2005 Feb 21
J04194127+2749484	LkCa 7 A+B	8.06±0.02	8.03±0.02	7.99±0.03	7.94±0.03	2005 Feb 20
		8.05±0.02	8.05±0.02	8.01±0.03	7.96±0.03	2005 Feb 21
J04194148+2716070	IRAS 04166+2708	11.13±0.02	10.31±0.02	9.91±0.03	9.24±0.03	2005 Feb 20
		11.25±0.02	10.36±0.02	9.92±0.03	9.31±0.03	2005 Feb 21
		11.19±0.02	out	9.75±0.03	out	2007 Oct 17
⋯	IRAS 04166+2706	⋯	11.01±0.03	10.22±0.03	9.59±0.03	2005 Feb 20
		⋯	11.03±0.03	10.40±0.03	9.67±0.03	2005 Feb 21
		⋯	11.26±0.03	10.43±0.03	9.90±0.03	2007 Oct 17
J04194657+2712552	[GKH94] 41	10.03±0.02	9.20±0.02	8.60±0.03	8.03±0.03	2005 Feb 20
		9.99±0.02	out	8.60±0.03	out	2005 Feb 21
		10.27±0.02	9.40±0.02	8.84±0.03	8.16±0.03	2007 Oct 17
J04195844+2709570	IRAS 04169+2702	8.45±0.02	7.20±0.02	6.30±0.03	5.36±0.03	2005 Feb 20
		8.43±0.02	out	6.32±0.03	out	2005 Feb 21
		8.31±0.02	7.08±0.02	6.21±0.03	5.28±0.03	2007 Oct 17
J04201611+2821325	⋯	11.81±0.02	11.40±0.02	11.11±0.03	10.56±0.03	2005 Feb 21
J04202144+2813491	⋯	12.71±0.02	12.29±0.02	12.09±0.04	11.56±0.04	2005 Feb 21
J04202555+2700355	⋯	10.95±0.02	10.71±0.02	10.44±0.03	9.73±0.03	2007 Oct 16
		10.93±0.02	10.68±0.02	10.43±0.03	9.75±0.03	2007 Oct 17
J04202583+2819237	IRAS 04173+2812	9.18±0.02	8.40±0.02	7.91±0.03	7.13±0.03	2005 Feb 21
J04202606+2804089	⋯	9.29±0.02	8.95±0.02	8.57±0.03	7.03±0.03	2005 Feb 21
J04203918+2717317	XEST 16-045	9.36±0.02	9.44±0.02	9.33±0.03	9.31±0.03	2005 Feb 21
		9.40±0.02	out	9.31±0.03	out	2007 Oct 17
J04205273+1746415	J2-157	10.44±0.02	10.35±0.02	10.31±0.03	10.28±0.03	2004 Mar 8
J04210795+2702204	⋯	8.10±0.02	7.28±0.02	6.63±0.03	5.54±0.03	2005 Feb 20
		7.58±0.02	6.59±0.02	6.00±0.03	5.12±0.03	2007 Oct 17
J04210934+2750368	⋯	10.00±0.02	9.72±0.02	9.58±0.03	9.20±0.03	2005 Feb 21
J04211038+2701372	IRAS 04181+2654 B	9.02±0.02	8.24±0.02	7.65±0.03	6.92±0.03	2005 Feb 20
		9.00±0.02	8.28±0.02	7.60±0.03	6.76±0.03	2007 Oct 17
J04211146+2701094	IRAS 04181+2654 A	8.39±0.02	7.36±0.02	6.48±0.03	5.46±0.03	2005 Feb 20
		8.61±0.02	7.51±0.02	6.69±0.03	5.67±0.03	2007 Oct 17
J04213459+2701388	⋯	9.91±0.02	9.61±0.02	9.34±0.03	8.98±0.03	2007 Oct 17
J04214013+2814224	XEST 21-026	10.63±0.02	10.58±0.02	10.54±0.03	10.52±0.03	2007 Oct 16
J04214323+1934133	IRAS 04187+1927	6.96±0.02	6.29±0.02	5.53±0.03	4.36±0.03	2005 Feb 20
J04214631+2659296	⋯	out	11.24±0.02	out	10.42±0.03	2007 Mar 28
		11.53±0.02	11.27±0.02	11.01±0.03	10.58±0.03	2007 Oct 17
J04215450+2652315	⋯	13.17±0.02	out	13.04±0.05	out	2005 Feb 20
		13.17±0.02	13.05±0.02	12.97±0.03	12.94±0.04	2007 Mar 28
		13.17±0.02	13.07±0.02	12.88±0.04	12.84±0.06	2007 Oct 17
J04215563+2755060	DE Tau	7.02±0.02	6.67±0.02	6.38±0.03	5.71±0.03	2005 Feb 20
		7.02±0.02	6.67±0.02	6.35±0.03	5.67±0.03	2007 Oct 16
⋯	IRAM 04191+1522	14.90±0.04	13.28±0.04	12.66±0.04	12.49±0.05	2004 Sep 10
		15.32±0.05	13.81±0.03	13.23±0.04	12.90±0.04	2005 Sep 17
J04215740+2826355	RY Tau	sat	sat	3.48±0.03	sat	2005 Feb 20
		sat	sat	3.51±0.03	sat	2005 Feb 21
J04215884+2818066	HD 283572	6.82±0.02	6.79±0.02	6.76±0.03	6.74±0.03	2005 Feb 20
		6.83±0.02	6.85±0.02	6.76±0.03	6.76±0.03	2005 Feb 21
J04215943+1932063	T Tau N+S	sat	sat	2.65±0.03	sat	2005 Feb 20
J04220007+1530248	IRAS 04191+1523 B	12.18±0.03	11.17±0.03	10.68±0.04	9.75±0.04	2004 Sep 10
		12.19±0.03	11.23±0.03	10.74±0.04	9.84±0.06	2005 Sep 17
J04220043+1530212	IRAS 04191+1523 A	9.48±0.02	8.30±0.02	7.38±0.03	6.41±0.03	2004 Sep 10
		9.56±0.02	8.29±0.02	7.31±0.03	6.26±0.03	2005 Sep 17
J04220069+2657324	Haro 6-5B	9.47±0.02	8.31±0.02	7.23±0.03	5.93±0.03	2005 Feb 20
		9.63±0.02	8.35±0.02	7.16±0.03	5.86±0.03	2007 Oct 17
J04220217+2657304	FS Tau A+B	6.88±0.02	6.35±0.02	5.93±0.03	5.14±0.03	2005 Feb 20
		6.76±0.02	6.37±0.02	5.76±0.03	4.89±0.03	2007 Oct 17
J04220313+2825389	LkCa 21	8.23±0.02	8.14±0.02	8.12±0.03	8.09±0.03	2005 Feb 20
		8.22±0.02	8.17±0.02	8.13±0.03	8.10±0.03	2005 Feb 21
J04221332+1934392	⋯	11.02±0.02	10.89±0.02	10.82±0.03	10.59±0.03	2007 Mar 29

TABLE 4 — *Continued*

2MASS[a]	Name	[3.6]	[4.5]	[5.8]	[8.0]	Date
J04221568+2657060	XEST 11-078	11.05±0.02	10.49±0.02	10.20±0.03	9.73±0.03	2007 Oct 17
J04221644+2549118	⋯	11.43±0.02	11.33±0.02	11.27±0.03	11.26±0.03	2006 Sep 28
		11.45±0.02	11.26±0.02	11.21±0.03	11.22±0.03	2007 Mar 30
J04221675+2654570	⋯	7.71±0.02	7.23±0.02	6.79±0.03	6.18±0.03	2007 Oct 17
J04222404+2646258	XEST 11-087	9.45±0.02	9.36±0.02	9.30±0.03	9.33±0.03	2007 Oct 17
J04224786+2645530	IRAS 04196+2638	8.06±0.02	7.49±0.02	7.09±0.03	6.24±0.03	2005 Feb 21
		8.11±0.02	7.55±0.02	7.02±0.03	6.27±0.03	2007 Oct 17
J04230607+2801194	⋯	10.60±0.02	out	9.98±0.03	out	2005 Feb 20
		10.58±0.02	10.22±0.02	9.93±0.03	9.35±0.03	2005 Feb 21
J04230776+2805573	IRAS 04200+2759	8.44±0.02	7.86±0.02	7.36±0.03	6.49±0.03	2005 Feb 20
		8.42±0.02	7.74±0.02	7.30±0.03	6.41±0.03	2005 Feb 21
J04231822+2641156	⋯	9.39±0.02	9.15±0.02	8.76±0.03	8.12±0.03	2005 Feb 21
J04233539+2503026	FU Tau A	out	7.68±0.02	out	6.44±0.03	2005 Feb 23
		8.34±0.02	7.87±0.02	7.33±0.03	6.71±0.03	2007 Mar 30
J04233573+2502596	FU Tau B	out	11.90±0.10	out	10.77±0.10	2005 Feb 23
		12.54±0.10	11.93±0.10	11.46±0.10	10.87±0.10	2007 Mar 30
J04233919+2456141	FT Tau	7.64±0.02	7.12±0.02	6.81±0.03	5.95±0.03	2005 Feb 23
		7.89±0.02	7.44±0.02	7.12±0.03	6.27±0.03	2007 Mar 30
J04242090+2630511	⋯	11.80±0.02	11.41±0.02	11.00±0.03	10.37±0.03	2005 Feb 21
J04242646+2649503	⋯	11.11±0.02	10.80±0.02	10.48±0.03	9.85±0.03	2005 Feb 21
J04244457+2610141	IRAS 04216+2603	7.80±0.02	7.24±0.02	6.78±0.03	6.00±0.03	2004 Mar 7
		8.07±0.02	7.56±0.02	7.07±0.03	6.25±0.03	2005 Feb 21
J04244506+2701447	J1-4423	10.18±0.02	10.11±0.02	10.08±0.03	10.04±0.03	2005 Feb 20
		10.18±0.02	10.14±0.02	10.02±0.03	10.06±0.03	2005 Feb 21
J04245708+2711565	IP Tau	7.70±0.02	7.43±0.02	7.20±0.03	6.53±0.03	2005 Feb 20
		7.76±0.02	7.42±0.02	7.22±0.03	6.60±0.03	2005 Feb 21
		7.67±0.02	7.38±0.02	7.20±0.03	6.61±0.03	2007 Oct 16
J04251767+2617504	J1-4872 B	9.06±0.04	8.94±0.04	8.88±0.04	8.86±0.04	2004 Mar 7
		9.02±0.04	8.95±0.04	8.82±0.04	8.88±0.04	2005 Feb 21
J04251767+2617504	J1-4872 A	8.33±0.04	8.32±0.04	8.25±0.04	8.22±0.04	2004 Mar 7
		8.32±0.04	8.24±0.04	8.30±0.04	8.18±0.04	2005 Feb 21
J04262939+2624137	KPNO 3	11.36±0.02	10.92±0.02	10.51±0.03	9.66±0.03	2004 Mar 7
		11.39±0.02	10.97±0.02	10.45±0.03	9.70±0.03	2005 Feb 22
J04263055+2443558	⋯	12.58±0.02	12.20±0.02	11.79±0.03	11.06±0.03	2007 Mar 28
		12.56±0.02	12.15±0.02	11.76±0.03	11.06±0.03	2007 Oct 16
J04265352+2606543	FV Tau A+B	6.12±0.02	5.49±0.02	4.88±0.03	4.08±0.03	2004 Mar 7
		6.32±0.02	5.79±0.02	5.20±0.03	4.42±0.03	2005 Feb 22
J04265440+2606510	FV Tau/c A+B	8.09±0.02	7.66±0.02	7.10±0.03	6.30±0.03	2004 Mar 7
		8.03±0.02	7.51±0.02	6.99±0.03	6.28±0.03	2005 Feb 22
J04265629+2443353	IRAS 04239+2436	7.62±0.02	6.25±0.02	5.29±0.03	4.45±0.03	2005 Feb 20
		7.57±0.02	6.27±0.02	5.34±0.03	4.49±0.03	2005 Feb 23
J04265732+2606284	KPNO 13	8.62±0.02	8.22±0.02	7.77±0.03	7.04±0.03	2004 Mar 7
		8.75±0.02	8.32±0.02	7.91±0.03	7.37±0.03	2005 Feb 22
J04270266+2605304	DG Tau B	8.86±0.02	7.21±0.02	5.85±0.03	4.83±0.03	2004 Mar 7
		8.78±0.02	7.07±0.02	5.72±0.03	4.62±0.03	2005 Feb 22
J04270280+2542223	DF Tau A+B	6.03±0.02	5.60±0.02	5.21±0.03	4.61±0.03	2004 Mar 7
		sat	5.36±0.02	4.99±0.03	4.42±0.03	2005 Feb 20
		sat	out	4.99±0.03	out	2005 Feb 22
J04270469+2606163	DG Tau	sat	sat	4.14±0.03	sat	2004 Mar 7
		sat	5.05±0.02	4.41±0.03	3.57±0.03	2005 Feb 22
J04270739+2215037	⋯	10.90±0.02	10.78±0.02	10.74±0.03	10.73±0.03	2008 Oct 31
J04272799+2612052	KPNO 4	12.56±0.02	12.35±0.02	12.23±0.04	12.11±0.04	2004 Mar 7
		12.54±0.02	12.32±0.02	12.23±0.04	12.13±0.05	2005 Feb 22
J04274538+2357243	⋯	13.20±0.02	13.05±0.02	12.98±0.04	13.00±0.07	2005 Feb 20
J04275730+2619183	IRAS 04248+2612	9.54±0.03	8.69±0.02	7.88±0.03	6.85±0.03	2004 Mar 7
		9.78±0.03	9.02±0.02	8.26±0.03	7.11±0.03	2005 Feb 22
⋯	L1521F-IRS	⋯	⋯	⋯	12.47±0.04	2004 Sep 9
		⋯	⋯	⋯	12.55±0.06	2005 Feb 24
		⋯	⋯	⋯	12.37±0.03	2006 Mar 25
J04284263+2714039	⋯	9.69±0.02	9.45±0.02	9.19±0.03	8.83±0.03	2005 Feb 24
J04290068+2755033	⋯	12.25±0.02	11.95±0.02	11.58±0.03	10.96±0.03	2005 Feb 24
J04290498+2649073	IRAS 04260+2642	10.01±0.02	9.37±0.02	8.82±0.03	8.03±0.03	2004 Mar 7
		10.03±0.02	9.34±0.02	8.86±0.03	8.08±0.03	2005 Feb 24
J04292071+2633406	J1-507	8.54±0.02	8.47±0.02	8.44±0.03	8.40±0.03	2004 Mar 7
		8.51±0.02	8.52±0.02	8.45±0.03	8.48±0.03	2005 Feb 24
J04292165+2701259	IRAS 04263+2654	8.07±0.02	7.64±0.02	7.27±0.03	6.64±0.03	2005 Feb 24
J04292373+2433002	GV Tau A+B	sat	sat	2.55±0.03	sat	2005 Feb 23
		sat	sat	2.57±0.03	sat	2005 Feb 24
		sat	sat	2.64±0.03	sat	2007 Oct 16
J04292971+2616532	FW Tau A+B+C	9.03±0.02	8.92±0.02	8.89±0.03	8.86±0.03	2004 Mar 7
		9.06±0.02	8.93±0.02	8.90±0.03	8.88±0.03	2005 Feb 24
		9.07±0.02	8.90±0.02	8.90±0.03	8.87±0.03	2006 Mar 25
J04293008+2439550	IRAS 04264+2433	10.19±0.02	9.48±0.02	8.79±0.03	6.97±0.03	2004 Sep 7
		out	9.13±0.02	out	6.44±0.03	2005 Feb 21
		10.16±0.02	9.40±0.02	8.55±0.03	6.70±0.03	2005 Feb 24
J04293209+2430597	⋯	out	9.20±0.02	out	7.26±0.03	2004 Sep 7
		10.42±0.02	9.20±0.02	8.24±0.03	7.35±0.03	2005 Feb 23

TABLE 4 — *Continued*

2MASS[a]	Name	[3.6]	[4.5]	[5.8]	[8.0]	Date
		10.36±0.02	9.22±0.02	8.29±0.03	7.31±0.03	2005 Feb 24
J04293606+2435556	XEST 13-010	out	7.73±0.02	out	7.04±0.03	2004 Sep 7
		7.99±0.02	7.71±0.02	7.42±0.03	6.96±0.03	2005 Feb 24
J04294155+2632582	DH Tau A+B	7.47±0.02	7.19±0.02	7.11±0.03	6.74±0.03	2004 Mar 7
		7.60±0.02	7.41±0.02	7.19±0.03	6.81±0.03	2005 Feb 24
J04294247+2632493	DI Tau A+B	8.16±0.02	8.25±0.02	8.16±0.03	8.11±0.03	2004 Mar 7
		8.22±0.02	8.20±0.02	8.11±0.03	8.10±0.03	2005 Feb 24
J04294568+2630468	KPNO 5	11.05±0.02	10.92±0.02	10.81±0.03	10.85±0.03	2004 Mar 7
		11.04±0.02	10.93±0.02	10.89±0.03	10.84±0.03	2005 Feb 24
J04295156+2606448	IQ Tau	6.94±0.02	6.49±0.02	6.12±0.03	5.57±0.03	2004 Mar 7
		6.73±0.02	6.32±0.02	6.02±0.03	5.46±0.03	2005 Feb 24
J04295422+1754041	⋯	out	out	out	out	⋯
J04295950+2433078	⋯	sat	out	8.28±0.03	out	2004 Oct 7
		9.03±0.02	8.56±0.02	8.31±0.03	7.80±0.03	2005 Feb 24
J04300357+1813494	UX Tau B	8.75±0.04	8.75±0.04	8.69±0.04	8.66±0.04	2005 Feb 19
J04300399+1813493	UX Tau A+C	6.66±0.02	6.37±0.02	6.16±0.03	5.93±0.03	2005 Feb 19
J04300724+2608207	KPNO 6	13.08±0.02	12.77±0.02	12.41±0.04	11.82±0.04	2004 Mar 7
		13.09±0.02	12.73±0.02	12.41±0.04	11.54±0.04	2005 Feb 24
J04302365+2359129	⋯	13.21±0.02	13.11±0.02	13.03±0.05	13.02±0.06	2005 Feb 24
J04302961+2426450	FX Tau A+B	7.21±0.02	6.92±0.02	6.62±0.03	5.90±0.03	2005 Feb 20
		7.17±0.02	6.87±0.02	6.66±0.03	5.94±0.03	2005 Feb 24
J04304425+2601244	DK Tau A	5.88±0.02	5.49±0.02	5.24±0.03	4.58±0.03	2004 Mar 7
		6.12±0.02	5.71±0.02	5.39±0.03	4.66±0.03	2005 Feb 24
J04304425+2601244	DK Tau B	8.02±0.10	7.30±0.10	7.24±0.10	6.60±0.10	2004 Mar 7
		7.77±0.10	7.41±0.10	7.39±0.10	6.63±0.10	2005 Feb 24
J04305028+2300088	IRAS 04278+2253 A+B	sat	sat	3.21±0.03	sat	2005 Feb 20
		sat	sat	3.33±0.03	sat	2005 Feb 24
J04305137+2442222	ZZ Tau	8.10±0.02	7.87±0.02	7.59±0.03	6.96±0.03	2005 Feb 23
		8.05±0.02	7.87±0.02	7.64±0.03	6.99±0.03	2005 Feb 24
J04305171+2441475	ZZ Tau IRS	8.15±0.02	7.35±0.02	6.67±0.03	5.75±0.03	2005 Feb 23
		8.06±0.02	7.32±0.02	6.66±0.03	5.72±0.03	2005 Feb 24
J04305718+2556394	KPNO 7	12.60±0.02	12.27±0.02	11.93±0.03	11.26±0.03	2004 Mar 7
		12.58±0.02	12.22±0.02	12.00±0.04	11.25±0.03	2005 Feb 24
J04311444+2710179	JH 56	8.77±0.02	8.73±0.02	8.69±0.03	8.64±0.03	2004 Mar 7
		8.70±0.02	8.72±0.02	8.70±0.03	8.60±0.03	2005 Feb 24
J04311578+1820072	MHO 9	10.04±0.02	9.96±0.02	9.86±0.03	9.94±0.03	2004 Oct 7
		out	9.93±0.02	out	9.88±0.03	2006 Mar 23
J04311907+2335047	⋯	11.65±0.02	11.52±0.02	11.53±0.03	11.47±0.04	2005 Feb 24
J04312382+2410529	V927 Tau A+B	8.52±0.02	8.45±0.02	8.41±0.03	8.39±0.03	2005 Feb 20
		8.52±0.02	8.40±0.02	8.37±0.03	8.38±0.03	2005 Feb 24
J04312405+1800215	MHO 4	10.12±0.02	9.99±0.02	9.94±0.03	9.93±0.03	2004 Oct 7
J04312669+2703188	⋯	12.85±0.02	out	12.73±0.04	out	2004 Mar 7
		12.88±0.02	12.69±0.02	12.68±0.04	12.68±0.04	2005 Feb 24
J04313407+1808049	L1551/IRS5	7.03±0.02	5.54±0.02	4.16±0.03	2.78±0.03	2004 Oct 7
J04313613+1813432	LkHa 358	8.45±0.02	7.72±0.02	7.12±0.03	6.43±0.03	2004 Oct 7
J04313747+1812244	HH 30	12.38±0.02	11.81±0.02	11.64±0.03	11.25±0.03	2004 Oct 7
J04313843+1813576	HL Tau	sat	sat	3.57±0.03	2.93±0.03	2004 Oct 7
J04314007+1813571	XZ Tau A+B	sat	5.04±0.02	4.40±0.03	3.57±0.03	2004 Oct 7
J04314444+1808315	L1551NE	8.66±0.02	7.06±0.02	5.98±0.03	5.03±0.03	2004 Oct 7
J04315056+2424180	HK Tau A+B	out	sat	out	6.61±0.03	2004 Oct 7
		7.78±0.02	7.39±0.02	7.08±0.03	6.52±0.03	2005 Feb 20
		7.68±0.02	7.30±0.02	7.06±0.03	6.55±0.03	2005 Feb 24
J04315779+1821380	V710 Tau A	7.95±0.04	7.55±0.04	7.16±0.04	6.36±0.04	2004 Oct 7
J04315779+1821350	V710 Tau B	8.34±0.04	8.13±0.05	8.11±0.07	7.91±0.10	2004 Oct 7
J04315844+2543299	J1-665	9.33±0.02	9.25±0.02	9.22±0.03	9.21±0.03	2004 Mar 7
		9.29±0.02	9.24±0.02	9.23±0.03	9.27±0.03	2005 Feb 24
J04315968+1821305	LkHa 267	8.78±0.02	8.24±0.02	7.82±0.03	7.31±0.03	2004 Oct 7
J04320329+2528078	⋯	10.27±0.02	10.14±0.02	10.09±0.03	10.09±0.03	2005 Feb 24
J04320926+1757227	L1551-51	out	8.69±0.02	out	8.64±0.03	2004 Oct 7
		8.79±0.02	8.72±0.02	8.71±0.03	8.67±0.03	2005 Feb 19
J04321456+1820147	V827 Tau	8.12±0.02	8.05±0.02	8.01±0.03	8.02±0.03	2004 Oct 7
J04321540+2428597	Haro 6-13	6.23±0.02	5.72±0.02	5.34±0.03	4.66±0.03	2005 Feb 20
		6.30±0.02	5.80±0.02	5.39±0.03	4.74±0.03	2005 Feb 24
J04321583+1801387	V826 Tau A+B	8.04±0.02	8.08±0.02	8.03±0.03	7.97±0.03	2004 Oct 7
J04321606+1812464	MHO 5	9.30±0.02	8.95±0.02	8.56±0.03	7.85±0.03	2004 Oct 7
J04321786+2422149	⋯	9.91±0.02	9.79±0.02	9.74±0.03	9.72±0.03	2005 Feb 20
		9.96±0.02	9.81±0.02	9.73±0.03	9.72±0.03	2005 Feb 24
J04321885+2422271	V928 Tau A+B	7.88±0.02	7.83±0.02	7.74±0.03	7.65±0.03	2005 Feb 20
		7.80±0.02	7.75±0.02	7.70±0.03	7.64±0.03	2005 Feb 24
J04322210+1827426	MHO 6	10.10±0.02	out	9.61±0.03	out	2004 Oct 7
		10.01±0.02	9.74±0.02	9.53±0.03	9.06±0.03	2005 Feb 19
J04322329+2403013	⋯	10.92±0.02	10.78±0.02	10.84±0.03	10.69±0.03	2005 Feb 24
J04322415+2251083	⋯	9.97±0.02	out	9.26±0.03	out	2005 Feb 24
		10.03±0.02	9.64±0.02	9.36±0.03	8.47±0.03	2007 Apr 3
J04322627+1827521	MHO 7	9.87±0.02	out	9.78±0.03	out	2004 Oct 7
		9.87±0.02	9.79±0.02	9.74±0.03	9.74±0.03	2005 Feb 19
J04323028+1731303	GG Tau Ba+Bb	9.20±0.02	8.80±0.02	8.40±0.03	7.61±0.03	2005 Feb 19

TABLE 4 — *Continued*

2MASS[a]	Name	[3.6]	[4.5]	[5.8]	[8.0]	Date
J04323034+1731406	GG Tau Aa+Ab	6.62±0.02	6.26±0.02	5.90±0.03	5.03±0.03	2005 Feb 19
J04323058+2419572	FY Tau	sat	sat	6.46±0.03	sat	2004 Oct 7
		7.20±0.02	6.82±0.02	6.50±0.03	6.02±0.03	2005 Feb 20
		7.12±0.02	6.72±0.02	6.45±0.03	5.97±0.03	2005 Feb 24
J04323176+2420029	FZ Tau	6.30±0.02	5.66±0.02	5.23±0.03	4.48±0.03	2005 Feb 20
		6.28±0.02	5.73±0.02	5.24±0.03	4.50±0.03	2005 Feb 24
J04323205+2257266	IRAS 04295+2251	8.60±0.02	7.70±0.02	6.78±0.03	5.49±0.03	2005 Feb 20
		8.56±0.02	7.70±0.02	6.81±0.03	5.50±0.03	2005 Feb 24
		out	7.62±0.02	out	5.06±0.03	2007 Apr 3
J04324282+2552314	UZ Tau Ba+Bb	7.68±0.10	7.55±0.10	7.17±0.10	6.50±0.10	2004 Mar 7
		7.71±0.07	7.38±0.07	7.12±0.07	6.41±0.07	2005 Feb 24
J04324303+2552311	UZ Tau A	5.91±0.02	5.39±0.02	5.00±0.03	4.20±0.03	2004 Mar 7
		6.41±0.02	5.87±0.02	5.45±0.03	4.59±0.03	2005 Feb 24
J04324373+1802563	L1551-55	9.19±0.02	9.16±0.02	9.12±0.03	9.10±0.03	2005 Feb 19
J04324911+2253027	JH 112	7.42±0.02	7.11±0.02	6.90±0.04	5.91±0.04	2005 Feb 20
		7.39±0.02	out	6.88±0.04	out	2005 Feb 24
		7.39±0.02	7.13±0.03	6.74±0.04	5.82±0.03	2007 Apr 3
J04324938+2253082	⋯	8.45±0.02	8.19±0.03	7.74±0.04	7.00±0.04	2005 Feb 20
		8.49±0.02	out	7.80±0.05	out	2005 Feb 24
		8.52±0.02	8.17±0.02	7.76±0.04	7.08±0.04	2007 Apr 3
J04325026+2422115	⋯	10.42±0.02	10.19±0.02	10.08±0.03	10.05±0.03	2004 Oct 7
		10.44±0.02	10.18±0.02	10.09±0.03	10.01±0.03	2005 Feb 20
		10.42±0.02	10.22±0.02	10.07±0.03	10.05±0.03	2005 Feb 24
J04325119+1730092	LH 0429+17	out	12.90±0.02	out	12.75±0.08	2004 Sep 7
J04330197+2421000	MHO 8	sat	9.16±0.02	9.13±0.03	9.07±0.03	2004 Oct 7
		9.30±0.02	9.16±0.02	9.12±0.03	9.08±0.03	2005 Feb 20
		9.26±0.02	9.27±0.02	9.09±0.03	9.10±0.03	2005 Feb 24
		9.30±0.02	out	9.12±0.03	out	2006 Mar 26
J04330622+2409339	GH Tau A+B	7.01±0.02	6.67±0.02	6.43±0.03	5.92±0.03	2005 Feb 20
		7.06±0.02	6.70±0.02	6.57±0.03	5.99±0.03	2005 Feb 24
J04330664+2409549	V807 Tau A+B	6.39±0.02	6.13±0.02	5.85±0.03	5.41±0.03	2005 Feb 20
		6.45±0.02	6.15±0.02	5.89±0.03	5.50±0.03	2005 Feb 24
J04330781+2616066	KPNO 14	9.78±0.02	9.60±0.02	9.59±0.03	9.53±0.03	2004 Mar 7
		9.72±0.02	9.64±0.02	9.59±0.03	9.58±0.03	2005 Feb 24
J04330945+2246487	⋯	10.77±0.02	10.54±0.02	10.31±0.03	9.93±0.03	2005 Feb 20
		10.80±0.02	10.53±0.02	10.27±0.03	9.80±0.03	2007 Mar 29
		10.78±0.02	10.56±0.02	10.32±0.03	9.95±0.03	2007 Apr 3
J04331003+2433433	V830 Tau	8.39±0.02	8.37±0.02	8.32±0.03	8.30±0.03	2005 Feb 20
		8.34±0.02	8.40±0.02	8.32±0.03	8.31±0.03	2005 Feb 24
J04331435+2614235	IRAS 04301+2608	11.84±0.02	11.44±0.02	11.02±0.03	9.45±0.03	2004 Mar 7
		12.04±0.02	11.67±0.02	11.27±0.03	9.55±0.03	2005 Feb 24
J04331650+2253204	IRAS 04302+2247	10.09±0.03	9.68±0.02	9.53±0.03	9.62±0.03	2005 Feb 20
		10.11±0.02	out	9.55±0.03	out	2005 Feb 24
		out	9.97±0.03	out	9.66±0.03	2007 Mar 29
		10.23±0.02	9.85±0.03	9.61±0.03	9.63±0.03	2007 Apr 3
J04331907+2246342	IRAS 04303+2240	6.16±0.02	5.36±0.02	4.68±0.03	3.96±0.03	2005 Feb 20
		sat	sat	4.33±0.03	3.67±0.03	2007 Apr 3
J04332621+2245293	XEST 17-036	9.53±0.02	9.44±0.02	9.31±0.03	9.35±0.03	2005 Feb 20
		9.54±0.02	9.39±0.02	9.32±0.03	9.31±0.03	2007 Apr 3
J04333278+1800436	⋯	out	8.71±0.02	out	7.33±0.03	2005 Feb 19
J04333297+1801004	HD 28867 B	out	6.72±0.04	out	6.19±0.04	2005 Feb 19
J04333297+1801004	HD 28867 A+C	out	6.15±0.04	out	6.13±0.04	2005 Feb 19
J04333405+2421170	GI Tau	6.80±0.02	6.23±0.02	5.72±0.03	4.76±0.03	2005 Feb 20
		6.80±0.02	6.22±0.02	5.74±0.03	4.78±0.03	2005 Feb 24
J04333456+2421058	GK Tau	6.43±0.02	6.05±0.02	5.77±0.03	4.84±0.03	2005 Feb 20
		6.43±0.02	6.05±0.02	5.72±0.03	4.81±0.03	2005 Feb 24
J04333678+2609492	IS Tau A+B	7.68±0.02	7.23±0.02	6.83±0.03	6.03±0.03	2004 Mar 7
		7.85±0.02	7.41±0.02	6.95±0.03	6.00±0.03	2005 Feb 24
J04333905+2227207	⋯	9.97±0.02	9.72±0.02	9.54±0.03	9.17±0.03	2007 Apr 3
J04333906+2520382	DL Tau	6.67±0.02	6.10±0.02	5.60±0.03	4.83±0.03	2004 Mar 7
		7.02±0.02	6.30±0.02	5.84±0.03	5.07±0.03	2005 Feb 24
J04333935+1751523	HN Tau A+B	6.92±0.02	6.22±0.02	5.62±0.03	4.70±0.03	2005 Feb 19
J04334171+1750402	⋯	9.97±0.02	9.79±0.02	9.56±0.03	9.07±0.03	2005 Feb 19
J04334291+2526470	⋯	out	12.60±0.02	out	12.56±0.05	2004 Mar 7
		12.69±0.02	12.56±0.04	12.47±0.04	12.45±0.05	2005 Feb 24
J04334465+2615005	⋯	8.67±0.02	8.22±0.02	7.83±0.03	7.20±0.03	2004 Mar 7
		8.80±0.02	8.25±0.02	7.76±0.03	7.14±0.03	2007 Oct 16
J04334871+1810099	DM Tau	9.35±0.02	9.30±0.02	9.25±0.03	8.70±0.03	2005 Feb 19
J04335200+2250301	CI Tau	6.76±0.02	6.27±0.02	5.82±0.03	4.92±0.03	2005 Feb 20
		7.03±0.02	6.38±0.02	6.09±0.03	5.37±0.03	2007 Apr 3
J04335245+2612548	⋯	13.13±0.02	12.67±0.02	12.24±0.04	11.49±0.05	2004 Mar 7
		13.07±0.02	12.64±0.02	12.25±0.04	11.42±0.04	2005 Feb 22
		13.18±0.02	12.70±0.02	12.28±0.04	11.52±0.04	2007 Oct 16
J04335252+2256269	XEST 17-059	out	8.65±0.02	out	8.62±0.03	2005 Feb 20
		8.77±0.02	out	8.59±0.03	out	2005 Feb 24
		8.80±0.02	8.62±0.02	8.61±0.03	8.57±0.03	2007 Apr 3
J04335470+2613275	IT Tau B	9.25±0.10	8.68±0.10	8.26±0.10	7.46±0.10	2004 Mar 7

TABLE 4 — *Continued*

2MASS[a]	Name	[3.6]	[4.5]	[5.8]	[8.0]	Date
		9.21±0.10	8.63±0.10	8.09±0.10	7.41±0.10	2005 Feb 23
		8.95±0.10	8.61±0.10	8.08±0.10	7.46±0.10	2007 Oct 16
J04335470+2613275	IT Tau A	7.25±0.02	6.89±0.02	6.57±0.03	5.96±0.03	2004 Mar 7
		7.22±0.02	6.84±0.02	6.53±0.03	5.96±0.03	2005 Feb 22
		7.27±0.02	6.88±0.02	6.50±0.03	5.91±0.03	2007 Oct 16
J04335546+1838390	J2-2041	9.39±0.02	9.37±0.02	9.32±0.03	9.29±0.03	2005 Feb 19
J04341099+2251445	JH 108	9.28±0.02	9.22±0.02	9.20±0.03	9.14±0.03	2005 Feb 20
		9.29±0.02	out	9.10±0.03	out	2005 Feb 24
		9.25±0.02	9.25±0.02	9.18±0.03	9.17±0.03	2007 Apr 3
J04341527+2250309	CFHT 1	11.22±0.02	11.07±0.02	10.95±0.03	10.98±0.03	2005 Feb 20
		11.17±0.02	11.04±0.02	10.96±0.03	10.99±0.03	2007 Apr 3
J04341803+1830066	HBC 407	9.82±0.02	9.79±0.02	9.81±0.03	9.76±0.03	2005 Feb 19
J04344544+2308027	· · ·	11.24±0.02	11.19±0.02	11.09±0.03	11.08±0.03	2005 Feb 24
J04345542+2428531	AA Tau	7.23±0.02	6.76±0.02	6.36±0.03	5.61±0.03	2005 Feb 20
		7.27±0.02	6.78±0.02	6.40±0.03	5.58±0.03	2005 Feb 21
J04345693+2258358	XEST 08-003	9.06±0.02	out	8.89±0.03	out	2005 Feb 24
		9.05±0.02	8.99±0.02	8.94±0.03	8.94±0.03	2007 Apr 3
J04350850+2311398	· · ·	11.19±0.02	11.06±0.02	11.02±0.03	10.98±0.03	2005 Feb 24
J04352020+2232146	HO Tau	8.97±0.02	8.58±0.02	8.46±0.03	7.82±0.03	2005 Feb 20
		8.88±0.02	8.49±0.02	8.36±0.03	7.72±0.03	2007 Apr 3
J04352089+2254242	FF Tau A+B	8.41±0.02	8.37±0.02	8.35±0.03	8.31±0.03	2005 Feb 20
		8.31±0.02	out	8.21±0.03	out	2005 Feb 24
		8.37±0.02	8.37±0.02	8.36±0.03	8.35±0.03	2007 Apr 3
J04352450+1751429	HBC 412 A+B	8.91±0.02	8.88±0.02	8.83±0.03	8.80±0.03	2005 Feb 19
J04352737+2414589	DN Tau	7.47±0.02	7.14±0.02	6.74±0.03	6.00±0.03	2005 Feb 20
		7.43±0.02	7.16±0.02	6.71±0.03	6.00±0.03	2005 Feb 21
		sat	sat	6.54±0.03	sat	2006 Mar 25
· · ·	IRAS 04325+2402 C	13.50±0.30	13.10±0.20	12.60±0.20	12.00±0.20	2005 Feb 20
		13.50±0.30	12.90±0.20	12.60±0.20	12.00±0.20	2005 Feb 21
		13.40±0.30	12.90±0.20	12.40±0.20	11.70±0.20	2006 Mar 25
J04353539+2408194	IRAS 04325+2402 A+B	9.89±0.02	9.26±0.02	8.99±0.03	8.49±0.03	2005 Feb 20
		9.85±0.02	9.18±0.02	8.96±0.03	8.46±0.03	2005 Feb 21
		9.90±0.02	9.34±0.02	9.12±0.03	8.52±0.03	2006 Mar 25
J04354093+2411087	CoKu Tau 3 A+B	7.28±0.02	6.83±0.02	6.33±0.03	5.59±0.03	2005 Feb 20
		7.35±0.02	6.87±0.02	6.42±0.03	5.57±0.03	2005 Feb 21
J04354183+2234115	KPNO 8	11.60±0.02	11.46±0.02	11.44±0.03	11.39±0.03	2005 Feb 20
		11.60±0.02	11.47±0.02	11.41±0.03	11.45±0.04	2007 Apr 3
J04354203+2252226	XEST 08-033	9.67±0.02	out	9.54±0.03	out	2005 Feb 21
		9.63±0.02	9.48±0.02	9.39±0.03	9.50±0.03	2007 Apr 3
J04354526+2737130	· · ·	13.12±0.02	13.04±0.02	12.89±0.04	13.04±0.07	2005 Feb 22
J04354733+2250216	HQ Tau	6.73±0.02	6.26±0.02	5.74±0.03	4.60±0.03	2005 Feb 20
		6.81±0.02	out	5.68±0.03	out	2005 Feb 21
		6.42±0.02	5.84±0.02	5.36±0.03	4.38±0.03	2007 Apr 3
J04355109+2252401	KPNO 15	9.73±0.02	9.74±0.02	9.60±0.03	9.67±0.03	2005 Feb 20
		9.74±0.02	out	9.66±0.03	out	2005 Feb 21
		9.76±0.02	9.69±0.02	9.64±0.03	9.63±0.03	2007 Apr 3
J04355143+2249119	KPNO 9	13.61±0.02	13.53±0.02	13.44±0.05	13.48±0.08	2005 Feb 20
		13.63±0.02	out	out	out	2005 Feb 21
		13.60±0.02	13.47±0.03	13.56±0.07	13.35±0.10	2007 Apr 3
J04355209+2255039	XEST 08-047	9.54±0.02	9.44±0.02	9.38±0.03	9.37±0.03	2005 Feb 20
		9.53±0.02	out	9.34±0.03	out	2005 Feb 21
		9.52±0.02	9.43±0.02	9.39±0.03	9.36±0.03	2007 Apr 3
J04355277+2254231	HP Tau	6.51±0.02	6.03±0.02	5.58±0.03	4.59±0.03	2005 Feb 20
		6.46±0.02	out	5.49±0.03	out	2005 Feb 21
		6.58±0.02	6.13±0.02	5.73±0.03	4.80±0.03	2007 Apr 3
J04355286+2250585	XEST 08-049	9.43±0.02	9.31±0.02	9.33±0.03	9.27±0.03	2005 Feb 20
		9.41±0.02	out	9.28±0.03	out	2005 Feb 21
		9.42±0.02	9.29±0.02	9.24±0.03	9.29±0.03	2007 Apr 3
J04355349+2254089	HP Tau/G3	8.58±0.02	8.53±0.02	8.49±0.03	8.48±0.03	2005 Feb 20
		8.56±0.02	out	8.51±0.03	out	2005 Feb 21
		8.61±0.02	8.52±0.02	8.47±0.03	8.48±0.03	2007 Apr 3
J04355415+2254134	HP Tau/G2	7.14±0.02	7.11±0.02	7.04±0.03	7.03±0.03	2005 Feb 20
		7.17±0.02	out	7.09±0.03	out	2005 Feb 21
		7.16±0.02	7.14±0.02	7.05±0.03	7.00±0.03	2007 Apr 3
J04355684+2254360	Haro 6-28 A+B	8.70±0.02	8.23±0.02	7.88±0.03	7.15±0.03	2005 Feb 20
		8.64±0.02	out	7.83±0.03	out	2005 Feb 21
		8.63±0.02	8.17±0.02	7.79±0.03	7.14±0.03	2007 Apr 3
J04355892+2238353	XEST 09-042	8.11±0.02	8.18±0.02	8.09±0.03	8.06±0.03	2007 Apr 3
J04361030+2159364	· · ·	12.96±0.02	12.66±0.02	12.35±0.03	11.72±0.03	2007 Mar 28
		12.99±0.02	12.70±0.02	12.37±0.04	11.79±0.04	2007 Apr 3
J04361038+2259560	CFHT 2	11.57±0.02	11.38±0.02	11.37±0.03	11.36±0.03	2005 Feb 20
		11.62±0.02	11.39±0.02	11.30±0.03	11.32±0.03	2005 Feb 21
		11.59±0.02	11.37±0.02	11.38±0.03	11.31±0.04	2007 Apr 3
J04361909+2542589	LkCa 14	8.53±0.02	8.51±0.02	8.47±0.03	8.45±0.03	2004 Mar 7
		8.41±0.02	8.47±0.02	8.44±0.03	8.44±0.03	2005 Feb 22
J04362151+2351165	· · ·	11.87±0.02	11.47±0.02	11.12±0.03	10.55±0.03	2005 Feb 21
J04363893+2258119	CFHT 3	11.77±0.02	11.62±0.02	11.56±0.03	11.54±0.03	2005 Feb 20

TABLE 4 — *Continued*

2MASS[a]	Name	[3.6]	[4.5]	[5.8]	[8.0]	Date
		11.77±0.02	11.65±0.02	11.68±0.03	11.59±0.04	2005 Feb 21
		11.77±0.02	11.78±0.02	11.53±0.03	11.53±0.04	2007 Apr 3
J04373705+2331080	⋯	14.16±0.02	13.88±0.03	13.59±0.05	13.30±0.08	2005 Feb 21
J04375670+2546229	ITG 1	11.95±0.02	11.47±0.02	10.71±0.03	9.89±0.03	2005 Feb 22
J04380083+2558572	ITG 2	9.57±0.02	9.42±0.02	9.33±0.03	9.34±0.03	2005 Feb 22
J04381486+2611399	⋯	10.79±0.02	10.14±0.02	9.61±0.03	8.91±0.03	2005 Feb 22
J04381630+2326402	⋯	out	out	out	out	⋯
J04382134+2609137	GM Tau	9.44±0.02	8.95±0.02	8.64±0.03	7.97±0.03	2004 Mar 7
		9.23±0.02	8.73±0.02	8.40±0.03	7.83±0.03	2005 Feb 22
J04382858+2610494	DO Tau	6.11±0.02	5.50±0.02	5.00±0.03	4.23±0.03	2004 Mar 7
		6.19±0.02	5.60±0.02	5.14±0.03	4.39±0.03	2005 Feb 22
J04383528+2610386	HV Tau A+B	7.65±0.02	7.54±0.02	7.46±0.03	7.43±0.03	2004 Mar 7
		7.71±0.02	7.55±0.02	7.44±0.03	7.43±0.03	2005 Feb 22
⋯	HV Tau C	11.37±0.05	10.74±0.05	10.20±0.05	9.27±0.05	2004 Mar 7
		11.29±0.05	10.73±0.05	10.21±0.05	9.35±0.05	2005 Feb 23
J04385859+2336351	⋯	10.49±0.02	out	9.84±0.03	out	2005 Feb 21
J04385871+2323595	⋯	out	out	out	out	⋯
J04390163+2336029	⋯	9.72±0.02	out	9.17±0.03	out	2005 Feb 21
J04390396+2544264	⋯	10.78±0.02	10.37±0.02	10.03±0.03	9.16±0.03	2005 Feb 22
J04390525+2337450	⋯	10.54±0.02	10.14±0.02	9.73±0.03	9.02±0.03	2005 Feb 21
J04390637+2334179	⋯	10.79±0.02	out	10.69±0.03	out	2005 Feb 21
J04391389+2553208	IRAS 04361+2547	8.54±0.02	7.62±0.02	7.14±0.03	5.88±0.03	2004 Mar 7
		7.95±0.02	7.01±0.02	6.42±0.03	4.77±0.03	2005 Feb 22
J04391741+2247533	VY Tau A+B	8.61±0.02	8.42±0.02	8.10±0.03	7.42±0.03	2005 Feb 20
J04391779+2221034	LkCa 15	7.57±0.02	7.34±0.02	7.18±0.03	6.50±0.03	2005 Feb 20
		7.70±0.02	7.35±0.02	7.28±0.03	6.59±0.03	2007 Apr 3
J04392090+2545021	GN Tau A+B	7.09±0.02	6.61±0.02	6.30±0.03	5.59±0.03	2004 Mar 7
		7.00±0.02	6.50±0.02	6.20±0.03	5.38±0.03	2005 Feb 22
J04393364+2359212	⋯	9.61±0.02	9.16±0.02	8.82±0.03	7.91±0.03	2005 Feb 21
J04393519+2541447	IRAS 04365+2535	7.54±0.02	6.07±0.02	5.09±0.03	4.37±0.03	2004 Mar 7
		7.16±0.02	5.73±0.02	4.81±0.03	4.08±0.03	2005 Feb 22
J04394488+2601527	ITG 15	8.41±0.02	8.14±0.02	7.72±0.03	7.08±0.03	2004 Mar 7
		8.45±0.02	8.12±0.02	7.69±0.03	7.11±0.03	2005 Feb 22
J04394748+2601407	CFHT 4	9.51±0.02	9.08±0.02	8.62±0.03	7.85±0.03	2004 Mar 7
		9.47±0.02	9.04±0.02	8.59±0.03	7.80±0.03	2005 Feb 22
⋯	IRAS 04368+2557	13.23±0.09	10.87±0.04	9.67±0.04	9.34±0.04	2004 Mar 7
		13.51±0.10	11.15±0.05	9.95±0.04	9.56±0.04	2005 Feb 22
J04395574+2545020	IC2087IR	sat	sat	3.33±0.03	2.76±0.03	2004 Mar 7
		sat	sat	3.43±0.03	2.75±0.03	2005 Feb 22
J04400067+2358211	⋯	10.90±0.02	10.61±0.02	10.35±0.03	9.69±0.03	2005 Feb 21
J04400174+2556292	⋯	10.07±0.02	out	9.81±0.03	out	2004 Mar 7
		10.13±0.02	9.91±0.02	9.84±0.03	9.81±0.03	2005 Feb 22
J04400800+2605253	IRAS 04370+2559	7.87±0.02	7.28±0.02	6.84±0.03	5.84±0.03	2004 Mar 7
		7.92±0.02	7.30±0.02	6.92±0.03	5.91±0.03	2005 Feb 22
J04403979+2519061	⋯	9.79±0.02	9.61±0.02	9.62±0.03	9.57±0.03	2005 Feb 21
J04404950+2551191	JH 223	8.87±0.02	8.55±0.02	8.23±0.03	7.72±0.03	2004 Feb 9
		sat	8.58±0.02	8.35±0.03	7.72±0.03	2004 Oct 8
		8.86±0.02	8.47±0.02	8.24±0.03	7.62±0.03	2005 Feb 23
		8.85±0.02	8.50±0.02	8.28±0.03	7.75±0.03	2007 Oct 16
J04410424+2557561	Haro 6-32	9.57±0.02	9.49±0.02	9.42±0.03	9.52±0.03	2004 Sep 8
		9.60±0.02	9.49±0.02	9.47±0.03	9.47±0.03	2004 Oct 8
		9.58±0.02	9.47±0.02	9.48±0.03	9.44±0.03	2005 Feb 23
J04410470+2451062	IW Tau A+B	8.11±0.02	8.09±0.02	8.02±0.03	7.99±0.03	2004 Feb 9
		8.10±0.02	8.12±0.02	8.06±0.03	8.03±0.03	2007 Oct 16
J04410826+2556074	ITG 33A	9.79±0.02	9.19±0.02	8.62±0.03	7.82±0.03	2004 Sep 8
		9.67±0.02	9.07±0.02	8.54±0.03	7.77±0.03	2004 Oct 8
		9.61±0.02	9.04±0.02	8.48±0.03	7.65±0.03	2005 Feb 23
J04411078+2555116	ITG 34	out	10.23±0.02	out	9.14±0.03	2004 Feb 9
		10.70±0.02	10.21±0.02	9.90±0.03	9.20±0.03	2004 Sep 8
		10.82±0.02	10.29±0.02	9.91±0.03	9.15±0.03	2004 Oct 8
		10.75±0.02	10.28±0.02	9.89±0.03	9.25±0.03	2005 Feb 23
J04411267+2546354	IRAS 04381+2540	9.18±0.02	7.85±0.02	6.84±0.03	5.83±0.03	2004 Feb 9
		9.11±0.02	7.77±0.02	6.74±0.03	5.67±0.03	2005 Feb 23
J04411681+2840000	CoKu Tau/4	8.47±0.02	8.39±0.02	8.34±0.03	8.13±0.03	2004 Feb 9
J04412464+2543530	ITG 40	10.37±0.02	9.83±0.02	9.33±0.03	8.88±0.03	2004 Oct 8
		10.48±0.02	9.78±0.02	9.40±0.03	8.87±0.03	2005 Feb 23
J04413882+2556267	IRAS 04385+2550	8.12±0.02	7.54±0.02	7.04±0.03	6.03±0.03	2004 Feb 9
		8.24±0.02	7.52±0.02	6.69±0.03	5.58±0.03	2004 Oct 8
		8.21±0.02	7.74±0.02	7.09±0.03	6.09±0.03	2005 Feb 23
J04414489+2301513	⋯	12.26±0.02	11.88±0.02	11.53±0.03	11.00±0.03	2007 Mar 28
J04414565+2301580	⋯	sat	9.48±0.02	9.37±0.03	9.22±0.03	2007 Mar 28
J04414825+2534304	⋯	out	10.87±0.02	out	9.59±0.03	2004 Oct 8
		11.38±0.02	10.87±0.02	10.47±0.03	9.54±0.03	2005 Feb 23
J04420548+2522562	LkHa 332/G2 A+B	7.94±0.02	7.87±0.02	7.75±0.03	7.69±0.03	2004 Feb 9
		7.91±0.02	7.83±0.02	7.73±0.03	7.69±0.03	2005 Feb 23
J04420732+2523032	LkHa 332/G1 A+B	7.66±0.02	7.58±0.02	7.50±0.03	7.44±0.03	2004 Feb 9
		7.59±0.02	7.56±0.02	7.48±0.03	7.50±0.03	2005 Feb 23

TABLE 4 — *Continued*

2MASS[a]	Name	[3.6]	[4.5]	[5.8]	[8.0]	Date
J04420777+2523118	V955 Tau A+B	6.90±0.02	6.46±0.02	6.05±0.03	5.34±0.03	2004 Feb 9
		6.93±0.02	6.53±0.02	6.06±0.03	5.33±0.03	2005 Feb 23
J04422101+2520343	CIDA 7	9.51±0.02	9.11±0.02	8.66±0.03	7.81±0.03	2004 Feb 9
		9.52±0.02	9.18±0.02	8.63±0.03	7.79±0.03	2005 Feb 23
J04423769+2515374	DP Tau	7.58±0.02	6.89±0.02	6.34±0.03	5.34±0.03	2004 Feb 9
		7.50±0.02	6.85±0.02	6.33±0.03	5.36±0.03	2005 Feb 23
J04430309+2520187	GO Tau	8.98±0.02	8.62±0.02	8.20±0.03	7.40±0.03	2004 Feb 9
		9.02±0.02	8.61±0.02	8.31±0.03	7.42±0.03	2005 Feb 23
J04432023+2940060	CIDA 14	8.94±0.02	8.64±0.02	8.32±0.03	7.65±0.03	2004 Feb 9
		8.90±0.02	8.60±0.02	8.25±0.03	7.53±0.03	2004 Mar 11
J04442713+2512164	IRAS 04414+2506	9.75±0.02	9.34±0.02	8.87±0.03	7.89±0.03	2004 Feb 9
		9.52±0.02	8.96±0.02	8.33±0.03	7.43±0.03	2005 Feb 23
J04455129+1555496	HD 30171	7.28±0.02	7.24±0.02	7.29±0.03	7.24±0.03	2004 Sep 7
J04455134+1555367	IRAS 04429+1550	8.55±0.02	8.20±0.02	7.80±0.03	6.73±0.03	2004 Sep 7
J04464260+2459034	RXJ 04467+2459	10.02±0.02	9.92±0.02	9.87±0.03	9.89±0.03	2004 Feb 9
		10.03±0.02	9.92±0.02	9.97±0.03	9.91±0.03	2005 Feb 24
J04465305+1700001	DQ Tau	7.05±0.02	6.58±0.02	6.07±0.03	5.20±0.03	2004 Mar 6
J04465897+1702381	Haro 6-37 A	6.64±0.04	6.14±0.04	5.80±0.05	5.24±0.05	2004 Mar 6
J04465897+1702381	Haro 6-37 B	7.85±0.07	7.28±0.07	7.12±0.07	5.99±0.07	2004 Mar 6
J04470620+1658428	DR Tau	sat	5.05±0.02	4.47±0.03	3.80±0.03	2004 Mar 6
J04474859+2925112	DS Tau	7.36±0.02	6.91±0.02	6.65±0.03	5.91±0.03	2004 Feb 9
J04484189+1703374	⋯	12.06±0.02	11.94±0.02	11.89±0.03	11.88±0.03	2006 Oct 26
J04514737+3047134	UY Aur A+B	6.08±0.02	5.53±0.02	4.98±0.03	3.92±0.03	2004 Feb 14
J04520668+3047175	IRAS 04489+3042	8.42±0.02	7.68±0.02	7.06±0.03	6.17±0.03	2004 Feb 14
J04551098+3021595	GM Aur	8.04±0.02	7.88±0.02	7.68±0.03	7.07±0.03	2004 Feb 14
J04552333+3027366	⋯	11.49±0.02	out	11.30±0.03	out	2004 Feb 15
		11.51±0.02	11.39±0.02	11.37±0.03	11.33±0.03	2005 Feb 20
		11.51±0.02	11.39±0.02	11.34±0.03	bad	2007 Mar 29
J04553695+3017553	LkCa 19	8.12±0.02	8.11±0.02	8.06±0.03	8.04±0.03	2004 Feb 14
		sat	sat	8.03±0.03	8.05±0.03	2005 Feb 20
J04554046+3039057	⋯	out	11.31±0.02	out	11.30±0.03	2004 Feb 14
		11.45±0.02	11.31±0.02	11.27±0.03	11.16±0.03	2005 Feb 20
		11.44±0.02	out	11.27±0.03	out	2008 Nov 1
J04554535+3019389	⋯	9.99±0.02	9.63±0.02	9.37±0.03	8.77±0.03	2004 Feb 14
		9.92±0.02	9.62±0.02	9.29±0.03	8.74±0.03	2005 Feb 20
		out	9.43±0.02	out	8.65±0.03	2008 Nov 1
J04554582+3033043	AB Aur	sat	sat	2.64±0.03	sat	2004 Feb 14
J04554757+3028077	⋯	9.63±0.02	out	9.49±0.03	out	2004 Feb 14
		9.60±0.02	9.51±0.02	9.48±0.03	9.43±0.03	2005 Feb 20
		9.65±0.02	9.52±0.02	9.50±0.03	9.46±0.03	2008 Nov 1
J04554801+3028050	⋯	11.43±0.02	out	10.78±0.03	out	2004 Feb 14
		11.38±0.02	11.00±0.02	10.68±0.03	10.02±0.03	2005 Feb 20
		11.42±0.02	11.09±0.02	10.75±0.03	10.09±0.03	2008 Nov 1
J04554820+3030160	XEST 26-052	10.64±0.02	10.53±0.02	10.52±0.03	10.52±0.03	2005 Feb 20
		10.67±0.02	10.55±0.02	10.56±0.03	10.38±0.03	2008 Nov 1
J04554969+3019400	⋯	out	11.21±0.02	out	out	2004 Feb 14
		11.36±0.02	11.15±0.02	10.95±0.03	10.62±0.03	2005 Feb 20
		out	11.11±0.02	out	10.66±0.03	2008 Nov 1
J04555288+3006523	⋯	10.39±0.02	10.31±0.02	10.26±0.03	10.24±0.03	2005 Feb 20
J04555605+3036209	XEST 26-062	8.68±0.02	8.36±0.02	8.01±0.03	7.16±0.03	2004 Feb 14
		out	8.41±0.02	out	7.18±0.03	2005 Feb 20
		8.69±0.02	8.37±0.02	7.99±0.03	7.20±0.03	2008 Nov 1
J04555636+3049374	⋯	10.75±0.02	10.65±0.02	10.58±0.03	10.58±0.03	2005 Feb 20
J04555938+3034015	SU Aur	sat	5.03±0.02	4.58±0.03	3.75±0.03	2004 Feb 14
		sat	sat	4.52±0.03	3.79±0.03	2008 Nov 1
J04560118+3026348	XEST26-071	9.42±0.02	9.08±0.02	8.68±0.03	7.99±0.03	2004 Feb 14
		out	9.02±0.02	out	8.07±0.03	2008 Nov 1
J04560201+3021037	HBC 427	8.09±0.02	8.10±0.02	8.06±0.03	8.02±0.03	2004 Feb 14
		sat	out	7.98±0.03	out	2005 Feb 20
		out	8.05±0.02	out	8.02±0.03	2008 Nov 1
J04574903+3015195	⋯	13.87±0.02	13.76±0.02	13.67±0.05	13.69±0.10	2005 Feb 20
		13.88±0.02	13.76±0.02	13.63±0.04	13.82±0.06	2006 Oct 26
J04584626+2950370	MWC 480	out	out	out	out	⋯
J05030659+2523197	V836 Tau	8.30±0.02	7.93±0.02	7.53±0.03	6.82±0.03	2004 Sep 7
J05044139+2509544	CIDA 8	9.21±0.02	8.88±0.02	8.65±0.03	8.00±0.03	2004 Feb 14
		9.15±0.02	8.86±0.02	8.61±0.03	7.96±0.03	2004 Feb 16
J05052286+2531312	CIDA 9	9.17±0.02	8.56±0.02	7.95±0.03	7.02±0.03	2004 Feb 14
J05061674+2446102	CIDA 10	9.59±0.02	9.45±0.02	9.44±0.03	9.41±0.03	2004 Feb 14
J05062332+2432199	CIDA 11	9.10±0.02	8.79±0.02	8.47±0.03	7.83±0.03	2004 Feb 14
J05064662+2104296	⋯	10.73±0.02	10.64±0.02	10.59±0.03	10.57±0.03	2008 Oct 31
J05071206+2437163	RXJ 05072+2437	9.23±0.02	9.24±0.02	9.18±0.03	9.14±0.03	2004 Feb 14
J05074953+3024050	RW Aur A+B	6.30±0.02	5.70±0.02	5.23±0.03	4.32±0.03	2004 Feb 12
J05075496+2500156	CIDA 12	10.06±0.02	9.84±0.02	9.51±0.03	8.72±0.03	2004 Feb 14

TABLE 4 — *Continued*

2MASS[a]	Name	[3.6]	[4.5]	[5.8]	[8.0]	Date

NOTE. — Entries of "···", "sat", "out", and "bad" indicate measurements that are absent because of non-detection, saturation, a position outside the field of view of the camera, and contamination by a cosmic ray, respectively.

[a] 2MASS Point Source Catalog.

TABLE 5
IRAC PHOTOMETRY FOR MEMBERS OF TAURUS WITH EXTENDED EMISSION

2MASS[a]	Name	Aperture[b]	[3.6]	[4.5]	[5.8]	[8.0]	Date
···	IRAS 04111+2800G	15	12.60±0.05	11.39±0.05	10.79±0.05	10.18±0.05	2005 Feb 19
		15	12.74±0.05	11.47±0.05	10.70±0.05	10.12±0.05	2007 Mar 29
···	IRAS 04166+2706	30	11.15±0.1	10.07±0.1	9.58±0.1	9.17±0.1	2005 Feb 20
		30	11.22±0.1	10.07±0.1	9.76±0.1	9.13±0.1	2005 Feb 21
		30	11.25±0.1	10.13±0.1	9.73±0.1	9.37±0.1	2007 Oct 17
J04195844+2709570	IRAS 04169+2702	30	8.32±0.05	7.13±0.05	···	···	2005 Feb 20
		30	8.29±0.05	out	···	···	2005 Feb 21
		30	8.19±0.05	7.03±0.05	···	···	2007 Oct 17
···	IRAM 04191+1522	15	13.79±0.05	12.30±0.05	11.74±0.1	12.17±0.15	2004 Sep 10
		15	14.06±0.05	12.62±0.05	12.14±0.05	12.39±0.1	2005 Sep 17
J04275730+2619183	IRAS 04248+2612	30	9.02±0.05	8.38±0.05	···	···	2004 Mar 7
		30	9.19±0.05	8.65±0.05	···	···	2005 Feb 22
···	L1521F-IRS	15	13.95±0.1	12.91±0.1	12.68±0.2	12.37±0.2	2004 Sep 9
		15	14.25±0.1	13.20±0.1	13.13±0.3	12.13±0.2	2005 Feb 24
		15	14.08±0.1	13.16±0.1	12.62±0.1	12.03±0.1	2006 Mar 25
J04313407+1808049	L1551/IRS5	30	6.74±0.05	5.32±0.05	···	···	2004 Oct 7
J04314444+1808315	L1551NE	30	8.39±0.05	6.94±0.05	···	···	2004 Oct 7
J04331650+2253204	IRAS 04302+2247	30	9.51±0.05	9.21±0.05	···	···	2005 Feb 20
		30	9.52±0.05	out	···	···	2005 Feb 24
		30	9.63±0.05	9.31±0.05	···	···	2007 Apr 3
J04353539+2408194	IRAS 04325+2402 A+B+C	30	8.98±0.05	8.55±0.05	8.49±0.05	8.16±0.05	2005 Feb 20
		30	9.00±0.05	8.47±0.05	8.45±0.05	8.17±0.05	2005 Feb 21
		30	9.07±0.05	8.61±0.05	8.56±0.05	8.24±0.05	2006 Mar 25
J04391389+2553208	IRAS 04361+2547	30	8.27±0.05	7.40±0.05	···	···	2004 Mar 7
		30	7.69±0.05	6.80±0.05	···	···	2005 Feb 22
···	IRAS 04368+2557	70	8.35±0.2	7.35±0.2	7.16±0.2	7.40±0.2	2004 Mar 7
		70	8.41±0.2	7.50±0.2	7.32±0.2	7.76±0.2	2005 Feb 22

NOTE. — Entries of "out" indicate measurements that are absent because of a position outside the field of view of the camera. We have not measured photometry with a large aperture if a source does not exhibit significant extended emission in a given band (···). Meausrements with the default 4-pixel apertures are available in Table 4.

[a] 2MASS Point Source Catalog.
[b] Aperture radius in pixels (1 pixel = 0.″86).

TABLE 6
MIPS 24 μM PHOTOMETRY FOR MEMBERS OF TAURUS

2MASS[a]	Name	[24]	Date
J04034930+2610520	HBC 358 A+B+C	8.98±0.08	2005 Feb 26
		8.67±0.13	2005 Mar 6
J04034997+2620382	XEST 06-006	out	···
J04035084+2610531	HBC 359	9.23±0.08	2005 Feb 26
J04043936+2158186	HBC 360	out	···
J04043984+2158215	HBC 361	out	···
J04044307+2618563	IRAS 04016+2610	sat	···
J04053087+2151106	HBC 362	9.40±0.06	2004 Sep 25
J04080782+2807280	···	out	···
J04131414+2819108	LkCa 1	8.13±0.07	2005 Feb 26
		8.21±0.07	2005 Mar 1
		8.07±0.05	2007 Feb 26
J04132722+2816247	Anon 1	7.28±0.07	2005 Feb 26
		6.90±0.04	2005 Mar 1
		6.94±0.04	2007 Feb 26
J04135328+2811233	IRAS 04108+2803 A	3.54±0.04	2005 Mar 1
		3.46±0.04	2007 Feb 26
J04135471+2811328	IRAS 04108+2803 B	1.36±0.04	2005 Mar 1
		1.04±0.04	2007 Feb 26
J04135737+2918193	IRAS 04108+2910	3.10±0.04	2007 Feb 26
J04141188+2811535	···	5.80±0.06	2005 Feb 26
		5.83±0.05	2007 Feb 26
···	IRAS 04111+2800G	3.48±0.04	2005 Mar 1
		3.45±0.04	2007 Feb 26
J04141291+2812124	V773 Tau A+B	1.43±0.04	2005 Mar 1

[a] 2MASS Point Source Catalog.

TABLE 6 — *Continued*

2MASS[a]	Name	[24]	Date
		1.56±0.04	2007 Feb 26
J04141358+2812492	FM Tau	2.79±0.04	2005 Mar 1
		2.91±0.04	2007 Feb 26
J04141458+2827580	FN Tau	1.86±0.04	2005 Mar 1
		2.00±0.04	2007 Feb 26
J04141700+2810578	CW Tau	1.51±0.04	2005 Mar 1
		1.61±0.04	2007 Feb 26
J04141760+2806096	CIDA 1	3.53±0.04	2005 Mar 1
		3.50±0.04	2007 Feb 26
J04142626+2806032	MHO 1+MHO 2[b]	sat	···
J04143054+2805147	MHO 3	sat	···
J04144730+2646264	FP Tau	4.28±0.04	2007 Feb 26
J04144739+2803055	XEST 20-066	9.14±0.10	2005 Mar 1
		9.37±0.23	2007 Feb 26
J04144786+2648110	CX Tau	3.38±0.04	2007 Feb 26
J04144797+2752346	LkCa 3 A+B	7.07±0.05	2005 Feb 26
		7.17±0.04	2005 Mar 1
		7.09±0.04	2007 Feb 26
J04144928+2812305	FO Tau A+B	2.77±0.04	2005 Mar 1
		2.88±0.04	2007 Feb 26
J04145234+2805598	XEST 20-071	7.04±0.04	2005 Mar 1
		7.15±0.05	2007 Feb 26
J04150515+2808462	CIDA 2	8.43±0.07	2005 Mar 1
		8.50±0.10	2007 Feb 26
J04151471+2800096	KPNO 1	···	···
J04152409+2910434	···	···	···
J04153916+2818586	···	4.28±0.04	2004 Sep 23
		4.20±0.04	2007 Feb 23
J04154278+2909597	IRAS 04125+2902	4.50±0.04	2007 Feb 23
J04155799+2746175	···	5.78±0.04	2007 Feb 23
J04161210+2756385	···	5.44±0.04	2004 Sep 23
		5.38±0.04	2007 Feb 23
J04161885+2752155	···	···	···
J04162725+2053091	···	out	···
J04162810+2807358	LkCa 4	7.92±0.04	2004 Sep 23
		7.96±0.06	2007 Feb 23
J04163048+3037053	···	out	···
J04163911+2858491	···	7.25±0.05	2007 Feb 23
J04173372+2820468	CY Tau	4.43±0.04	2004 Sep 23
		4.44±0.04	2005 Feb 28
		4.41±0.04	2007 Feb 23
J04173893+2833005	LkCa 5	8.44±0.07	2004 Sep 19
		8.67±0.06	2004 Sep 23
		8.60±0.08	2007 Feb 23
J04174955+2813318	KPNO 10	5.92±0.04	2004 Sep 23
		5.99±0.04	2005 Feb 28
		5.93±0.04	2007 Feb 23
J04174965+2829362	V410 X-ray 1	3.92±0.04	2004 Sep 19
		3.96±0.04	2004 Sep 23
		3.85±0.04	2005 Feb 28
		3.81±0.04	2007 Feb 23
J04180796+2826036	V410 X-ray 3	9.19±0.06	2004 Sep 23
		8.74±0.16	2005 Feb 28
J04181078+2519574	V409 Tau	4.49±0.04	2007 Feb 23
J04181710+2828419	V410 Anon 13	6.07±0.04	2004 Sep 23
		6.06±0.04	2005 Feb 28
		6.03±0.04	2007 Feb 23
J04182147+1658470	HBC 372	out	···
J04182909+2826191	V410 Anon 25	8.18±0.05	2004 Sep 23
		8.00±0.07	2005 Feb 28
		8.18±0.09	2007 Feb 23
J04183030+2743208	KPNO 11	···	···
J04183110+2827162	V410 Tau A+B+C	7.13±0.04	2004 Sep 23
		7.12±0.05	2005 Feb 28
		7.11±0.05	2007 Feb 23
J04183112+2816290	DD Tau A+B	1.73±0.04	2004 Sep 23
		1.67±0.04	2005 Feb 28
J04183158+2816585	CZ Tau A+B	1.96±0.04	2004 Sep 23
		1.94±0.04	2005 Feb 28
J04183203+2831153	IRAS 04154+2823	1.90±0.04	2004 Sep 23
		2.06±0.04	2005 Feb 28
		1.82±0.04	2007 Feb 23
J04183444+2830302	V410 X-ray 2	3.42±0.04	2004 Sep 23
		3.48±0.04	2005 Feb 28
		3.34±0.04	2007 Feb 23
J04184023+2824245	V410 X-ray 4	8.07±0.06	2004 Sep 23

Luhman et al.

TABLE 6 — *Continued*

2MASS[a]	Name	[24]	Date
		7.90±0.08	2005 Feb 28
		8.20±0.10	2007 Feb 23
J04184061+2819155	V892 Tau	sat	⋯
J04184133+2827250	LR1	4.61±0.04	2004 Sep 23
		4.63±0.04	2005 Feb 28
		4.64±0.04	2007 Feb 23
J04184250+2818498	V410 X-ray 7	⋯	⋯
J04184703+2820073	Hubble 4	6.99±0.23	2004 Sep 23
		6.62±0.10	2005 Feb 28
		6.60±0.15	2007 Feb 23
J04185115+2814332	KPNO 2	⋯	⋯
J04185147+2820264	CoKu Tau/1	0.83±0.04	2004 Sep 23
		0.85±0.04	2005 Feb 28
		0.84±0.04	2007 Feb 23
J04185170+1723165	HBC 376	8.95±0.08	2004 Sep 25
J04185813+2812234	IRAS 04158+2805	2.71±0.04	2004 Sep 23
		2.74±0.04	2005 Feb 28
		2.73±0.04	2007 Feb 23
J04190110+2819420	V410 X-ray 6	3.63±0.04	2004 Sep 23
		3.62±0.04	2005 Feb 28
		3.69±0.04	2007 Feb 23
J04190126+2802487	KPNO 12	⋯	⋯
J04190197+2822332	V410 X-ray 5a	8.84±0.07	2004 Sep 23
		9.09±0.17	2005 Feb 28
		9.08±0.24	2007 Feb 23
J04191281+2829330	FQ Tau A+B	4.92±0.04	2004 Sep 23
		4.84±0.04	2005 Feb 28
		4.82±0.04	2007 Feb 23
J04191583+2906269	BP Tau	2.51±0.04	2007 Feb 23
J04192625+2826142	V819 Tau	6.33±0.04	2004 Sep 23
		6.30±0.04	2005 Feb 28
		6.36±0.04	2007 Feb 23
J04193545+2827218	FR Tau	4.79±0.04	2004 Sep 23
		4.84±0.04	2005 Feb 28
		4.82±0.04	2007 Feb 23
J04194127+2749484	LkCa 7 A+B	7.74±0.05	2005 Feb 26
		7.71±0.06	2005 Feb 28
		7.79±0.06	2007 Oct 28
J04194148+2716070	IRAS 04166+2708	3.19±0.04	2005 Feb 28
		3.25±0.04	2007 Oct 28
⋯	IRAS 04166+2706	2.91±0.04	2005 Feb 28
		2.90±0.04	2007 Oct 28
J04194657+2712552	[GKH94] 41	4.07±0.04	2005 Feb 28
		4.07±0.04	2007 Oct 28
J04195844+2709570	IRAS 04169+2702	sat	⋯
J04201611+2821325	⋯	8.16±0.06	2005 Feb 28
		8.20±0.09	2007 Feb 23
J04202144+2813491	⋯	8.63±0.15	2005 Feb 28
		8.46±0.13	2007 Feb 23
		8.68±0.09	2007 Oct 29
J04202555+2700355	⋯	6.11±0.04	2005 Feb 28
		6.07±0.04	2007 Oct 28
J04202583+2819237	IRAS 04173+2812	3.73±0.04	2005 Feb 28
		3.83±0.04	2007 Feb 23
J04202606+2804089	⋯	3.25±0.04	2005 Feb 28
J04203918+2717317	XEST 16-045	9.06±0.13	2005 Feb 28
		8.91±0.11	2007 Oct 28
J04205273+1746415	J2-157	out	⋯
J04210795+2702204	⋯	1.69±0.04	2005 Feb 28
		1.50±0.04	2007 Oct 28
J04210934+2750368	⋯	7.13±0.05	2005 Feb 28
		7.17±0.05	2007 Oct 28
J04211038+2701372	IRAS 04181+2654 B	2.64±0.04	2005 Feb 28
		2.67±0.04	2007 Oct 28
J04211146+2701094	IRAS 04181+2654 A	1.65±0.04	2005 Feb 28
		1.52±0.04	2007 Oct 28
J04213459+2701388	⋯	7.18±0.05	2005 Feb 28
		7.02±0.05	2007 Feb 28
		7.19±0.05	2007 Oct 28
J04214013+2814224	XEST 21-026	⋯	⋯
J04214323+1934133	IRAS 04187+1927	out	⋯
J04214631+2659296	⋯	7.21±0.05	2005 Feb 28
		7.42±0.05	2007 Feb 28
		7.23±0.05	2007 Oct 28
J04215450+2652315	⋯	⋯	⋯
J04215563+2755060	DE Tau	2.56±0.04	2005 Feb 27
		2.58±0.04	2007 Oct 28

TABLE 6 — *Continued*

2MASS[a]	Name	[24]	Date
$\cdots$	IRAM 04191+1522	6.65±0.04	2005 Sep 26
		6.64±0.04	2007 Sep 23
J04215740+2826355	RY Tau	sat	$\cdots$
J04215884+2818066	HD 283572	6.70±0.05	2004 Sep 19
		6.75±0.04	2005 Feb 27
J04215943+1932063	T Tau N+S	out	$\cdots$
J04220043+1530212	IRAS 04191+1523 A+B	1.89±0.04	2005 Sep 26
		1.68±0.04	2007 Sep 23
J04220069+2657324	Haro 6-5B	1.62±0.04	2005 Feb 28
		1.45±0.04	2007 Feb 28
		1.47±0.04	2007 Oct 28
J04220217+2657304	FS Tau A+B	1.34±0.04	2005 Feb 28
		0.93±0.04	2007 Feb 28
		1.25±0.04	2007 Oct 28
J04220313+2825389	LkCa 21	7.95±0.08	2004 Sep 19
		7.76±0.08	2005 Feb 27
J04221332+1934392	$\cdots$	out	$\cdots$
J04221568+2657060	XEST 11-078	3.73±0.04	2005 Feb 28
		3.79±0.04	2007 Feb 28
		3.81±0.04	2007 Oct 28
J04221644+2549118	$\cdots$	$\cdots$	$\cdots$
J04221675+2654570	$\cdots$	3.29±0.04	2007 Feb 28
		3.31±0.04	2007 Oct 28
J04222404+2646258	XEST 11-087	8.63±0.09	2007 Feb 28
		8.98±0.12	2007 Oct 28
J04224786+2645530	IRAS 04196+2638	3.35±0.04	2005 Feb 27
		3.01±0.04	2007 Feb 28
		3.25±0.04	2007 Oct 28
J04230607+2801194	$\cdots$	6.41±0.04	2005 Feb 27
J04230776+2805573	IRAS 04200+2759	3.26±0.04	2005 Feb 27
J04231822+2641156	$\cdots$	4.63±0.04	2005 Feb 27
		4.53±0.04	2007 Sep 23
		4.54±0.04	2007 Oct 28
J04233539+2503026	FU Tau A	4.62±0.04	2007 Feb 28
J04233573+2502596	FU Tau B	$\cdots$	$\cdots$
J04233919+2456141	FT Tau	3.15±0.04	2007 Feb 28
J04242090+2630511	$\cdots$	7.48±0.05	2005 Feb 27
J04242646+2649503	$\cdots$	6.79±0.04	2005 Feb 27
J04244457+2610141	IRAS 04216+2603	3.51±0.04	2005 Feb 27
J04244506+2701447	J1-4423	$\cdots$	$\cdots$
J04245708+2711565	IP Tau	3.56±0.04	2005 Feb 27
		3.46±0.04	2005 Mar 1
J04251767+2617504	J1-4872 A+B	7.65±0.06	2005 Feb 27
J04262939+2624137	KPNO 3	6.81±0.05	2005 Feb 28
		6.87±0.04	2005 Mar 1
J04263055+2443558	$\cdots$	8.61±0.18	2005 Feb 27
		9.13±0.21	2005 Mar 1
J04265352+2606543	FV Tau A+B	1.43±0.04	2005 Feb 28
		1.46±0.04	2005 Mar 1
J04265440+2606510	FV Tau/c A+B	$\cdots$	$\cdots$
J04265629+2443353	IRAS 04239+2436	sat	$\cdots$
J04265732+2606284	KPNO 13	5.27±0.04	2005 Feb 28
		5.30±0.04	2005 Mar 1
J04270266+2605304	DG Tau B	sat	$\cdots$
J04270280+2542223	DF Tau A+B	2.20±0.04	2005 Feb 28
		2.23±0.04	2005 Mar 1
J04270469+2606163	DG Tau	sat	$\cdots$
J04270739+2215037	$\cdots$	out	$\cdots$
J04272799+2612052	KPNO 4	$\cdots$	$\cdots$
J04274538+2357243	$\cdots$	$\cdots$	$\cdots$
J04275730+2619183	IRAS 04248+2612	2.25±0.04	2005 Feb 28
		2.23±0.04	2005 Mar 1
$\cdots$	L1521F-IRS	6.09±0.04	2004 Sep 25
		6.11±0.04	2005 Mar 2
		6.10±0.04	2007 Sep 25
J04284263+2714039	$\cdots$	6.23±0.04	2005 Mar 2
		6.27±0.04	2007 Sep 25
J04290068+2755033	$\cdots$	8.08±0.07	2005 Mar 2
J04290498+2649073	IRAS 04260+2642	3.59±0.04	2005 Mar 2
		3.35±0.04	2007 Sep 25
J04292071+2633406	J1-507	8.03±0.07	2005 Mar 2
		8.19±0.05	2007 Feb 24
		8.25±0.08	2007 Sep 25
J04292165+2701259	IRAS 04263+2654	3.42±0.04	2005 Mar 2
J04292373+2433002	GV Tau A+B	sat	$\cdots$
J04292971+2616532	FW Tau A+B+C	7.56±0.07	2005 Mar 2
		7.64±0.04	2007 Feb 24

TABLE 6 — *Continued*

2MASS[a]	Name	[24]	Date
J04293008+2439550	IRAS 04264+2433	0.97±0.04	2005 Mar 2
		1.09±0.04	2007 Sep 23
J04293209+2430597	· · ·	3.90±0.04	2005 Mar 2
		3.94±0.04	2007 Sep 23
J04293606+2435556	XEST 13-010	4.15±0.04	2005 Mar 2
		4.11±0.04	2007 Sep 23
J04294155+2632582	DH Tau A+B	3.32±0.04	2004 Sep 25
		3.34±0.04	2005 Mar 2
		3.21±0.04	2007 Feb 24
J04294247+2632493	DI Tau A+B	· · ·	· · ·
J04294568+2630468	KPNO 5	· · ·	· · ·
J04295156+2606448	IQ Tau	2.81±0.04	2005 Mar 2
		2.84±0.04	2007 Feb 24
J04295422+1754041	· · ·	out	· · ·
J04295950+2433078	· · ·	4.92±0.04	2005 Mar 2
		4.86±0.04	2007 Sep 23
J04300399+1813493	UX Tau A+B+C	1.83±0.04	2004 Sep 25
J04300724+2608207	KPNO 6	9.10±0.22	2005 Mar 2
		9.20±0.09	2007 Feb 24
J04302365+2359129	· · ·	· · ·	· · ·
J04302961+2426450	FX Tau A+B	3.04±0.04	2005 Feb 26
		3.04±0.04	2005 Mar 2
		2.88±0.04	2007 Sep 23
J04304425+2601244	DK Tau A+B	1.84±0.04	2005 Mar 2
J04305028+2300088	IRAS 04278+2253 A+B	sat	· · ·
J04305137+2442222	ZZ Tau	4.42±0.04	2004 Sep 25
		4.54±0.04	2005 Mar 2
J04305171+2441475	ZZ Tau IRS	2.06±0.04	2004 Sep 25
		2.02±0.04	2005 Mar 2
J04305718+2556394	KPNO 7	8.44±0.09	2005 Mar 2
J04311444+2710179	JH 56	6.72±0.04	2005 Mar 1
J04311578+1820072	MHO 9	9.80±0.15	2006 Feb 19
J04311907+2335047	· · ·	· · ·	· · ·
J04312382+2410529	V927 Tau A+B	8.25±0.07	2004 Sep 25
		8.20±0.08	2005 Mar 2
J04312405+1800215	MHO 4	9.62±0.12	2006 Feb 19
J04312669+2703188	· · ·	· · ·	· · ·
J04313407+1808049	L1551/IRS5	sat	· · ·
J04313613+1813432	LkHα 358	2.48±0.04	2004 Feb 20
		2.64±0.05	2006 Feb 19
J04313747+1812244	HH 30	6.84±0.06	2004 Feb 20
		6.40±0.04	2006 Feb 19
J04313843+1813576	HL Tau	sat	· · ·
J04314007+1813571	XZ Tau A+B	sat	· · ·
J04314444+1808315	L1551NE	0.55±0.04	2006 Feb 19
J04315056+2424180	HK Tau A+B	2.35±0.04	2004 Sep 25
		2.31±0.04	2005 Mar 2
		2.28±0.04	2007 Sep 23
J04315779+1821380	V710 Tau A+B	3.65±0.04	2004 Feb 20
		3.64±0.04	2004 Sep 25
		3.67±0.04	2006 Feb 19
J04315844+2543299	J1-665	9.26±0.18	2005 Mar 1
J04315968+1821305	LkHα 267	4.51±0.04	2004 Feb 20
		4.55±0.04	2004 Sep 25
		4.50±0.04	2006 Feb 19
J04320329+2528078	· · ·	· · ·	· · ·
J04320926+1757227	L1551-51	8.81±0.07	2004 Feb 20
		8.56±0.08	2004 Sep 23
		8.49±0.06	2006 Feb 19
J04321456+1820147	V827 Tau	7.95±0.06	2004 Feb 20
		7.81±0.05	2006 Feb 19
J04321540+2428597	Haro 6-13	sat	· · ·
J04321583+1801387	V826 Tau A+B	7.78±0.05	2004 Feb 20
		7.88±0.04	2006 Feb 19
J04321606+1812464	MHO 5	5.68±0.04	2004 Feb 20
		5.64±0.04	2006 Feb 19
J04321786+2422149	· · ·	9.69±0.10	2007 Sep 23
J04321885+2422271	V928 Tau A+B	7.59±0.05	2004 Sep 25
		7.52±0.05	2005 Mar 1
		7.58±0.04	2007 Sep 23
J04322210+1827426	MHO 6	6.27±0.04	2004 Feb 20
		6.43±0.04	2006 Feb 19
J04322329+2403013	· · ·	· · ·	· · ·
J04322415+2251083	· · ·	6.12±0.04	2005 Mar 2
J04322627+1827521	MHO 7	9.82±0.24	2006 Feb 19
J04323028+1731303	GG Tau Ba+Bb	out	· · ·
J04323034+1731406	GG Tau Aa+Ab	out	· · ·

TABLE 6 — *Continued*

2MASS[a]	Name	[24]	Date
J04323058+2419572	FY Tau	3.79±0.04	2004 Sep 25
		3.67±0.04	2005 Mar 1
		3.75±0.04	2007 Sep 23
J04323176+2420029	FZ Tau	1.78±0.04	2004 Sep 25
		2.07±0.04	2005 Mar 1
		1.90±0.04	2007 Sep 23
J04323205+2257266	IRAS 04295+2251	1.25±0.04	2005 Mar 2
		1.12±0.04	2007 Feb 27
J04324303+2552311	UZ Tau A+Ba+Bb	1.57±0.04	2005 Mar 1
J04324373+1802563	L1551-55	8.85±0.15	2004 Feb 20
		9.11±0.10	2004 Sep 25
		9.12±0.09	2006 Feb 19
J04324911+2253027	JH 112	2.50±0.04	2005 Mar 2
		2.54±0.04	2007 Feb 26
J04324938+2253082	⋯	⋯	⋯
J04325026+2422115	⋯	9.81±0.25	2004 Sep 25
		9.40±0.07	2005 Sep 25
		9.42±0.10	2007 Sep 24
J04325119+1730092	LH 0429+17	out	⋯
J04330197+2421000	MHO 8	8.72±0.07	2004 Sep 25
		9.24±0.15	2005 Mar 1
		8.87±0.05	2005 Sep 25
		8.83±0.09	2007 Sep 24
J04330622+2409339	GH Tau A+B	3.25±0.04	2005 Feb 26
		3.19±0.04	2005 Mar 1
		3.26±0.04	2007 Sep 24
J04330664+2409549	V807 Tau A+B	3.04±0.04	2005 Feb 26
		2.95±0.04	2005 Mar 1
		3.06±0.04	2007 Sep 24
J04330781+2616066	KPNO 14	9.27±0.25	2005 Mar 1
		9.21±0.21	2007 Oct 27
J04330945+2246487	⋯	8.25±0.08	2005 Mar 1
		8.25±0.08	2007 Feb 26
J04331003+2433433	V830 Tau	8.30±0.09	2004 Sep 18
		8.25±0.08	2005 Feb 26
		8.18±0.07	2005 Mar 1
J04331435+2614235	IRAS 04301+2608	3.23±0.04	2005 Mar 1
		3.35±0.04	2007 Oct 27
J04331650+2253204	IRAS 04302+2247	3.56±0.04	2005 Mar 1
		3.46±0.04	2007 Feb 27
J04331907+2246342	IRAS 04303+2240	1.27±0.04	2005 Mar 1
		1.44±0.04	2007 Feb 26
J04332621+2245293	XEST 17-036	8.34±0.09	2005 Mar 1
		8.27±0.08	2007 Feb 26
J04333278+1800436	⋯	out	⋯
J04333297+1801004	HD 28867 A+B+C	out	⋯
J04333405+2421170	GI Tau	1.93±0.04	2004 Sep 18
		2.09±0.05	2005 Feb 26
		2.05±0.04	2005 Mar 1
J04333456+2421058	GK Tau	1.64±0.04	2004 Sep 18
		1.69±0.04	2005 Mar 1
J04333678+2609492	IS Tau A+B	3.69±0.04	2005 Mar 1
J04333905+2227207	⋯	4.89±0.04	2007 Feb 26
J04333906+2520382	DL Tau	2.17±0.04	2005 Mar 1
		2.12±0.04	2007 Oct 27
J04333935+1751523	HN Tau A+B	out	⋯
J04334171+1750402	⋯	out	⋯
J04334291+2526470	⋯	⋯	⋯
J04334465+2615005	⋯	4.54±0.04	2005 Mar 1
J04334871+1810099	DM Tau	out	⋯
J04335200+2250301	CI Tau	2.12±0.04	2005 Mar 1
		2.15±0.04	2007 Feb 26
J04335245+2612548	⋯	8.26±0.09	2005 Mar 1
J04335252+2256269	XEST 17-059	8.41±0.10	2005 Mar 1
J04335470+2613275	IT Tau A+B	3.51±0.04	2005 Mar 1
J04335546+1838390	J2-2041	out	⋯
J04341099+2251445	JH 108	8.75±0.12	2005 Mar 1
		8.64±0.21	2007 Feb 27
J04341527+2250309	CFHT 1	⋯	⋯
J04341803+1830066	HBC 407	out	⋯
J04344544+2308027	⋯	⋯	⋯
J04345542+2428531	AA Tau	2.80±0.04	2005 Mar 1
		2.78±0.04	2006 Feb 26
J04345693+2258358	XEST 08-003	8.34±0.07	2005 Mar 1
		8.31±0.08	2007 Feb 26
J04350850+2311398	⋯	⋯	⋯
J04352020+2232146	HO Tau	4.90±0.04	2007 Feb 26

Luhman et al.

TABLE 6 — *Continued*

2MASS[a]	Name	[24]	Date
J04352089+2254242	FF Tau A+B	8.18±0.12	2005 Mar 1
		8.25±0.11	2007 Feb 26
J04352450+1751429	HBC 412 A+B	8.75±0.07	2004 Sep 23
J04352737+2414589	DN Tau	3.04±0.04	2005 Mar 1
		2.95±0.04	2006 Feb 26
J04353539+2408194	IRAS 04325+2402 A+B+C	1.40±0.04	2005 Mar 1
		1.29±0.04	2006 Feb 26
J04354093+2411087	CoKu Tau 3 A+B	3.29±0.04	2005 Feb 26
		3.28±0.04	2005 Mar 1
		3.13±0.04	2006 Feb 26
J04354183+2234115	KPNO 8	⋯	⋯
J04354203+2252226	XEST 08-033	9.00±0.17	2005 Mar 1
		8.84±0.12	2007 Feb 26
J04354526+2737130	⋯	⋯	⋯
J04354733+2250216	HQ Tau	1.39±0.04	2005 Mar 1
		1.53±0.04	2007 Feb 26
J04355109+2252401	KPNO 15	⋯	⋯
J04355143+2249119	KPNO 9	⋯	⋯
J04355209+2255039	XEST 08-047	⋯	⋯
J04355277+2254231	HP Tau	1.12±0.04	2005 Mar 1
		1.27±0.04	2007 Feb 26
J04355286+2250585	XEST 08-049	8.87±0.15	2005 Mar 1
		8.93±0.15	2007 Feb 26
J04355349+2254089	HP Tau/G3	⋯	⋯
J04355415+2254134	HP Tau/G2	⋯	⋯
J04355684+2254360	Haro 6-28 A+B	4.38±0.04	2005 Mar 1
		4.43±0.04	2007 Feb 26
J04355892+2238353	XEST 09-042	⋯	⋯
J04361030+2159364	⋯	8.62±0.09	2007 Feb 26
J04361038+2259560	CFHT 2	⋯	⋯
J04361909+2542589	LkCa 14	8.44±0.06	2004 Sep 25
		8.19±0.07	2005 Mar 1
		8.19±0.08	2006 Feb 20
J04362151+2351165	⋯	7.83±0.06	2005 Mar 1
J04363893+2258119	CFHT 3	⋯	⋯
J04373705+2331080	⋯	⋯	⋯
J04375670+2546229	ITG 1	7.13±0.05	2005 Mar 4
J04380083+2558572	ITG 2	9.25±0.25	2005 Mar 5
J04381486+2611399	⋯	5.03±0.04	2005 Mar 4
J04381630+2326402	⋯	⋯	⋯
J04382134+2609137	GM Tau	5.33±0.04	2005 Feb 26
		5.32±0.04	2005 Mar 4
J04382858+2610494	DO Tau	0.79±0.04	2005 Feb 26
		0.90±0.04	2005 Mar 4
J04383528+2610386	HV Tau A+B	⋯	⋯
⋯	HV Tau C	3.48±0.04	2005 Feb 26
		3.50±0.04	2005 Mar 4
J04385859+2336351	⋯	6.40±0.04	2005 Mar 4
J04385871+2323595	⋯	⋯	⋯
J04390163+2336029	⋯	6.25±0.04	2005 Mar 4
J04390396+2544264	⋯	6.44±0.04	2005 Mar 4
J04390525+2337450	⋯	3.47±0.04	2005 Mar 4
J04390637+2334179	⋯	⋯	⋯
J04391389+2553208	IRAS 04361+2547	sat	⋯
J04391741+2247533	VY Tau A+B	4.61±0.04	2007 Feb 26
J04391779+2221034	LkCa 15	3.09±0.04	2007 Feb 26
J04392090+2545021	GN Tau A+B	2.83±0.04	2005 Mar 4
J04393364+2359212	⋯	5.23±0.04	2005 Mar 4
J04393519+2541447	IRAS 04365+2535	sat	⋯
J04394488+2601527	ITG 15	3.94±0.04	2005 Mar 4
J04394748+2601407	CFHT 4	4.96±0.04	2005 Mar 4
⋯	IRAS 04368+2557	2.73±0.04	2005 Mar 4
J04395574+2545020	IC2087IR	sat	⋯
J04400067+2358211	⋯	6.37±0.04	2005 Mar 4
J04400174+2556292	⋯	8.94±0.13	2005 Mar 5
J04400800+2605253	IRAS 04370+2559	2.46±0.04	2005 Mar 4
J04403979+2519061	⋯	7.52±0.06	2005 Feb 28
		7.47±0.06	2005 Mar 4
J04404950+2551191	JH 223	5.19±0.04	2004 Sep 25
		5.10±0.04	2005 Feb 28
		5.19±0.04	2007 Sep 24
J04410424+2557561	Haro 6-32	9.52±0.17	2004 Sep 25
		9.70±0.27	2007 Sep 24
J04410470+2451062	IW Tau A+B	7.91±0.07	2005 Feb 26
		7.83±0.06	2005 Feb 28
		8.08±0.11	2005 Mar 4
J04410826+2556074	ITG 33A	4.80±0.04	2004 Sep 25

TABLE 6 — *Continued*

2MASS[a]	Name	[24]	Date
		4.64±0.04	2005 Feb 26
		4.65±0.04	2005 Feb 28
		4.40±0.04	2007 Sep 24
J04411078+2555116	ITG 34	6.53±0.04	2004 Sep 25
		6.58±0.04	2005 Feb 26
		6.46±0.04	2005 Feb 28
		6.52±0.04	2007 Sep 24
J04411267+2546354	IRAS 04381+2540	1.43±0.04	2004 Sep 25
		1.37±0.04	2005 Feb 26
		1.35±0.04	2005 Feb 28
		1.33±0.04	2007 Sep 24
J04411681+2840000	CoKu Tau/4	2.30±0.04	2007 Sep 25
J04412464+2543530	ITG 40	5.54±0.04	2004 Sep 25
		5.70±0.04	2005 Feb 26
		5.65±0.04	2005 Feb 28
		5.52±0.04	2007 Sep 25
J04413882+2556267	IRAS 04385+2550	1.81±0.04	2004 Sep 25
		1.84±0.04	2005 Feb 28
		1.91±0.04	2007 Sep 25
J04414489+2301513	· · ·	out	· · ·
J04414565+2301580	· · ·	out	· · ·
J04414825+2534304	· · ·	6.26±0.04	2004 Sep 25
		6.32±0.04	2005 Feb 28
		6.31±0.04	2007 Sep 25
J04420548+2522562	LkHa 332/G2 A+B	7.26±0.07	2004 Sep 25
		7.09±0.05	2005 Feb 28
		7.24±0.09	2007 Sep 25
J04420732+2523032	LkHa 332/G1 A+B	· · ·	· · ·
J04420777+2523118	V955 Tau A+B	2.86±0.04	2004 Sep 25
		2.78±0.04	2005 Feb 28
		2.73±0.04	2007 Sep 25
J04422101+2520343	CIDA 7	4.22±0.04	2004 Sep 25
		4.26±0.04	2005 Feb 28
J04423769+2515374	DP Tau	1.85±0.04	2005 Feb 28
J04430309+2520187	GO Tau	4.35±0.04	2005 Feb 28
J04432023+2940060	CIDA 14	5.56±0.04	2004 Sep 23
J04442713+2512164	IRAS 04414+2506	4.30±0.04	2005 Feb 28
J04455129+1555496	HD 30171	· · ·	· · ·
J04455134+1555367	IRAS 04429+1550	2.55±0.04	2005 Mar 3
J04464260+2459034	RXJ 04467+2459	· · ·	· · ·
J04465305+1700001	DQ Tau	out	· · ·
J04465897+1702381	Haro 6-37 A+B	out	· · ·
J04470620+1658428	DR Tau	out	· · ·
J04474859+2925112	DS Tau	out	· · ·
J04484189+1703374	· · ·	out	· · ·
J04514737+3047134	UY Aur A+B	out	· · ·
J04520668+3047175	IRAS 04489+3042	out	· · ·
J04551098+3021595	GM Aur	2.48±0.04	2005 Mar 5
J04552333+3027366	· · ·	· · ·	· · ·
J04553695+3017553	LkCa 19	6.99±0.04	2004 Oct 12
		7.09±0.04	2005 Mar 5
J04554046+3039057	· · ·	· · ·	· · ·
J04554535+3019389	· · ·	6.41±0.04	2004 Oct 12
		6.49±0.04	2005 Mar 5
J04554582+3033043	AB Aur	sat	· · ·
J04554757+3028077	· · ·	· · ·	· · ·
J04554801+3028050	· · ·	7.05±0.04	2005 Mar 5
J04554820+3030160	XEST 26-052	· · ·	· · ·
J04554969+3019400	· · ·	8.16±0.08	2004 Sep 25
		7.94±0.07	2004 Oct 12
		8.19±0.08	2005 Mar 5
J04555288+3006523	· · ·	out	· · ·
J04555605+3036209	XEST 26-062	3.74±0.04	2004 Sep 25
		3.77±0.04	2005 Mar 5
J04555636+3049374	· · ·	· · ·	· · ·
J04555938+3034015	SU Aur	sat	· · ·
J04560118+3026348	XEST26-071	5.81±0.04	2005 Mar 5
J04560201+3021037	HBC 427	7.67±0.08	2004 Sep 25
		7.55±0.11	2005 Mar 5
J04574903+3015195	· · ·	out	· · ·
J04584626+2950370	MWC 480	out	· · ·
J05030659+2523197	V836 Tau	3.83±0.04	2004 Sep 25
J05044139+2509544	CIDA 8	5.18±0.04	2008 Apr 17
J05052286+2531312	CIDA 9	out	· · ·
J05061674+2446102	CIDA 10	out	· · ·
J05062332+2432199	CIDA 11	out	· · ·
J05064662+2104296	· · ·	out	· · ·

TABLE 6 — *Continued*

2MASS[a]	Name	[24]	Date
J05071206+2437163	RXJ 05072+2437	out	⋯
J05074953+3024050	RW Aur A+B	out	⋯
J05075496+2500156	CIDA 12	out	⋯

NOTE. — Entries of "⋯", "sat", and "out" indicate measurements that are absent because of non-detection, saturation, and a position outside the field of view of the camera, respectively.

[a] 2MASS Point Source Catalog.

[b] 2MASS J04142639+2805597.

TABLE 7
SPECTRAL SLOPES FOR MEMBERS OF TAURUS

2MASS[a]	Name	Spectral Type	α(2–8 μm)	α(2–24 μm)	α(3.6–8 μm)	α(3.6–24 μm)	SED Class
J04034930+2610520	HBC 358 A+B+C	M3.5	−2.49/−2.49	−2.68/−2.68	−2.74/−2.74	−2.83/−2.83	III
J04034997+2620382	XEST 06-006	M5.25	⋯	⋯	⋯	⋯	III?
J04035084+2610531	HBC 359	M2	−2.58/−2.58	−2.77/−2.77	−2.74/−2.74	−2.88/−2.88	III
J04043936+2158186	HBC 360	M3.5	−2.54/−2.54	⋯	−2.75/−2.75	⋯	III
J04043984+2158215	HBC 361	M3	−2.55/−2.55	⋯	−2.73/−2.73	⋯	III
J04044307+2618563	IRAS 04016+2610	K3	1.74	⋯	0.85	⋯	I
J04053087+2151106	HBC 362	M2	−2.58/−2.58	−2.63/−2.63	−2.77/−2.77	−2.73/−2.73	III
J04080782+2807280	⋯	M3.75	⋯	⋯	⋯	⋯	III?
J04131414+2819108	LkCa 1	M4	−2.64/−2.71	−2.69/−2.73	−2.76/−2.79	−2.76/−2.77	III
J04132722+2816247	Anon 1	M0	−2.51/−2.65	−2.71/−2.79	−2.69/−2.76	−2.84/−2.87	III
J04135328+2811233	IRAS 04108+2803 A	M3.5–M6[c]	−0.09	−0.23	−0.13	−0.28	I
J04135471+2811328	IRAS 04108+2803 B	K6–M3.5[c]	0.96	0.91	1.14	0.97	I
J04135737+2918193	IRAS 04108+2910	M0	−0.23/−0.43	−0.47/−0.57	−0.61/−0.70	−0.68/−0.72	II
J04141188+2811535	⋯	M6.25	−0.85/−0.94	−0.63/−0.68	−0.55/−0.60	−0.45/−0.47	II
⋯	IRAS 04111+2800G	K6–M3.5[c]	⋯	⋯	0.22	1.74	I
J04141291+2812124	V773 Tau A+B	K3	−1.48/−1.62	−1.06/−1.14	−0.99/−1.05	−0.75/−0.78	II
J04141358+2812492	FM Tau	M0	−1.03/−1.13	−0.60/−0.65	−0.92/−0.97	−0.44/−0.46	II
J04141458+2827580	FN Tau	M5	−1.03/−1.11	−0.47/−0.51	−0.81/−0.84	−0.23/−0.25	II
J04141700+2810578	CW Tau	K3	−0.80/−1.01	−0.73/−0.84	−1.11/−1.21	−0.85/−0.89	II
J04141760+2806096	CIDA 1	M5.5	−0.40/−0.62	−0.43/−0.55	−0.52/−0.62	−0.48/−0.53	II
J04142626+2806032	MHO 1	M2.5	−0.31/−1.09	⋯	−0.41/−0.77	⋯	II
J04142639+2805597	MHO 2	M2.5	−0.79/−1.35	⋯	−0.10/−0.37	⋯	II
J04143054+2805147	MHO 3	K7	−0.41/−0.92	⋯	−0.10/−0.34	⋯	II
J04144730+2646264	FP Tau	M4	−1.63/−1.72	−1.11/−1.15	−1.63/−1.66	−0.97/−0.99	II
J04144739+2803055	XEST 20-066	M5.25	−2.50/−2.50	−2.60/−2.60	−2.64/−2.64	−2.68/−2.68	III
J04144786+2648110	CX Tau	M2.5	−1.22/−1.26	−0.79/−0.81	−0.73/−0.75	−0.47/−0.48	II
J04144797+2752346	LkCa 3 A+B	M1	−2.65/−2.68	−2.77/−2.78	−2.76/−2.77	−2.84/−2.85	III
J04144928+2812305	FO Tau A+B	M3.5	−1.16/−1.31	−0.84/−0.91	−0.87/−0.93	−0.63/−0.66	II
J04145234+2805598	XEST 20-071	M3.25	−2.44/−2.56	−2.65/−2.71	−2.64/−2.70	−2.78/−2.81	III
J04150515+2808462	CIDA 2	M5.5	−2.52/−2.56	−2.64/−2.66	−2.72/−2.74	−2.76/−2.76	III
J04151471+2800096	KPNO 1	M8.5	−2.19/−2.21	⋯	−2.55/−2.56	⋯	III
J04152409+2910434	⋯	M7	−2.22/−2.30	⋯	−2.54/−2.58	⋯	III
J04153916+2818586	⋯	M3.75	−1.56/−1.65	−0.95/−1.00	−1.49/−1.53	−0.77/−0.79	II
J04154278+2909597	IRAS 04125+2902	M1.25	−2.56/−2.64	−1.00/−1.04	−2.82/−2.85	−0.71/−0.73	II
J04155799+2746175	⋯	M5.5	−1.24/−1.24	−1.05/−1.05	−1.29/−1.29	−1.03/−1.03	II
J04161210+2756385	⋯	M4.75	−1.32/−1.40	−0.98/−1.03	−1.63/−1.67	−1.03/−1.04	II
J04161885+2752155	⋯	M6.25	−2.31/−2.35	⋯	−2.57/−2.59	⋯	III
J04162725+2053091	⋯	M5	−2.42/−2.42	⋯	−2.65/−2.65	⋯	III
J04162810+2807358	LkCa 4	K7	−2.57/−2.59	−2.74/−2.75	−2.60/−2.61	−2.79/−2.80	III
J04163048+3037053	⋯	M4.5	−2.51/−2.54	⋯	−2.78/−2.80	⋯	III
J04163911+2858491	⋯	M5.5	−1.45/−1.57	−1.33/−1.39	−1.65/−1.70	−1.38/−1.40	II
J04173372+2820468	CY Tau	M1.5	−1.39/−1.46	−1.27/−1.31	−1.44/−1.47	−1.26/−1.28	II
J04173893+2833005	LkCa 5	M2	−2.58/−2.59	−2.71/−2.71	−2.71/−2.71	−2.79/−2.79	III
J04174955+2813318	KPNO 10	M5	−1.38/−1.44	−1.01/−1.05	−0.58/−0.61	−0.58/−0.60	II
J04174965+2829362	V410 X-ray 1	M4	−0.88/−1.14	−0.88/−1.02	−0.67/−0.79	−0.79/−0.84	II
J04180796+2826036	V410 X-ray 3	M6	−2.34/−2.38	−2.39/−2.41	−2.66/−2.68	−2.54/−2.55	III
J04181078+2519574	V409 Tau	M1.5	−0.83/−1.02	−1.13/−1.23	−0.83/−0.92	−1.21/−1.25	II
J04181710+2828419	V410 Anon 13	M5.75	−1.24/−1.51	−0.99/−1.13	−1.22/−1.34	−0.91/−0.96	II
J04182147+1658470	HBC 372	K5	−2.70/−2.70	⋯	−2.79/−2.79	⋯	III
J04182909+2826191	V410 Anon 25	M1	−1.68/−2.69	−2.19/−2.73	−2.27/−2.74	−2.57/−2.76	III
J04183030+2743208	KPNO 11	M5.5	−2.42/−2.45	⋯	−2.65/−2.66	⋯	III
J04183110+2827162	V410 Tau A+B+C	K7	−2.50/−2.50	−2.69/−2.69	−2.69/−2.69	−2.82/−2.82	III
J04183112+2816290	DD Tau A+B	M3.5	−0.30/−0.54	−0.50/−0.62	−0.45/−0.56	−0.61/−0.65	II
J04183158+2816585	CZ Tau A+B	M3	0.37/0.32	−0.02/−0.05	1.18/1.16	0.22/0.21	II
J04183203+2831153	IRAS 04154+2823	M2.5	0.65/−0.20	0.34/−0.12	−0.23/−0.62	−0.11/−0.27	I
J04183444+2830302	V410 X-ray 2	M0	−1.62/−2.56	−0.64/−1.15	−2.07/−2.50	−0.58/−0.77	III
J04184023+2824245	V410 X-ray 4	M4	−1.88/−2.68	−2.25/−2.69	−2.36/−2.74	−2.56/−2.71	III
J04184061+2819155	V892 Tau	B9	⋯	⋯	⋯	⋯	II
J04184133+2827250	LR1	K4.5	−0.56/−1.65	−0.40/−0.98	−1.18/−1.68	−0.62/−0.83	II

TABLE 7 — *Continued*

2MASS[a]	Name	Spectral Type	α(2–8 μm)	α(2–24 μm)	α(3.6–8 μm)	α(3.6–24 μm)	SED Class
J04184250+2818498	V410 X-ray 7	M0.75	$-1.93/-2.38$	$\cdots$	$-1.99/-2.20$	$\cdots$	II
J04184703+2820073	Hubble 4	K7	$-2.53/-2.64$	$-2.65/-2.71$	$-2.61/-2.67$	$-2.71/-2.74$	III
J04185115+2814332	KPNO 2	M7.5	$-2.18/-2.23$	$\cdots$	$-2.51/-2.53$	$\cdots$	III
J04185147+2820264	CoKu Tau/1	M0	$0.94/0.67$	$1.03/0.89$	$2.17/2.05$	$1.58/1.52$	I
J04185170+1723165	HBC 376	K7	$-2.69/-2.69$	$-2.76/-2.76$	$-2.73/-2.73$	$-2.79/-2.79$	III
J04185813+2812234	IRAS 04158+2805	M5.25	$0.30/-0.03$	$0.38/0.21$	$-0.13/-0.28$	$0.22/0.16$	I
J04190110+2819420	V410 X-ray 6	M5.5	$-2.16/-2.32$	$-0.76/-0.85$	$-2.23/-2.30$	$-0.44/-0.47$	II
J04190126+2802487	KPNO 12	M9	$-1.12/-1.15$	$\cdots$	$-1.33/-1.34$	$\cdots$	II
J04190197+2822332	V410 X-ray 5a	M5.5	$-2.28/-2.53$	$-2.40/-2.54$	$-2.62/-2.74$	$-2.57/-2.62$	III
J04191281+2829330	FQ Tau A+B	M3	$-1.42/-1.47$	$-1.16/-1.19$	$-1.35/-1.38$	$-1.07/-1.08$	II
J04191583+2906269	BP Tau	K7	$-1.30/-1.36$	$-0.86/-0.90$	$-0.97/-1.00$	$-0.62/-0.63$	II
J04192625+2826142	V819 Tau	K7	$-2.53/-2.59$	$-2.08/-2.11$	$-2.69/-2.72$	$-2.03/-2.04$	II
J04193545+2827218	FR Tau	M5.25	$-0.84/-0.84$	$-0.89/-0.89$	$-0.36/-0.36$	$-0.70/-0.70$	II
J04194127+2749484	LkCa 7 A+B	M0	$-2.57/-2.59$	$-2.69/-2.70$	$-2.73/-2.74$	$-2.79/-2.79$	III
J04194148+2716070	IRAS 04166+2708	K6–M3.5[c]	-0.39	0.75	-0.64	0.93	I
$\cdots$	IRAS 04166+2706	K6–M3.5[c]	$\cdots$	$\cdots$	$\cdots$	$\cdots$	I
J04194657+2712552	[GKH94] 41	M7.5	$-0.07/-1.20$	$0.14/-0.47$	$-0.52/-1.05$	$0.00/-0.22$	I?
J04195844+2709570	IRAS 04169+2702	K6–M3.5[c]	1.72	$\cdots$	0.71	$\cdots$	I
J04201611+2821325	$\cdots$	M6.5	$-1.36/-1.36$	$-1.19/-1.19$	$-1.40/-1.40$	$-1.17/-1.17$	II
J04202144+2813491	$\cdots$	M1	$-1.00/-1.08$	$-0.78/-0.83$	$-1.52/-1.56$	$-0.95/-0.97$	II
J04202555+2700355	$\cdots$	M5.25	$-1.52/-1.60$	$-0.79/-0.83$	$-1.46/-1.50$	$-0.58/-0.60$	II
J04202583+2819237	IRAS 04173+2812	mid-M	$0.51/0.51$	$0.18/0.18$	$-0.48/-0.48$	$-0.32/-0.32$	II
J04202606+2804089	$\cdots$	M3.5	$-0.87/-0.87$	$-0.39/-0.39$	$-0.23/-0.23$	$0.00/0.00$	II
J04203918+2717317	XEST 16-045	M4.5	$-2.62/-2.62$	$-2.66/-2.66$	$-2.77/-2.77$	$-2.74/-2.74$	III
J04205273+1746415	J2-157	M5.5	$-2.44/-2.44$	$\cdots$	$-2.68/-2.68$	$\cdots$	III
J04210795+2702204	$\cdots$	M5.25	$0.92/0.44$	$0.57/0.32$	$0.08/-0.14$	$0.13/0.04$	II
J04210934+2750368	$\cdots$	M5.25	$-1.96/-1.96$	$-1.65/-1.65$	$-1.94/-1.94$	$-1.55/-1.55$	II
J04211038+2701372	IRAS 04181+2654 B	K7	0.26	0.38	-0.35	0.15	I
J04211146+2701094	IRAS 04181+2654 A	M3	0.63	0.50	0.55	0.43	I
J04213459+2701388	$\cdots$	M5.5	$-1.74/-1.81$	$-1.61/-1.65$	$-1.77/-1.80$	$-1.59/-1.60$	II
J04214013+2814224	XEST 21-026	M5.75	$-2.43/-2.43$	$\cdots$	$-2.73/-2.73$	$\cdots$	III
J04214323+1934133	IRAS 04187+1927	M0	$-0.16/-0.45$	$\cdots$	$0.15/0.02$	$\cdots$	II
J04214631+2659296	$\cdots$	M5.75	$-1.62/-1.71$	$-1.01/-1.06$	$-1.68/-1.71$	$-0.88/-0.90$	II
J04215450+2652315	$\cdots$	M8.5	$-2.08/-2.12$	$\cdots$	$-2.55/-2.57$	$\cdots$	III
J04215563+2755060	DE Tau	M1	$-1.27/-1.33$	$-0.86/-0.89$	$-1.32/-1.34$	$-0.78/-0.79$	II
$\cdots$	IRAM 04191+1522	$\cdots$	$\cdots$	$\cdots$	-0.16	1.17	0
J04215740+2826355	RY Tau	K1	$\cdots$	$\cdots$	$\cdots$	$\cdots$	II
J04215884+2818066	HD 283572	G5	$-2.71/-2.74$	$-2.83/-2.85$	$-2.77/-2.79$	$-2.89/-2.89$	III
J04215943+1932063	T Tau N+S	K0	$\cdots$	$\cdots$	$\cdots$	$\cdots$	II
J04220007+1530248	IRAS 04191+1523 B	M6–M8[c]	0.33	$\cdots$	-0.08	$\cdots$	I
J04220043+1530212	IRAS 04191+1523 A	K6–M3.5[c]	1.47	1.09^{b}	0.82	0.77^{b}	I
J04220069+2657324	Haro 6-5B	K5	1.42	1.07	1.38	0.97	I
J04220217+2657304	FS Tau A+B	M0	$-0.53/-0.84$	$-0.19/-0.36$	$-0.79/-0.93$	$-0.21/-0.27$	II
J04220313+2825389	LkCa 21	M3	$-2.54/-2.56$	$-2.66/-2.68$	$-2.70/-2.71$	$-2.76/-2.77$	III
J04221332+1934392	$\cdots$	M8	$-2.12/-2.12$	$\cdots$	$-2.35/-2.35$	$\cdots$	III
J04221568+2657060	XEST 11-078	M1	$-1.14/-1.18$	$0.31/0.28$	$-1.33/-1.35$	$0.59/0.59$	I?
J04221644+2549118	$\cdots$	M7.75	$-2.29/-2.31$	$\cdots$	$-2.62/-2.63$	$\cdots$	III
J04221675+2654570	$\cdots$	M1.5	$-0.76/-0.92$	$-0.68/-0.76$	$-1.08/-1.16$	$-0.79/-0.82$	II
J04222404+2646258	XEST 11-087	M4.75	$-2.48/-2.52$	$-2.51/-2.53$	$-2.72/-2.74$	$-2.62/-2.62$	III
J04224786+2645530	IRAS 04196+2638	M1	$-0.61/-0.80$	$-0.54/-0.64$	$-0.73/-0.82$	$-0.57/-0.61$	II
J04230607+2801194	$\cdots$	M6	$-1.46/-1.48$	$-1.03/-1.04$	$-1.42/-1.43$	$-0.90/-0.91$	II
J04230776+2805573	IRAS 04200+2759	M3.5–M6[c]	$0.06/-0.28$	$-0.12/-0.30$	$-0.57/-0.72$	$-0.42/-0.49$	II
J04231822+2641156	$\cdots$	M3.5	$-1.31/-1.71$	$-0.71/-0.93$	$-1.39/-1.57$	$-0.59/-0.67$	II
J04233539+2503026	FU Tau A	M7.25	$-0.83/-0.91$	$-1.06/-1.11$	$-0.83/-0.87$	$-1.13/-1.14$	II
J04233573+2502596	FU Tau B	M9.25	$-0.99/-0.99$	$\cdots$	$-0.87/-0.87$	$\cdots$	II
J04233919+2456141	FT Tau	K6–M3.5[c]	$-1.03/-1.16$	$-0.78/-0.85$	$-0.96/-1.02$	$-0.69/-0.71$	II
J04242090+2630511	$\cdots$	M6.5	$-1.31/-1.31$	$-0.97/-0.97$	$-1.20/-1.20$	$-0.84/-0.84$	II
J04242646+2649503	$\cdots$	M5.75	$-1.41/-1.43$	$-0.96/-0.97$	$-1.39/-1.40$	$-0.84/-0.84$	II
J04244457+2610141	IRAS 04216+2603	M0.5	$-0.70/-0.89$	$-0.74/-0.85$	$-0.75/-0.84$	$-0.78/-0.81$	II
J04244506+2701447	J1-4423	M5	$-2.50/-2.52$	$\cdots$	$-2.71/-2.71$	$\cdots$	III
J04245708+2711565	IP Tau	M0	$-1.52/-1.61$	$-1.02/-1.07$	$-1.54/-1.58$	$-0.90/-0.91$	II
J04251767+2617504	J1-4872 B	M1	$-2.13/-2.13$	$\cdots$	$-2.66/-2.66$	$\cdots$	III
J04251767+2617504	J1-4872 A	K7	$-2.25/-2.25$	$-2.54/-2.54^{b}$	$-2.71/-2.71$	$-2.83/-2.83^{b}$	III
J04262939+2624137	KPNO 3	M6	$-1.06/-1.13$	$-0.86/-0.90$	$-0.89/-0.92$	$-0.74/-0.75$	II
J04263055+2443558	$\cdots$	M8.75	$-1.11/-1.11$	$-1.15/-1.15$	$-1.11/-1.11$	$-1.16/-1.16$	II
J04265352+2606543	FV Tau A+B	K5	$-0.53/-0.87$	$-0.56/-0.75$	$-0.61/-0.77$	$-0.61/-0.68$	II
J04265440+2606510	FV Tau/c A+B	M2.5	$-0.94/-1.21$	$\cdots$	$-0.81/-0.93$	$\cdots$	II
J04265629+2443353	IRAS 04239+2436	K6–M3.5[c]	1.18	$\cdots$	0.76	$\cdots$	I
J04265732+2606284	KPNO 13	M5	$-1.11/-1.22$	$-1.22/-1.28$	$-1.18/-1.23$	$-1.28/-1.30$	II
J04270266+2605304	DG Tau B	<K6[c]	$\cdots$	$\cdots$	1.87	$\cdots$	I
J04270280+2542223	DF Tau A+B	M2	$-1.20/-1.28$	$-1.14/-1.18$	$-1.11/-1.14$	$-1.08/-1.10$	II
J04270469+2606163	DG Tau	K6	$-0.33/-0.49$	$\cdots$	$\cdots$	$\cdots$	II
J04270739+2215037	$\cdots$	M6.75	$-2.39/-2.40$	$\cdots$	$-2.66/-2.67$	$\cdots$	III
J04272799+2612052	KPNO 4	M9.5	$-1.96/-1.96$	$\cdots$	$-2.35/-2.35$	$\cdots$	III

TABLE 7 — *Continued*

2MASS[a]	Name	Spectral Type	$\alpha(2\text{–}8~\mu m)$	$\alpha(2\text{–}24~\mu m)$	$\alpha(3.6\text{–}8~\mu m)$	$\alpha(3.6\text{–}24~\mu m)$	SED Class
J04274538+2357243	⋯	M8.25	−2.30/−2.30	⋯	−2.63/−2.63	⋯	III
J04275730+2619183	IRAS 04248+2612	M4.5	0.10/−0.21	0.51/0.34	0.24/0.09	0.67/0.61	I
⋯	L1521F-IRS	M6–M8[c]	⋯	⋯	⋯	⋯	I
J04284263+2714039	⋯	M5.25	−1.63/−1.65	−1.26/−1.27	−1.86/−1.87	−1.26/−1.27	II
J04290068+2755033	⋯	M8.25	−1.43/−1.43	−1.04/−1.04	−1.36/−1.36	−0.91/−0.91	II
J04290498+2649073	IRAS 04260+2642	K5.5	−0.04	0.36	−0.58	0.24	II
J04292071+2633406	J1-507	M4	−2.54/−2.59	−2.64/−2.67	−2.75/−2.78	−2.76/−2.77	III
J04292165+2701259	IRAS 04263+2654	M5.25	−1.29/−1.45	−0.83/−0.92	−1.20/−1.28	−0.68/−0.71	II
J04292373+2433002	GV Tau A+B	K5	⋯	⋯	⋯	⋯	I
J04292971+2616532	FW Tau A+B+C	M5.5	−2.42/−2.46	−2.20/−2.22	−2.64/−2.66	−2.24/−2.25	III
J04293008+2439550	IRAS 04264+2433	M1	0.35	1.02	1.08	1.50	I
J04293209+2430597	⋯	K6–M3.5[c]	1.82	0.90	0.71	0.21	I?
J04293606+2435556	XEST 13-010	M3	−1.60/−1.72	−1.13/−1.20	−1.71/−1.77	−1.06/−1.08	II
J04294155+2632582	DH Tau A+B	M1	−1.79/−1.89	−1.00/−1.05	−1.97/−2.02	−0.87/−0.89	II
J04294247+2632493	DI Tau A+B	M0	−2.59/−2.60	⋯	−2.76/−2.76	⋯	III
J04294568+2630468	KPNO 5	M7.5	−2.30/−2.33	⋯	−2.62/−2.64	⋯	III
J04295156+2606448	IQ Tau	M0.5	−1.17/−1.29	−0.97/−1.04	−1.32/−1.38	−0.98/−1.01	II
J04295422+1754041	⋯	M4	⋯	⋯	⋯	⋯	III?
J04295950+2433078	⋯	M5	−1.35/−1.44	−0.98/−1.03	−1.43/−1.47	−0.92/−0.94	II
J04300357+1813494	UX Tau B	M2	−2.60/−2.64	⋯	−2.75/−2.77	⋯	III
J04300399+1813493	UX Tau A+C	K5	−1.63/−1.69	−0.78/−0.81[b]	−2.01/−2.04	−0.66/−0.68[b]	II
J04300724+2608207	KPNO 6	M8.5	−1.36/−1.39	−1.14/−1.16	−1.26/−1.27	−1.05/−1.05	II
J04302365+2359129	⋯	M8.25	−2.31/−2.31	⋯	−2.64/−2.64	⋯	III
J04302961+2426450	FX Tau A+B	M1	−1.35/−1.45	−0.98/−1.03	−1.38/−1.43	−0.90/−0.92	II
J04304425+2601244	DK Tau A	K7	−0.77/−0.90	−0.81/−0.88[b]	−1.25/−1.31	−0.99/−1.02[b]	II
J04304425+2601244	DK Tau B	K6–M3.5[c]	−1.08	⋯	−1.35	⋯	II
J04305028+2300088	IRAS 04278+2253 A+B	G8	⋯	⋯	⋯	⋯	I
J04305137+2442222	ZZ Tau	M3	−1.74/−1.81	−1.36/−1.39	−1.58/−1.61	−1.19/−1.21	II
J04305171+2441475	ZZ Tau IRS	M5	0.50/0.18	0.31/0.14	−0.11/−0.26	0.01/−0.06	II
J04305718+2556394	KPNO 7	M8.25	−1.34/−1.36	−1.02/−1.03	−1.31/−1.32	−0.92/−0.93	II
J04311444+2710179	JH 56	M0.5	−2.67/−2.67	−2.08/−2.08	−2.72/−2.72	−1.96/−1.96	II
J04311578+1820072	MHO 9	M4.25	−2.51/−2.52	−2.69/−2.70	−2.71/−2.72	−2.82/−2.82	III
J04311907+2335047	⋯	M7.75	−2.27/−2.29	⋯	−2.65/−2.66	⋯	III
J04312382+2410529	V927 Tau A+B	M4.75	−2.52/−2.55	−2.68/−2.69	−2.70/−2.71	−2.79/−2.80	III
J04312405+1800215	MHO 4	M7	−2.34/−2.38	−2.52/−2.54	−2.64/−2.67	−2.69/−2.70	III
J04312669+2703188	⋯	M7.5	−2.24/−2.26	⋯	−2.64/−2.65	⋯	III
J04313407+1808049	L1551/IRS5	<K6[c]	2.27	⋯	2.06	⋯	I
J04313613+1813432	LkHa 358	K8	−0.45/−0.92	−0.13/−0.39	−0.52/−0.74	−0.08/−0.17	I
J04313747+1812244	HH 30	M0	−1.27	−0.28	−1.55	−0.15	I
J04313843+1813576	HL Tau	K7	0.43/0.10	⋯	⋯	⋯	I
J04314007+1813571	XZ Tau A+B	M2	−0.11/−0.28	⋯	⋯	⋯	II
J04314444+1808315	L1551NE	<K6[c]	1.80	1.31	1.34	1.00	I
J04315056+2424180	HK Tau A+B	M0.5	−1.33/−1.54	−0.46/−0.57	−1.50/−1.60	−0.31/−0.35	II
J04315779+1821380	V710 Tau A	M0.5	−1.07/−1.07	−1.26/−1.26[b]	−1.01/−1.01	−1.13/−1.13[b]	II
J04315779+1821350	V710 Tau B	M2	−2.37	⋯	−2.36	⋯	II?
J04315844+2543299	J1-665	M5.5	−2.56/−2.64	−2.77/−2.81	−2.78/−2.81	−2.91/−2.92	III
J04315968+1821305	LkHa 267	M1.5	−0.83/−1.04	−0.75/−0.86	−1.15/−1.25	−0.87/−0.91	II
J04320329+2528078	⋯	M6.25	−2.34/−2.34	⋯	−2.64/−2.64	⋯	III
J04320926+1757227	L1551-51	K7	−2.65/−2.66	−2.81/−2.81	−2.70/−2.70	−2.86/−2.86	III
J04321456+1820147	V827 Tau	K7	−2.64/−2.67	−2.75/−2.76	−2.74/−2.75	−2.81/−2.82	III
J04321540+2428597	Haro 6-13	M0	−0.35/−0.76	⋯	−1.05/−1.24	⋯	II
J04321583+1801387	V826 Tau A+B	K7	−2.59/−2.60	−2.73/−2.73	−2.77/−2.77	−2.84/−2.84	III
J04321606+1812464	MHO 5	M6	−1.20/−1.25	−1.18/−1.21	−1.18/−1.20	−1.17/−1.18	II
J04321786+2422149	⋯	M5.75	−2.32/−2.32	−2.62/−2.62	−2.61/−2.61	−2.82/−2.82	III
J04321885+2422271	V928 Tau A+B	M0.5	−2.46/−2.62	−2.68/−2.77	−2.63/−2.70	−2.80/−2.83	III
J04322210+1827426	MHO 6	M4.75	−1.65/−1.69	−1.23/−1.25	−1.71/−1.73	−1.14/−1.15	II
J04322329+2403013	⋯	M7.75	−2.33/−2.33	⋯	−2.58/−2.58	⋯	III
J04322415+2251083	⋯	M4.5	−1.31/−1.39	−1.18/−1.22	−1.09/−1.12	−1.05/−1.06	II
J04322627+1827521	MHO 7	M5.25	−2.48/−2.51	−2.75/−2.77	−2.70/−2.71	−2.91/−2.92	III
J04323028+1731303	GG Tau Ba+Bb	M5.5	−1.10/−1.13	⋯	−1.02/−1.04	⋯	II
J04323034+1731406	GG Tau Aa+Ab	K7	−1.11/−1.20	⋯	−1.01/−1.06	⋯	II
J04323058+2419572	FY Tau	K5	−1.31/−1.61	−1.22/−1.38	−1.51/−1.64	−1.27/−1.33	II
J04323176+2420029	FZ Tau	M0	−0.74/−1.05	−0.79/−0.96	−0.78/−0.92	−0.83/−0.89	II
J04323205+2257266	IRAS 04295+2251	K7	0.62	0.58	0.82	0.65	I
J04324282+2552314	UZ Tau Ba+Bb	M2	−1.45/−1.57	⋯	−1.40/−1.46	⋯	II
J04324303+2552311	UZ Tau A	M1	−0.53/−0.80	−0.73/−0.87[b]	−0.78/−0.90	−0.79/−0.84[b]	II
J04324373+1802563	L1551-55	K7	−2.64/−2.67	−2.80/−2.81	−2.74/−2.76	−2.88/−2.89	III
J04324911+2253027	JH 112	K6	−1.13/−1.40	−0.70/−0.84	−1.08/−1.20	−0.57/−0.62	II
J04324938+2253082	⋯	M4.25	−1.24/−1.37	⋯	−1.18/−1.24	⋯	II
J04325026+2422115	⋯	M7.5	−1.90/−2.36	−2.17/−2.42	−2.40/−2.62	−2.46/−2.55	III
J04325119+1730092	LH 0429+17	M8.25	−2.21/−2.21	⋯	⋯	⋯	III
J04330197+2421000	MHO 8	M6	−2.33/−2.41	−2.55/−2.59	−2.62/−2.66	−2.73/−2.74	III
J04330622+2409339	GH Tau A+B	M2	−1.47/−1.53	−1.12/−1.16	−1.60/−1.63	−1.09/−1.10	II
J04330664+2409549	V807 Tau A+B	K5	−1.71/−1.76	−1.36/−1.39	−1.74/−1.76	−1.28/−1.29	II

TABLE 7 — *Continued*

2MASS[a]	Name	Spectral Type	α(2–8 μm)	α(2–24 μm)	α(3.6–8 μm)	α(3.6–24 μm)	SED Class
J04330781+2616066	KPNO 14	M6	−2.28/−2.41	−2.49/−2.55	−2.63/−2.69	−2.68/−2.71	III
J04330945+2246487	⋯	M6	−1.61/−1.72	−1.61/−1.67	−1.83/−1.88	−1.70/−1.73	II
J04331003+2433433	V830 Tau	K7	−2.71/−2.74	−2.81/−2.83	−2.79/−2.80	−2.87/−2.88	III
J04331435+2614235	IRAS 04301+2608	M0	−0.64/−0.89	0.67/0.54	−0.02/−0.14	1.27/1.22	II
J04331650+2253204	IRAS 04302+2247	K6–M3.5[c]	−1.29	0.29	−2.26	0.29	I
J04331907+2246342	IRAS 04303+2240	M0.5	−0.04/−0.54	−0.44/−0.72	−0.18/−0.42	−0.61/−0.71	II
J04332621+2245293	XEST 17-036	M4	−2.37/−2.53	−2.26/−2.35	−2.62/−2.69	−2.34/−2.37	III
J04333278+1800436	⋯	M1	−1.16/−1.16	⋯	⋯	⋯	II
J04333297+1801004	HD 28867 B	B9.5	−2.35	⋯	⋯	⋯	II
J04333297+1801004	HD 28867 A+C	B9	−2.77	⋯	⋯	⋯	III
J04333405+2421170	GI Tau	K7	−0.55/−0.66	−0.62/−0.68	−0.50/−0.56	−0.62/−0.64	II
J04333456+2421058	GK Tau	K7	−0.89/−0.99	−0.64/−0.70	−1.00/−1.04	−0.62/−0.64	II
J04333678+2609492	IS Tau A+B	M0	−0.90/−1.04	−0.97/−1.04	−0.82/−0.88	−0.95/−0.98	II
J04333905+2227207	⋯	M1.75	−1.68/−1.74	−0.63/−0.66	−1.93/−1.95	−0.47/−0.48	II
J04333906+2520382	DL Tau	K7	−0.64/−0.77	−0.64/−0.70	−0.64/−0.70	−0.64/−0.66	II
J04333935+1751523	HN Tau A+B	K5	−0.14/−0.41	⋯	−0.29/−0.41	⋯	II
J04334171+1750402	⋯	M4	−1.90/−1.91	⋯	−1.81/−1.81	⋯	II
J04334291+2526470	⋯	M8.75	−2.20/−2.20	⋯	−2.64/−2.64	⋯	III
J04334465+2615005	⋯	M4.75	−0.94/−1.07	−0.87/−0.94	−1.04/−1.10	−0.89/−0.92	II
J04334871+1810099	DM Tau	M1	−2.20/−2.23	⋯	−2.11/−2.12	⋯	II
J04335200+2250301	CI Tau	K7	−0.93/−1.03	−0.70/−0.75	−0.87/−0.92	−0.61/−0.63	II
J04335245+2612548	⋯	M8.5	−0.98/−1.12	−0.67/−0.74	−0.94/−1.01	−0.57/−0.60	II
J04335252+2256269	XEST 17-059	M5.75	−2.42/−2.42	−2.61/−2.61	−2.63/−2.63	−2.75/−2.75	III
J04335470+2613275	IT Tau B	M3.5–M6[c]	−0.94	⋯	−0.87	⋯	II
J04335470+2613275	IT Tau A	K2	−1.31/−1.63	−1.21/−1.38[b]	−1.35/−1.50	−1.20/−1.27[b]	II
J04335546+1838390	J2-2041	M3.5	−2.56/−2.58	⋯	−2.74/−2.75	⋯	III
J04341099+2251445	JH 108	M1	−2.60/−2.67	−2.62/−2.65	−2.72/−2.75	−2.67/−2.68	III
J04341527+2250309	CFHT 1	M7	−2.17/−2.41	⋯	−2.61/−2.72	⋯	III
J04341803+1830066	HBC 407	G8	−2.70	⋯	−2.79	⋯	III
J04344544+2308027	⋯	M5.25	−2.35/−2.42	⋯	−2.67/−2.70	⋯	III
J04345542+2428531	AA Tau	K7	−1.03/−1.10	−0.85/−0.89	−0.94/−0.97	−0.77/−0.78	II
J04345693+2258358	XEST 08-003	M1.5	−2.56/−2.64	−2.52/−2.57	−2.72/−2.76	−2.58/−2.60	III
J04350850+2311398	⋯	M6	−2.35/−2.35	⋯	−2.61/−2.61	⋯	III
J04352020+2232146	HO Tau	M0.5	−1.39/−1.45	−1.02/−1.05	−1.52/−1.55	−0.98/−0.99	II
J04352089+2254242	FF Tau A+B	K7	−2.61/−2.69	−2.74/−2.79	−2.81/−2.85	−2.86/−2.88	III
J04352450+1751429	HBC 412 A+B	M2	−2.59/−2.61	−2.76/−2.77	−2.73/−2.73	−2.86/−2.86	III
J04352737+2414589	DN Tau	M0	−1.34/−1.39	−0.94/−0.97	−1.18/−1.20	−0.77/−0.78	II
⋯	IRAS 04325+2402 C	M6–M8[c]	−0.86	⋯	−1.07	⋯	II
J04353539+2408194	IRAS 04325+2402 A+B	K6–M3.5[c]	−0.56	1.08[b]	−1.25	1.19[b]	I
J04354093+2411087	CoKu Tau 3 A+B	M1	−0.75/−1.11	−0.89/−1.08	−0.84/−1.01	−0.96/−1.03	II
J04354183+2234115	KPNO 8	M5.75	−2.38/−2.40	⋯	−2.65/−2.66	⋯	III
J04354203+2252226	XEST 08-033	M4.75	−2.44/−2.51	−2.46/−2.50	−2.68/−2.71	−2.57/−2.59	III
J04354526+2737130	⋯	M9.25	−2.31/−2.31	⋯	−2.76/−2.76	⋯	III
J04354733+2250216	HQ Tau	K2	−0.90/−1.08	−0.69/−0.79	−0.33/−0.42	−0.40/−0.43	II
J04355109+2252401	KPNO 15	M2.75	−2.54/−2.62	⋯	−2.74/−2.78	⋯	III
J04355143+2249119	KPNO 9	M8.5	−2.26/−2.33	⋯	−2.65/−2.69	⋯	III
J04355209+2255039	XEST 08-047	M4.5	−2.47/−2.55	⋯	−2.66/−2.70	⋯	III
J04355277+2254231	HP Tau	K3	−0.70/−0.95	−0.40/−0.54	−0.76/−0.88	−0.35/−0.40	II
J04355286+2250585	XEST 08-049	M4.25	−2.45/−2.50	−2.56/−2.59	−2.69/−2.71	−2.68/−2.69	III
J04355349+2254089	HP Tau/G3	K7	−2.57/−2.67	⋯	−2.74/−2.78	⋯	III
J04355415+2254134	HP Tau/G2	G0	−2.64/−2.76	⋯	−2.69/−2.75	⋯	III
J04355684+2254360	Haro 6-28 A+B	M3	−1.08/−1.25	−0.90/−1.00	−1.10/−1.19	−0.87/−0.91	II
J04355892+2238353	XEST 09-042	M0	−2.57/−2.59	⋯	−2.81/−2.81	⋯	III
J04361030+2159364	⋯	M8.5	−1.43/−1.43	−0.94/−0.94	−1.44/−1.44	−0.82/−0.82	II
J04361038+2259560	CFHT 2	M7.5	−2.19/−2.27	⋯	−2.55/−2.59	⋯	III
J04361909+2542589	LkCa 14	M0	−2.70/−2.70	−2.78/−2.78	−2.82/−2.82	−2.86/−2.86	III
J04362151+2351165	⋯	M5.25	−1.58/−1.63	−1.18/−1.21	−1.33/−1.36	−0.98/−0.99	II
J04363893+2258119	CFHT 3	M7.75	−2.21/−2.28	⋯	−2.60/−2.64	⋯	III
J04373705+2331080	⋯	L0	−1.26/−1.26	⋯	−1.87/−1.87	⋯	III
J04375670+2546229	ITG 1	M3.5–M6[c]	−0.77/−0.77	−0.73/−0.73	−0.47/−0.47	−0.60/−0.60	II
J04380083+2558572	ITG 2	M7.25	−2.25/−2.39	−2.56/−2.63	−2.59/−2.65	−2.78/−2.81	III
J04381486+2611399	⋯	M7.25	0.14/0.14	0.19/0.19	−0.68/−0.68	−0.14/−0.14	II
J04381630+2326402	⋯	M4.75	⋯	⋯	⋯	⋯	III
J04382134+2609137	GM Tau	M6.5	−0.83/−1.08	−0.83/−0.97	−1.19/−1.30	−0.98/−1.03	II
J04382858+2610494	DO Tau	M0	−0.65/−0.86	−0.39/−0.50	−0.74/−0.83	−0.36/−0.40	II
J04383528+2610386	HV Tau A+B	M1	−2.45/−2.56	⋯	−2.56/−2.61	⋯	III
⋯	HV Tau C	K6	⋯	⋯	−0.53	0.87	I?
J04385859+2336351	⋯	M4.25	⋯	−1.09/−1.09	⋯	−0.95/−0.95	II
J04385871+2323595	⋯	M6.5	⋯	⋯	⋯	⋯	III
J04390163+2336029	⋯	M6	⋯	−1.36/−1.40	⋯	−1.25/−1.26	II
J04390396+2544264	⋯	M7.25	−1.20/−1.27	−0.98/−1.01	−0.98/−1.01	−0.83/−0.84	II
J04390525+2337450	⋯	M3.5–M6[c]	−0.97/−0.97	0.24/0.24	−1.10/−1.10	0.50/0.50	I?
J04390637+2334179	⋯	M7.5	⋯	⋯	⋯	⋯	III
J04391389+2553208	IRAS 04361+2547	<K6[c]	0.83	⋯	0.24	⋯	I

TABLE 7 — *Continued*

2MASS[a]	Name	Spectral Type	$\alpha(2\text{–}8\ \mu m)$	$\alpha(2\text{–}24\ \mu m)$	$\alpha(3.6\text{–}8\ \mu m)$	$\alpha(3.6\text{–}24\ \mu m)$	SED Class
J04391741+2247533	VY Tau A+B	M0	−1.69/−1.71	−1.20/−1.22	−1.48/−1.49	−0.99/−1.00	II
J04391779+2221034	LkCa 15	K5	−1.63/−1.68	−0.92/−0.95	−1.59/−1.62	−0.73/−0.74	II
J04392090+2545021	GN Tau A+B	M2.5	−0.95/−1.20	−0.86/−1.00	−1.07/−1.18	−0.89/−0.94	II
J04393364+2359212	· · ·	M5	−1.09/−1.14	−0.93/−0.96	−0.89/−0.92	−0.81/−0.82	II
J04393519+2541447	IRAS 04365+2535	<K6[c]	1.95	· · ·	0.78	· · ·	I
J04394488+2601527	ITG 15	M5	−1.46/−1.65	−0.95/−1.05	−1.31/−1.40	−0.76/−0.79	II
J04394748+2601407	CFHT 4	M7	−0.99/−1.21	−0.81/−0.93	−0.93/−1.03	−0.74/−0.78	II
· · ·	IRAS 04368+2557	· · ·	· · ·	· · ·	1.66	2.23	0
J04395574+2545020	IC2087IR	<K6[c]	−0.26	· · ·	· · ·	· · ·	I
J04400067+2358211	· · ·	M6	−1.50/−1.50	−0.91/−0.91	−1.46/−1.46	−0.74/−0.74	II
J04400174+2556292	· · ·	M5.5	−2.11/−2.32	−2.18/−2.29	−2.52/−2.62	−2.37/−2.41	III
J04400800+2605253	IRAS 04370+2559	K6–M3.5[c]	−0.64/−1.27	−0.41/−0.75	−0.52/−0.81	−0.30/−0.42	II
J04403979+2519061	· · ·	M5.25	−2.32/−2.42	−1.83/−1.88	−2.61/−2.65	−1.82/−1.84	II
J04404950+2551191	JH 223	M2	−1.51/−1.58	−1.21/−1.25	−1.52/−1.55	−1.14/−1.16	II
J04410424+2557561	Haro 6-32	M5	−2.45/−2.50	−2.74/−2.77	−2.73/−2.76	−2.93/−2.94	III
J04410470+2451062	IW Tau A+B	K7	−2.60/−2.66	−2.74/−2.77	−2.75/−2.77	−2.84/−2.85	III
J04410826+2556074	ITG 33A	M3	−0.39/−0.78	−0.40/−0.60	−0.61/−0.78	−0.49/−0.56	II
J04411078+2555116	ITG 34	M5.5	−1.17/−1.27	−0.98/−1.04	−1.04/−1.08	−0.88/−0.90	II
J04411267+2546354	IRAS 04381+2540	K6–M3.5[c]	1.37	1.05	1.07	0.84	I
J04411681+2840000	CoKu Tau/4	M1.5	−2.42/−2.58	−0.43/−0.52	−2.46/−2.54	0.06/0.03	II
J04412464+2543530	ITG 40	M3.5	−0.72/−1.84	−0.51/−1.11	−1.06/−1.58	−0.60/−0.81	II
J04413882+2556267	IRAS 04385+2550	M0	−0.46/−0.83	−0.05/−0.25	−0.27/−0.45	0.14/0.07	II
J04414489+2301513	· · ·	M8.5	−1.24/−1.28	· · ·	−1.40/−1.41	· · ·	II
J04414565+2301580	· · ·	M4.5	−2.33/−2.35	· · ·	· · ·	· · ·	III
J04414825+2534304	· · ·	M7.75	−0.88/−0.99	−0.60/−0.66	−0.76/−0.81	−0.47/−0.49	II
J04420548+2522562	LkHa 332/G2 A+B	M0	−2.41/−2.59	−2.48/−2.57	−2.59/−2.67	−2.57/−2.61	III
J04420732+2523032	LkHa 332/G1 A+B	M1	−2.45/−2.65	· · ·	−2.67/−2.76	· · ·	III
J04420777+2523118	V955 Tau A+B	K7	−0.92/−1.16	−0.90/−1.02	−1.03/−1.14	−0.94/−0.98	II
J04422101+2520343	CIDA 7	M4.75	−1.09/−1.13	−0.59/−0.62	−0.88/−0.90	−0.38/−0.39	II
J04423769+2515374	DP Tau	M0.5	−0.34/−0.55	−0.21/−0.33	−0.32/−0.41	−0.17/−0.21	II
J04430309+2520187	GO Tau	M0	−1.41/−1.49	−0.96/−1.00	−1.01/−1.05	−0.68/−0.69	II
J04432023+2940060	CIDA 14	M5	−1.49/−1.52	−1.40/−1.41	−1.32/−1.34	−1.30/−1.31	II
J04442713+2512164	IRAS 04414+2506	M7.25	−0.61/−0.70	−0.38/−0.43	−0.63/−0.67	−0.33/−0.35	II
J04455129+1555496	HD 30171	G5	−2.72/−2.75	· · ·	−2.80/−2.81	· · ·	III
J04455134+1555367	IRAS 04429+1550	M2.5	−1.09/−1.16	−0.35/−0.39	−0.76/−0.79	−0.03/−0.04	II
J04464260+2459034	RXJ 04467+2459	M4	−2.48/−2.48	· · ·	−2.71/−2.71	· · ·	III
J04465305+1700001	DQ Tau	M0	−0.79/−0.90	· · ·	−0.70/−0.76	· · ·	II
J04465897+1702381	Haro 6-37 A	K7	−1.11/−1.35	· · ·	−1.23/−1.34	· · ·	II
J04465897+1702381	Haro 6-37 B	M1	−0.85	· · ·	−0.70	· · ·	II
J04470620+1658428	DR Tau	K5	−0.58/−0.74	· · ·	· · ·	· · ·	II
J04474859+2925112	DS Tau	K5	−1.26/−1.38	· · ·	−1.17/−1.23	· · ·	II
J04484189+1703374	· · ·	M7	−2.36/−2.36	· · ·	−2.65/−2.65	· · ·	III
J04514737+3047134	UY Aur A+B	M0	−0.41/−0.58	· · ·	−0.36/−0.44	· · ·	II
J04520668+3047175	IRAS 04489+3042	M4	0.24/−0.49	· · ·	−0.25/−0.59	· · ·	I
J04551098+3021595	GM Aur	K7	−1.92/−1.94	−0.64/−0.65	−1.73/−1.74	−0.24/−0.24	II
J04552333+3027366	· · ·	M6.25	−2.33/−2.39	· · ·	−2.65/−2.68	· · ·	III
J04553695+3017553	LkCa 19	K0	−2.72/−2.78	−2.46/−2.49	−2.77/−2.79	−2.41/−2.42	III
J04554046+3039057	· · ·	M5.25	−2.41/−2.42	· · ·	−2.61/−2.62	· · ·	III
J04554535+3019389	· · ·	M4.75	−1.54/−1.54	−1.33/−1.33	−1.43/−1.43	−1.23/−1.23	II
J04554582+3033043	AB Aur	B9	· · ·	· · ·	· · ·	· · ·	II
J04554757+3028077	· · ·	M4.75	−2.40/−2.40	· · ·	−2.64/−2.64	· · ·	III
J04554801+3028050	· · ·	M5.6	−1.28/−1.28	−0.91/−0.91	−1.28/−1.28	−0.82/−0.82	II
J04554820+3030160	XEST 26-052	M4.5	−2.44/−2.44	· · ·	−2.63/−2.63	· · ·	III
J04554969+3019400	· · ·	M6	−1.91/−1.91	−1.43/−1.43	−2.02/−2.02	−1.35/−1.35	II
J04555288+3006523	· · ·	M5.25	−2.44/−2.47	· · ·	−2.68/−2.70	· · ·	III
J04555605+3036209	XEST 26-062	M4	−1.29/−1.37	−0.75/−0.80	−1.12/−1.16	−0.54/−0.56	II
J04555636+3049374	· · ·	M5	−2.43/−2.44	· · ·	−2.66/−2.67	· · ·	III
J04555938+3034015	SU Aur	G2	−1.20/−1.33	· · ·	· · ·	· · ·	II
J04560118+3026348	XEST26-071	M3.5	−1.34/−1.39	−1.25/−1.28	−1.24/−1.27	−1.18/−1.20	II
J04560201+3021037	HBC 427	K5	−2.72/−2.75	−2.69/−2.71	−2.77/−2.79	−2.71/−2.72	III
J04574903+3015195	· · ·	M9.25	−2.29/−2.29	· · ·	−2.76/−2.76	· · ·	III
J04584626+2950370	MWC 480	A2	· · ·	· · ·	· · ·	· · ·	II
J05030659+2523197	V836 Tau	K7	−1.51/−1.55	−1.04/−1.06	−1.14/−1.16	−0.76/−0.77	II
J05044139+2509544	CIDA 8	M3.5	−1.63/−1.74	−1.18/−1.24	−1.47/−1.52	−0.99/−1.01	II
J05052286+2531312	CIDA 9	K8	0.19	· · ·	−0.37	· · ·	II
J05061674+2446102	CIDA 10	M4	−2.50/−2.54	· · ·	−2.66/−2.67	· · ·	III
J05062332+2432199	CIDA 11	M3.5	−1.62/−1.66	· · ·	−1.38/−1.40	· · ·	II
J05064662+2104296	· · ·	M5.25	−2.40/−2.42	· · ·	−2.67/−2.68	· · ·	III
J05071206+2437163	RXJ 05072+2437	K6	−2.68/−2.71	· · ·	−2.76/−2.77	· · ·	III
J05074953+3024050	RW Aur A+B	K3	−0.85/−0.96	· · ·	−0.56/−0.61	· · ·	II
J05075496+2500156	CIDA 12	M4	−1.59/−1.62	· · ·	−1.31/−1.32	· · ·	II

TABLE 7 — *Continued*

2MASS[a]	Name	Spectral Type	$\alpha(2\text{--}8\ \mu m)$	$\alpha(2\text{--}24\ \mu m)$	$\alpha(3.6\text{--}8\ \mu m)$	$\alpha(3.6\text{--}24\ \mu m)$	SED Class

NOTE. — Entries consist of observed and dereddened values, respectively. Only the observed values are listed if extinction estimates are unavailable.

[a] 2MASS Point Source Catalog.

[b] Because this multiple system is unresolved at 24 μm, this slope was computed with the total flux of the system in the band at shorter wavelengths.

[c] The spectral type bin in which this source was placed in Table 8 based on its bolometric luminosity.

TABLE 8
STATISTICS OF SED CLASSES

Spectral Type[b]	All of Taurus			XEST Fields		
	I	II	III	I	II	III
<K6	10	23	8	9	14	3
≥K6 and ≤M3.5	22	90	40	19	56	23
>M3.5 and <M6	5	44	42	2	20	23
≥M6 and ≤M8	3	18	25	1	7	12
>M8	0	9	11	0	3	3
Total	42	184	126	31	100	64

[a] Spectral types have been estimated from bolometric luminosities for stars that lack spectral classifications, most of which are class I sources. The spectral type bins in which these sources appear are indicated in Table 7.

TABLE 9
IRAC PHOTOMETRY FOR PROBABLE MEMBERS OF η CHA

ID[a]	[3.6]	[4.5]	[5.8]	[8.0]	Date
1	7.18±0.02	7.20±0.02	7.13±0.03	7.09±0.03	2004 Jun 10
2	out	out	5.63±0.03	out	2004 Jun 10
3	9.28±0.02	9.23±0.02	9.11±0.03	9.18±0.03	2004 Jun 10
4	8.46±0.02	8.44±0.02	8.37±0.03	8.37±0.03	2004 Jun 10
5	9.62±0.02	9.51±0.02	9.36±0.03	8.95±0.03	2004 Jun 10
6	9.19±0.02	9.11±0.02	9.09±0.03	9.04±0.03	2004 Jun 10
7	7.53±0.02	7.54±0.02	7.48±0.03	7.48±0.03	2004 Jun 10
8	sat	sat	5.38±0.03	5.41±0.03	2004 Jun 10
9	8.98±0.02	8.79±0.02	8.55±0.03	7.99±0.03	2004 Jun 10
10	8.59±0.02	8.60±0.02	8.53±0.03	8.52±0.03	2004 Jun 10
11	7.10±0.02	6.85±0.02	6.56±0.03	5.93±0.03	2004 Jun 10
12	8.19±0.02	8.15±0.02	8.10±0.03	8.10±0.03	2004 Jun 10
13	6.98±0.02	6.96±0.02	6.95±0.03	6.94±0.03	2004 Jun 10
14	10.53±0.02	10.28±0.02	10.04±0.03	9.51±0.03	2004 Jun 10
15	8.40±0.02	7.90±0.02	7.41±0.03	6.54±0.03	2004 Jun 10
16	11.02±0.02	10.74±0.02	10.44±0.03	9.79±0.03	2004 Jun 10
17	10.09±0.02	9.97±0.02	9.93±0.03	9.92±0.03	2004 Jun 10
18	10.57±0.02	10.44±0.02	10.41±0.03	10.35±0.03	2004 Jun 10

[a] Identifications from Mamajek et al. (1999) and Luhman & Steeghs (2004).

TABLE 10
MIPS PHOTOMETRY FOR PROBABLE MEMBERS OF η CHA

ID[a]	[24]	Date
1	7.07±0.05	2005 Mar 9
	7.01±0.04	2005 Apr 8
2	4.37±0.04	2004 Feb 21
	4.40±0.04	2005 Apr 8
3	8.68±0.05	2005 Mar 9
	8.65±0.07	2005 Apr 8
4	7.62±0.05	2005 Mar 8
	7.73±0.04	2005 Apr 8
	7.62±0.04	2008 May 18
5	5.18±0.04	2004 Feb 21
	5.10±0.04	2005 Apr 8
6	8.84±0.05	2005 Apr 8
7	7.47±0.05	2005 Mar 8
	7.39±0.04	2005 Apr 8
	7.36±0.04	2008 May 18

Luhman et al.

TABLE 10 — *Continued*

IDa	[24]	Date
8	5.50±0.04	2005 Mar 8
	5.39±0.04	2005 Apr 8
	5.41±0.04	2008 May 18
9	5.40±0.04	2005 Apr 8
10	8.40±0.05	2005 Apr 8
11	3.81±0.05	2004 Feb 21
	3.61±0.04	2004 Sep 18
	3.75±0.04	2005 Apr 8
	3.68±0.04	2008 May 18
12	7.95±0.05	2004 Jun 22
	7.91±0.04	2005 Apr 8
13	6.99±0.04	2005 Mar 9
	7.00±0.04	2005 Apr 8
14	7.18±0.04	2005 Apr 8
15	3.40±0.04	2005 Mar 8
	3.53±0.04	2005 Apr 8
	3.47±0.04	2008 May 18
16	7.17±0.04	2005 Apr 8
17	9.81±0.17	2008 May 18
18	out	⋯

a Identifications from Mamajek et al. (1999) and Luhman & Steeghs (2004).

TABLE 11
MIPS Photometry for Probable Members of ε Cha

IDa	[24]	Date
1	⋯	⋯
2	4.99±0.04	2006 Feb 22
3+4+5+6	sat	⋯
7	2.1±0.2	2006 Feb 22
8	6.69±0.04	2006 Feb 27
9	9.9±0.2	2006 Feb 27
10	6.68±0.04	2006 Feb 27
11	5.30±0.04	2006 Feb 27
12	9.8±0.2	2006 Feb 27

a Identifications from Feigelson et al. (2003) and Luhman (2004a).

TABLE 12
Spitzer Photometry for Probable Members of TWA

TWA	[3.6]	[4.5]	[5.8]	[8.0]	Date	[24]	Date
1	7.14±0.02	7.04±0.02	6.90±0.03	5.98±0.03	2003 Dec 20	1.24±0.04	2004 Feb 2
2	out	out	out	out	⋯	6.37±0.04	2004 Jan 30
3	6.49±0.02	6.37±0.02	6.15±0.03	5.15±0.03	2004 May 27	1.62±0.04	2004 Feb 2
4	5.59±0.02	5.54±0.02	5.43±0.03	4.79±0.03	2003 Dec 20	sat	⋯
5	out	out	out	out	⋯	6.35±0.04	2004 Feb 2
6	out	out	out	out	⋯	7.66±0.04	2004 May 9
7	out	out	out	out	⋯	5.97±0.04	2004 Jan 30
8A	out	out	out	out	⋯	6.98±0.04	2004 Jan 31
8B	out	out	out	out	⋯	8.17±0.05	2004 Jan 31
9	out	out	out	out	⋯	7.21±0.04	2004 Feb 2
10	out	out	out	out	⋯	7.75±0.04	2004 Feb 20
11A+B	out	out	out	out	⋯	0.97±0.04	2004 Jan 31
11C	out	8.61±0.02	out	8.52±0.03	2007 Aug 7	8.23±0.08	2004 Jan 31
13	out	out	out	out	⋯	6.55±0.05	2004 Jun 21
14	out	out	out	out	⋯	8.11±0.05	2004 Feb 20
15	out	out	out	out	⋯	8.41±0.06	2004 Feb 20
16	out	out	out	out	⋯	7.84±0.05	2004 Feb 20
20	out	out	out	out	⋯	8.01±0.05	2006 Feb 20
21	out	out	out	out	⋯	7.09±0.04	2005 Jan 31,2006 Feb 27
23	out	out	out	out	⋯	7.35±0.04	2005 Feb 1
25	out	out	out	out	⋯	7.07±0.05	2005 Jun 26
26	10.93±0.02	10.81±0.02	10.71±0.03	10.61±0.03	2005 Jun 10	10.31±0.07	2005 Feb 1
27	11.30±0.02	10.98±0.02	10.70±0.03	10.18±0.03	2005 Jun 14	8.10±0.04	2005 Jan 27
28	11.19±0.02	10.80±0.02	10.45±0.03	9.95±0.03	2007 Jul 4	8.09±0.04	2007 Jul 12
29	12.72±0.02	12.64±0.02	12.56±0.03	12.51±0.03	2009 Mar 19	out	⋯

TABLE 13   — *Continued*

Spectral Type	$J - H$	$H - K_s$	$K_s - [3.6]$	$[3.6] - [4.5]$	$[4.5] - [5.8]$	$[5.8] - [8.0]$	$[8.0] - [24]$

TABLE 13
COLORS OF YOUNG STELLAR PHOTOSPHERES

Spectral Type	$J - H$	$H - K_s$	$K_s - [3.6]$	$[3.6] - [4.5]$	$[4.5] - [5.8]$	$[5.8] - [8.0]$	$[8.0] - [24]$
K4	0.53	0.10	0.06	0.00	0.04	0.00	0.04
K5	0.61	0.12	0.08	0.00	0.04	0.00	0.06
K6	0.66	0.14	0.10	0.00	0.04	0.00	0.08
K7	0.68	0.15	0.10	0.00	0.04	0.00	0.11
M0	0.70	0.16	0.10	0.00	0.04	0.00	0.13
M1	0.71	0.18	0.11	0.01	0.04	0.00	0.15
M2	0.70	0.20	0.14	0.03	0.04	0.00	0.17
M3	0.68	0.22	0.17	0.05	0.04	0.00	0.19
M4	0.63	0.26	0.20	0.07	0.04	0.00	0.21
M5	0.56	0.29	0.28	0.09	0.04	0.00	0.23
M6	0.55	0.33	0.39	0.11	0.04	0.00	0.25
M7	0.59	0.37	0.42	0.12	0.05	0.00	0.27
M8	0.65	0.44	0.52	0.12	0.07	0.03	0.29
M9	0.72	0.55	0.63	0.14	0.13	0.12	0.31
L0	0.98	0.66	0.72	0.16	0.22	0.25	0.33
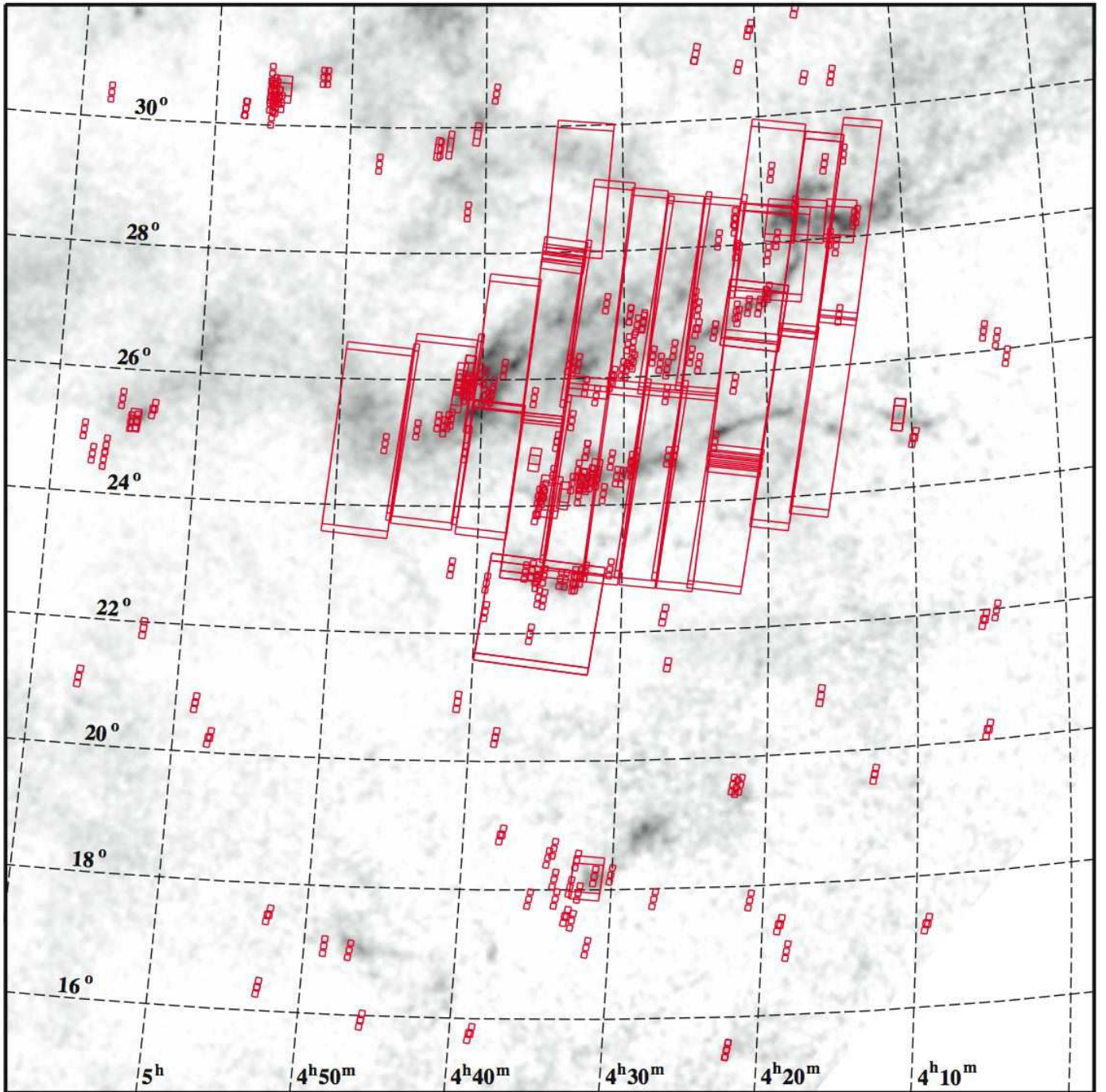
FIG. 1.— Fields in the Taurus star-forming region that have been imaged at 3.6–8.0 μm by IRAC on the *Spitzer Space Telescope* (Table 1). The dark clouds in Taurus are displayed with a map of extinction (*grayscale*, Dobashi et al. 2005).
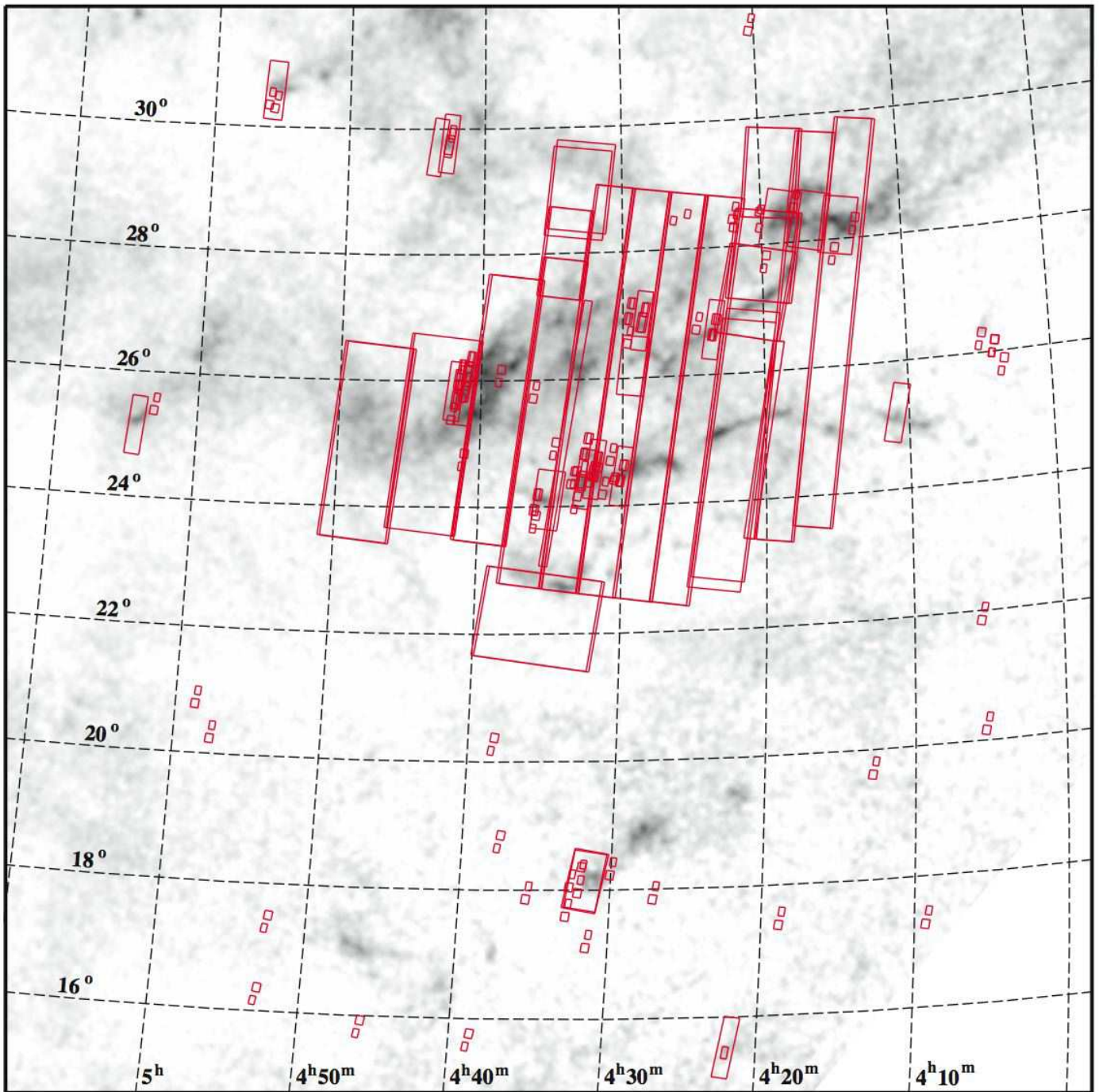
FIG. 2.— Fields in the Taurus star-forming region that have been imaged at 24 μm with MIPS on the *Spitzer Space Telescope* (Table 2).
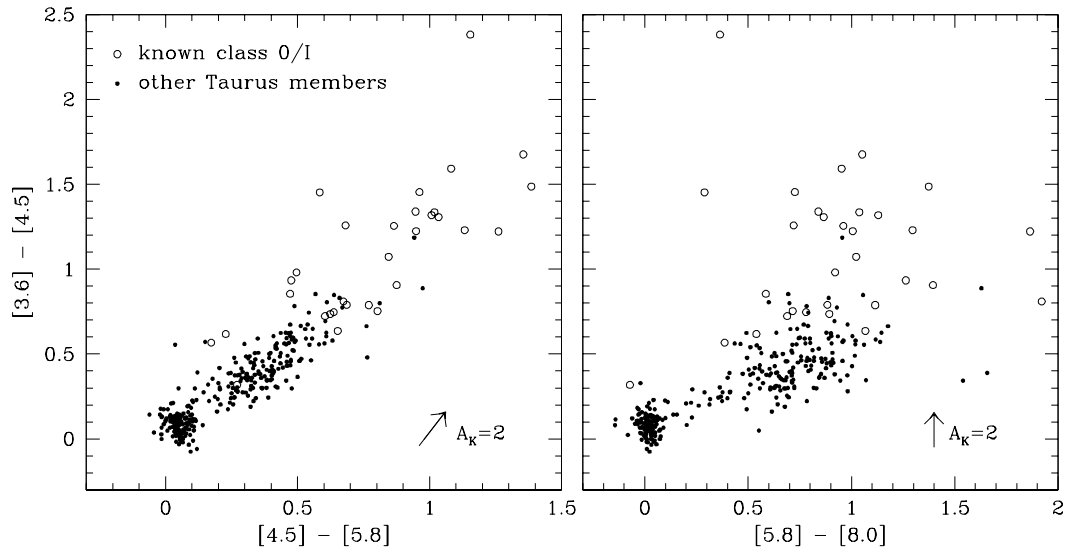
FIG. 3.— *Spitzer* IRAC color-color diagrams for members of the Taurus star-forming region. Stars that have been previously identified as class 0 and class I sources through mid-IR spectroscopy and other diagnostics are indicated (*open circles*, § 3.1). The reddening vectors are based on the extinction law from Flaherty et al. (2007).
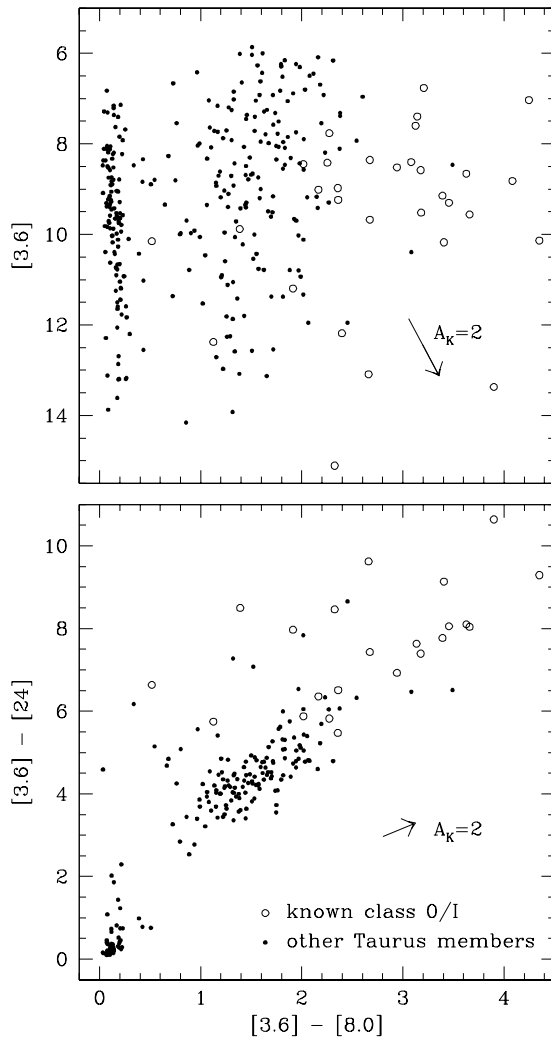
FIG. 4.— *Spitzer* color-magnitude and color-color diagrams for members of the Taurus star-forming region. Stars that have been previously identified as class 0 and class I sources through mid-IR spectroscopy and other diagnostics are indicated (*open circles*, § 3.1). The reddening vectors are based on the extinction law from Flaherty et al. (2007).

Luhman et al.
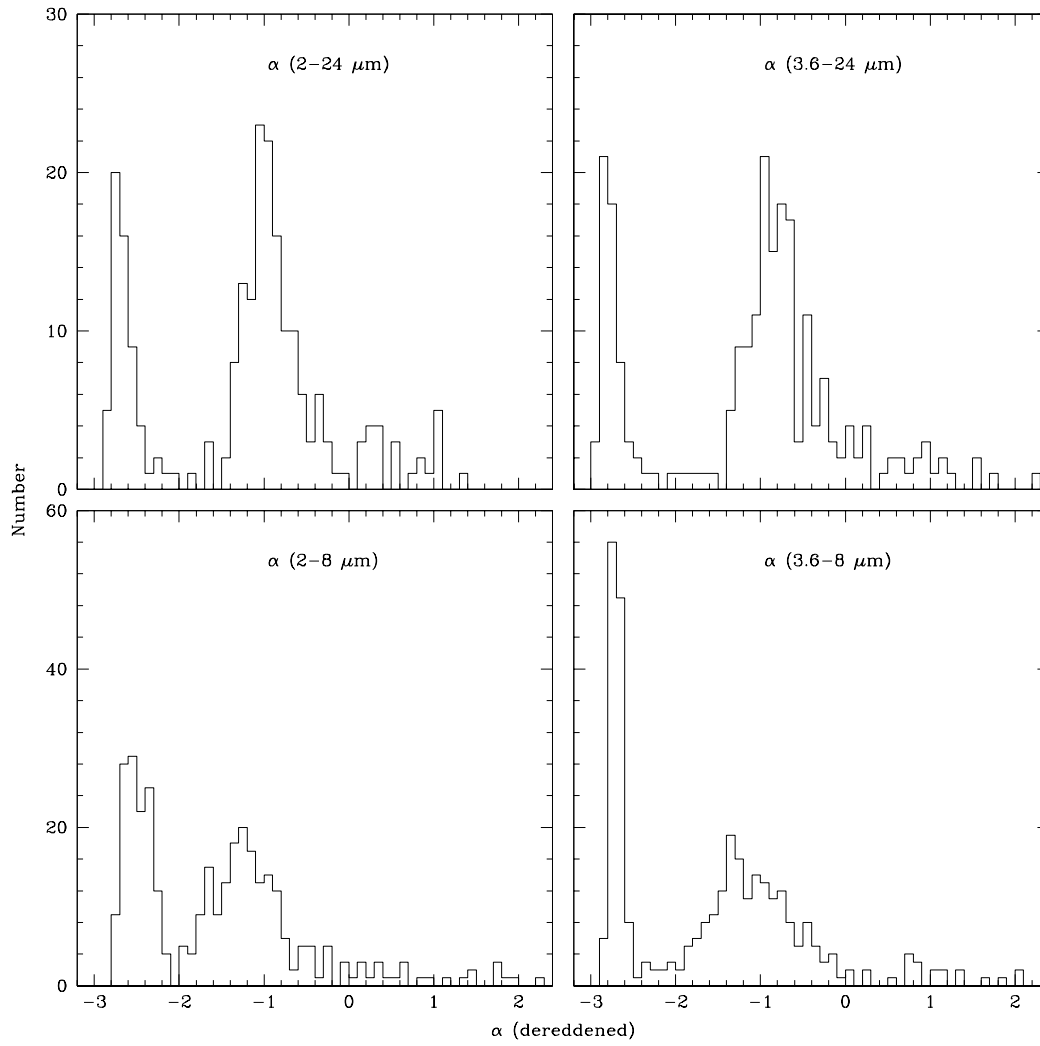
FIG. 5.— Distributions of spectral slopes for members of Taurus (Table 7).
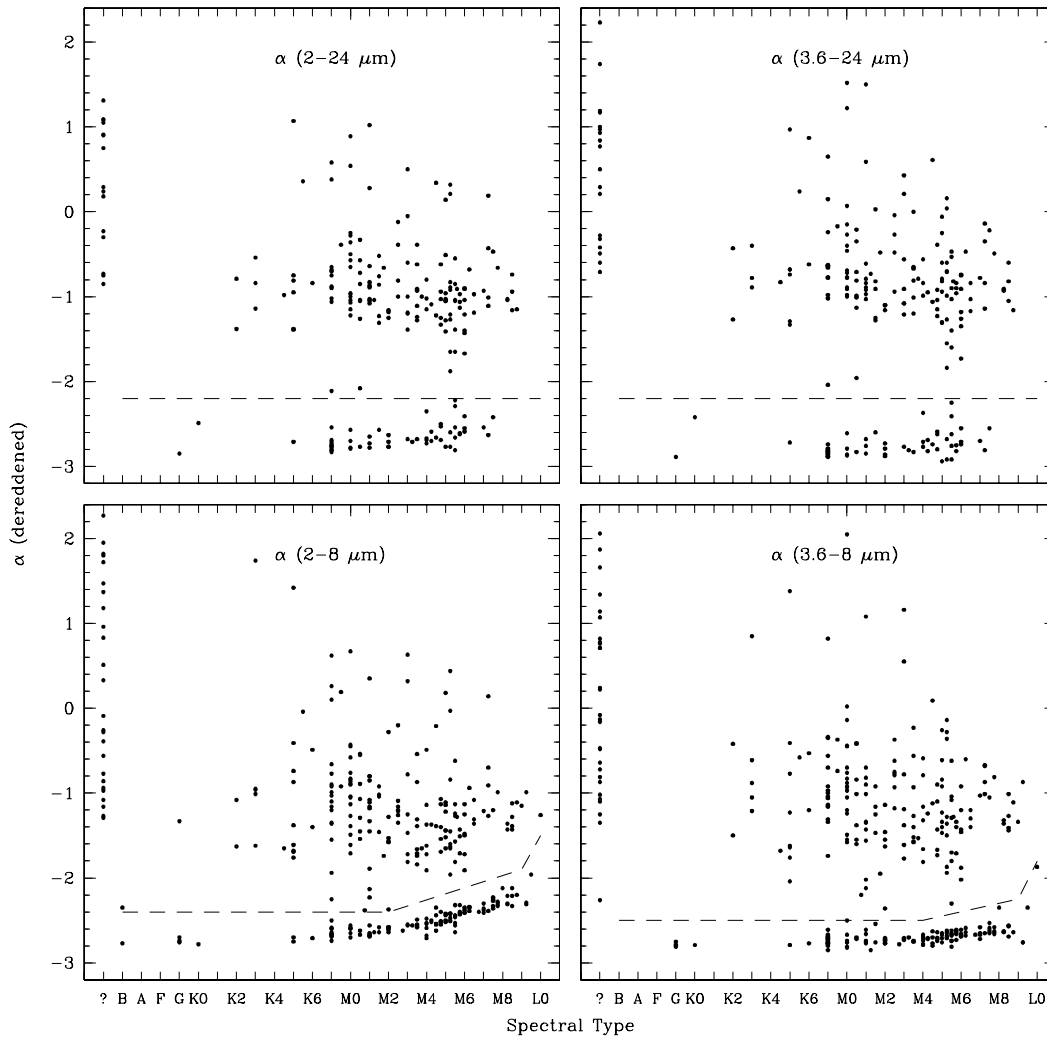
Fig. 6.— Spectral slopes as function of spectral type for members of Taurus (Table 7). Our adopted boundaries for separating classes II and III are indicated (*dashed lines*).

Luhman et al.
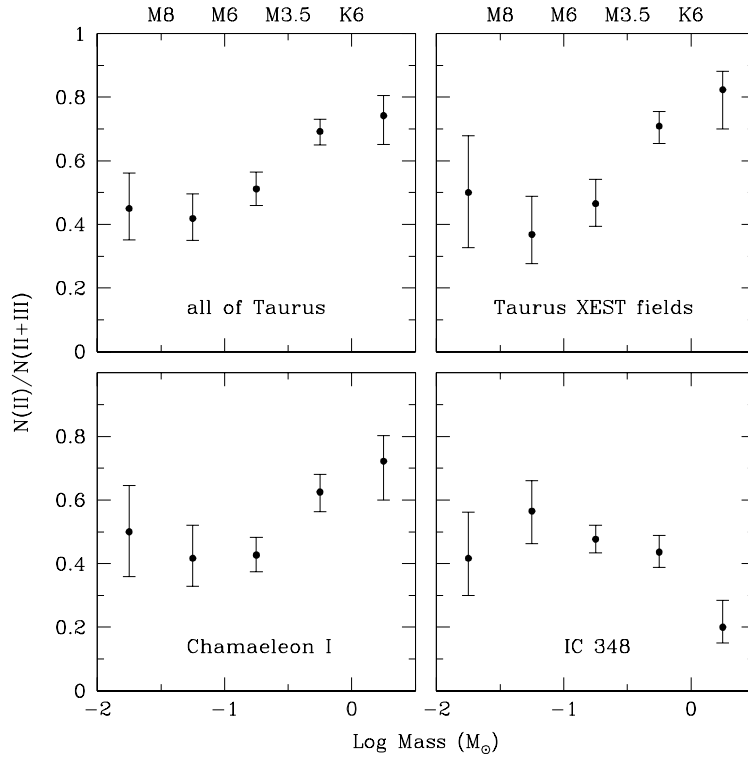
FIG. 7.— Disk fraction as a function of stellar mass and spectral type among all known members of Taurus and the members within the XEST fields. Similar measurements for Chamaeleon I and IC 348 are included for comparison (Lada et al. 2006; Muench et al. 2007; Luhman et al. 2005, 2008a).
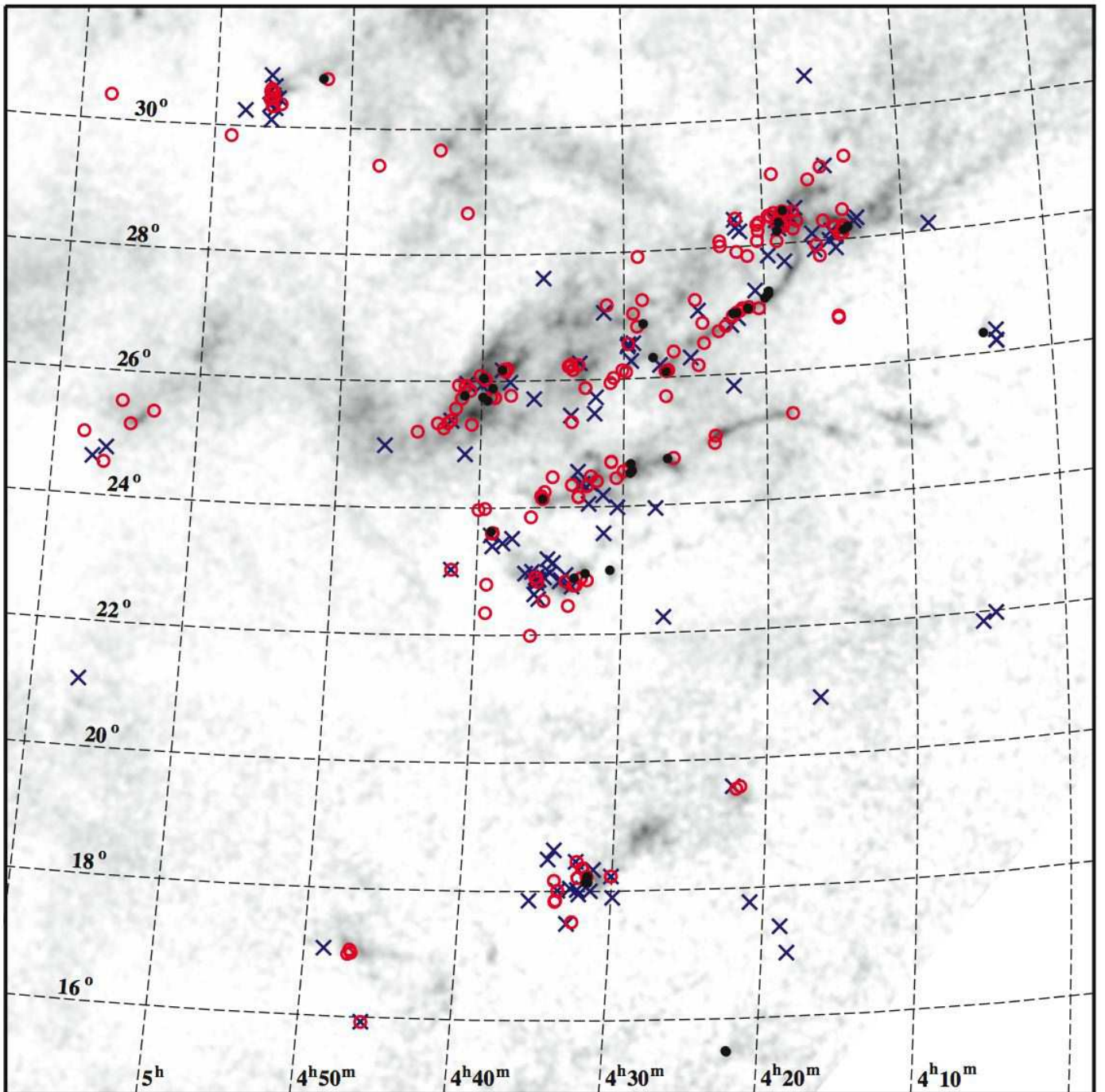
FIG. 8.— Spatial distributions of classes 0/I (*black filled circles*), II (*red open circles*), and III (*blue crosses*) in the Taurus star-forming region.
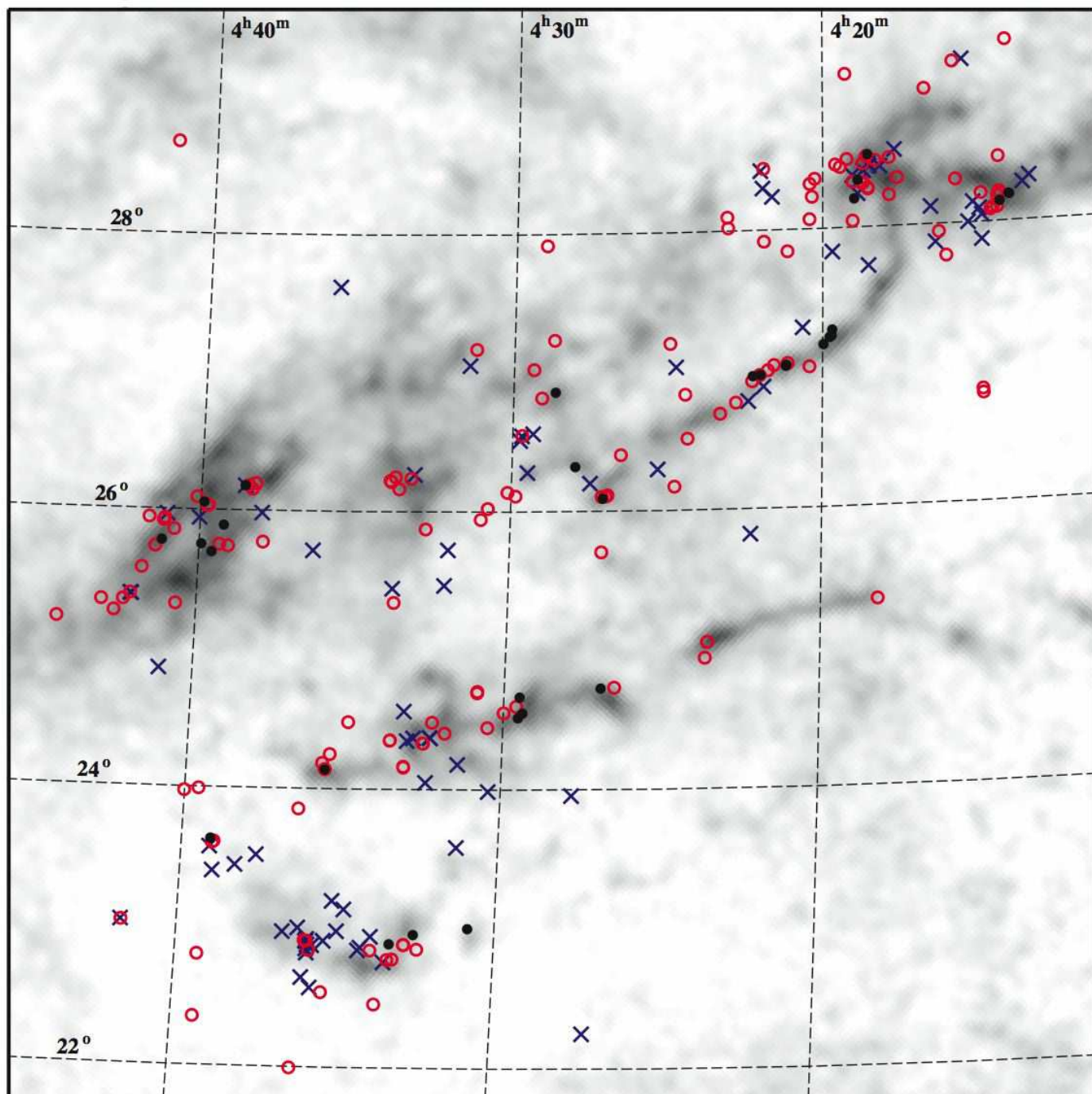
FIG. 9.— Same as Figure 8, but for the central clouds in Taurus.
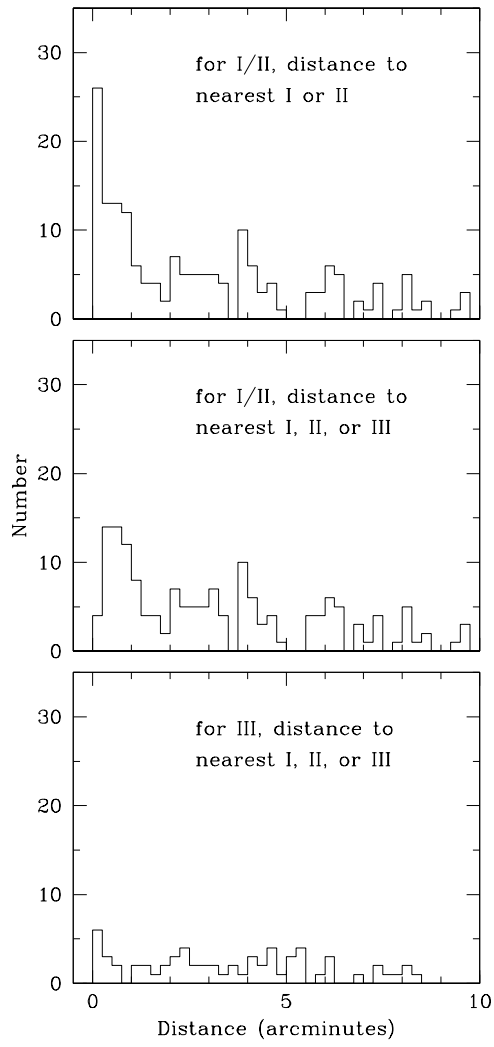
FIG. 10.— Distributions of projected angular distances to the nearest neighbor for different SED classes in Taurus. The bin size is 15″, corresponding to ∼ 0.01 pc at the distance of Taurus.
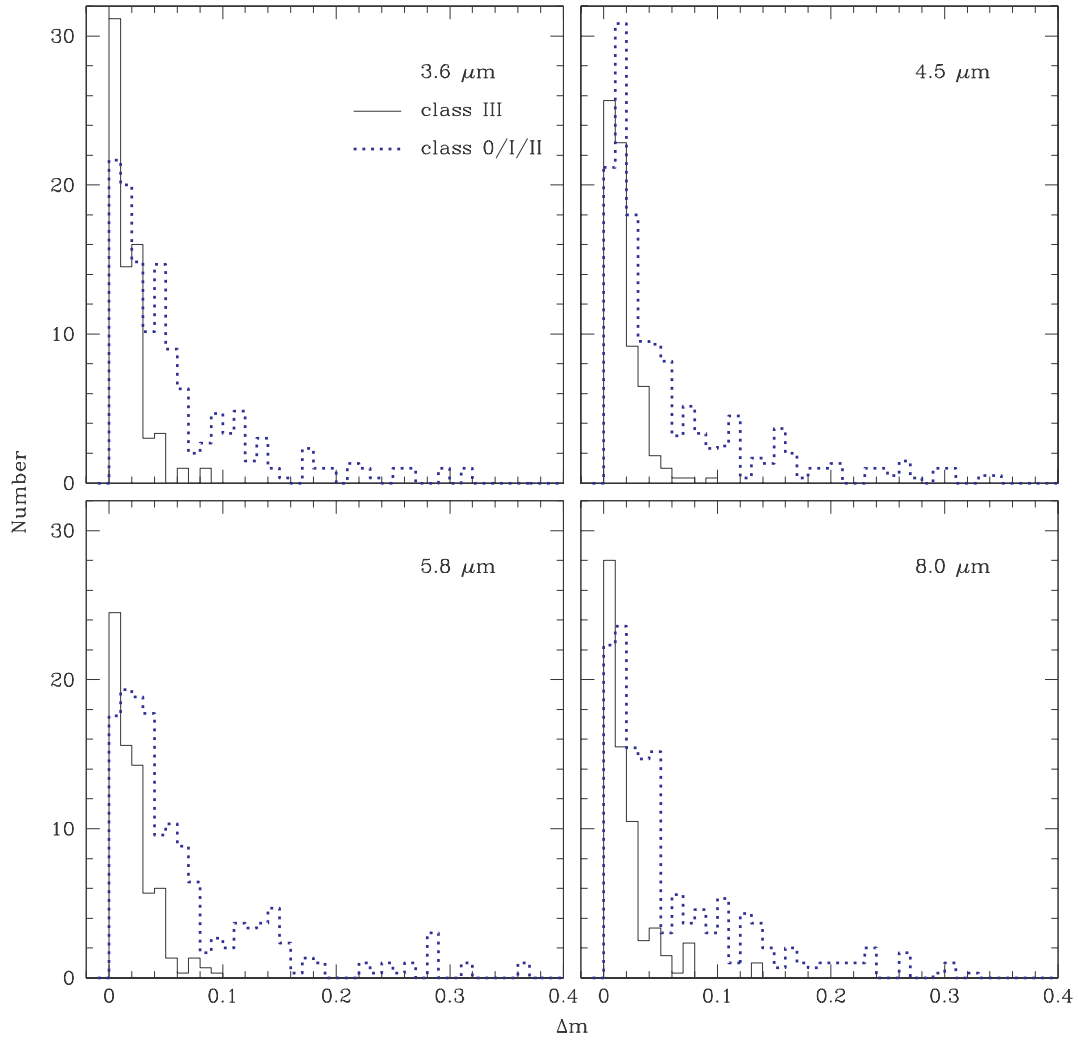
FIG. 11.— Variability of IRAC magnitudes for members of Taurus that have disks (classes 0, I, and II, *dotted histograms*) and members without disks (class III, *solid histograms*). The histograms represent distributions of differences between a magnitude and the average magnitude for a given source and band. Each magnitude difference is weighted by the inverse of the number of measurements so that all members contribute equally.
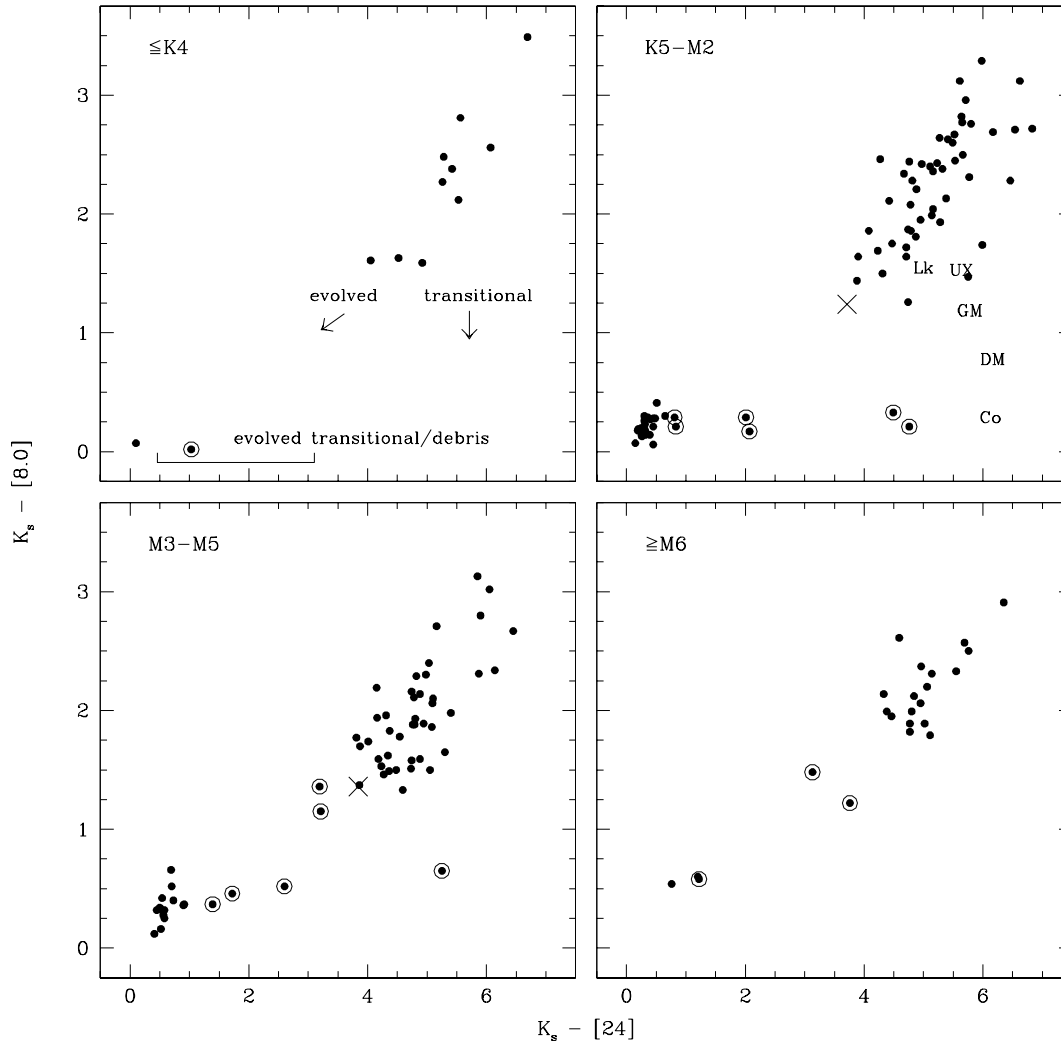
FIG. 12.— $K_s - [8.0]$ versus $K_s - [24]$ for class II and class III members of Taurus in four ranges of spectral types. The colors predicted by a model of an optically thick disk with a low accretion rate and a high degree of dust settling are shown for stellar masses of 0.2 and 0.7 $M_\odot$ (M3–M5 and K5–M2, *crosses*). These models demonstrate that the large, continuous population of red colors can be explained in terms of optically thick disks, which we refer to as primordial disks. In the upper left panel, we indicate the colors expected for optically thick disks that have developed inner holes (transitional), disks that are becoming optically thin throughout their inner regions (evolved), optically thin disks with inner holes (evolved transitional), and disks of second-generation dust (debris). The SEDs of systems that appear to be in these stages according to this diagram (*circles*) are shown in Figs. 15, 16, and 17. For reference, abbreviated names are used as the symbols for the pre-transitional and transitional systems UX Tau A, LkCa 15, GM Aur, DM Tau, and CoKu Tau/4.
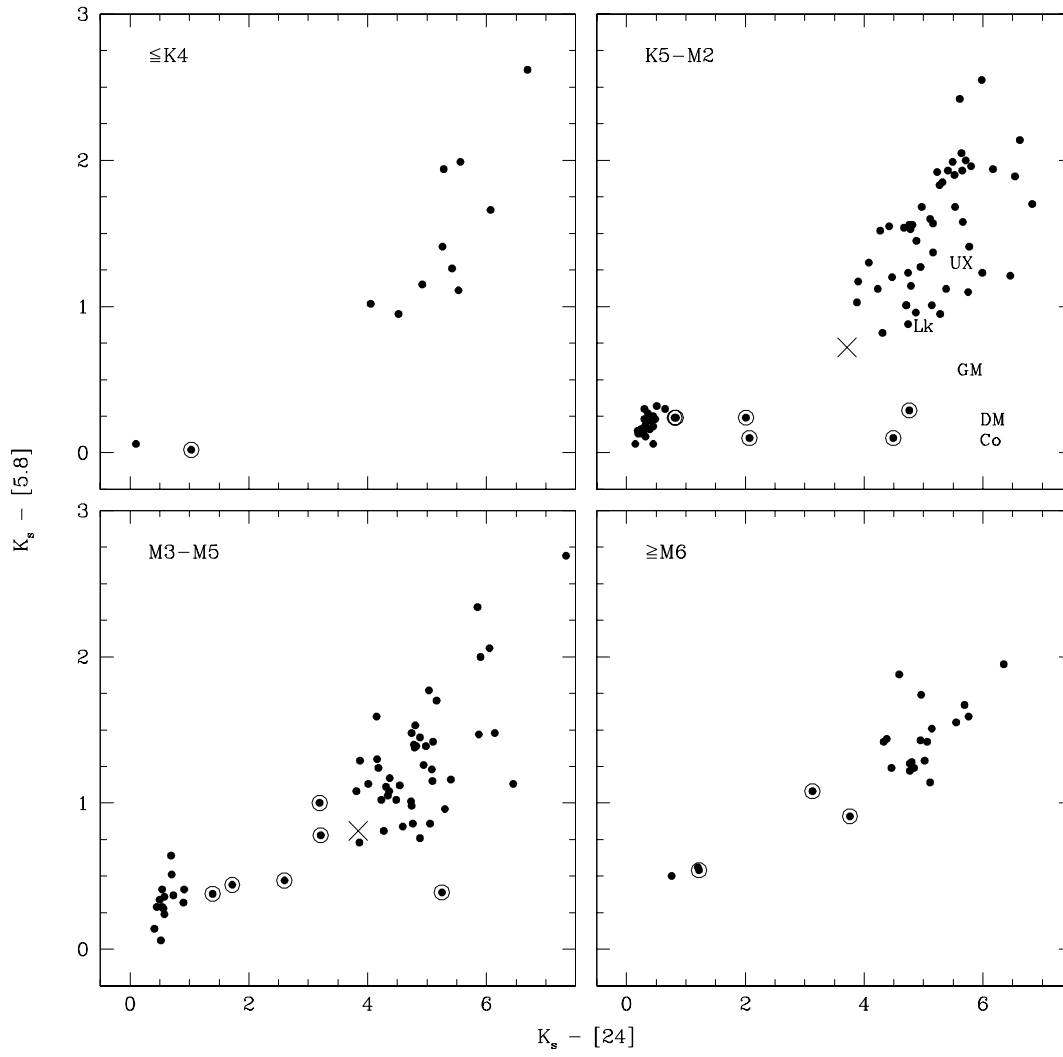
FIG. 13.— Same as Figure 12, but for $K_s - [5.8]$ versus $K_s - [24]$.
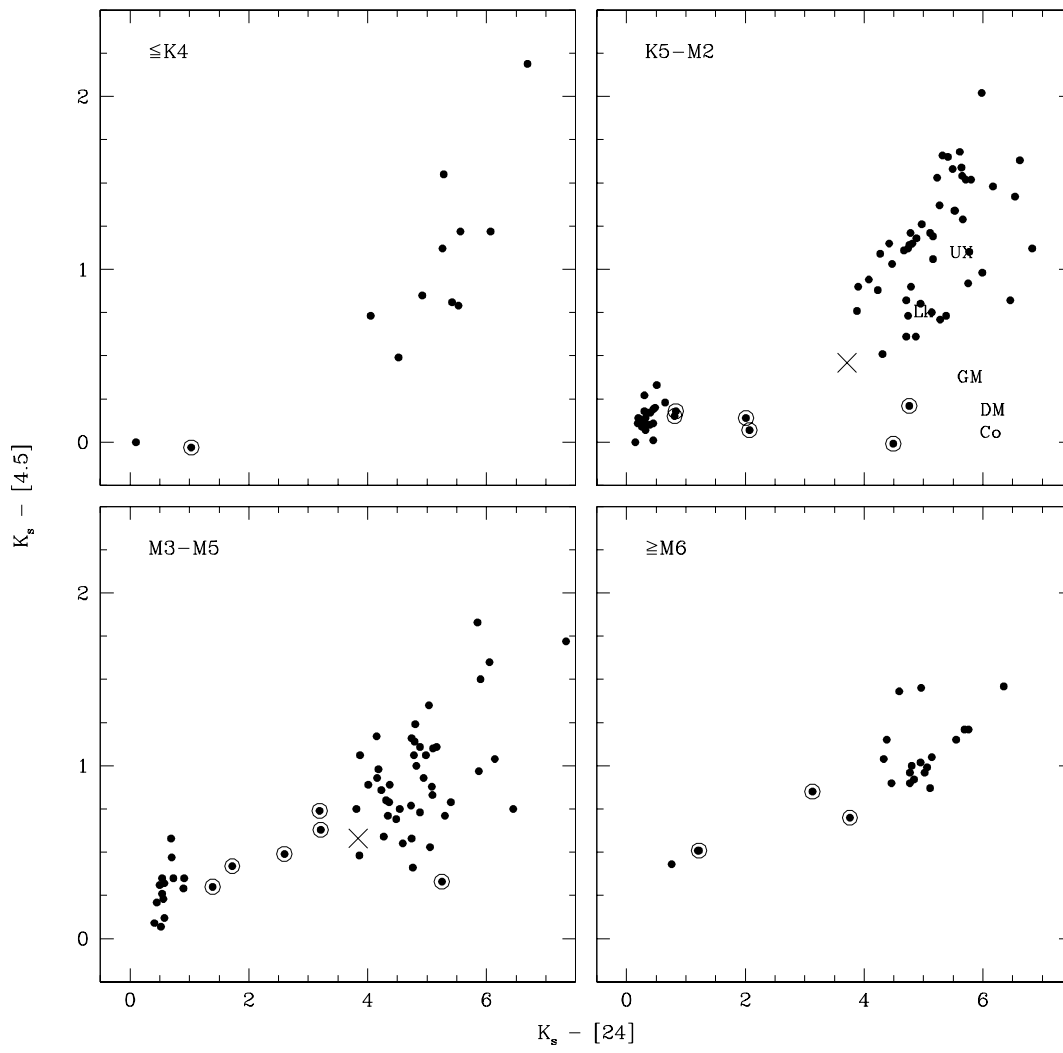
FIG. 14.— Same as Figure 12, but for $K_s - [4.5]$ versus $K_s - [24]$.
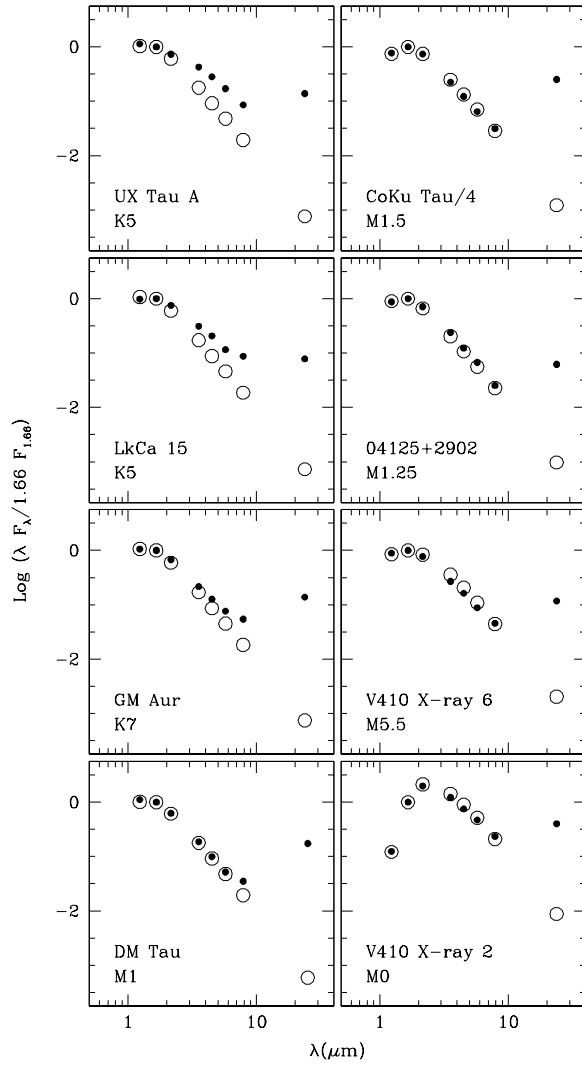
FIG. 15.— SEDs in Taurus that exhibit large 24 μm excesses but less excess emission at shorter wavelengths, which indicate the presence of disks with gaps and inner holes (pre-transitional and transitional disks). Each SED is compared to the SED of a stellar photosphere at the same spectral type (*circles*), which has been reddened by the extinction of the Taurus source and scaled to its *H*-band flux.
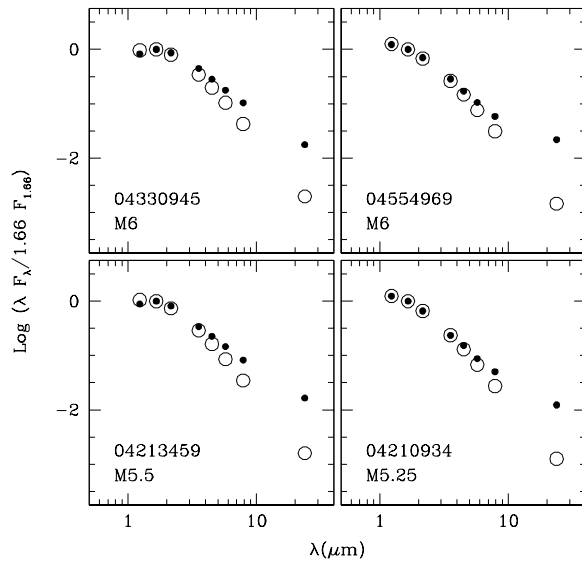
FIG. 16.— SEDs in Taurus that exhibit small excesses at 8 and 24 μm, which indicate the presence of disks that are becoming optically thin at these wavelengths (evolved disks). Each SED is compared to the SED of a stellar photosphere at the same spectral type (*circles*), which has been reddened by the extinction of the Taurus source and scaled to its *H*-band flux.

Luhman et al.
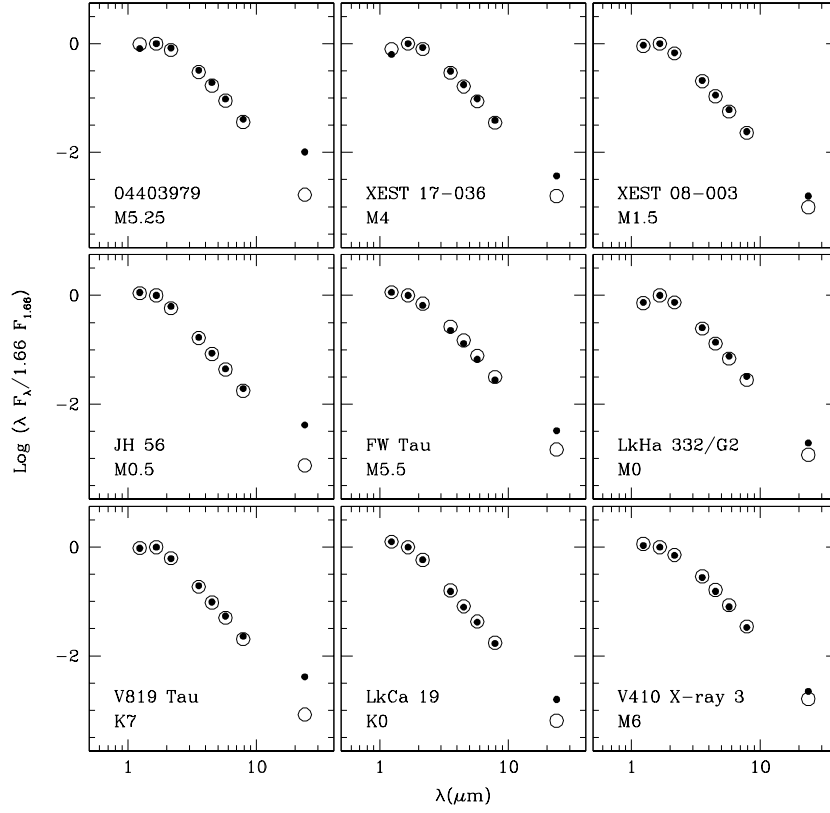
FIG. 17.— SEDs in Taurus that exhibit no excess emission at $\lambda < 10$ μm and small excesses at 24 μm, which may indicate the presence of disks that have inner holes and are becoming optically thin at 24 μm (evolved transitional disks) or disks that are composed of second-generation dust from collisions among planetesimals (debris disks). Each SED is compared to the SED of a stellar photosphere at the same spectral type (*circles*), which has been reddened by the extinction of the Taurus source and scaled to its *H*-band flux.
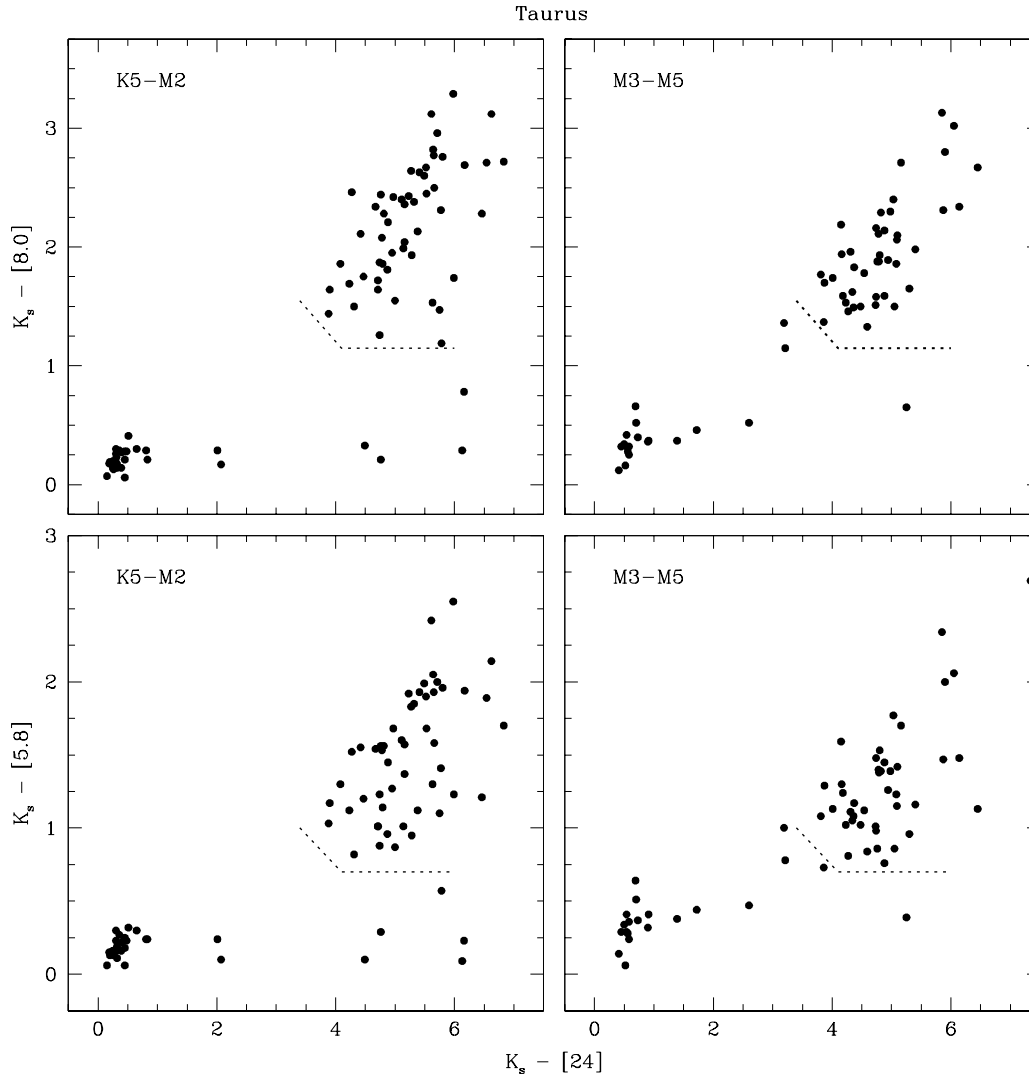
FIG. 18.— $K_s - [8.0]$ and $K_s - [5.8]$ versus $K_s - [24]$ for K5–M2 and M3–M5 members of Taurus ($\tau \sim 1$ Myr). We have marked the lower boundary of the primordial disks (*dotted lines*), which is plotted with data for other clusters in Figs. 19–25.
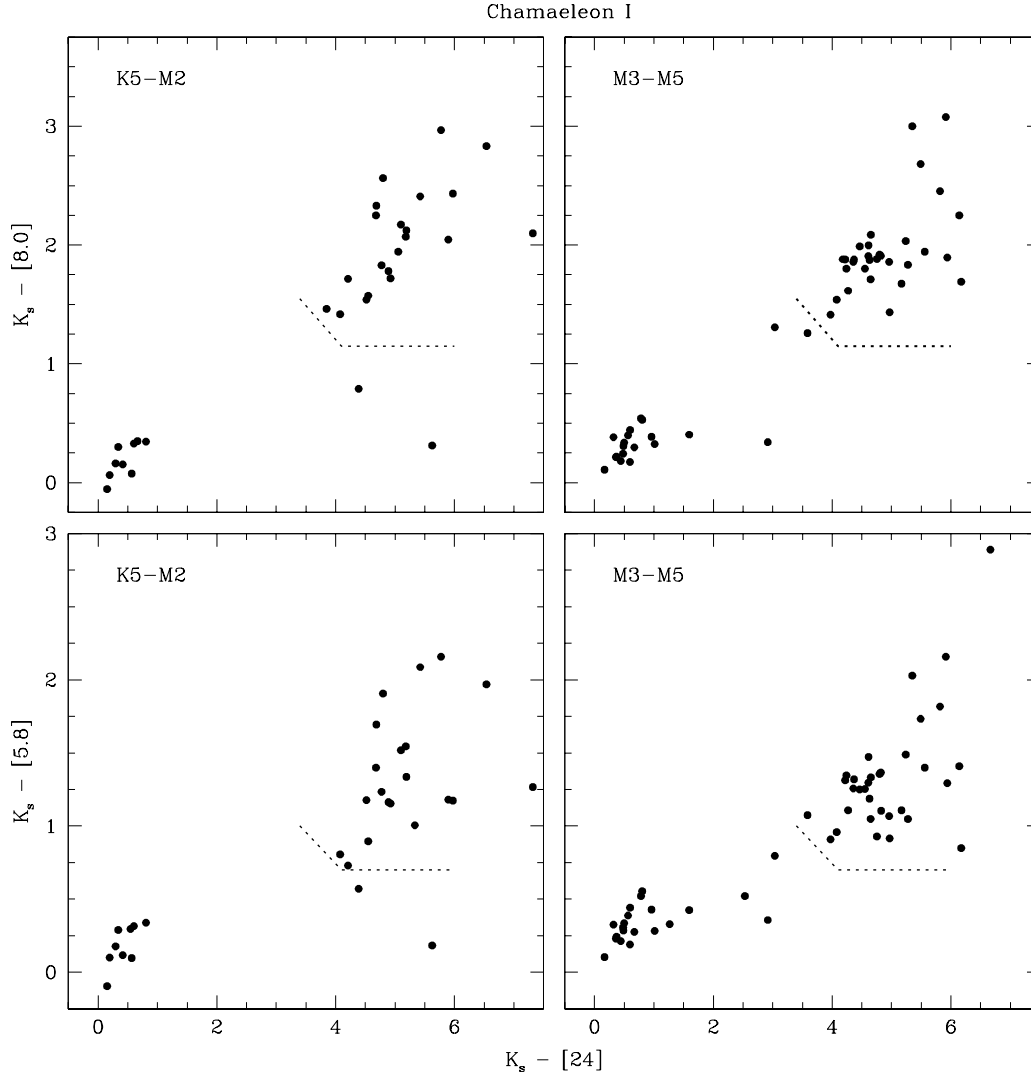
FIG. 19.— $K_s - [8.0]$ and $K_s - [5.8]$ versus $K_s - [24]$ for K5–M2 and M3–M5 members of Chamaeleon I ($\tau \sim 2 - 3$ Myr, Luhman et al. 2008a; Luhman & Muench 2008). The lower boundary of the primordial disks in Taurus is indicated (*dotted lines*).
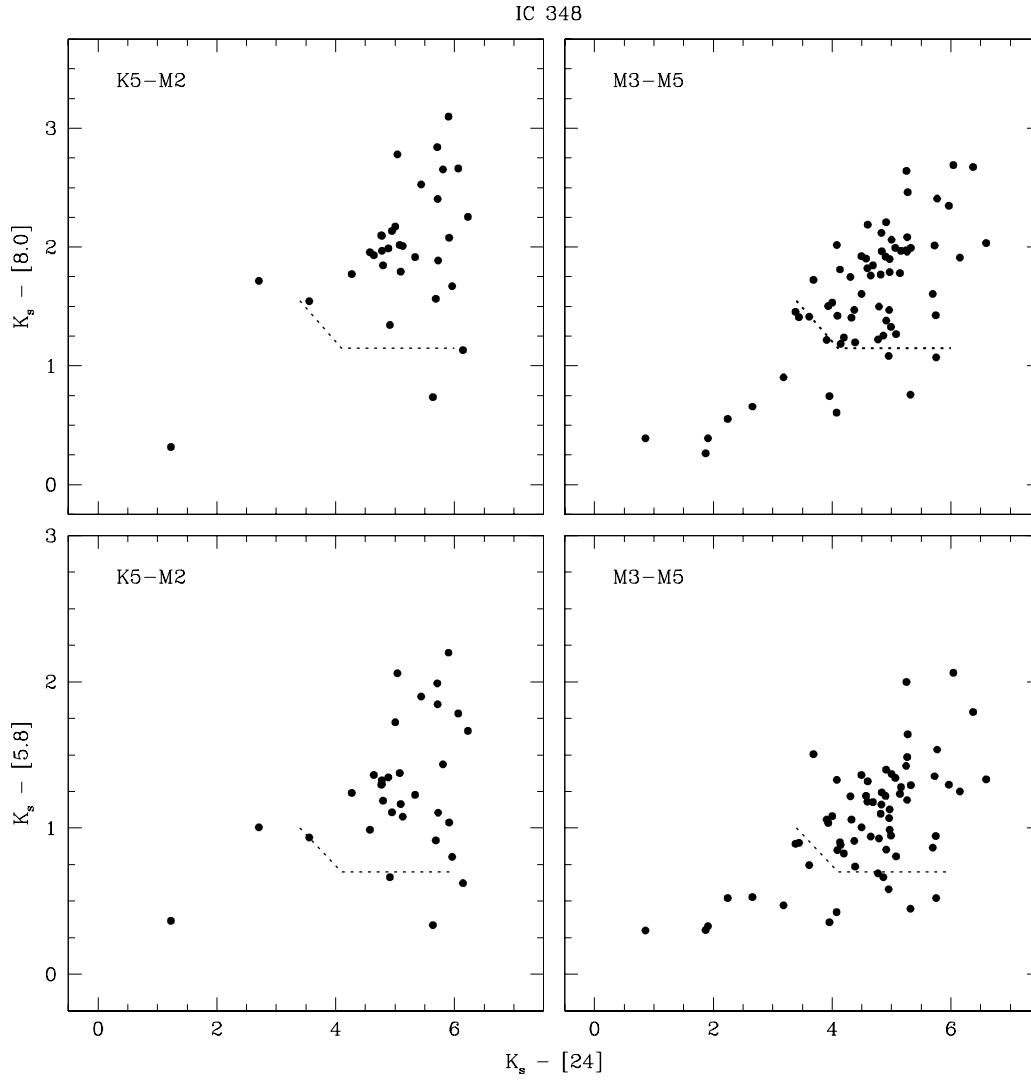
FIG. 20.— $K_s - [8.0]$ and $K_s - [5.8]$ versus $K_s - [24]$ for K5–M2 and M3–M5 members of IC 348 ($\tau \sim 2 - 3$ Myr, Lada et al. 2006; Muench et al. 2007). The lower boundary of the primordial disks in Taurus is indicated (*dotted lines*).
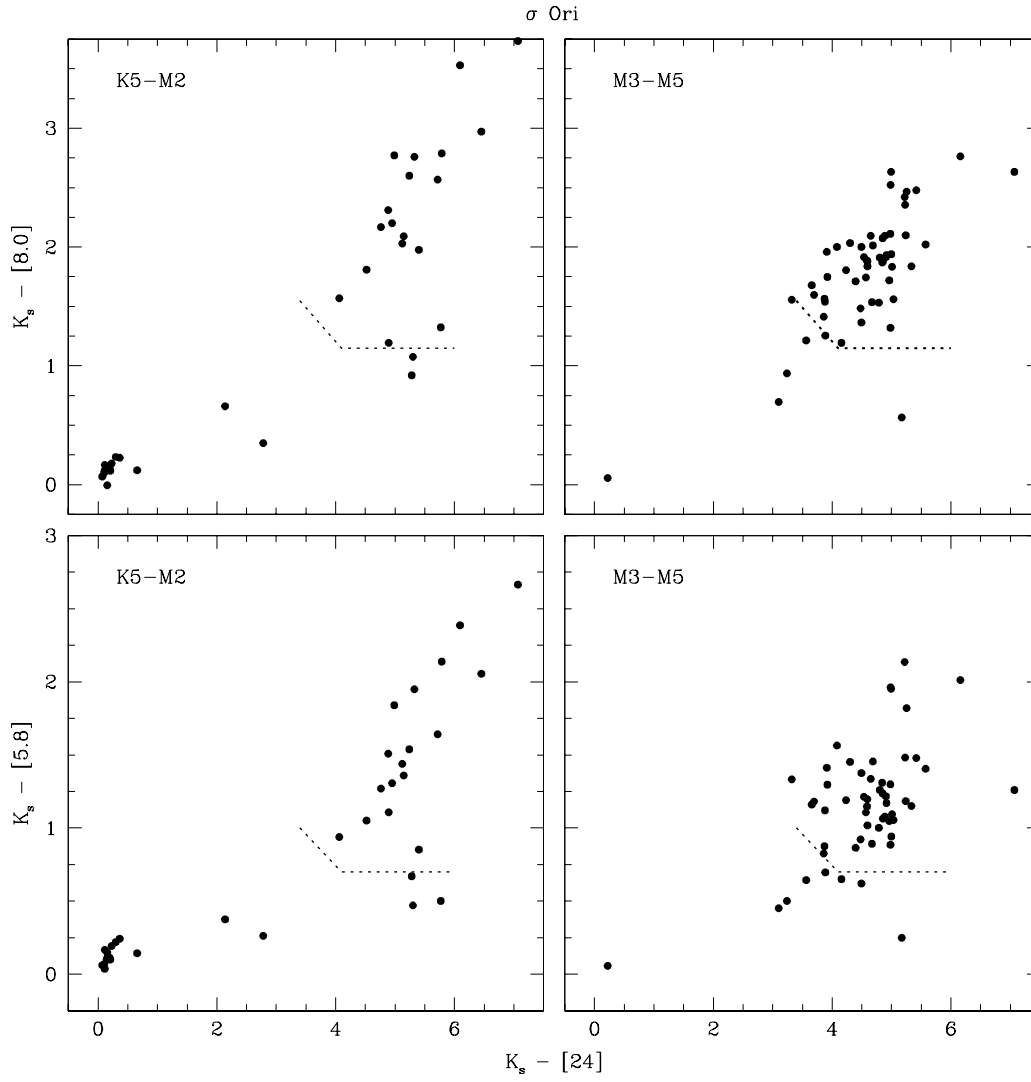
FIG. 21.— $K_s - [8.0]$ and $K_s - [5.8]$ versus $K_s - [24]$ for K5–M2 and M3–M5 members of σ Ori ($\tau \sim 2 - 3$ Myr, Hernández et al. 2007a; Luhman et al. 2008b). The lower boundary of the primordial disks in Taurus is indicated (*dotted lines*).
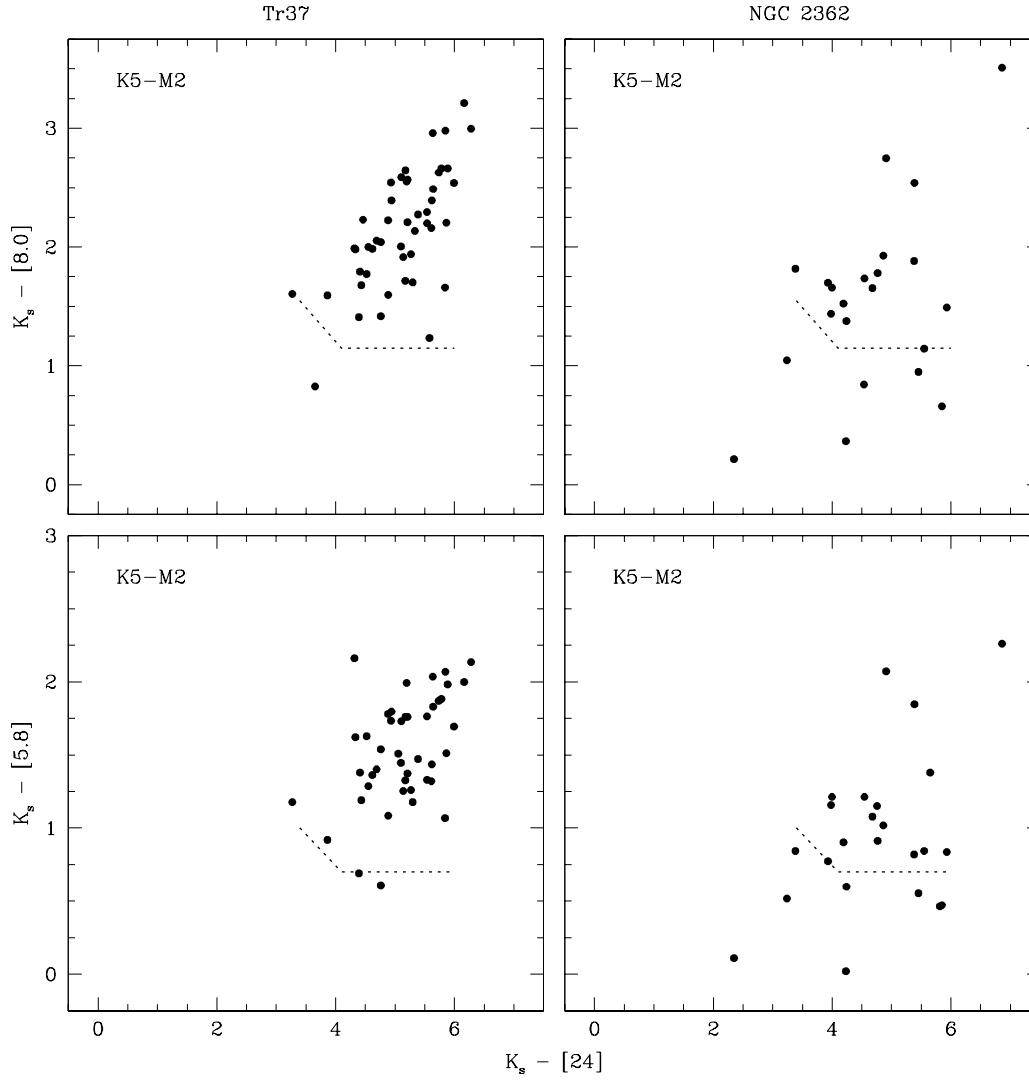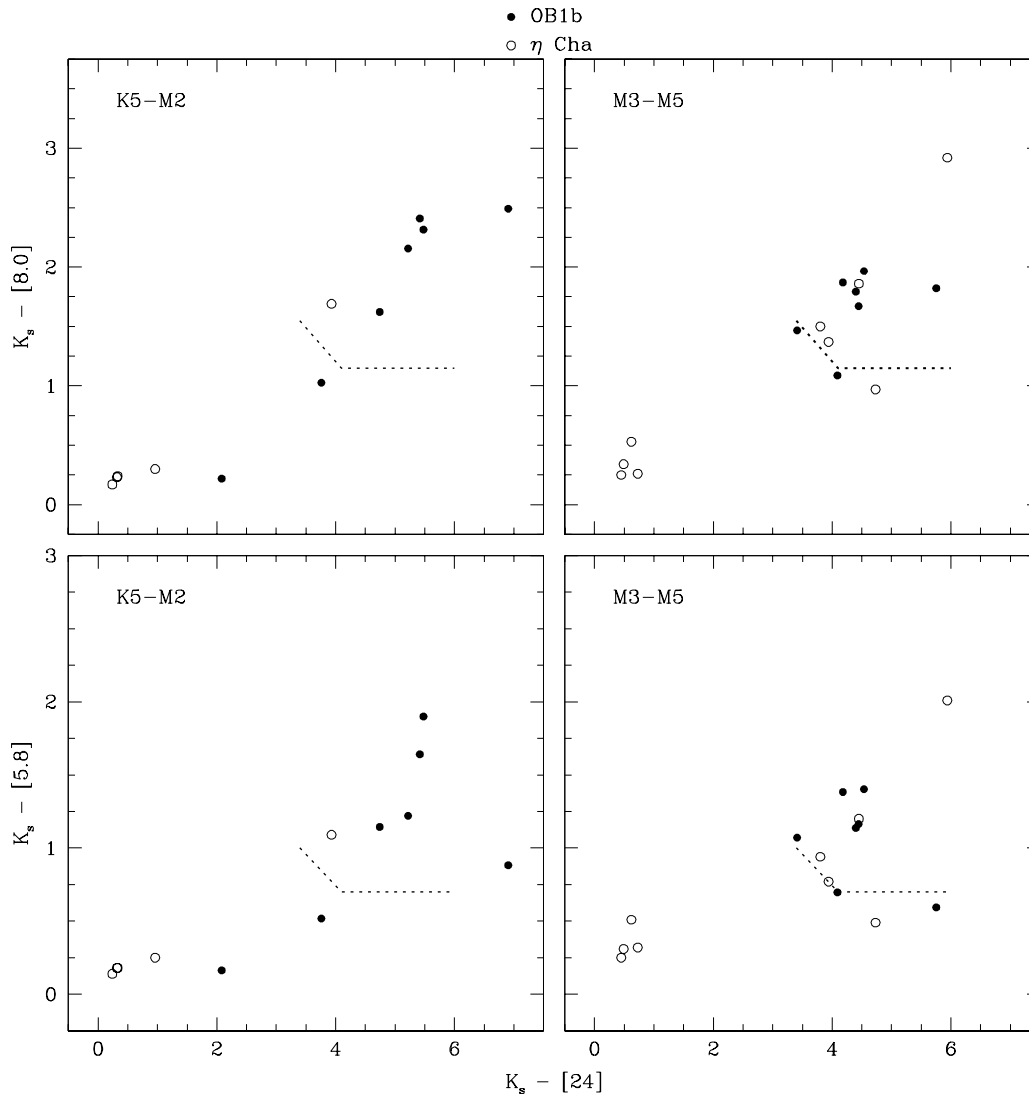
FIG. 22.— $K_s - [8.0]$ and $K_s - [5.8]$ versus $K_s - [24]$ for K5–M2 members of Tr 37 and NGC 2362 ($\tau \sim 4$ and 5 Myr, Sicilia-Aguilar et al. 2006; Dahm & Hillenbrand 2007; Currie et al. 2009a). The lower boundary of the primordial disks in Taurus is indicated (*dotted lines*).

Luhman et al.
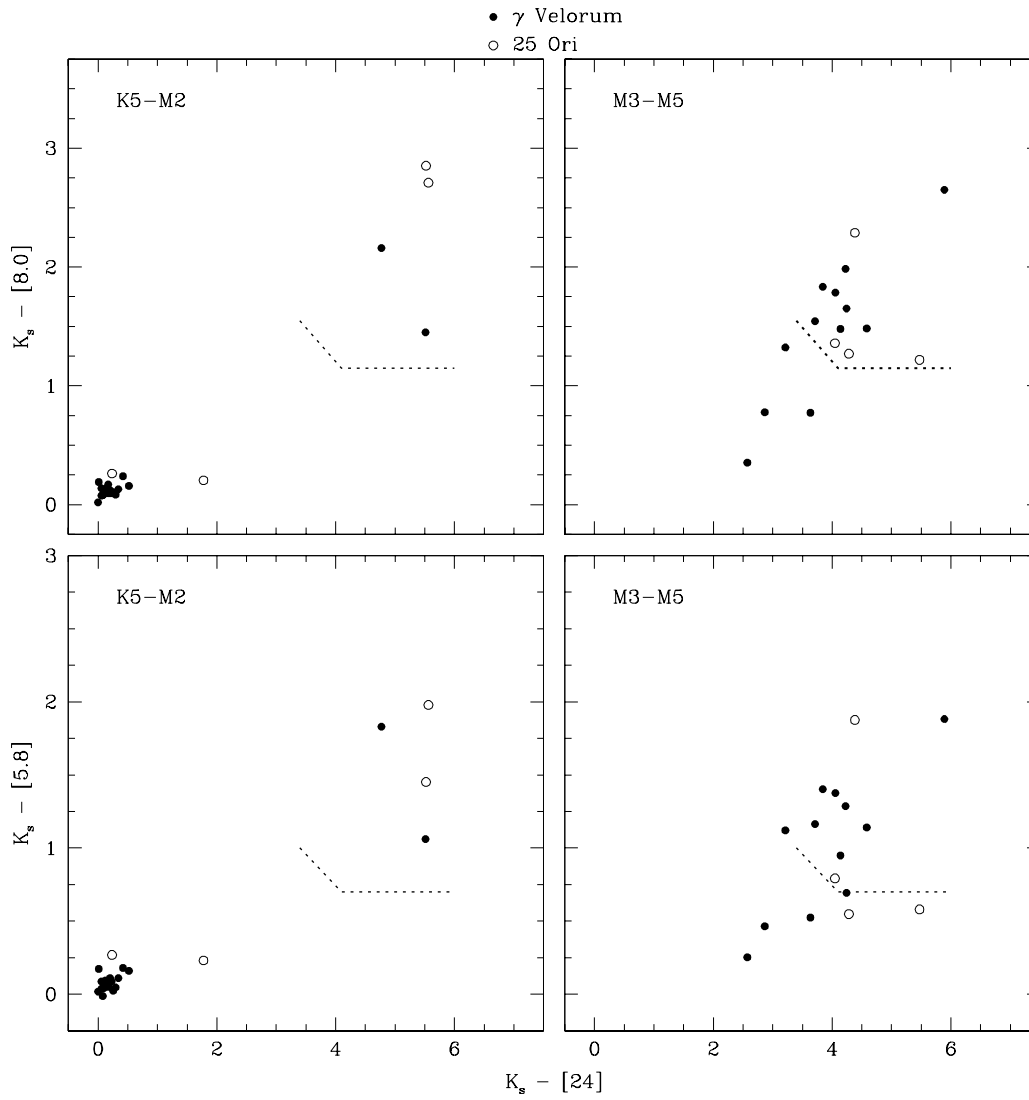
FIG. 23.— $K_s - [8.0]$ and $K_s - [5.8]$ versus $K_s - [24]$ for K5–M2 and M3–M5 members of γ Velorum and 25 Ori ($\tau \sim 5$ and 10 Myr, Hernández et al. 2007b, 2008). The lower boundary of the primordial disks in Taurus is indicated (*dotted lines*).

FIG. 24.— $K_s - [8.0]$ and $K_s - [5.8]$ versus $K_s - [24]$ for K5–M2 and M3–M5 members of Orion OB1b and η Cha ($\tau \sim 5$ and 6 Myr, Megeath et al. 2005; Hernández et al. 2007b). The lower boundary of the primordial disks in Taurus is indicated (*dotted lines*).
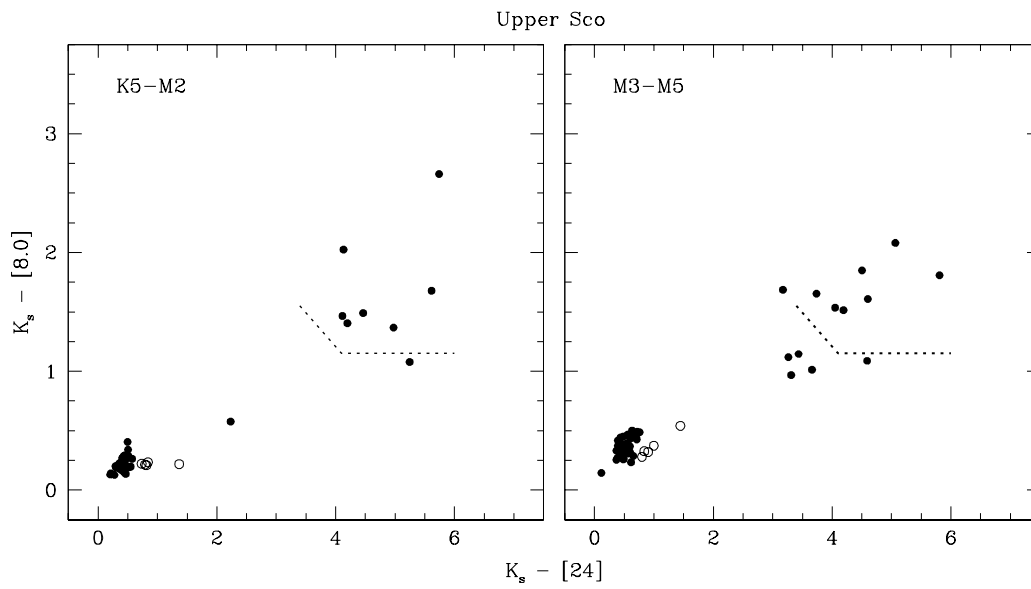
FIG. 25.— $K_s - [8.0]$ versus $K_s - [24]$ for K5–M2 and M3–M5 members of Upper Sco ($\tau \sim 5$ Myr, Carpenter et al. 2006, 2009). Candidate debris disks that were identified by Carpenter et al. (2009) are shown as open circles. The lower boundary of the primordial disks in Taurus is indicated (*dotted lines*).
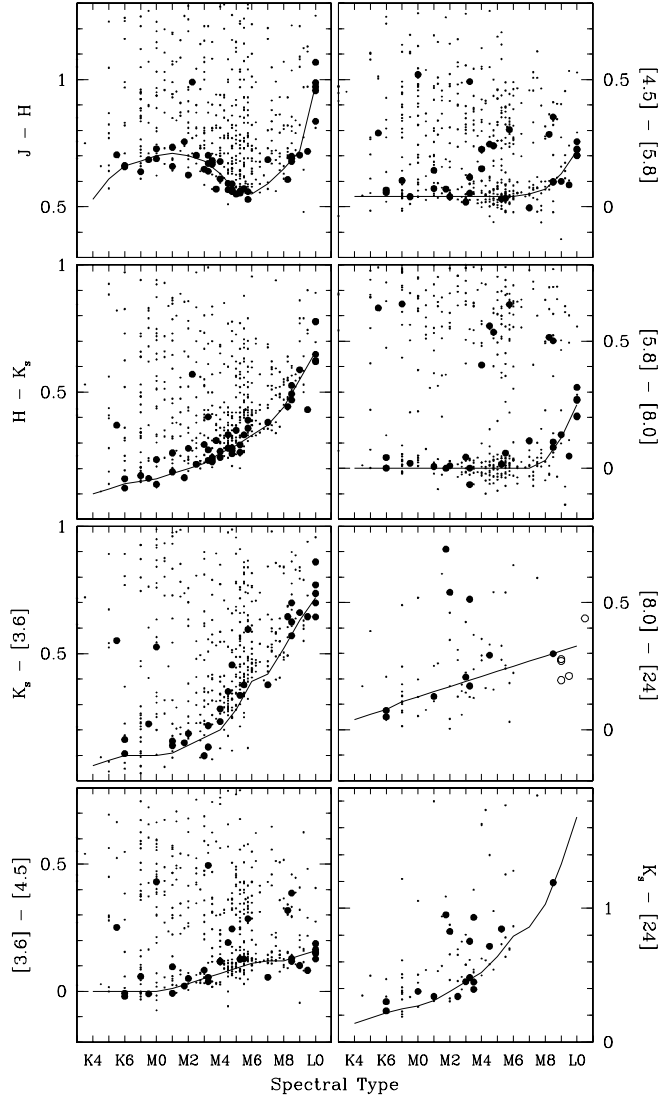
FIG. 26.— Infrared colors as a function of spectral type for members of the Taurus and Chamaeleon I star-forming regions (*small filled circles*) and young sources in the η Cha, ε Cha, and TW Hya associations and in the solar neighborhood (*large filled circles*). The latter samples should have negligible extinction ($A_V < 1$). We have used these data to estimate the intrinsic colors of young stellar photospheres (*solid lines*, Table 13). Because few young late-type objects have been measured at 24 μm, we also show data for field dwarfs at M9–L0 in the diagram of [8.0] − [24] colors (*open circles*).